



**Development of chemosensors for endocrine
disrupting chemicals (EDCs):
synthesis and evaluation of solid-phase bound
estrogen modelreceptors**

Steven Van der Plas

Promotor: Prof. Dr. A. Madder

**Thesis submitted to obtain the degree of
Doctor in Sciences: Chemistry**

I. Preface.....	1
II. Introduction	3
II.1. General Background.....	3
II.2. Endocrine disruption	5
II.2.1. Mechanism of disruption	5
II.2.2. Effects on animals	6
II.2.3. Effects on human health: is there a problem?.....	7
II.2.4. Exposure	9
II.2.5. Biological monitoring of estrogenic compounds.....	14
II.2.6. Chemical monitoring of estrogenic compounds	17
II.2.7. SPE techniques for the enrichment of EDCs	18
II.3. Rationally designed artificial receptors.....	24
II.3.1. One-armed receptors.....	25
II.3.2. Tweezers.....	26
II.3.3. Tripodal scaffolds	27
III. Project aim and objectives.....	33
IV. Synthesis of hER mimics	35
IV.1. Synthesis of the tripodal scaffold	35
IV.1.1. Synthesis of the triamine core	36
IV.1.2. Synthesis of the arms	38
IV.1.3. Coupling of the arms to the triamine backbone	39
IV.1.4. Establishing the anchor point.....	40
IV.2. Solid phase synthesis of possible EDC receptors	42
IV.2.1. Synthetic and analytical strategies	42
IV.2.2. Coupling of scaffold IV.1 to a solid phase.....	49
IV.2.3. Capping of the remaining spacer amines	54
IV.2.4. Attachment of the first amino acids	57
IV.2.5. Reconsidering the orthogonality scheme: synthesis of new glycine derivatives	60
IV.2.6. Incorporation of the new glycine derivatives	79

IV.2.7. Selection of the key amino acids.....	81
IV.2.8. Size of the parallel library	83
IV.2.9. Automated solid phase synthesis of 120 receptors.....	85
IV.2.10. Side chain deprotection	87
IV.3. Conclusion	90
V. Screening of the library	91
V.1. SPE tests	92
V.1.1. Tentagel based SPE material	92
V.1.2. Alternatives for Tentagel.....	95
V.2. Affinity LC	100
V.2.1. Development of a new estradiol column	100
V.2.2. Evaluation the estradiol column	101
V.2.3. Testing of the library via affinity LC.....	103
V.2.4. Development of a norethindrone column	105
V.2.5. Competition experiments.....	106
V.3. Reconsidering the SPE test	109
V.3.1. General strategy.....	109
V.3.2. ‘Clicking’ of the alkyne derivatives to silica.....	120
V.4. Results of the SPE tests.....	122
V.5. Conclusion	125
VI. Considering the chirality of the scaffold	129
VII. General conclusions	133
VIII. Experimental part	139
VIII.1. Methods and materials	139
VIII.2. Synthesis of the Tripodal Scaffold IV.1	141
VIII.2.1. Synthesis of the triamine core IV.2	141
VIII.2.2. Synthesis of the arms.....	143
VIII.2.3. Coupling of the arms to the triamine core	150
VIII.2.4. Establishing the anchor point	154
VIII.3. Solid phase synthesis	158
VIII.3.1. Standard operating protocols	158

VIII.3.2. Coupling of the scaffold IV.1 to Tentagel.....	160
VIII.3.3. Synthesis of new glycine derivatives.....	163
VIII.3.4. Incorporation of the glycine derivatives.....	167
VIII.3.5. Automated synthesis of 120 members.....	170
VIII.3.6. Side chain deprotection of the library.....	173
VIII.4. Screening of the library: development of the first SPE tests.....	180
VIII.4.1. Preparation of Tentagel-bound Tozzi-tetrapeptide	180
VIII.4.2. Synthesis on silica	183
VIII.5. Screening of the library: development of affinity LC	189
VIII.5.1. Development of the estradiol column V.11	189
VIII.5.2. Synthesis of the Tozzi peptides	191
VIII.5.3. Development of the norethindrone column V.19	195
VIII.5.4. Development of a second generation estradiol column V.23	196
VIII.6. Screening of the library: development of new SPE cartridges.....	200
VIII.6.1. Synthesis of alkyne substituted components	200
IX. List of publications.....	219
IX.1. Poster presentations	219
IX.2. Peer reviewed publications	219

List of Abbreviations

AA	amino acid
Abz	aminobenzoic acid
AcOH	acetic acid
Ala	alanine
Alloc	allyloxycarbonyl
AMP	adenosine monophosphate
APCI	atmospheric pressure chemical ionisation
APE	alkylphenol polyethoxylates
Arg	arginine
Boc	<i>tert</i> -butyloxycarbonyl
BPA	bisphenol-A
CSA	campher sulphonic acid
DCC	N, N'-dicyclohexylcarbodiimide
DCM	dichloromethane
DCU	N, N'-dicyclohexylurea
DDD	dichloro-diphenyl-dichloroethane
DDE	dichloro-diphenyl-dichloroethylene
DDT	dichloro-diphenyl-trichloroethane
DEHP	di-2-ethyl-hexylphthalate

DES	diethylstilbesterol
DIC	N, N'-diisopropylcarbodiimide
DIEA	di-isopropylethylamine
DMF	N, N'-dimethylforamide
DOTD	3,6-dioxa-1,8-octanedithiol
E1	estrone
E2	estradiol
EDC	endocrine disrupting chemical
EE2	ethinylestradiol
EI	electron impact
ELISA	enzyme linked immuno assay
EPA	environmental protection agency
ESI	electron spray ionisation
Fmoc	9-fluorenylmethoxycarbonyl
FTIR	fourier transform infrared
GC	gas chromatography
Gln	glutamine
Glu	glutamic acid
Gly	glycine
HATR	horizontal attenuated total reflection
HBD	hormone binding domain
HBTU	O-Benzotriazole-N,N',N'-tetramethyl-uronium-hexafluoro-phosphate

hER	human estrogen receptor
HFIP	hexafluoroisopropanol
His	histidine
HOAt	1-hydroxy-7-azabenzotriazole
HOBt	N-Hydroxybenzotriazole
HPLC	high-pressure liquid chromatography
HRMS	high resolution mass spectroscopy
IR	infra red
<i>iv</i> Dde	2- <i>iso</i> -valerydimedone
K _d	dissociation constant
LC	liquid chromatography
Leu	leucine
Lys	lysine
MALDI-TOF	matrix assisted laser desorption-time of flight
Met	methionine
MIP	molecular imprinted polymer
MS	mass spectrometry
NHS	N-hydroxysuccinimide
NMR	nuclear magnetic resonance
NP	nonylphenol
OBt	oxobenzotriazole
oNBS	<i>ortho</i> -nitrobenzenesulfonyl

Pbf	2,2,4,6,7-pentamethyldihydrobenzofuran-5-sulfonyl
PG	protecting group
pH	pontentia hydrongenii
Phe	phenylalanine
Pro	proline
PyBOP	benzotriazol-1-yl- oxytripyrrolidinophosphonium hexafluorophosphate
RaNi	Raney Nickel
RBA	relative binding affinity
RF	ratio to front
Ser	serine
SPE	solid phase extracion
SPPS	solid phase peptide synthesis
TAC	triazacyclophane
TBS	<i>tert</i> -butyl-dimethylsilyl
TBSCI	<i>tert</i> -butyl-dimethylsilylchloride
<i>t</i> Bu	<i>tert</i> -butyl
TCV	cyclotrimeratrylene
Tes	testosteron
TFA	trifluoroactetic acid
TFE	trifluoroethanol
TFFH	N, N'-tetramethylfluoroformamidinium hexafluorophosphate
TIS	triisopropylsilane

TLC	thin layer chromatography
Trt	trityl
UV	ultra violet
Val	valine
WHO	world health organisation
YES	yeast estrogen screen

I. Preface

Worldwide concern has been growing on the increasing distribution of endocrine disrupting chemicals (EDCs) during the last decade. The overall anxiety is caused by their effect on the endocrine system of wildlife and humans. While the influence on the reproductive systems of several animals has been thoroughly documented, the effects on human health are still the subject of intense debate.

Establishing a causal relationship between the presence of EDCs in the environment and their possible effects on human health is a challenging quest. Besides their low physiologically active concentrations, the complex environmental matrices in which they are present, makes it very difficult to identify and quantify different EDCs.

This problem can be tackled by a pre-concentration step before the actual analysis. In general, solid-phase extraction (SPE) of aqueous samples is a widely applied technique to enrich pollutants. With the current SPE cartridges, the extraction efficiency of the pollutants depends on their polarity. Thus polar compounds stay in the water sample while apolar compounds are retained on the solid phase. As a consequence the selectivity of the SPE is poor. A solid-phase material which could selectively bind the different EDCs would thus greatly simplify the analysis.

This PhD will focus on the development of an artificial receptor that shows high affinity towards common EDCs and low or no affinity to other compounds present in environmental samples. By constructing this receptor on a solid phase, a new affinity based SPE material can be developed, resulting in a more accurate and selective determination of EDCs.

II. Introduction

II.1. General Background

Since World War II, the world has witnessed a large increase in the production of chemicals. Some of these chemicals, like pesticides, were designed for wide spread use in the environment. Others, like PCBs, were rather accidentally released into the environment by leakages or waste dumping. At the time, little or no attention was paid to the possible consequences that could result from the use and distribution of these chemicals.

This ignorance changed with the publication of Rachel Carson's *Silent Spring* in 1962.¹ This book documented for the first time the detrimental effects of pesticides on wildlife. More particularly, the link was proven between egg shell thinning of birds and the pollution of the surrounding environment with dichloro-diphenyl-trichloroethane (DDT). From this time, public awareness was born and grew ever since.

Only three decades later, a new disturbing event was signalled in an article by Theo Colborn.² This article described the deleterious influence that certain chemicals had on the development of endocrine systems. These endocrine disrupting chemicals (EDCs) were linked to reproductive problems like the decrease in fertility with birds and the demasculinisation and feminisation of fish. The last twenty years that followed this paper have witnessed a growing scientific concern, public debate and media attention over the possible effects in wildlife and humans that may result from exposure to chemicals that have the potential of interfering with the endocrine system.³

¹ Carson, R. 1962. *Silent Spring*. Mariner Books, Boston, 400p.

² Colborn, T.; Saal, F. S. V.; Soto, A. M. *Environmental Health Perspectives* **1993**, 101, 378-384.

³ Matthiessen, P. *Pure Appl. Chem.* **2003**, 75, 2197-2206.

The international programme for chemical safety (IPCS) defined endocrine disruptors as follows:⁴

An endocrine disrupter is an exogenous substance or mixture that alters function(s) of the endocrine system and consequently causes adverse health effects in an intact organism, or its progeny, or (sub)populations.

Currently, the European commission has listed 320 chemicals⁵ as possible EDCs. The list encompasses a variety of chemical classes, including natural and synthetic hormones, plant constituents, pesticides, compounds used in the plastic industry and in consumer products and other industrial by-products and pollutants. Some EDCs are persistent organic molecules and bio-accumulate in the food chain, others are rapidly degraded and excreted into the environment.

In the next chapter a brief overview is presented of the mechanism of endocrine disruption and the effects on wildlife and humans. A focus will be put on estrogen related problems. Next, the different classes of EDCs are discussed and finally a summary is given of analytical strategies used for the determination of the potency and the concentration of EDCs. Though a complete review of scientific literature is beyond the scope of this chapter, the most important and disturbing events are listed.

⁴ WHO/IPCS *Global assesment of the state-of-the-science of endocrine disruptors*, **2002**.

⁵ Commission staff working document on the implementation of the community for endocrine disruptors, a range of substances suspected of interfering with the hormone systems of humans and wildlife, SEC (2004) 1372, COMM (2001) 262, SEC (2007) 1635, Brussels Belgium.

II.2. Endocrine disruption

II.2.1. Mechanism of disruption

Communication inside the body can proceed via fast, electrical signalling coordinated by the central nervous system or via slower, chemical signalling coordinated by the endocrine system. The chemical messengers employed by the latter are called hormones and consist of two classes: peptide hormones and steroid hormones. These hormones generate specific responses in other parts of the body by interacting with their specific receptor. The concentrations at which the hormones are present vary in time, but wild swings in concentrations are avoided so that a homeostasis is maintained.

Chemicals originating from outside the body can influence the endocrine system via several pathways:

- Binding to the hormone receptor and acting as an agonist (activating the receptor).
- Binding to the hormone receptor and acting as an antagonist (deactivating the receptor).
- Influencing the production, metabolism or transport of the endogeneous hormones.

The most disturbing effects originate from the binding of chemicals with the hormone receptors at the cell surface, cytoplasm or nucleus.⁶ From these hormone receptors, especially the estrogen receptor (ER) seems to behave promiscuous.

The estrogen receptor, part of the family of nuclear receptors, is a ligand-inducible transcription factor. With humans, two forms, ER α and ER β , are present. Though they are very similar, the two receptor types have distinctly different localisations and

⁶ Harry, F.; Robert, G. *Pure Appl. Chem.* **2003**, 75, 2181-2193.

concentrations within our body. Both are activated upon binding with small, lipophilic molecules. After activation, a dimer (e.g. ER β - ER β , ER α - ER α or ER β - ER α) is formed and this complex binds to the cell's DNA. The DNA is then transcribed into mRNA that leaves the nucleus to be translated in proteins. In this way, growth and reproduction of the body are regulated.

The human estrogen receptor (hER) is unique in its ability to embrace a wide variety of non-steroidal compounds. This overall promiscuity can be ascribed to the large size of the hormone binding domain (HBD) which has an accessible volume (450 Å³), twice the size of estradiol (250 Å³).⁷ A distinct feature is a pincer like arrangement of amino acids around the phenolic ring of estradiol that imposes an absolute requirement on effective ligands to contain an aromatic ring. The length and the breadth of the estradiol skeleton are well matched by the receptor, but there are large unoccupied cavities at the two sides of the molecule.

Consequently, a lot of chemicals can bind with the ER and influence the endocrine system. This will eventually result in a disturbed reproductive system and explains the observed phenotypes with decrease in fertility, change of sex, ...⁸

II.2.2. Effects on animals

A direct effect of chemicals on the endocrine system of animals was observed in the 1980s with the alligator population of Lake Apopka, central Florida (USA). It was noticed that this population declined while the populations in the rest of Northern America increased. This decline was the consequence of the contamination of the lake with the pesticide dichloro-diphenyl-dichloroethylene DDE.⁹ The pesticide pollution was linked to reproductive

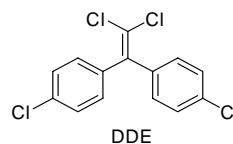


Figure II.1: DDE.

⁷ Brzozowski, A. M.; Pike, A. C. W.; Dauter, Z.; Hubbard, R. E.; Bonn, T.; Engstrom, O.; Ohman, L.; Greene, G. L.; Gustafsson, J. A.; Carlquist, M. *Nature* **1997**, 389, 753-758.

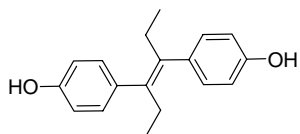
⁸ Harrison, P. T. C.; Humfrey, C. D. N.; Litchfield, M.; Peakall, D.; Shuker, L. K. *IEH assesment on environmental oestrogens: consequences to human health and wildlife*; Page Bros.: Norwich, **1995**.

abnormalities like a smaller penis size, lower plasma concentrations of testosterone and higher concentrations estradiol with juvenile, male alligators.

Another notable and convincing biological response to the presence EDCs, is the production of the female fish hormone vitellogenin in male fish. Although this hormone is normally produced by the yolk of the female, high values of it have been found in male fish in a variety of water bodies in Europe, Japan and North America. In the UK, domestic waste effluents are a major source of pollution of the rivers.¹⁰ The effluents are contaminated with EDCs that cause the feminisation of male fish which is reflected in the production of vitellogenin.

These two examples are only a few of the well documented effects on wildlife. The influence on animals continues to raise a lot of concern because it can be seen as an indicator for the overall contamination of the environment with EDCs. Indeed, problems with wildlife can be regarded as a warning for humans.

II.2.3. Effects on human health: is there a problem?



Diethylstilbesterol (DES)

Figure II.2: DES.

The effects on humans resulting from different chemicals are not only predicted by studying the effects on animals, some significant conclusions can be drawn from the DES case. Diethylstilbesterol or DES (**Figure II.2**) is a drug that was administered to several million women between the late 1930's until its ban as a drug in 1971. The drug was described to prevent habitual abortion but was banned later on with the discovery that some women exposed in utero (the DES daughters) developed a vaginal cancer.¹¹ Also an increased infertility and an irregular menstrual cycle were observed

⁹ Guillette, L. J.; Gross, T. S.; Masson, G. R.; Matter, J. M.; Percival, H. F.; Woodwar, A. R. *Environ. Health Perspect.* **1994**, *102*, 680-688.

¹⁰ Tyler, C. R.; Routledge, E. J. *Pure Appl. Chem.* **1998**, *70*, 1795-1804.

¹¹ Fisch, H.; Golden, R. *Pure Appl. Chem.* **2003**, *75*, 2181-2193.

with the female offspring. Adverse effects on the male reproductive system resulting from the in utero exposure to DES consisted in a decreased sperm count, increased incidence in abnormal sperm and smaller penises. Because of the wide spread use of this drug, a clear relationship could be established between the use of the endocrine disrupting DES and the effects on humans.

Nevertheless, there is a big difference between the high amounts of DES given to pregnant women and the low concentrations of EDCs present in the environment. DES was administered in high doses and is more active than endogenous estrogens while common pollutants with estrogenic activity are not only present in very low concentrations, they are also less active than the endogenous estrogens. Consequently, reports of low-dose effects of exogenous EDCs are highly controversial and subject of intense debate.¹²

Exposure to EDCs does generate some concerns. This is because analysis of human data shows that there are human health effects in which EDCs can play a role. With males in particular the decrease in the sperm count/quality and the increase in testicular cancer have been linked to the exposure of estrogenic chemicals during the foetal development.^{13,14} For women, it has been proposed they begin menstruation and undergo sexual maturation (early puberty) at lower ages than usual because of the exposure to EDCs. Another effect that has been described to EDCs is the steadily increase in breast cancers over the past decades in different countries.¹⁵

One of the reasons that makes it so difficult to establish causal relationships between EDCs and their effects is the time of exposure. For adults, contamination to EDCs can be corrected by the homeostasis mechanism. Exposure to EDCs during foetal and post-natal life can however result in permanent changes because during this period the

¹² a) Safe, S. H. *Environ. Health Perspect.* **2000**, *108*, 487-493. b) Safe, S. *Toxicology* **2004**, *205*, 3-10. c) Inoue, T. *Pure Appl. Chem.* **2003**, *75*, 2555-2561.

¹³ Carlsen, E.; Giwercman, A.; Keiding, N.; Skakkebaek, N. E. *Brit. Med. J.* **1992**, *305*, 609-613.

¹⁴ Moller, H. *Eur. Urol.* **1993**, *23*, 8-15.

¹⁵ Wolff, M. S.; Toniolo, P. G.; Lee, E. W.; Rivera, M.; Dubin, N. *J. Natl. Cancer I.* **1993**, *85*, 648-662.

endocrine system is programmed. Wrong conclusions can be drawn from measuring the concentrations of EDCs in the blood of adult humans and for example the occurrence of breast cancer.¹⁶

In conclusion, the effects of EDCs on the human health are unknown at this moment. More information is needed to accurately quantify the human burden of hormonally active environmental chemicals.

II.2.4. Exposure

There are numerous chemicals in the environment that are hormonally active. These include synthetic and natural hormones, industrial chemicals (insecticides, household detergents, ...) and phyto-estrogens (plant derived).

II.2.4.1. Natural and synthetic hormones

Hormones produced by humans and animals are constantly excreted into the environment. Many of these hormones are peptides that are rapidly destroyed. However, the steroid hormones like estrogenic compounds (**Figure II.3**) are very stable and not fully removed during waste water treatment. Human females excrete about 5µg/day each of estrone and estradiol. When pregnant, women can excrete a 1000 fold of these hormones, depending on the stage of pregnancy.¹⁷ Next to human excretion, animals contribute to the estrogen production as well. Cows, sheep, pigs and chickens produce estrogens that are excreted in the urine and especially in the faeces. The natural estrogens represent one of the most active class of compounds that can interfere with the endocrine system. As described above, they have been shown to be responsible for vitellogenin production in male fish.¹⁰

¹⁶ a) Westin, J. B.; Richter, E. *Trends in Cancer Mortality in Industrial Countries* **1990**, 609, 269-279. b) Mendez, M. A.; Arab, L. *Pure Appl. Chem.* **2003**, 75, 1973-2012.

¹⁷ Shore, L. S.; Shemesh, M. *Pure Appl. Chem.* **2003**, 75, 1859-1871.

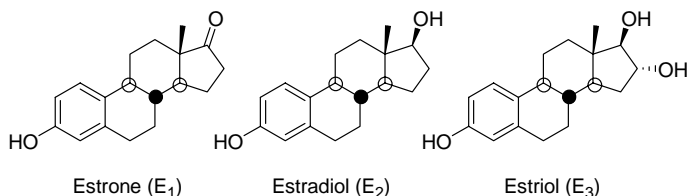


Figure II.3: Natural estrogens.

Many synthetic estrogens have been prepared in search for estrogen pharmaceuticals (**Figure II.4**). These compounds are designed to have a greater estrogenic potency than the natural estrogens by enhancing binding to the receptor or by retarding metabolism. The best known example is the use of ethinylestradiol (EE_2) in birth control pills. After intake in tablet form, the EE_2 can be excreted via the urine or the faeces.¹⁸ Other pharmaceutical compounds include DES that had a past as drug (*vide supra*) but that is also used as an anabolic agent in livestock feedings. Sometimes natural hormones are administered as pharmaceutical compounds, such as the use of E_2 in the hormone replacement therapy with post-menopausal women or in the treatment of breast cancer. Another source of estradiol is its use as anabolic agent in feedings for cattle.¹⁹

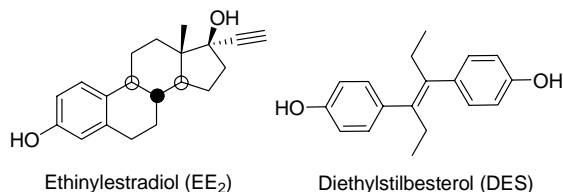


Figure II.4: Pharmaceutical estrogens.

II.2.4.2. Phyto-estrogens

A more surprising source of EDCs can be found in plants. They produce non-steroidal phyto-estrogens that encompass two main classes: the isoflavones and the

¹⁸ Ingerslev, F.; Vaclavik, E.; Halling-Sorensen, B. *Pure Appl. Chem.* **2003**, 75, 1881-1893.

¹⁹ Katzenellenbogen, J. A.; Muthyala, R. *Pure Appl. Chem.* **2003**, 75, 1797-1817.

lignans (**Figure II.5**). Humans consume isoflavones via soybeans and other legumes. The lignans are consumed by eating grains, fibres and fruits.

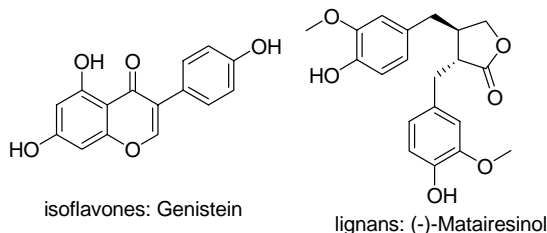


Figure II.5: Phyto-estrogens.

Actually, the first endocrine disrupting effect on animals described in 1948 was linked to phyto-estrogens.²⁰ Sheep in Western Australia suffered from a decrease in fertility by eating red clover. Apparently, the red clover contained high percentages of isoflavones that can disturb the endocrine system resulting in infertility.²¹ The role of phyto-estrogens however, is not totally clear. On one hand, they are linked with a lot of beneficial effects on human health involving cardiovascular diseases, breast cancer and post-menopausal osteoporosis.²² The reduced risk of breast cancer in women in Singapore was found to correlate with a daily, high soy intake.²³ On the other hand, studies on animals have shown that phyto-estrogens can act as endocrine disruptors. Probably, the time of exposure is very important and that is why particular attention is given to babies who are fed with soy-based infant formulas.²⁴

²⁰ Bennetts H.W., U. E. J., Shier, F.L. *Aust. Vet. J.* **1948**, 22, 2-12.

²¹ Adams, N. R. *J. Anim. Science* **1995**, 73, 1509-1515.

²² Wanibuchi, H.; Kang, J. S.; Salim, E. I.; Morimura, K.; Fukushima, S. *Pure Appl. Chem.* **2003**, 75, 2047-2053.

²³ Lee, H. P.; Gourly, L.; Duffy, S. W.; Esteve, J.; Lee, J.; Day, N. E. *Lancet* **1991**, 331, 1197-1200.

²⁴ Verger, P.; Leblanc, J. C. *Pure Appl. Chem.* **2003**, 75, 1873-1880.

II.2.4.3. Industrial chemicals

An intriguing variety of men-made compounds, or their metabolites, seem to be estrogenically active. Though their potency is rarely high, some are very lipophilic and have the tendency to bio-accumulate throughout the food chain. The most important estrogenic chemicals are summarised below.

One class of chemicals that were released intentionally into the environment are the chlorinated aromatic insecticides (**Figure II.6**) like the notorious DDT. In the 1940's, it was used on a large scale against insect vectors for diseases as typhus and malaria, helping to finally eliminate malaria in Europe and Northern America. From 1950 till 1980 DDT found wide spread use as a general insecticide in agriculture. After the publication of *Silent Spring*, it became clear that the release of large quantities of DDT in the environment had it's consequences on wildlife and humans.¹ Thus it was banned from world wide agricultural use, but an exception was made for the fight against malaria in developing countries.

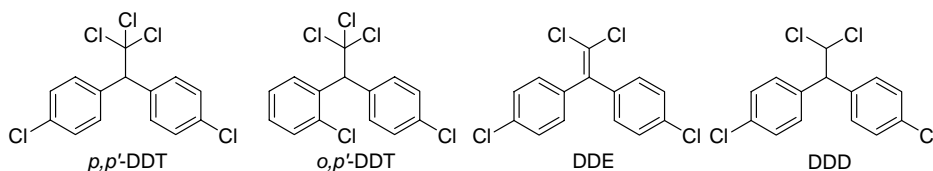


Figure II.6: Chlorinated aromatic insecticides.

Commercially available DDT is actually a mixture consisting for the main part out of the *p,p'*- and the *o,p'*- DDT isomers (**Figure II.6**). A minor fraction consists of DDE and DDD, which are also the breakdown products of DDT.²⁵

These chlorinated aromatic insecticides are persistent organic molecules which are very hydrophobic. A study in 2002²⁶ found detectable levels of DDT or metabolites in

²⁵ WHO/IPCS *Environmental Health Criteria 9: DDT and its derivatives*, 1979.

²⁶ CDCP *National Report on Exposure to Environmental Chemicals*, 2005.

the blood samples of more than half of the subjects tested. These values are the direct consequence of the past world wide use of the insecticides. This bio-accumulation is the reason why they continue to raise much concern, although they are only weak estrogenic compounds. In vitro binding assays showed that the highest estrogenic activity was displayed by *o,p'*-DDT.²⁷ Several studies were undertaken to determine a relationship between DDT levels in adipose tissue and breast cancer, but failed to find a significant link.⁸ However, concentrations were determined in the patients at the moment they already developed the cancers, but maybe the exposure during foetal development and childhood plays a more important role.

Another threat is posed by the substances shown in **Figure II.7**. These are estrogenically active chemicals that are unintentionally released into the environment. A disturbing example is bisphenol-A (BPA) which is a frequently used monomer for the preparation of polycarbonates and epoxy resins. These polymers are used in plastic water bottles, baby bottles, plastic food containers and dental materials. The monomer BPA is known to leach from these products. With baby bottles, leaching occurs during heating of the bottle and this exposes infants fed with liquid formula to BPA. A study by the European Food Safety Authority showed that daily intake with these infants can be as high as 13µg/kg/day.²⁸ Although it was already shown in 1936 that bisphenol-A is an estrogenically active compound, only Canada intends to put a ban on the use of BPA.²⁹ While Europe and the USA conclude that there is a potential danger, they state that current human exposure levels are too low to induce adverse effects. Nevertheless, the first bisphenol-A free bottles are on the market, trying to benefit from the growing public concern.³⁰

²⁷ Forster, M. S.; Wilder, E. L.; Heinrichs, W. L. *Biochem Pharmacol* **1975**, *24*, 1777-80.

²⁸ EFSA *Opinion of the Scientific Panel on food additives, flavourings, processing aids and materials in contact with food (AFC) related to 2,2-BIS(4-HYDROXYPHENYL)PROPANE*, **2006**.

²⁹ Dodds, C. E.; Lawson, W. *Nature* **1936**, *137*, 996-996.

³⁰ BPA free plastic bottles can be ordered via <http://www.babybornfree.co.uk>

Phthalates in plastics are another source of estrogenic chemicals. These chemicals are called plasticizers because they soften hard plastics when added. They are not chemically bound to the polymeric framework and can thus migrate to the surface. Phthalates are found in soft toys, cosmetics, flooring, medical equipment and colourful prints on children's clothing. In vitro tests showed that they have weak estrogenic properties.³¹ The most potent phthalate, bis(2-ethylhexyl)phthalate (DEHP), used in medical tubing, catheters and blood bags, may harm sexual development in male infants.³² Based on these and other results, including animal testing, the European Commission has banned the use of phthalates in children's toys.

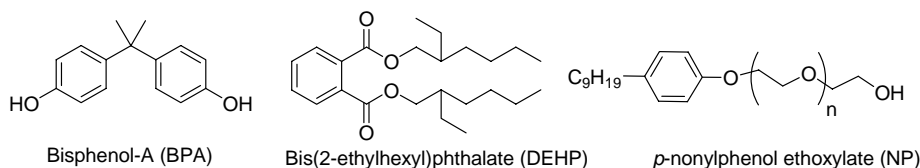


Figure II.7: Industrial estrogenic chemicals.

Alkylphenol polyethoxylates (APEs) are non-ionic surfactants, used extensively in household detergents. This implies that they are disposed into the sewage system where they are broken down by micro-organisms. The remaining alkylphenols are resistant to further biological degradation and show up in rivers.³³ Although there are many different APEs, 80% of them is composed of *p*-nonylphenol (NP). This compound showed in vitro and in vivo estrogenic activity and is not only exposed to aquatic life, but also to humans via drinking water and the consumption of fish.⁸ The use of nonylphenol ethoxylates is now restricted by the European Commission.

³¹ Johnson, A.; Jurgens, M. *Pure Appl. Chem.* **2003**, 75, 1895-1904.

³² Fisher, J. S. *Reproduction* **2004**, 127, 305-15.

³³ Preziosi, P. *Pure Appl. Chem.* **1998**, 70, 1617-1631.

These examples show that we are exposed to EDCs on a daily basis in products that are used without suspicion. Careful monitoring of the concentrations and the potencies of the EDCs to which we are exposed is thus very important.

II.2.5. Biological monitoring of estrogenic compounds

The total estrogenic activity of a solution can be determined using in vitro or in vivo assays.

Biologically based in vitro methods can be categorised as follows:

Receptor binding assays measure binding of agonists (or antagonists) to the human estrogen receptor (hER). These methods rely on the displacement of a high-affinity radioligand (^3H -labeled estradiol) by a possible estrogenic chemical. Its value is then compared to the displacement caused by the unlabeled estradiol and is expressed in relative binding affinities (RBA of E_2 being 100%). They have the advantage of being very sensitive, RBAs of 0,0003% can be detected.¹⁹

Cell proliferation assays depend on the ability of possible estrogens to induce rapid, uncontrolled cellular growth in the human breast cancer cell line MCF-7.⁴ These cells have high levels of estrogen receptors and consequently proliferation can be induced with very low concentrations of estrogenic substances.

Receptor-dependent gene expression assays measure the ability of a compound to stimulate a receptor dependent response in genes. The most popular assay for the determination of estrogenic activity is the Yeast Estrogen Screen (YES assay).³⁴ It consists of yeast cells in which the hER is expressed. When an estrogen binds to the hER, a reporter gene is transcribed and eventually translated into the enzyme β -galactosidase. This enzyme catalyses the hydrolysis of *o*-nitrophenol- β -D-galactopyranoside after which the concentration of the *o*-nitrophenol can be determined via UV-measurements at 420 nm.

³⁴ Arnold, S. F.; Robinson, M. K.; Notides, A. C.; Guillette, L. J.; McLachlan, J. A. *Environ. Health Perspect.* **1996**, *104*, 544-548.

For the *in vivo* assessment of estrogenic activity, the following tests are frequently used:

With the *uterotrophic assay* the ovary from mouse is removed, reducing the intrinsic female hormone levels to a minimum and thus shrinking the uterus. After administrating the test compound, the inflation of the uterus is monitored and the estrogenic activity of the compound can be determined.^{12c}

The induction of *vitellogenin* production in juvenile male fish is an approach to measure the estrogenicity of the aquatic environment. The concentration of this biomarker in the blood is measured and can be correlated with the estrogenic potency of the mixture.³⁵

The *in vitro* and *in vivo* assays give complementary results and should be used together in a battery of tests.³⁶ Although *in vitro* tests are easier in use because of the lack of animal testing, they have significant drawbacks. They do not take into account the effects of bioaccumulation and metabolism and other possible pathways of interaction are neglected. *In vivo* tests on the other hand, lack standardisation which makes it difficult to compare results obtained with the same method.

Biological methods to measure the concentration of an EDC depend on the antibody–antigen interaction and are thus called *immunoassays*.³⁷ If antibodies are to be generated against small molecules like EDCs, they first have to be conjugated with a large protein like the bovine serum albumin to render them immunogenic.³⁸ The immunoresponse to this ligated molecule or hapten, yields different antibodies. When extracted from the serum, these polyclonal antibodies can be used directly or first be purified to get only one type of monoclonal antibodies. The latter are much more selective and have less cross reactivity than the polyclonal antibodies.

³⁵ Eggen, R. I. L.; Bengtsson, B. E.; Bowmer, C. T.; Gerritsen, A. A. M.; Gibert, M.; Hylland, K.; Johnson, A. C.; Leonards, P.; Nakari, T.; Norrgren, L.; Sumpter, J. P.; Suter, M. J. F.; Svenson, A.; Pickering, A. D. *Pure Appl. Chem.* **2003**, *75*, 2445-2450.

³⁶ Zacharewski, T. *Environ Health Perspect* **1998**, *106 Suppl 2*, 577-82.

³⁷ Eggen, R. I.; Segner, H. *Anal Bioanal Chem* **2003**, *377*, 386-96.

³⁸ Schneider, C.; Scholer, H. F.; Schneider, R. J. *Steroids* **2004**, *69*, 245-253.

When using immunoassays, the binding event is usually visualised by an auxiliary reaction, in which a second labelled immunoreactant binds to the analyte. With *enzyme-linked immunoassays* (ELISAs), this label is an enzyme that can convert a colourless substrate into a coloured product, from which the concentration can then be measured using UV-spectroscopy.³⁹

Immunoassays are technically simple and allow a rapid screening of high sample numbers. Their production however, is a time consuming, trial and error based process. Another big disadvantage is that they are too selective, only one or a few chemicals can be quantified and not a whole set of related compounds.

II.2.6. Chemical monitoring of estrogenic compounds

To establish a link between a certain EDC and its possible effects on human health, quantitative exposure levels should be determined at different stages of life. Because most biological tests do not give away the identity and the amount of the chemical that is causing the endocrine disruption, these tests need to go hand in hand with chemical analysis.

Quantifying EDCs in environmental matrices is a difficult process not only because of the low concentrations at which the EDCs are present but also because of the complex constitution of the matrices (e.g. sewage water, serum, urine samples, ...).⁴⁰ Before the actual measurements take place, the desired compounds have to be extracted from the matrix. For liquid samples, this is usually done via solid-phase extraction (SPE) techniques.⁴¹ The sample is sent over a SPE-cartridge which is packed with an adsorbent like C₁₈ silica or styrene based polymers. The analytes are retained on the cartridge, depending on their water-octanol partitioning coefficient (log P value). The higher this value for a certain chemical, the better it is retained on an apolar phase like

³⁹ Campbell, C. G.; Borglin, S. E.; Green, F. B.; Grayson, A.; Wozel, E.; Stringfellow, W. T. *Chemosphere* **2006**, 65, 1265-1280.

⁴⁰ de Alda, M. J. L.; Barcelo, D. *J. Chromatogr. A* **2001**, 938, 145-153.

⁴¹ Holland, P. T. *Pure Appl. Chem.* **2003**, 75, 1843-1857.

C₁₈. After extraction, the chemicals can be washed from the packing material using a small amount of organic solvent. This pre-concentration step can be followed by GC-MS or LC-MS analysis.

GC separation of the compounds followed by detection with MS has developed into a primary technique for the identification and quantification of EDCs. Electron impact (EI) is the most common used ionisation technique and yields smaller fragments of the molecule. By comparing the retention time and the corresponding fragments of a compound with a database, the identity of the compound can be established. If this technique is used with an internal standard, an isotope of the analyte, low detection limits and high accuracy are possible. However, EDCs with polar functionalities like estradiol are more difficult to evaporate due to hydrogen bonding. This can be solved via derivatisation reactions (e.g. silylating or capping the alcohols).⁴²

With LC-MS, the most common used ionisation techniques are electrospray ionisation (ESI) or atmospheric pressure chemical ionization (APCI). Both yield the hydrogen or sodium adduct of the molecule, giving direct information about the molecular weight and identity of the compound. Low detection limits can be reached without the need for derivatisation.⁴³

II.2.7. SPE techniques for the enrichment of EDCs

The most crucial step in the whole analysis protocol, whether GC- or LC-MS is used, is the pre-concentration step. Instead of just extracting apolar compounds, current research is focussing on the extraction of specific classes of compounds, like EDCs. A lot of progress has been made using biologically based interactions, but a trend towards

⁴² a) Tan, B. L. L.; Mohd, M. A. *Talanta* **2003**, *61*, 385-391. b) Lerch, O.; Zinn, P. *J. Chromatogr. A* **2003**, *991*, 77-97.

⁴³ a) Giese, R. W. *J. Chromatogr. A* **2003**, *1000*, 401-412. b) de Alda, M. J. L.; Diaz-Cruz, S.; Petrovic, M.; Barcelo, D. *J. Chromatogr. A* **2003**, *1000*, 503-526.

synthetic systems like molecular imprinted polymers (MIPs) and synthetic proteins is visible.⁴⁴

II.2.7.1. SPE based on immuno-affinity sorbents

The underlying principle of immuno-affinity sorbents, which is outlined in **Figure II.8**, is basically the same as with immunoassays. The sorbent consists of antibodies specific to the target analytes. These antibodies are produced in the same way as described before and can thus encompass polyclonal or monoclonal antibodies. Monoclonal antibodies are frequently used because they give more reproducible results.⁴⁵ Nevertheless, polyclonal antibodies are preferred since they recognise more than one compound. Due to the heterogeneity of the polyclonal antibodies they are able to bind structural variants of the analyte.⁴⁶

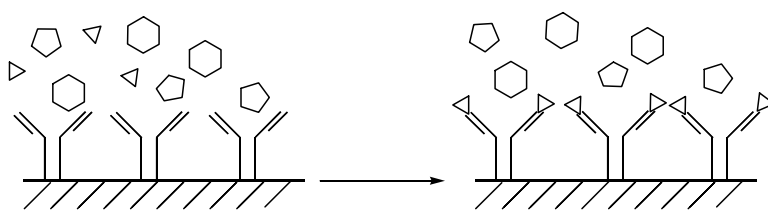


Figure II.8: Principle of immuno-affinity sorbents.

When eluting the analytes from the sorbent, organic solvents have to be applied. These can cause irreversible unfolding of the antibodies with loss of activity as a result. Another drawback, as with immunoassays, is the high selectivity of the technique, making it more attractive for a single residue then for a multiple residue analysis, where 20 to 30 analytes have to be determined.

⁴⁴ Tozzi, C.; Anfossi, L.; Giraudi, G. *J. Chromatogr. B* **2003**, 797, 289-304.

⁴⁵ Hennion, M.-C.; Pichon, V. *J. Chromatogr. A* **2003**, 1000, 29-52.

⁴⁶ Su, P.; Zhang, X.-X.; Chang, W.-B. *J. Chromatogr. B* **2005**, 816, 7-14.

II.2.7.2. SPE based on molecular imprinted polymers (MIPs)

Molecular imprinting is a technique to create template-shaped cavities in polymeric frameworks and has been applied to pre-concentrate several EDCs from aqueous samples.⁴⁷ MIPs are generated by first adding a template to a mixture of functionalised monomers (**Figure II.9**). These monomers can organise themselves around the template creating a non covalent 3D structure that fits around the template. This structure is locked by initiating the polymerisation process and thus creating covalent bonds between the different monomers. After the template is washed away, a cavity remains in the polymer network that has the shape of the template. It is claimed that these recognition sites mimic the binding sites of antibodies and receptors.⁴⁸

When packed into a SPE cartridge, this polymer can then be used to selectively concentrate the template and structural look-a-likes. These MIPs are chemically and physically more robust than the biological immuno-affinity sorbents.

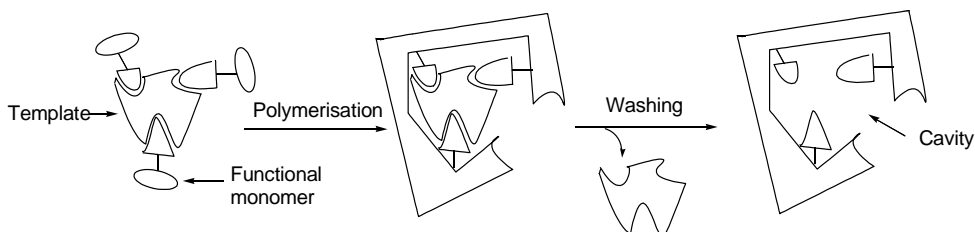


Figure II.9: Preparation of MIPs.

Though the principle of MIPs looks nice, there are a lot of practical drawbacks with these artificial receptors. A first problem is the leaching of the analyte, resulting in a positive error. Due to insufficient washing, some of the template molecules can stay

⁴⁷ a) Bravo, J. C.; Fernandez, P.; Durand, J. S. *Analyst* **2005**, 130, 1404-1409. b) Meng, Z. H.; Chen, W.; Mulchandani, A. *Environmental Science & Technology* **2005**, 39, 8958-8962. c) Bravo, J. C.; Garcinuno, R. M.; Fernandez, P.; Durand, J. S. *Anal. Bioanal. Chem.* **2007**, 388, 1039-1045.

⁴⁸ Haupt, K. *Chem. Commun.* **2003**, 171-178.

behind and leach during the analysis. The washing step is therefore crucial during the preparation of MIPs, but complete removal of the template is not always possible.

Another problem is the solvent based effects. Care must be taken in which solvent the organisation and polymerisation of the monomers is carried out. Effects like hydrogen bonding are less pronounced in water, while hydrophobic interactions are enhanced. This can result in the absence of selectivity between the MIP and the non-imprinted polymer blank.⁴⁹ However, selectivity can be enhanced by performing the polymerisation in an organic solvent, but this renders the MIP unusable for the analysis of aqueous matrices as is the case for EDCs.

II.2.7.3. SPE based on synthetic peptides

In the search for more robust systems that work in an aqueous environment, combinatorial solid phase techniques are used to develop new materials with biomimetic recognition properties.⁵⁰ Using these synthetic protocols, Tozzi et al prepared small polypeptides that could selectively bind estradiol and other similar structures in aqueous media.⁵¹

The monomers used for the peptide synthesis were Arg, Ser, Pro, Val, Leu, Gln, Gly and Ala. These were chosen because they are part of the HBD of the human steroid binding protein, a transport protein present in the serum of humans. With these amino acids, a first library was made consisting of dipeptides. By incubating the different solid-phase bound members with tritium-labelled estradiol, the dipeptide with the best binding characteristics was selected. This dipeptide was then the starting material for a second library, now consisting of tetrapeptides. Again the best tetrapeptide was selected

⁴⁹ a) Tse Sum Bui, B.; Belmont, A. S.; Witters, H.; Haupt, K. *Anal. Bioanal. Chem.* **2008**, 8, 2081-2088. b) Ye, L. *The Analyst* **2001**, 126, 760-765. c) Rachkov, A.; McNiven, S.; Cheong, S. H.; El'Skaya, A.; Yano, K.; Karube, I. *Supramol. Chem.* **1998**, 9, 317-323. d) Giraudi, G.; Giovannoli, C.; Tozzi, C.; Baggiani, C.; Anfossi, L. *Chem. Commun.* **2000**, 1135-1136.

⁵⁰ Diaz-Garcia, M. E.; Pina-Luis, G.; Rivero, I. A. *TrAC, Trends Anal. Chem.* **2006**, 25, 112-121.

⁵¹ Tozzi, C.; Anfossi, L.; Giraudi, G.; Giovannoli, C.; Baggiani, C.; Vanni, A. *J. Chromatogr. A* **2002**, 966, 71-79.

by measuring the radioactivity of the beads. These steps were repeated until the stage of the octapeptide.

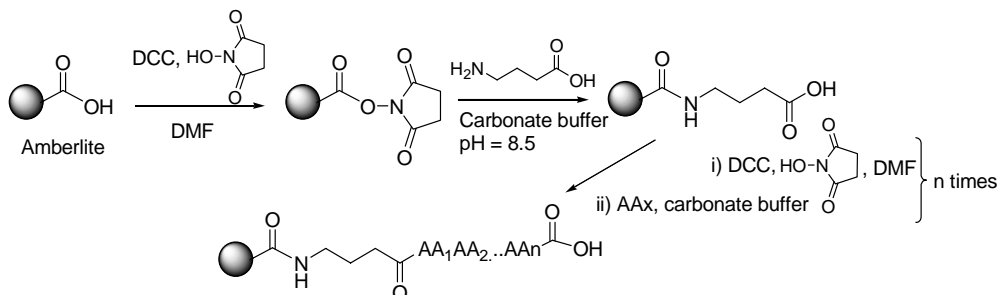


Figure II.10: Employed synthetic strategy.

The peptides were synthesised on Amberlite, an acrylic acid based polymer that was cross-linked to a high degree with divinylbenzene. Consequently, it has no swelling properties, unlike other frequently used commercial resins for peptide synthesis like Tentagel and Merrifield resin.⁵²

A rather unusual synthetic strategy was adopted for the peptide synthesis (**Figure II.10**). Instead of synthesising in the conventional $\text{C} \rightarrow \text{N}$ direction, the opposite direction was chosen. The carboxylic acid functions on bead were first pre-activated as their N-hydroxysuccinimide esters. An aqueous basic solution of an amino acid was then added to the activated beads to generate an amide bond.

This manner of coupling seems very odd when compared to standard protocols where the N- α -protected amino acid is activated in an organic solution like DMF or DCM, and is subsequently added to the amine-functionalised beads. Instead, Tozzi et al used unprotected amino acids that were dissolved in a carbonate buffer. The article does not give any proof of the identity and purity of the synthesised peptides, only the

⁵² Adams, J. H.; Cook, R. M.; Hudson, D.; Jammalamadaka, V.; Lyttle, M. H.; Songster, M. F. *J. Org. Chem.* **1998**, *63*, 3706-3716.

dissociation constants K_d towards estradiol are displayed. These are shown in **Table II.1**.

Table II.1: K_d values for estradiol and the ratio ($R_{\text{estradiol/testosterone}}$) of bound estradiol/bound testosterone.

Peptide	K_d (μM)	$R_{\text{estradiol/testosterone}}$
Arg-Ser	32	6
Arg-Ser-Ser-Val	17	10,1
Arg-Ser-Ser-Val-Gly-Ser	12	5,6
Arg-Ser-Ser-Val-Gly-Ser-Gln-Ser	15	3,4

A trend in decreasing dissociation constants can be observed until the hexapeptide, the octapeptide already has less affinity for estradiol. The selectivity was tested by determining how much testosterone was retained on the beads and comparing this with the values for estradiol. The higher R , the more selective the peptide is for estradiol over testosterone. It seems that after the tetrapeptide, the selectivity declines.

Because of their good selectivity and affinity properties, the beads containing the tetrapeptide were selected to be packed into a pre-concentration column. This was tested on a mixture of natural and synthetic hormones and good recoveries were obtained.

To summarise this chapter, it can be said that in search for a new, selective SPE material, a trend is visible towards synthetic systems that are more robust and furthermore are useful for the simultaneous determination of more than one compound (multi residue method). However, a real rational design for a receptor that can selectively entrap EDCs is still missing.

II.3. Rationally designed artificial receptors

The solid phase extraction materials like the MIPs and the Tozzi peptides are examples of systems synthesised in a random manner. Once the monomers are selected to make an MIP, a random equilibrium is generated between the template and the functionalised monomers. Although there is a 3D structure formed upon polymerisation, this cavity is not designed (nor does anybody know how it looks). Randomness also played a great role in the development of the Tozzi peptides. All the possible combinations were made and then the best one was selected. No effort was made in trying to characterise the nature of the interactions and so, no lessons could be learned from it.

Another approach to make artificial receptors relies more on the rational design of a molecule. Such a rationally designed molecule should contain the right functional groups that allow binding of the target. When these functionalities are organised in a specific orientation, a cavity can be formed in which the target can fit.

The design of artificial receptors that can bind a target in water still remains quite challenging. Although electrostatic interactions, such as ion pairs or H-bonds, are important for imposing selectivity in supramolecular complexes, they are weakened in water because of competitive solvation by the polar water molecules.

In the next chapter, the progress that has been made in designing such receptors is presented. Some attention is also paid to how the [receptor-target] complex is characterised.

II.3.1. One-armed receptors

A lot of pioneering work in the field of one-armed receptors has been carried out by Schmuck.⁵³ His group focuses on the recognition of small peptides in water. As the binding site for the tetrapeptide's carboxylate, a cationic guanidiniocarbonylpyrrole moiety was used (**Figure II.11**). Additional interaction sites in the form of a linear tripeptide unit were attached. The peptidic nature of the receptor allowed the formation of a hydrogen bonded antiparallel β -sheet with the backbone of target peptide. Based on this receptor design, a combinatorial receptor library was synthesised on Tentagel.

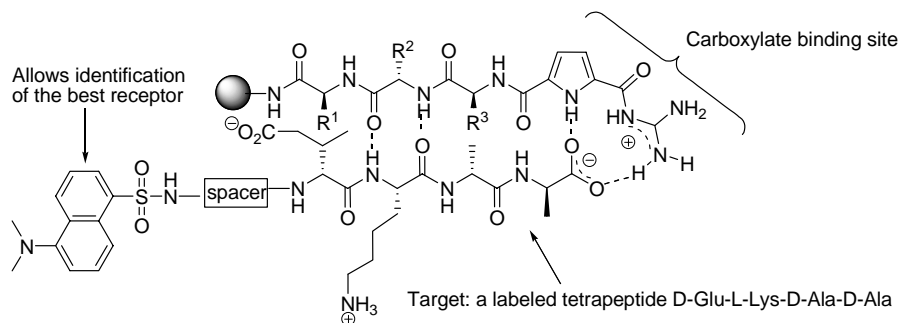


Figure II.11: Schematic representation of complex formation of a library member with the target tetrapeptide D-Glu-L-Lys-D-Ala-D-Ala.

The best receptor of the library was identified by labelling the target compound with the fluorescent Dansyl group. The peptide sequence of this receptor was deciphered to be Lys-Lys-Phe.

The binding strength of the complex was determined via UV titrations in water. The UV absorbance of the pyrrole ring was monitored while increasing amounts of the unlabeled tetrapeptide were added. From these data a K_d of 65 μ M was obtained.

⁵³ a) Schmuck, C.; Heil, M. *Chem. Eur. J.* **2006**, *12*, 1339-1348. b) Schmuck, C.; Rupprecht, D.; Wienand, W. *Chem. Eur. J.* **2006**, *12*, 9186-9195. c) Schmuck, C.; Rupprecht, D.; Junkers, M.; Schrader, T. *Chem. Eur. J.* **2007**, *13*, 6864-6873.

Selectivity was tested by determining the K_d for the receptor and the reversed tetrapeptide Ala-Ala-Lys-Glu which was only 208 μM .

With the design of this receptor, two strategies were combined. The first one was the rational design of the carboxylate binding motif. This was then combined with the random generation of different structures via combinatorial chemistry. Although no cavity around the target peptide was formed, a receptor consisting of only one arm was obtained that showed some selectivity.

II.3.2. Tweezers

In attempt to create receptors with a cavity like structure, two-armed receptors or tweezers were designed. The structure of such a dipodal group consists of a scaffold which is conformationally restricted and directs, or pre-organises the functionalised receptor arms.

Figure II.12 shows two frequently used scaffolds. Structure **II.1** is based upon the cholic acid skeleton which has a very rigid, predefined structure.⁵⁴ The two built in arms are directed in a parallel orientation. The carboxylic acid function was used to couple the scaffold to a Tentagel solid support, allowing the generation of a combinatorial library.

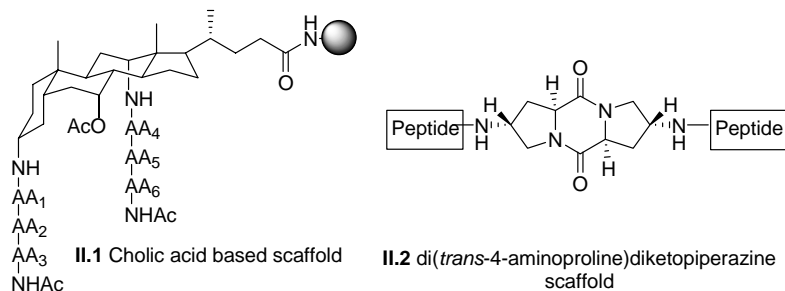


Figure II.12: Dipodal scaffolds or tweezers.

⁵⁴ Barry, J. F.; Davis, A. P.; Perez-Payas, M. N.; Elsegood, M. R. J.; Jackson, R. F. W.; Gennari, C.; Piarulli, U.; Gude, M. *Tetrahedron Lett.* **1999**, *40*, 2849-2852.

Using this dipodal scaffold our group has mimicked the cavity of a protease enzyme that could hydrolyse an ester bond.⁵⁵ Because its predefined structure it is currently also being used for the synthesis of epitope mimics of the measles virus.⁵⁶

Dipodal scaffold **II.2** is based on a diketopiperazine skeleton. Though this backbone is less rigid than the cholic acid derived scaffold **II.1**, X-ray analysis showed that the two peptide arms were pointing in the same direction, forming a cavity that was able to recognise small peptides.⁵⁷ To determine which small peptide was a suitable target for a receptor, the receptor molecules were labelled with a disperse red dye. The labelled receptors were then added to a combinatorial library of small peptides. After incubation, the beads were washed and those that stayed red, contained a peptide that was a suitable target for the tested receptor.

II.3.3. Tripodal scaffolds

The next logical step towards a better cavity for the molecular recognition of target molecules is the development of a three-armed or tripodal scaffold. In this way, the target can be captured by three arms, providing more coverage of the molecular surface of the target.

⁵⁵ De Muynck, H.; Madder, A.; Farcy, N.; De Clercq, P. J.; Perez-Payan, M. N.; Ohberg, L. M.; Davis, A. P. *Angew. Chem. Int. Ed.* **2000**, *39*, 145-148.

⁵⁶ Bode, C. A.; Muller, C. P.; Madder, A. *J. Pept. Sci.* **2007**, *13*, 702-708.

⁵⁷ Wennemers, H.; Nold, M. C.; Conza, M. M.; Kulicke, K. J.; Neuburger, M. *Chem. Eur. J.* **2003**, *9*, 442-448.

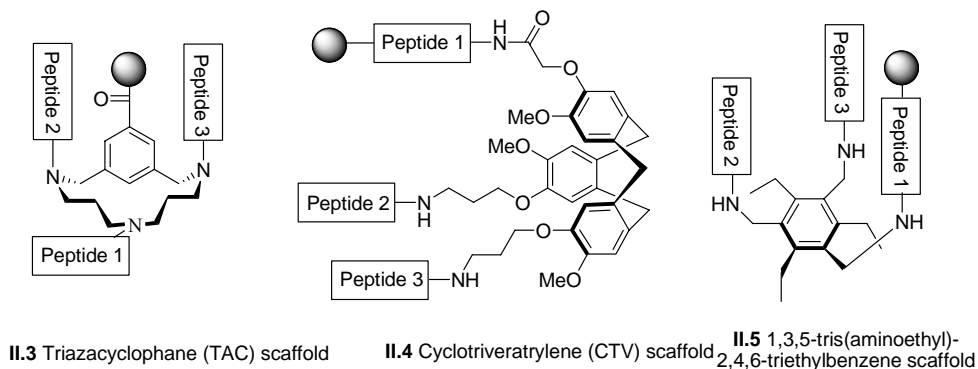


Figure II.13: Tripodal scaffolds.

In the recent years, a lot of tripodal scaffolds have been designed of which the most important ones are represented in **Figure II.13**.⁵⁸ All three of them allow the incorporation of three different peptide chains that are pointing in the same direction. The TAC scaffold **II.3** has an extra functionality that acts as an anchoring point to the solid phase. With **II.4** and **II.5**, the first one of the three peptide arms has to be synthesised on solid phase, after which the scaffold can be coupled and the two other arms can be constructed.

Scaffolds **II.3** and **II.4** have been designed and used by Liskamp in the search for a receptor for the dipeptides D-Ala-D-Ala.⁵⁹ This dipeptide is a precursor for the bacterial cell wall. Consequently, receptors that are able to bind the dipeptide, can play an important role in the next generation of antibiotics. Based on these two scaffolds, large combinatorial libraries were generated and screened for affinity against the D-Ala-D-Ala sequence. With the TAC backbone, a library of 46656 members was screened by adding a labelled peptide to the beads. The CTV based library consisted of 2197 possible receptors and the most active one was selected by screening with the same

⁵⁸ Guarise, C.; Zaupa, G.; Prins, L. J.; Scrimin, P. *Eur. J. Org. Chem.* **2008**, 3559-3568.

⁵⁹ a) Chamorro, C.; Hofman, J. W.; Liskamp, R. M. J. *Tetrahedron* **2004**, 60, 8691-8697. b) Chamorro, C.; Liskamp, R. M. J. *Tetrahedron* **2004**, 60, 11145-11157.

labelled target as depicted in **Figure II.14**. In both cases, the screening was performed in an aqueous buffer which resulted in a few positive hits. By using different fluorescent labels, it was shown that the reporter group had a profound, albeit not decisive influence on the binding by the receptor. After identification of the active receptors, they were tested for inhibition of bacterial growth, but no inhibition was observed. No attempt was made to determine K_d values.

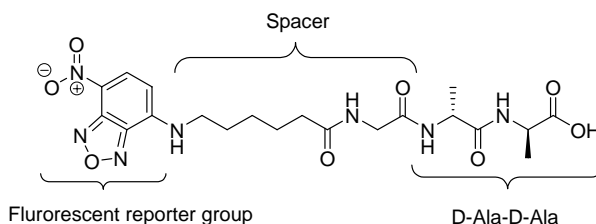


Figure II.14: Labelled D-Ala-D-Ala.

Scaffold **II.5** was employed by Schmuck for the synthesis of a receptor for carbohydrates in water.⁶⁰ Carbohydrates represent difficult substrates for recognition in water, as their dominant functional group (the OH group) is difficult to distinguish from water molecules. Nevertheless, a prototype was synthesised that showed weak affinity ($K_d \sim 357 \mu\text{M}$) towards an adenosine monophosphate (AMP) molecule. Binding constants were obtained by adding increasing amounts of AMP to the receptor and monitoring the decrease in absorbance. A further improvement of binding capacities might be achieved by varying the amino acid substituents. For this purpose, a combinatorial approach is currently under research by the group of Schmuck.

Having some experience with tweezers, our group decided to explore the possibilities of tripodal scaffolds and see if the cavity of a protease enzyme could be better mimicked in this way.

⁶⁰ Schmuck, C.; Heller, M. *Org. Biomol. Chem.* **2007**, 5, 787-791.

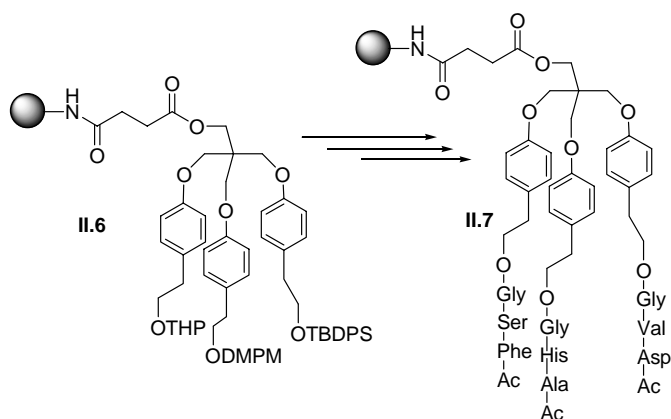


Figure II.15: A tripodal scaffold with a flexible but preorganised geometry.

The scaffold **II.6** in **Figure II.15** was designed starting from a flexible pentaerythritol backbone to which three different protected aromatic moieties were attached.⁶¹ Though the aromatic interactions between these three cores keep the attached chains together, the molecule still is flexible enough to be able to cope with targets of different sizes.

After the synthesis, the scaffold was tested by synthesising one member of a library of possible protease mimics. During synthesis, however, some problems arose due to the instability of the scaffold against certain deprotection conditions. It appeared that the benzylic ethers were stable neither against conditions used for the deprotection of the alcohol functions nor against conditions to deprotect the side chains of the amino acids. The employed acidic conditions also led to the loss of one or more of the arms. Although the conditions for the synthesis of one library member were carefully optimised, a full library was never made.⁶²

⁶¹ Farcy, N.; De Muynck, H.; Madder, A.; Hosten, N.; De Clercq, P. J. *Org. Lett.* **2001**, 3, 4299-4301.

⁶² Gea, A.; Farcy, N.; Rossell, N. R. I.; Martins, J. C.; De Clercq, P. J.; Madder, A. *Eur. J. Org. Chem.* **2006**, 4135-4146.

Based upon these literature results and upon previous experience in the lab with dipodal and tripodal scaffolds, the notion grew that in order to arrive at an efficient receptor for EDCs, a tripodal scaffold could be useful for obtaining a binding cavity for EDCs.

III. Project aim and objectives

The main aim of this PhD is the development of a new artificial receptor for endocrine disrupting chemicals. Once attached to a solid support, this receptor can be used to pre-concentrate EDCs, allowing a more accurate and sensitive determination of EDCs in different environmental samples. In this way, this project could help to fill some current data gaps about EDCs in our environment, leading to a better understanding of the effects of EDCs on human health.

A biomimetic approach will be used in the construction of EDC receptors. Based on the knowledge that most EDCs directly exert their effect through binding with the ER, the cavity of the hormone binding domain of the hER will be mimicked. Building the key amino acids of the hormone binding domain of the hER into the flexible, but preorganised structure **III.1** allows to build such a system in a combinatorial way. For this purpose, quantities of the scaffold will be required and thus an efficient synthesis for tripodal scaffold **III.1** has to be developed. Once synthesised, the scaffold has to be coupled to a suitable solid phase, and protocols for the independent incorporation of three different peptide chains have to be established.

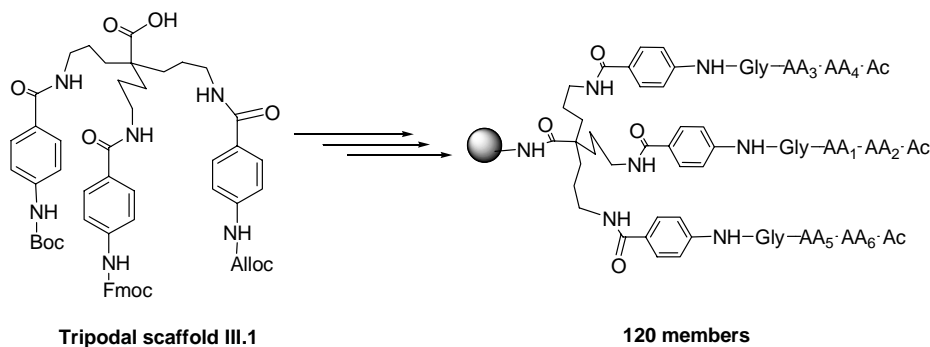


Figure III.1: Library of possible estrogen receptor mimics.

Molecular diversity will be created by using automated solid-phase peptide synthesis (SPPS). In this way a parallel library of 120 possible estrogen receptor mimics will be created. These first generation receptors will be screened for affinity towards a few

selected estrogenic chemicals. For this screening, a close collaboration with the laboratory of separation sciences of Prof. Dr. P. Sandra will be set up. Once the best receptor is identified, an attempt will be made to characterise the nature of the [target-receptor] complex. Lessons learned from these preliminary studies will be used to design a second generation of possible receptors with improved binding affinities.

Finally, the optimised receptor will be coupled to a solid support that will then be packed into a SPE cartridge. This cartridge will be evaluated in the analysis protocol of aqueous samples and compared with commercially available SPE materials. In this way, we hope to obtain an improved enrichment and selectivity.

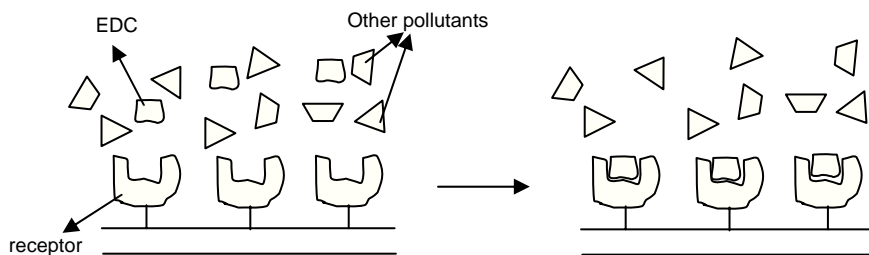
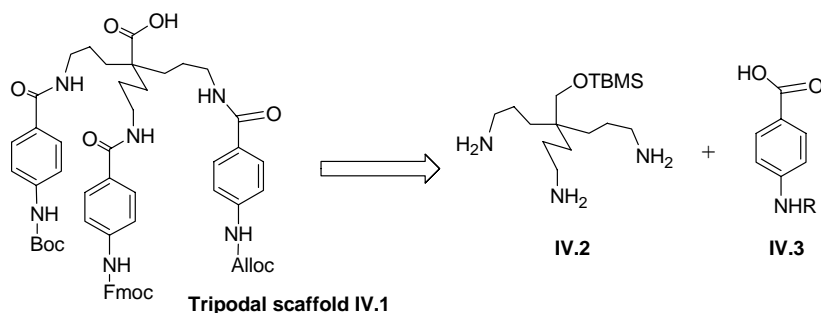


Figure III.2: Development of EDC selective SPE material.

IV. Synthesis of hER mimics

IV.1. Synthesis of the tripodal scaffold

The design of new artificial receptors requires a suitable scaffold that allows incorporation of various chemical functionalities and at the same time pre-organises the different incorporated residues. Based on previous experiences, tripodal structure **IV.1** (Scheme IV.1) was designed.



Scheme IV.1: Retrosynthetic analysis.

The scaffold consists of a flexible triamine core **IV.2** and three differently protected *p*-aminobenzoic acid derivatives **IV.3**. Pre-organisation of the three arms is possible due to the π - π interactions between the three aminobenzoic cores. By starting from a flexible backbone, the receptor will be able to recognise different which may that can vary in size. Hence, this flexible but pre-organised scaffold is a suitable starting point for the synthesis of receptors that can be used for pre-concentration in a multi residue analysis method.

The parallel orientation of the three arms was indicated by modelling studies using MacroModel V.6.0 (force field MM2). To reduce calculation times, the carboxylic acid was replaced by a methyl group and the three different amine protecting groups were simplified as acetyl groups. **Figure IV.1** shows the two most energetically favoured conformations in water. Extra stabilisation is achieved via hydrogen bonding,

represented by the dotted lines. From these modelling studies it can be deduced that some conformational freedom is possible, but a parallel orientation of the three arms is dominant.

Another feature of the scaffold is the carboxylic acid head group that will function as an anchoring point, allowing attachment to a solid support. In this way, solid-phase peptide synthesis protocols can be employed in a manual or automated fashion. This

has the advantage that for each reaction, a large excess of reagents can be used, driving the reaction to completion and enabling fast reaction kinetics. When the reaction has finished, the excess of reagents can simply be washed away.

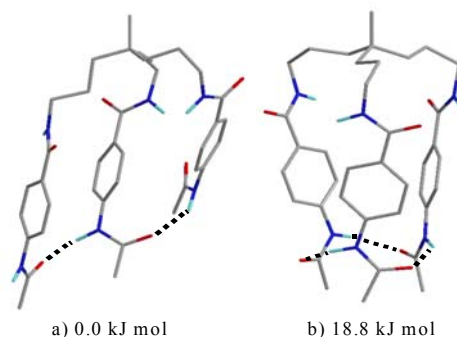
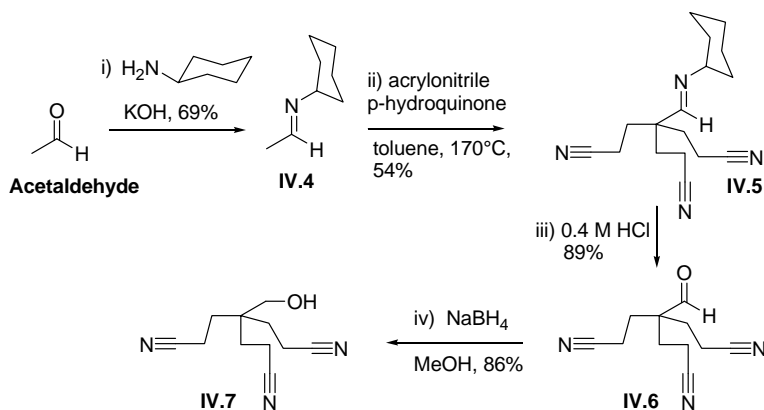


Figure IV.1: Two most energetically favoured conformations of a simplified version of IV.1 in water

IV.1.1. Synthesis of the triamine core

Thanks to the work of Dr. An Gea, a great deal of the building blocks for the triamine core were already available in the lab. Starting from acetaldehyde, she prepared multi gram quantities of the alcohol **IV.7** via a previously described method.⁶³

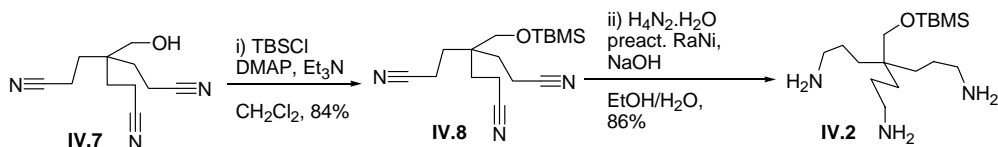
⁶³ Imbert, D.; Thomas, F.; Baret, P.; Serratrice, G.; Gaude, D.; Pierre, J.L.; Laulhère, J.P. *New. J. Chem.* **2000**, *24*, 281-288.



Scheme IV.2: Synthesis of alcohol IV.7

After protection of the aldehyde with cyclohexylamine (**Scheme IV.2**), the 1,4-addition on acrylonitrile was performed in an autoclave at a temperature of 170 °C. To prevent any radical polymerisation of acrylonitrile, some *p*-hydroquinone was added to trap unintentionally formed radicals. The addition product was subsequently hydrolysed and the resulting aldehyde reduced with NaBH₄ to give the alcohol **IV.7**.

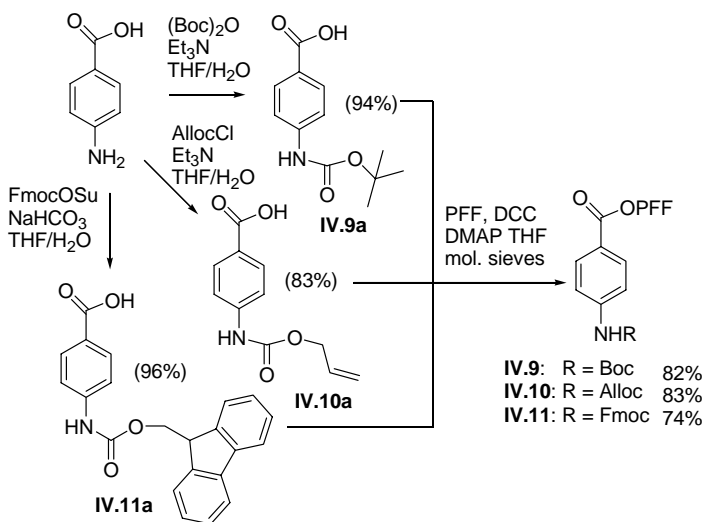
Scheme IV.3 shows the synthesis of the triamine backbone starting from this alcohol. First a *t*-butyldimethylsilyl (TBS) group was introduced. Next, the nitriles were reduced but this reaction did not proceed smoothly. Although according to the published procedure, complete nitrile reduction should be achieved using hydrazine in the presence of preactivated RaNi-catalyst, TLC-monitoring showed the reduction not to be fully complete, with some mono- and di-nitriles still present. Changing the reaction variables and the type of catalyst did not result in a significant improvement. However, the crude product could be used as such and the impurities could be removed on a later stage in the synthesis.



Scheme IV.3: Protection of the alcohol and subsequent reduction of the nitriles.

IV.1.2. Synthesis of the arms

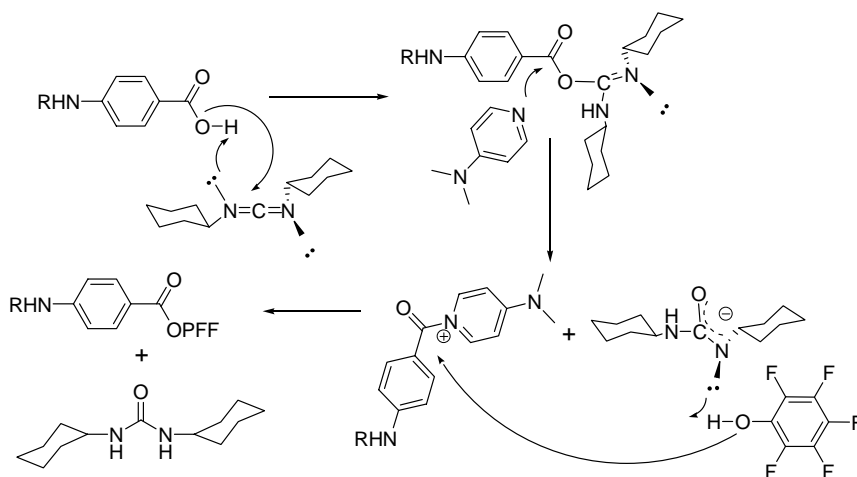
The three different aromatic moieties were synthesized starting from 4-aminobenzoic acid. The aromatic amines were protected as carbamates. An acid labile (Boc), Pd⁰ labile (Alloc) and base labile (Fmoc) protecting group were chosen to ensure complete orthogonality during later attachment of the three different peptide chains.⁶⁴ Protection of the amines proceeded in all cases smoothly, the products were easily purified by acidifying the solution and collecting the precipitate (**Scheme IV.4**).



Scheme IV.4: Synthesis of the protected arms.

⁶⁴ Mu, F.; Coffing, S.L.; Riese, D.J.; David, J. *J. Med. Chem.* **2001**, *44*, 441-452

Before the arms were coupled to the triamine **IV.2**, they were first pre-activated as their pentafluorophenol (PFP) esters. This was achieved via a condensation between PFF and the three acids using DCC as a coupling reagent and DMAP as a nucleophilic catalyst (**Scheme IV.5**). The products were purified from the DMAP and the urea side product by column chromatography. The yield for the Fmoc-derivative was a little lower due to an extra crystallisation step necessary to remove some remaining urea side product.

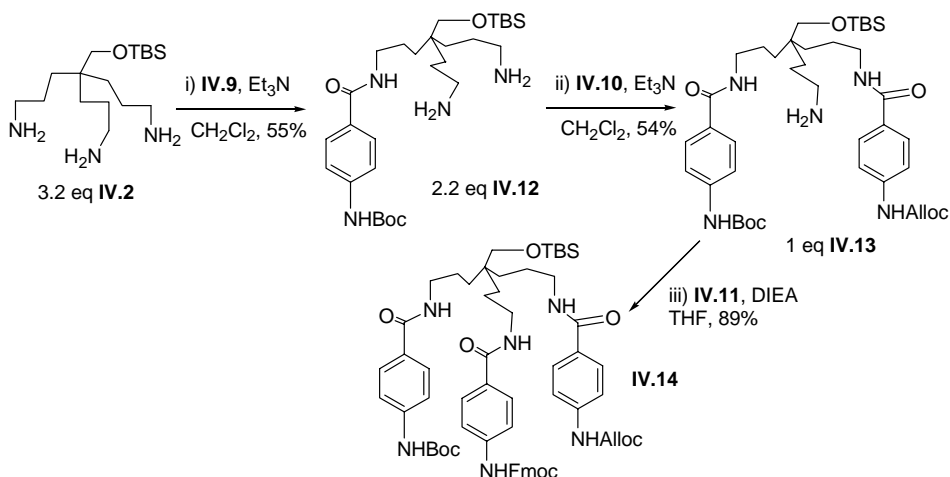


Scheme IV.5: Mechanism of activation with DCC using DMAP as a catalyst.

IV.1.3. Coupling of the arms to the triamine backbone

In general, the synthesis of tripodal structures is a challenging, sometimes frustrating quest because differentiation of three equal functionalities requires the use of an excess of starting material. Thus, in order to maximize the yield of mono derivatisation in the first step of **Scheme IV.6**, 3.2 equivalents of triamine **IV.2** were used and activated **IV.9** was added over a period of 8 h. Separation of the monopodal product from the excess starting material and the side products was achieved via chromatography using a DCM/MeOH/NH₃ mixture. The second aromatic residue **IV.10** was added over a period of 8 h to a solution of 2.2 equivalents of the monopodal **IV.12**. Also in this case, the

desired dipodal product **IV.13** was isolated via chromatography with DCM/MeOH/NH₃. For the coupling of the last Fmoc arm **IV.11**, only one equivalent of dipodal **IV.13** was necessary and since all the amines were acylated, the chromatographic separation with a DCM/MeOH mixture was much easier.

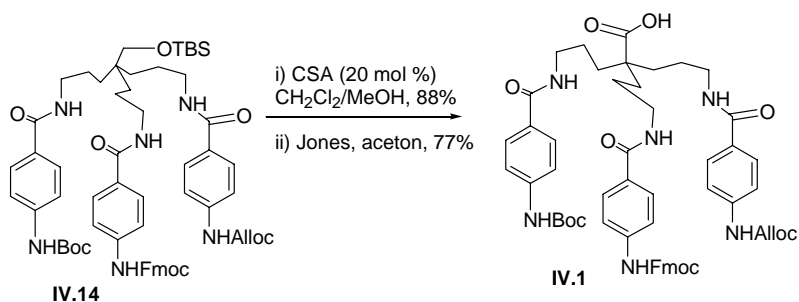


Scheme IV.6: Coupling of the arms.

IV.1.4. Establishing the anchor point

Silyl ethers can be deprotected using either strong nucleophiles or acidic conditions. Good nucleophiles in this context are the MeO⁻ and the F⁻ anion. These are however also basic enough to cause Fmoc deprotection. Therefore, the deprotection of the silyl ether had to be done under acidic conditions, without removing the acid labile Boc group (**Scheme IV.7**). This was achieved with catalytic amounts of (±)-camphor sulphonic acid (CSA)⁶⁵ and only a very small amount of Boc deprotection (< 1%) was observed.

⁶⁵ Garcia-Rubio, S.; Meinwald, J. *J. Org. Chem.* **2001**, *66*, 1082-1096.



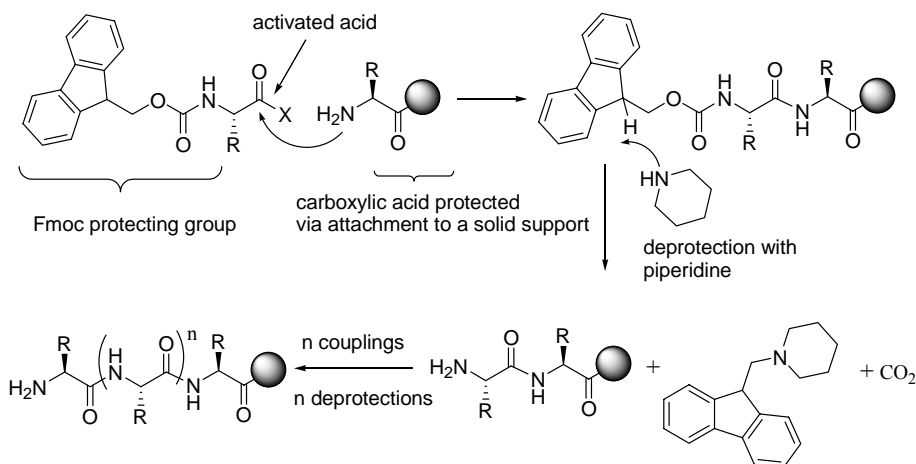
Scheme IV.7: Deprotection and oxidation.

Finally, oxidation to the carboxylic acid **IV.1** was carried out using Jones reagent. In total, an amount of 4.5 g of **IV.1** was synthesised, which proved to be sufficient for the rest of the PhD.

IV.2. Solid phase synthesis of possible EDC receptors

IV.2.1. Synthetic and analytical strategies

To create a cavity that can encompass different endocrine chemicals, small peptide strands have to be incorporated into scaffold **IV.1**. This implies the repeated formation of amide bonds between amino acids (AAs). The condensation between two amino acids is only possible if one of the carboxylic acid functions is activated, enabling nucleophilic attack of the amine function of the other amino acid. This means that the correct protecting groups have to be employed to avoid undesired side reactions.



Scheme IV.8: Solid phase peptide synthesis.

Scheme IV.8 shows the principles of solid phase peptide synthesis or SPPS according to the Fmoc strategy. The first AA is attached to the solid phase via its carboxylic acid. In this way, the carboxylic acid is protected and no activation can occur during the peptide coupling. Moreover, after the condensation, the excess of reagents can be filtered away while the product stays behind on the resin, making time-consuming chromatographic separations unnecessary. The α -amino group of the AA

that is built into the peptide chain is protected as a carbamate. Consequently, when activating the acid, no homopolymerisation can occur.

Amino acids are building blocks of nature, which has provided them with a great diversity of chemical functions, incorporated in their side chains. When the side chains contain nucleophilic or electrophilic groups, these need to be properly protected to avoid any side reactions during the coupling of the next AA. With the Fmoc/*t*Bu strategy, the N- α group is protected with a base labile Fmoc group and the side chains with acid labile groups, ensuring orthogonality during the synthesis. Deprotection of the side chains is usually performed with a mixture of trifluoroacetic acid (TFA) and various nucleophiles, called scavengers, that neutralise the formed cations.

The selection of a suitable solid support can have a big influence on the synthesis outcome. Crucial properties of the solid phase include good physical and chemical stability as well as good swelling of the resin in solvents used for peptide synthesis. Gel type resins possess all of these qualities and are the most used in SPPS. The structures of some of the frequently used resins are shown in **Figure IV.2**.

The two most known examples are the classic Merrifield resin and Tentagel resin. Both consist of a polystyrene framework that is crosslinked with 1 or 2 % divinylbenzene. With Tentagel, extra polyethyleneglycol chains are grafted onto this network, rendering the resin more compatible with polar solvents like water.⁶⁶

Resins that do not consist of a large hydrophobic core are represented by PEGA and CLEAR. The first one is based on acrylamide monomers cross linked with polyethylene glycol chains, resulting in a very polar resin that has good swelling properties. Due to the presence of the amide bonds, a peptide like environment is created which is thought to be beneficial for peptide synthesis.⁶⁷ CLEAR, on the other hand, consists of ester linkages with a high degree of cross linking and a high percentage of polyethylene

⁶⁶ Adams, J. H.; Cook, R. M.; Hudson, D.; Jammalamadaka, V.; Lyttle, M. H.; Songster, M. F. *J. Org. Chem.* **1998**, *63*, 3706-3716.

⁶⁷ Atherton, E.; Clive, D. L.; Sheppard, R. C. *J. Am. Chem. Soc.* **1975**, *97*, 6584-6585.

glycol chains. Consequently, the polar resin shows a high degree of swelling in especially polar solvents including water.⁶⁸

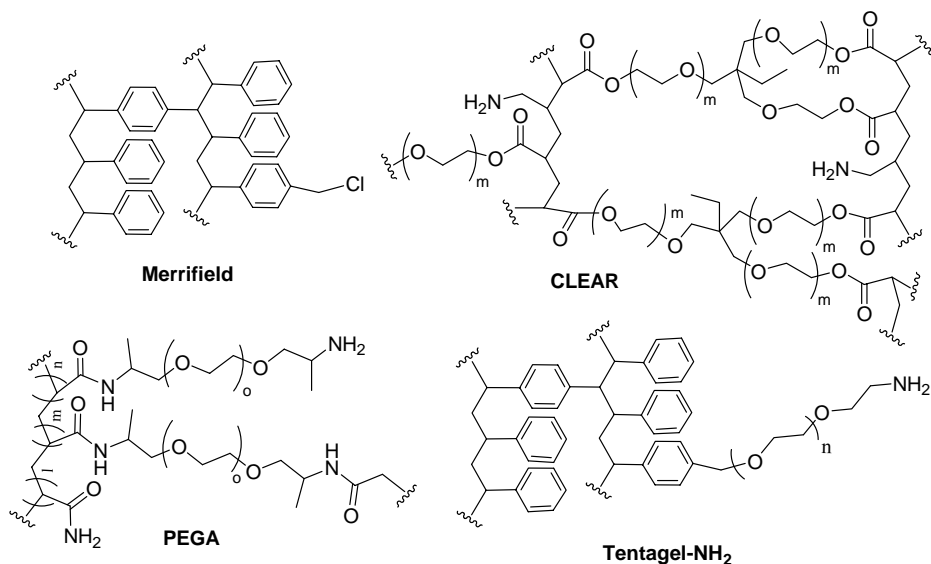


Figure IV.2: Structures of Merrifield, Tentagel, PEGA and CLEAR.

Based on previous expertise in the lab, Tentagel was chosen as the solid support for the synthesis of the receptors. Due to its reported good swelling properties in water,⁶⁹ an on-bead screening of the receptors for the affinity towards EDCs is possible.

For the synthesis of linear peptide chains, the Merrifield support was chosen. This resin has a high loading and moreover, it is available with a variety of linkers that allow attachment of the first AA to the resin and cleavage of the final peptide from the resin. For this purpose, the acid labile linkers like the 2'-chlorotrityl linker (**Figure IV.3**) are very popular. With the 2'-chlorotrityl linker, the peptide can be cleaved from the resin

⁶⁸ Kempe, M.; Barany, G. *J. Am. Chem. Soc.* **1996**, *118*, 7083-7093.

⁶⁹ Santini, R.; Griffith, M. C.; Qi, M. *Tetrahedron Lett.* **1998**, *39*, 8951-8954.

as a fully, side chain protected segment,⁷⁰ or the cleavage of the peptide can be combined with the deprotection of the side chains.

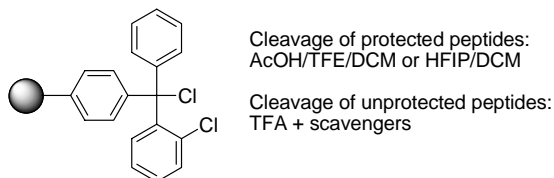
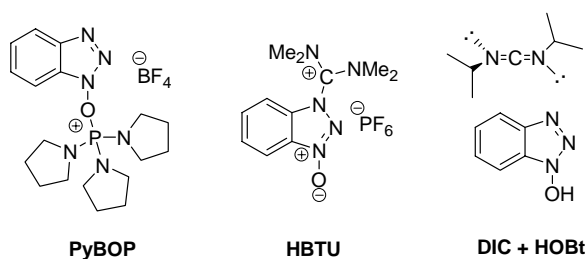


Figure IV.3: 2'-chlorotrityl resin.

A carboxylic acid can be activated using a plethora of methods and strategies.⁷¹ Usually, an intermediate active oxobenzotriazole ester (OBt ester) is formed by mixing the acid with an appropriate activating agent. The reagents routinely used in our lab are depicted in Scheme IV.9. The most reactive agents are PyBOP, a phosphonium based coupling reagent, and HBTU, an uronium based agent, and are used in the presence of a base like DIEA. The more classical carbodiimide based couplings are somewhat slower but represent a useful alternative if base free circumstances are necessary.

⁷⁰ a) Barlos, K.; Gatos, D.; Kallitsis, J.; Papaphoti, G.; Sotiriu, P.; Wenging, Y.; Schäfer, W. *Tetrahedron Lett.* **1989**, *30*, 3943-3945. b) Bollhagen, R.; Schmiedberger, M.; Barlos, K.; Grell, E. *J. Chem. Soc., Chem. Commun.* **1994**, 2559-2561.

⁷¹ Montalbetti, C.; Falque, V. *Tetrahedron* **2005**, *61*, 10827-10852.



Scheme IV.9: Coupling reagents.

Before further chain elongation can occur, the N- α protecting group has to be removed. By adding a secondary amine like piperidine to the resin, the base labile Fmoc group is deprotected, giving rise to fulvene and carbamic acid (**Scheme IV.8**). While the carbamic acid dissociates in CO_2 and the free amine, the fulvene undergoes a 1,4-addition by the excess of piperidine. The concentration of the formed complex can be determined by UV measurements and correlated to the amount of product on the resin.

Another way of monitoring reactions on bead is cleaving the peptide from the resin and analysing the cleavage solution via LC/MS. With acid labile linkers this is rather difficult, because the scavengers present in the cleavage cocktail can interfere with the analysis and each time a fresh cleavage solution should be prepared. In order to facilitate monitoring of reactions on solid support, a photocleavable linker (**Figure IV.4**) was used which releases the product upon irradiation at 365 nm.⁷² Only small amounts of resin are needed (typically 1 mg or less) and the solution obtained upon irradiation can be directly analyzed by LC-ES-MS. Using the photocleavable linker, in some cases yellow coloration of the solid support was observed, lowering the sensitivity of the TNBS-test (*vide infra*). This problem could be circumvented by using the NF31-test which has a higher sensitivity.

⁷² Holmes, C.P. *J. Org. Chem.* **1997**, 62, 2370-2380

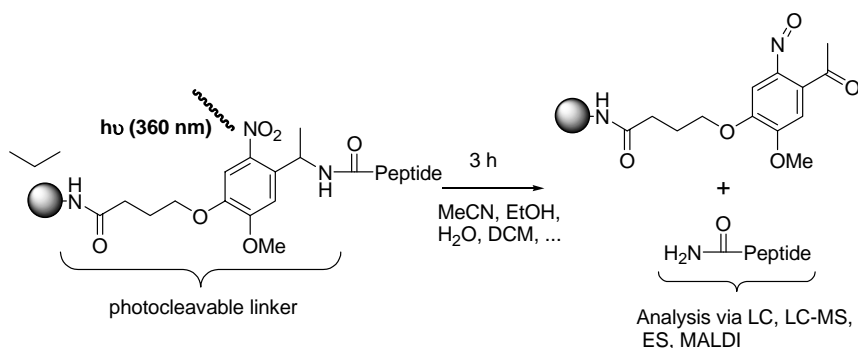
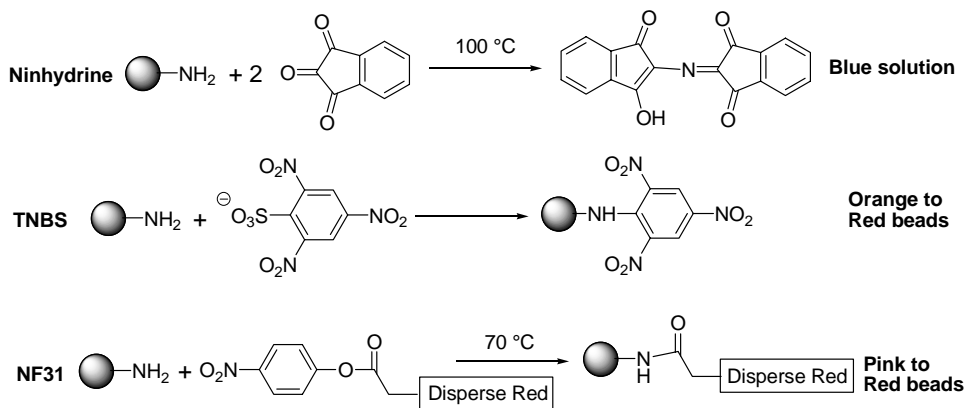


Figure IV.4: Photocleavable linker.

For very fast routine assessment of the completeness of a coupling reaction, colour tests are used. (Scheme IV.10). An incomplete coupling results in free amine functionalities on the beads. These can be detected with various reagents giving an intense colour after reaction with the amines.⁷³ One of these colour tests, NF31,⁷⁴ was developed in our lab. This very efficient reagent is currently available via Bachem.



Scheme IV.10: Colour tests for the detection of amines.

⁷³ a) Hancock, W. S.; Battersby, J. E. *Anal. Biochem.* **1976**, *71*, 260-264. b) Sarin, V. K.; Kent, S. B. H.; Tam, J. P.; Merrifield, R. B. *Anal. Biochem.* **1981**, *117*, 147-157.

⁷⁴ Madder, A.; Farcy, N.; Hosten, N.; De Munck, H.; De Clercq, P.J.; Barry, J.; Davis, A.P. *Eur. J. Org. Chem.* **1999**, *11*, 2787-2791.

IV.2.1.1. Fast and easy detection of aromatic amines on solid support

Once scaffold **IV.1** is coupled to a solid phase, the protecting groups have to be removed to allow the incorporation of different peptide chains. Deprotection of the carbamates provides an aromatic amine that is subsequently acylated with the desired amino acid. Monitoring of the completeness of this coupling reaction by colour tests has proven to be very difficult. The two most commonly used colour tests, the ninhydrine and TNBS test, are not applicable in case of aromatic amines. To date, only the so called chloranil test has been reported to monitor the progress of these reactions with high sensitivity.⁷⁵ During this Phd, the NF31 test was established as a reliable method for the on bead detection of primary aromatic amines.⁷⁶

In order to tackle the sensitivity issue, mixtures of Fmoc-Gly-OH and Boc-Gly-OH were coupled in varying ratios to Tentagel (loading 0.21 mmol/g) using the PyBOP /DIPEA protocol. After selective Fmoc deprotection with 20 % piperidine in DMF, Fmoc-protected *p*-aminobenzoic acid (Fmoc-*p*-Abz) was coupled using PyBOP and DIPEA. The amount of Fmoc-*p*-Abz on the resin was determined by the previously described method, giving values of 3.4, 13 and 18 $\mu\text{mol g}^{-1}$. Finally the Fmoc-group was deprotected with a 20% piperidine/DMF solution.

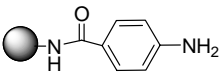
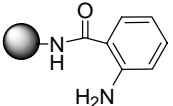
In order to check if the sensitivity of the colorimetric tests is influenced by sterical hindrance we further prepared resin loaded with 5.4 and 11 $\mu\text{mol g}^{-1}$ of *o*-Abz in the same manner.

The resins were treated with a 0.002 M solution of NF31 in acetonitrile and heated at 70°C for 10 min. The results are summarized in **Table IV.1**.

⁷⁵ Marik, J.; Song, A.; Lam, K. S. *Tetrahedron Lett.* **2003**, *44*, 4319-4320.

⁷⁶ Van der Plas, S. E.; De Clercq, P. J.; Madder, A. *Tetrahedron Lett.* **2007**, *48*, 2587-2589.

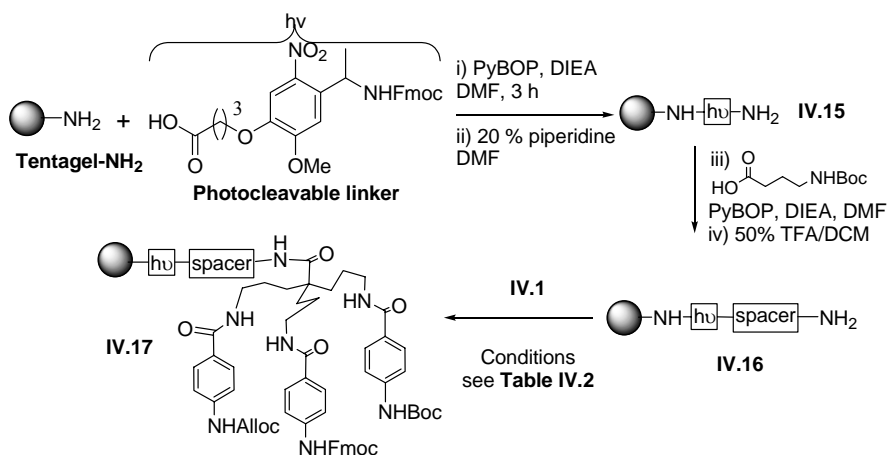
Table IV.1: Detection of resin bound aromatic amines with NF31. Tentagel resin (loading 0.21 mmol/g) was used in these experiments. A single plus indicates that it still is possible to observe the free amines. The ++ indicates a strong coloration of the beads.

	Resin substitution ($\mu\text{mol g}^{-1}$)	Result
	3.4 (~2%)	+
	13 (~5%)	++
	18 (~9%)	++
	5.4 (~3%)	+
	11 (~5%)	++

In conclusion reagent NF31 offers a simple and sensitive test for the monitoring of coupling reactions to free aromatic amines during solid phase synthesis. Previously validated for the monitoring of peptide coupling, the use of NF31 is now extended to the detection of free aromatic amines, rendering it a versatile and useful tool for the solid phase chemist.

IV.2.2. Coupling of scaffold IV.1 to a solid phase

The photocleavable linker was coupled to Tentagel (loading: 0.21 mmol/g) by activating the acid with PyBOP in the presence of DIEA (**Scheme IV.11**). Boc- γ -aminobutyric acid was used as a spacer to minimize sterical hindrance when performing coupling reactions to the secondary amine of **IV.15**. It was noted that the use of Fmoc- γ -aminobutyric acid led to undesired alkylation of the spacer upon Fmoc deprotection with piperidine.



Scheme IV.11: Coupling of the linker, spacer and scaffold to the resin.

Following Boc-deprotection, coupling of the scaffold **IV.1** to the solid support was first tested (**entry 1**, Table IV.2) using a five-fold excess of **IV.1** in the presence of PyBOP (5 eq) and DIEA (10 eq) for 3 h, yielding a loading of $0.077 \text{ mmol g}^{-1}$ (maximal theoretical loading is $0.176 \text{ mmol g}^{-1}$). LC control of the reaction mixture (**Figure IV.5**) showed that a small amount of Fmoc-deprotected compound was present. Taking into account the percentage of Fmoc deprotected compound (4 %), the total loading was 0.080 mmol/g . These experiments were repeated several times and the loading values were always between 0.077 and 0.084 mmol/g .

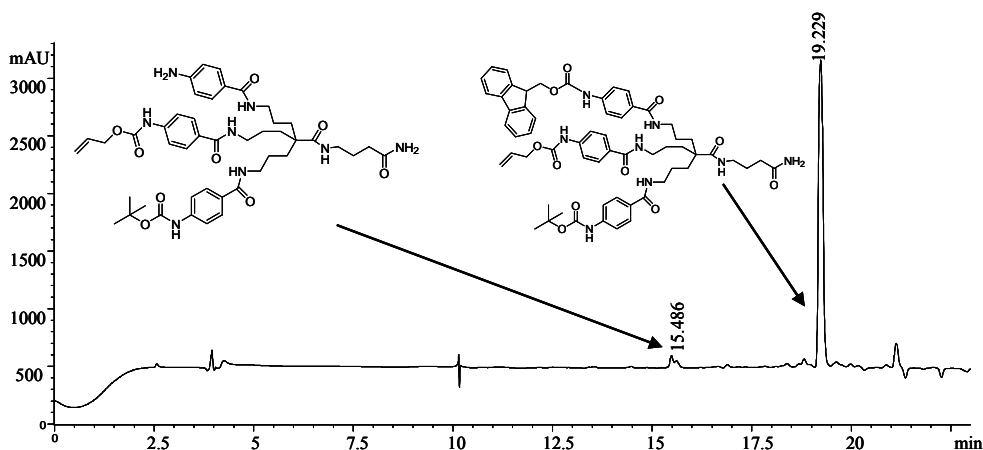


Figure IV.5: HPLC at 214 nm of IV.17 (entry 1, Table IV.2) after photocleavage in MeCN.

The efforts undertaken to optimise the coupling of **IV.1** are summarised in Table IV.2. In a first attempt to improve the coupling yield (**entry 2**), the more reactive N, N'-tetramethylfluoroformamidinium hexafluorophosphate (TFFH) was used as coupling reagent (**Figure IV.6**). By adding TFFH, the carboxylic acid is transformed to the corresponding acylfluoride. This reactive intermediate is known to give good results for the coupling of sterically hindered AA.⁷⁷ In our case however, no improvement was observed.

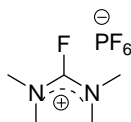


Figure IV.6: TFFH.

⁷⁷ Carpino, L. A.; Elfaham, A. *J. Am. Chem. Soc.* **1995**, *117*, 5401-5402.

Table IV.2: Optimisation of the coupling conditions.

Entry	Coupling reagent	IV.1 (eq)	DIEA (eq)	Coupling time (h)	T	Total loading (mmol/g)	Remarks
1	PyBOP	5	10	3	rT	0.077-0.086	Fmoc-depr.: 3 to 25%
2	TFFH	5	10	3	rT	0.084	Fmoc-depr.: 3 to 25%
3	PyBOP	6	12	3	rT	0.085	Fmoc-depr.: 3 to 25%
4	PyBOP	3	6	3	rT	0.100	Double coupling
5	DIC/HOAt	5	10	18	rT	0.084	Guanidine formation
6	HBTU	5	10	3	rT	0.082	Guanidine formation
7	PyBOP	5	15	3	rT	0.95-0.105	Fmoc-depr.: 3 to 25%
8	PyBOP	3	9	18	50 °C	0.085-0.100	up to 50% Fmoc depr.
9	PyBOP	1.5	4.5	18	50 °C	0.085-0.100	up to 50% Fmoc depr.
10	PyBOP	1.5	4.5	18	rT	0.085-0.104	Fmoc-depr.: 3 to 25%
11	DIC/HOAt	1.5	4.5	18	rT	0.059	Guanidine formation

Increasing the number of equivalents of **IV.1** (**entry 3**) did not result in a higher loading. A higher loading was observed after a double coupling (**entry 4**), using 3 equivalents for each coupling. In total, 6 equivalents are used, which is not very economical.

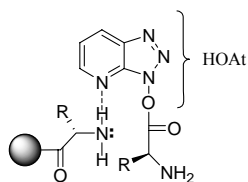
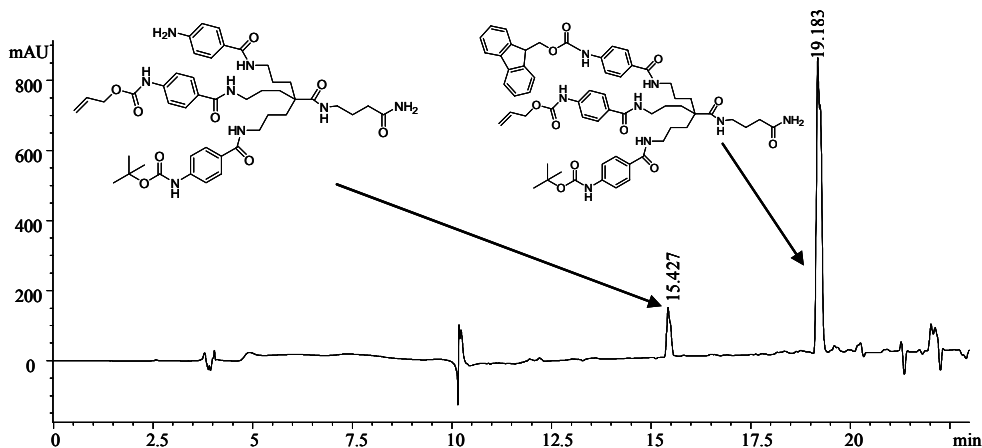


Figure IV.7: HOAt

The undesired removal of the Fmoc group could be prevented by using DIC in the presence of the coupling additive HOAt (**entry 5**), the more active variant of HOBt. By replacing the benzene ring with pyridine, reaction kinetics are enhanced by a neighbouring group effect.⁷⁸ After performing the coupling, the TNBS and NF31 colour test indicated that all the amines were acylated. Loading determination however, did not indicate a significantly higher loading. After photocleavage from the resin, the LC-MS analysis showed that the uncoupled spacer amines had attacked directly on the DIC resulting in the guanidilation of the molecule. A similar side reaction was observed with the coupling reagent HBTU (**entry 6**).

During one of the coupling experiments, 15 instead of 10 equivalents of DIEA were accidentally added. This apparently led to better loading values (**entry 7**). It was decided to use a scaffold/base ratio of 1:3. The amount of Fmoc deprotected compound did not seem to increase significantly under these circumstances (**entry 8**).

Figure IV.8: HPLC at 214 nm of IV.17 (**entry 10**) after photocleavage in MeCN.

⁷⁸ Carpino, L. A. *J. Am. Chem. Soc.* **1993**, *115*, 4397-4398.

It goes without saying that the less scaffold that is used for a coupling, the better it is. On the other hand, when lowering the number of equivalents, the overall concentrations drop because a minimum volume of solvent has to be used to ensure good swelling of the resin. This can be compensated by raising the temperature and prolonging the reaction time. Indeed, only 1.5 equivalents were needed to obtain the same loadings as with 5 equivalents (**entry 9**). These conditions were repeated at rT and it seemed that this was sufficient to get the same loading (**entry 10**). These circumstances were repeated but now with DIC in the presence of HOAt resulting however in a lower loading (**entry 11**).

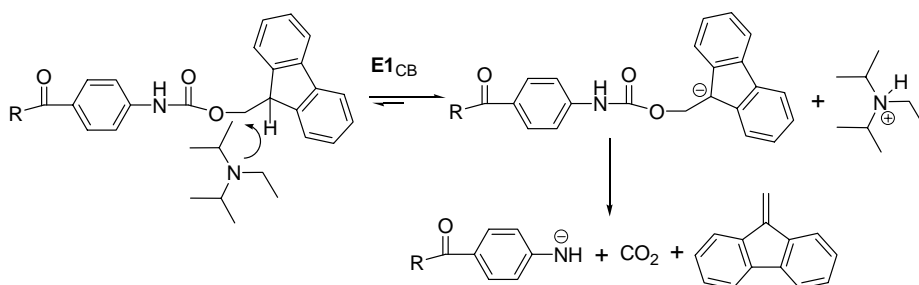
In conclusion, by activating only 1.5 equivalents of scaffold **IV.1** with PyBOP in the presence of 4.5 equivalents of DIEA, a loading of 0.085-0.104 mmol g⁻¹ was obtained, correlating with a coupling yield of 48 to 59%. The only problem associated with this reaction was the partial Fmoc removal during the coupling (**Figure IV.8**).

IV.2.3. Capping of the remaining spacer amines

The Fmoc deprotection occurring during the coupling was rather unexpected. Indeed, with standard coupling procedures, 2 equivalents of DIEA with respect to the activated AA, are classically added and no Fmoc deprotection is observed. The sterically hindered base is known to remove very small amounts of the Fmoc group only after prolonged reaction times (> 3 h).⁷⁹ In our case, it could be that the free amines the resin are acting as a base, but this option does not apply when the scaffold was activated with DIC in the presence of HOAt. Under these circumstances, no Fmoc deprotection was observed, even after a coupling time of 18 h. Therefore, it was concluded that Fmoc-aminobenzoic acid derivatives are more base labile than their aliphatic counterparts.

⁷⁹ Chang, C. D.; Waki, M.; Ahmad, M.; Meienhofer, J.; Lundell, E. O.; Haug, J. D. *Int. J. Pept. Protein Res.* **1980**, *15*, 59-66.

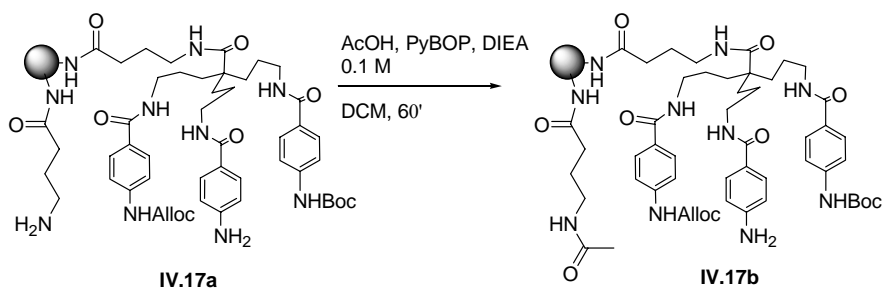
When looking at the mechanism of the Fmoc deprotection however⁸⁰ (**Scheme IV.12**), it is difficult to come up with a rational explanation. The rate determining step is the abstraction of the fulvene proton, so the reaction kinetics should not be influenced by the better leaving group capacities of the aminobenzoic acid. Probably, the electron withdrawing aminobenzoic acid influences the acidity of the fulvene proton but no proof of this theory was found in literature.



Scheme IV.12: Fmoc deprotection.

The attachment of the scaffold did not proceed in a 100 % yield, leaving unreacted spacer amino groups free for a subsequent coupling. Consequently, these had to be capped before any new amide bond could be formed. Capping had to be selective in order not to block one of the arms of the scaffold. This ruled out the use of Ac₂O in the presence of a base, because as well aliphatic as aniline amino groups are capped under these circumstances.

⁸⁰ Carpino, L. A.; Han, G. Y. *J. Org. Chem.* **1972**, 37, 3404-3409.



Scheme IV.13: Capping of the free spacer amines.

Selectivity could be obtained by taking into account that aliphatic spacer amines are more reactive than anilines. The difference in reactivity could be exploited by capping with AcOH that is activated with PyBOP and DIEA. The in situ formed OB_t ester is less reactive than the usually employed acetic acid anhydride. The reaction was monitored with the ninhydrine test and after 1 h, a negative colour test was obtained. Analysis after photocleavage showed that less than 2 % of deprotected tripodal construct **IV.17a** was acetylated (**Figure IV.9**).

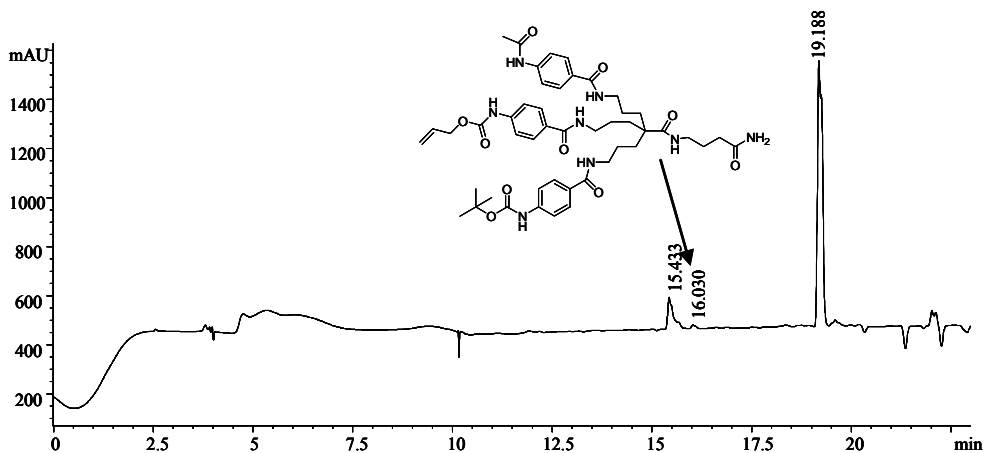


Figure IV.9: HPLC at 214 nm of IV.17b after photocleavage in MeCN.

IV.2.4.Attachment of the first amino acids

After the deprotection of one of the protecting groups of construct **IV.17** (**Scheme**

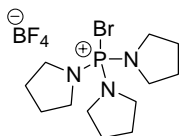


Figure IV.10: PyBrOP

IV.11) an aniline derivative is generated. In addition to being conjugated to the aromatic system, this amine can be regarded as a vinylogous ureum derivative with very poor nucleophilic properties (cfr. the pKa of protonated Abz = 2.38).

Acetylation with standard coupling reagents as PyBOP, HBTU or DIC/HOBt gives incomplete reactions even after repeated couplings.⁸¹ A few examples of aniline acetylations are described using PyBrOP,⁸² acid chlorides,⁸³ DIC activation,⁸⁴ symmetrical anhydrides⁸⁵ and unsymmetrical anhydrides.⁸⁶

Activation with PyBrOP yields the acyl bromide, a very reactive intermediate. Nevertheless, 10 equivalents of AA and PyBrOP in the presence of 20 equivalents of DIEA were needed for 18 h to finish the reaction. Keeping in mind that prolonged exposure to tertiary bases can remove the Fmoc group, it was decided not to use this method.

The acyl chlorides of an amino acid can be prepared in advance with thionyl chloride (SOCl₂) or oxalylchloride. This however, requires an extra synthesis and purification step and therefore other alternatives were first explored.

Unsymmetrical anhydrides are known to be very reactive species. They can be generated by reacting the AA with (Boc)₂O in the presence of a weak base (**Scheme IV.14**). After 1 h, the activated species is added to the resin to acylate the free amine. Ten equivalents of the activated species for 18 h were not sufficient to drive the reaction to completion. Therefore the coupling had to be repeated. In a few cases, the Boc

⁸¹ Pascal, R.; Sola, R.; Labeguere, F.; Jouin, P. *Eur. J. Org. Chem.* **2000**, 3755-3761.

⁸² a) Neustadt, B. R.; Smith, E. M.; Nechuta, T.; Zhang, Y. *Tetrahedron Lett.* **1998**, 39, 5317-5320. b) Kilburn, J. P.; Lau, J.; Jones, R. C. F. *Tetrahedron Lett.* **2000**, 41, 5419-5421.

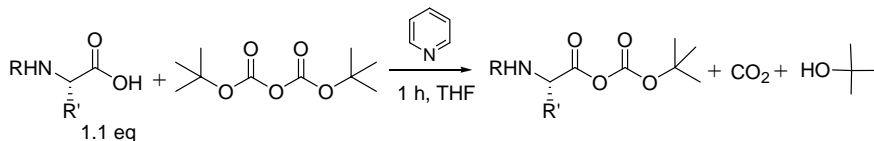
⁸³ Spivey, A. C.; McKendrick, J.; Srikanan, R.; Helm, B. A. *J. Org. Chem.* **2003**, 68, 1843-1851.

⁸⁴ Kawato, H. C.; Nakayama, K.; Inagaki, H.; Ohta, T. *Org. Lett.* **2001**, 3, 3451-3454.

⁸⁵ Franke, R.; Doll, C.; Eichler, J. *Tetrahedron Lett.* **2005**, 46, 4479-4482.

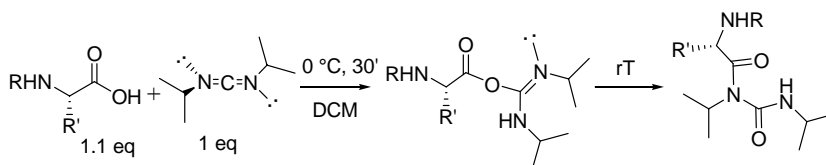
⁸⁶ Hamze, A.; Martinez, J.; Hernandez, J. F. *J. Org. Chem.* **2004**, 69, 8394-8402.

protected scaffold was obtained, probably resulting from insufficient preactivation or attack on the wrong carbonyl centre.



Scheme IV.14: Unsymmetrical anhydrides.

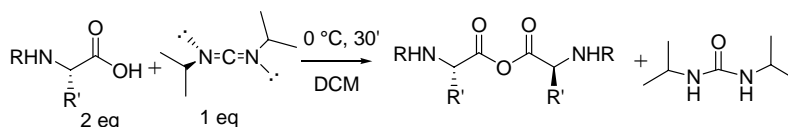
To avoid these problems, activation of an AA with DIC was tried. Here, the reactive species is the O-acylureum (**Scheme IV.15**). Normally this intermediate is intercepted by HOBT to give the OBt ester, but in the absence of this nucleophilic catalyst, the O-acylureum stays the reactive intermediate. Activation occurs preferably in DCM and by lowering the temperature, the formation of the less reactive N-acylureum is avoided. A slight excess of AA should be used to prevent guanidylation of the free amine by the unreacted DIC. Although the coupling proceeded well using DIC activation, in some cases, guanidinylated side product was noticed.



Scheme IV.15: Activation with DIC: formation of N-acylureum at room temperature.

We then focussed our attention on the symmetrical anhydrides, which possesses a reactivity similar to acetyl chlorides. When an acid is activated with DIC, the O-acylureum intermediate can be intercepted by a second equivalent of acid to yield the symmetrical anhydride (**Scheme IV.16**). The symmetrical anhydride is formed by preactivating the AA with DIC at 0 °C for half an hour. The solvent of choice is DCM,

because carboxylic acids form a hydrogen bonded stabilised dimer in DCM that then rapidly reacts with DIC to give the symmetrical anhydride.⁸⁷ Depending on the amino acid, some DMF can be added to increase the solubility of the anhydride.



Scheme IV.16: Activation to symmetrical anhydrides.

Upon activating 12 equivalents of AA with 6 equivalents of DIC, a clean coupling of the AA to the scaffold was obtained after overnight reaction. Occasionally, the reaction had to be repeated due to incomplete coupling, but more importantly, no side reactions were observed.

Using this protocol, three different AAs were attached to the resin-bound scaffold **IV.17** and in this manner, proof was delivered for its use in the construction of tripodal libraries.⁸⁸

One drawback is that this protocol is less suited for automated synthesis. With automated synthesis, all necessary solutions are made in advance (AA, coupling reagent, base) and then mixed with each other and the resin by the robot arm. Being a volatile solvent, DCM easily evaporates and this can cause clogging of the needle of the robot arm. Moreover, the necessity to cool at $0\text{ }^\circ\text{C}$ is difficult to achieve in the robotic setup.

For this reason, a glycine residue will first be manually incorporated into each chain. The starting material for the automated synthesis will now be the tripodal structure **IV.17** but where the three aromatic units are elongated with a glycine residue (**Figure IV.11**). In order to keep the orthogonality, glycines with the correct N-protecting groups will have to be coupled.

⁸⁷ DeTar, D. F.; Silverstein, R. *J. Am. Chem. Soc.* **1965**, 88, 1013-1019.

⁸⁸ Van der Plas, S. E.; Gea, A.; Figaroli, S.; De Clercq, P. J.; Madder, A. *Eur. J. Org. Chem.* **2008**, 1582-1588.

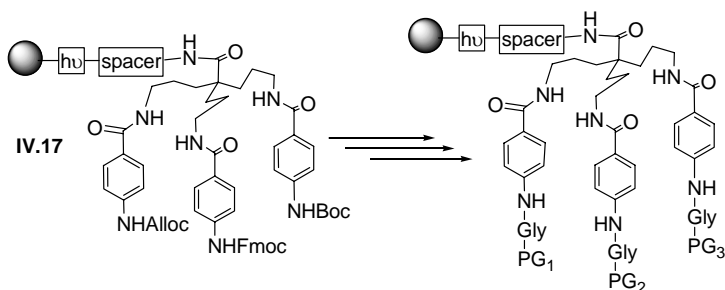


Figure IV.11: A new starting point for automated synthesis.

IV.2.5. Reconsidering the orthogonality scheme: synthesis of new glycine derivatives

Now that a protocol was established for attaching the scaffold **IV.1** to Tentagel resin, and for the coupling of the first AA, peptide chains could be constructed on to this backbone. The scaffold is designed in such a way that three different peptide chains can be incorporated. In theory, by coupling FmocGlyOH, AllocGlyOH and BocGlyOH, the same orthogonality scheme is applicable.

IV.2.5.1. Replacing the acid labile Boc group

In the present scheme, the Boc group restricts the use of side chain protected amino acids in previous chains. If for example, a glutamic acid residue is introduced in the first chain, this side chain will be deprotected when applying 50 % TFA/DCM to access the second arm. To increase diversity and flexibility of the synthesis, a new protecting group had to be selected and a suitably protected glycine was thus needed.

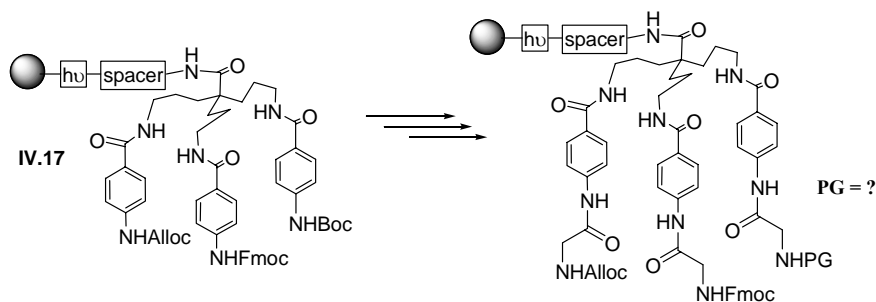
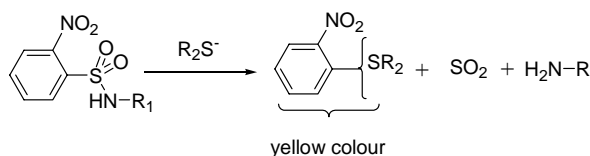


Figure IV.12: New orthogonality scheme.

The possibilities for protecting an α -amino group of an AA are truly enormous⁸⁹ and even today, new protecting groups are designed and tested.⁹⁰ In the search for a new, compatible group, the *ortho*-nitrobenzenesulfonyl (*o*NBS) group caught our attention. It offers a number of features justifying its use as a temporary amino protecting group.⁹¹ A first advantage is that upon deprotection with a thiolate via S_NAr , a yellow coloured chromophore is released allowing simple visual confirmation of deprotection (**Scheme IV.17**).

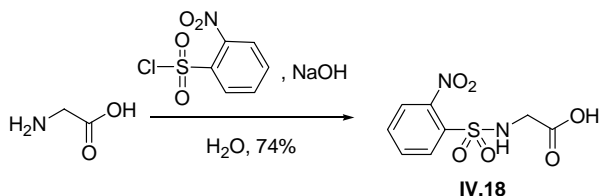
Scheme IV.17: Deprotection of *o*NBS protected amines.

The second advantage is that the reagent necessary for the synthesis of *o*NBS amino acids, is commercially available and considerably cheaper than e.g. Fmoc-Cl. This protecting group has also been used by Liskamp in the synthesis of the earlier mentioned tripodal TAC scaffold.^{59a}

⁸⁹ Albericio, F. *Biopolymers* **2000**, 55, 123-139.

⁹⁰ Pothukanuri, S.; Pianowski, Z.; Winssinger, N. *Eur. J. Org. Chem.* **2008**, 3141-3148.

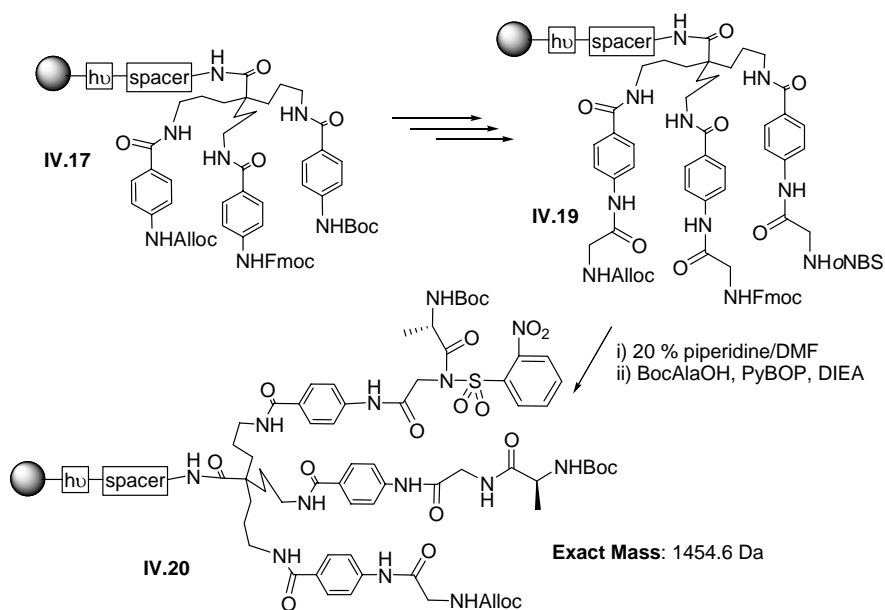
⁹¹ Miller, S. C.; Scanlan, T. S. *J. Am. Chem. Soc.* **1998**, 120, 2690-2691.



Scheme IV.18: Preparation of *o*NBSGlyOH.

The glycine derivative **IV.18** was easily prepared following previously published procedures concerning the preparation of benzenesulfonyl amino acids (**Scheme IV.18**).⁹² It was incorporated into construct **IV.17** together with AllocGlyOH and FmocGlyOH (as later described in more detail in **Chapter IV.2.6**) and its orthogonality was tested by attaching BocAlaOH after Fmoc deprotection (**Scheme IV.19**).

⁹² Milne, H. *J. Am. Chem. Soc.* **1957**, 79, 639-644.

Scheme IV.19: Testing of the *o*NBS group.

After the photocleavage of a small sample, the product was analysed by LC-MS. From **Figure IV.13** it can be seen that the main peak had a mass corresponding to the desired product plus an extra BocAlaOH residue.

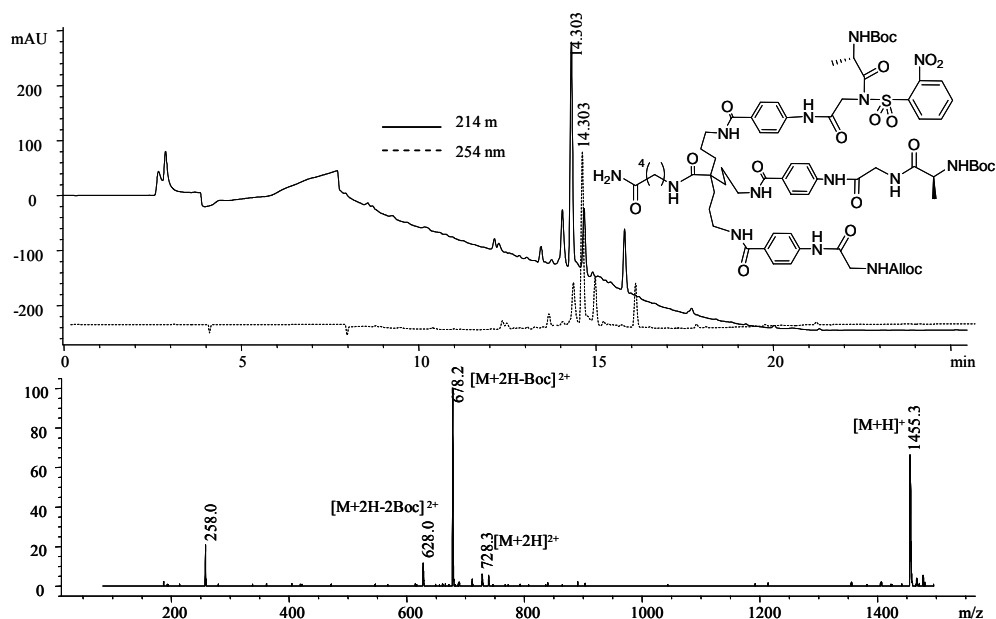
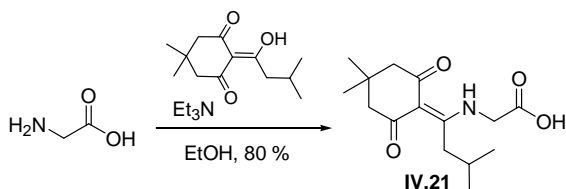


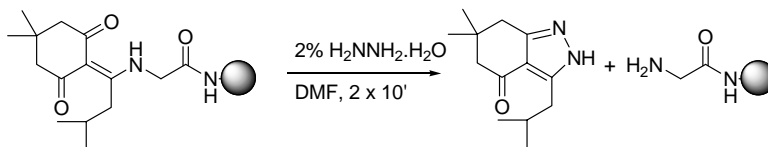
Figure IV.13: LC-ESI-MS of IV.20 after photocleavage in EtOH. The ESI- spectrum of the main peak is included, indicating that a double acetylation had occurred.

The formation of this product could be explained by assuming that during the coupling of the BocAlaOH (step ii in **Scheme IV.19**) the DIEA deprotonated the sulphonamide, generating a reactive nucleophile capable of attacking a second equivalent of activated amino acid. Indeed, it is for this reason that the *o*NBS group is sometimes used for the selective alkylation of amines.⁹³ However, the *o*NBS has also been used as a replacement for the Fmoc group in the synthesis of small peptides without any problems.⁹¹ Nevertheless, this side reaction showed the *o*NBS group to be unsuitable for our purposes and a new protecting group had to be found.

⁹³ Fukuyama, T.; Cheung, M.; Kan, T. *Synlett* **1999**, 1301-1303.

Scheme IV.20: Synthesis of *ivDdeGlyOH*.

Another potentially useful group is the 2-*iso*-valeryldimedone (*ivDde*) group. This group has become a valuable tool in the synthesis of branched or side chain modified protected peptides by the Fmoc/*t*Bu solid phase approach.⁹⁴ The group can be introduced in good yield by a condensation reaction (Scheme IV.20). Deprotection can be carried out using a 2 % hydrazine solution in DMF (Scheme IV.21). After incorporation, the group was tested for orthogonality towards Fmoc and Alloc deprotection conditions and no side reactions were observed.

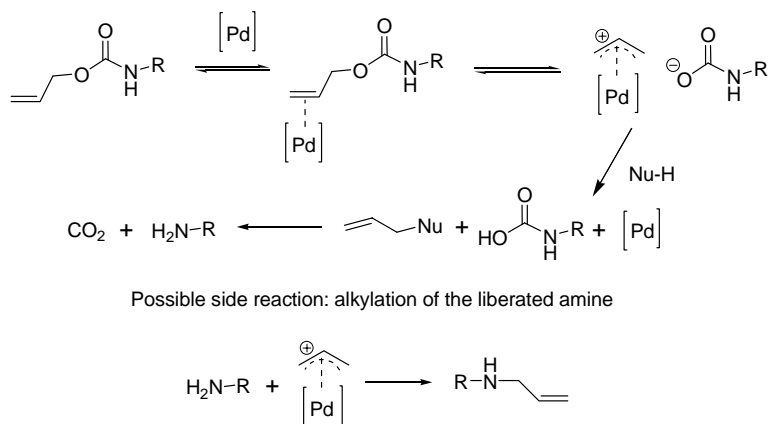
Scheme IV.21: Deprotection of the *ivDde* group.

IV.2.5.2. Orthogonality of the Alloc group

The allyloxycarbonyl (Alloc) group is widely used in combination with a Fmoc/*t*Bu strategy⁹⁵ and is also used in different dipodal⁵⁶ and tripodal scaffolds.⁵⁷ Cleavage is achieved by catalytic amounts of (PPh₃)₄Pd in the presence of an appropriate nucleophile, a so called scavenger. Moreover, the Alloc group is stable under Boc, Fmoc and *ivDde* deprotecting conditions.

⁹⁴ Chhabra, S. R.; Hothi, B.; Evans, D. J.; White, P. D.; Bycroft, B. W.; Chan, W. C. *Tetrahedron Lett.* **1998**, 39, 1603-1606.

⁹⁵ Brase, S.; Kirchhoff, J. H.; Kobberling, J. *Tetrahedron* **2003**, 59, 885-939.



Scheme IV.22: Mechanism of Alloc deprotection and undesired alkylation.

The scavenger plays an important role in trapping the cationic π -allyl-Pd-complex, thus preventing attack of the liberated amine on this cation which would lead to undesired alkylation (**Scheme IV.22**). For this reason, 10 equivalents of scavenger or more are usually added to the reaction mixture. In literature, a range of scavengers are described⁹⁶ and some of them were tested for their effectiveness (**Table IV.3**).

⁹⁶ Guibe, F. *Tetrahedron* **1998**, *54*, 2967-3042.

Table IV.3: Scavengers tested for the Alloc deprotection.

Entry	Scavenger	Equivalents	Time	Solvent	Remarks
1	Morpholine	180	18 h	DMF	- Concurrent Fmoc deprotection. - Incomplete Alloc deprotection.
2	Bu ₃ SnH	10	1 h	DCM	- Concurrent Fmoc deprotection. - Incomplete Alloc deprotection. - Undesired alkylation.
3	Bu ₃ SnH	20	2 x 30'	DCM	- Concurrent Fmoc deprotection. - Complete Alloc deprotection..
4	Anilinium <i>p</i> -toluenesulfinate	70	1 h	DMF	- Incomplete Alloc deprotection
5	Bu ₃ SnH + anilinium <i>p</i> -toluenesulfinate	20 + 10	2 x 60'	DCM	- Complete Alloc deprotection.
6	PhSiH ₃	25	2 x 10'	DCM	- Incomplete Alloc deprotection..
7	PhSiH ₃	25	2 x 60'	DCM	- Complete Alloc deprotection - Irreproducible results
8	TIS	75	45'	DCM	- Incomplete Alloc deprotection.

Test reactions were performed on derivatives of construct **IV.22** (**Figure IV.14**) and conditions were optimised for the removal of an Alloc group attached to an aromatic amine.

The scavenger previously used in our lab was morpholine which was applied in a very large excess for 18 h (**entry 1**). Besides causing Fmoc deprotection, this secondary amine was apparently not performant enough as incomplete deprotection was observed using this reagent.

The first explored alternative was Bu_3SnH (**entry 2**).⁹⁷ This Sn derivative, though effective, is less used nowadays due to its toxicity. In a first experiment it was noticed that 10 equivalents were not sufficient for complete deprotection of the Alloc group. Moreover, some alkylation was observed. Increasing the equivalents (**entry 3**) gave a complete deprotection without alkylation. However, the hydride appeared basic enough to cause undesired Fmoc deprotection.

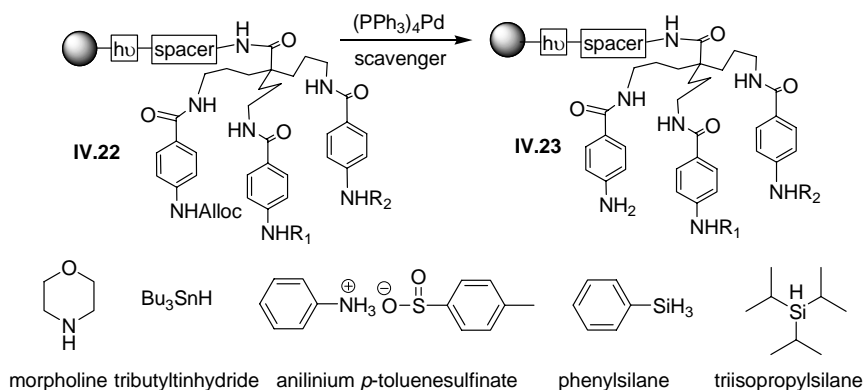


Figure IV.14: Tested scavengers for the Alloc deprotection.

Sulfenic acids are also known to be able to scavenge the cationic π -allyl-Pd-complex generated during the Alloc deprotection.⁹⁸ Using the salt of *p*-toluenesulfinic acid and aniline did not lead to a complete deprotection (**entry 4**), even when a very large excess

⁹⁷ Dangles, O.; Guibe, F.; Balavoine, G.; Lavielle, S.; Marquet, A. *J. Org. Chem.* **1987**, 52, 4984-4993.

⁹⁸ Honda, M.; Morita, H.; Nagakura, I. *J. Org. Chem.* **1997**, 62, 8932-8936.

was applied. The advantage is that the Fmoc group is not deprotected and no alkylation is observed.

When combining the sulfenic acid with Bu_3SnH in a 1:2 ratio, a complete deprotection was observed without removal of the Fmoc group (**entry 5**). This is probably due to a decrease in pH of the solution when the acidic salt is added. The combined scavengers also prevented alkylation of the liberated amine.

Another, commonly used scavenger is phenylsilane. The allyl group is transferred under neutral conditions using PhSiH_3 and consequently, no Fmoc deprotection is observed.⁹⁹ Additionally, no trace of the alkylated side product was observed using this scavenger. The reported reaction time of 10 min seemed insufficient to completely deprotect the Alloc group (**entry 6**). Prolonging the reaction time until 60 min led to a complete removal in most cases. However, the deprotection showed to be irreproducible (**entry 7**). Sometimes only one hour was sufficient but in other cases, the deprotection had to be repeated for three times. Interestingly, triisopropylsilane, a known hydride donor routinely used in our lab during the side chain deprotection of peptides (*vide infra*), was unable to give good results (**entry 8**).

In conclusion, two systems (PhSiH_3 and anilinium *p*-toluenesulfinate/ Bu_3SnH) were found to be effective in the deprotection of the Alloc group. The silyl reagent was preferred due to the lower toxicity but each time the deprotection was carefully monitored via LC(-MS) to make sure that all the starting material had disappeared. According to literature, when using PhSiH_3 as a scavenger, the liberated amine should be rapidly and quantitatively acylated in the presence of a suitably activated carboxylic acid.¹⁰⁰ When performing the deprotection in the presence of pre-activated FmocGlyOH (**Figure IV.15**), it appeared that not only was the Alloc removal incomplete but also only 20 % of the liberated amine was acylated. In a second experiment, the symmetrical anhydride was only added to the deprotection mixture after 30 min but no improvement

⁹⁹ Thieriet, N.; Alsina, J.; Giralt, E.; Guibe, F.; Albericio, F. *Tetrahedron Lett.* **1997**, 38, 7275-7278.

¹⁰⁰ Thieriet, N.; Gomez-Martinez, P.; Guibe, F. *Tetrahedron Lett.* **1999**, 40, 2505-2508.

was seen. Therefore, the deprotection and subsequent coupling were carried out separately.

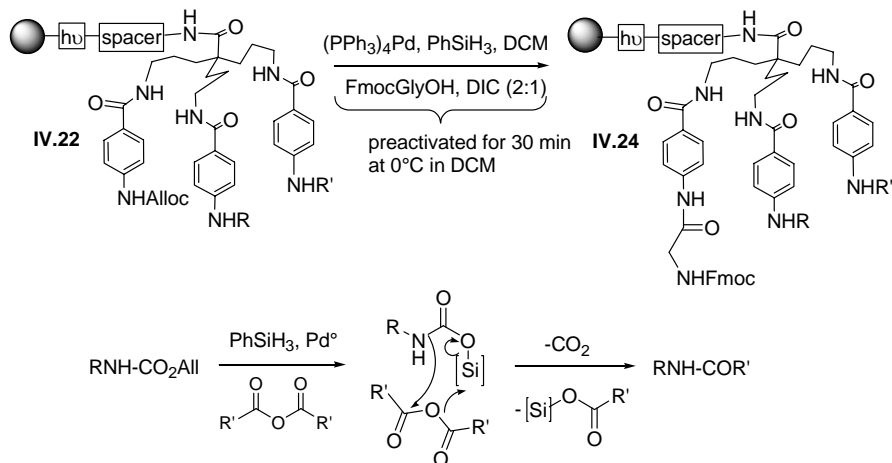
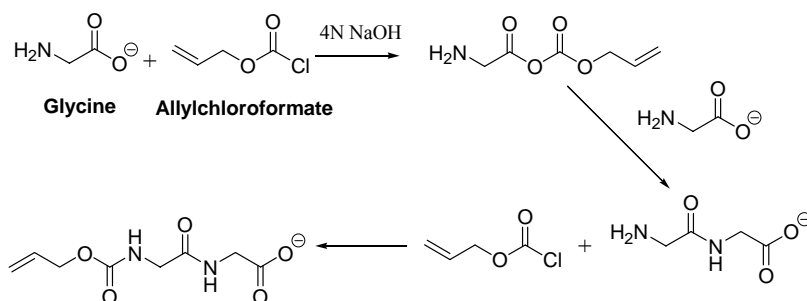


Figure IV.15: Tandem deprotection-coupling.

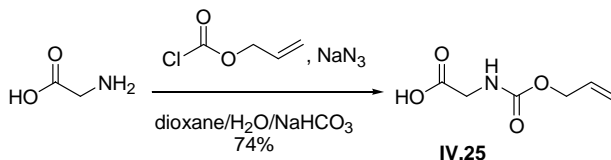
Once the Alloc group was removed, AllocGlyOH had to be coupled to ensure complete orthogonality.

Not being commercially available, AllocGlyOH first had to be synthesised. The Alloc group can be introduced using allyl chloroformate (**Scheme IV.23**). However, this reagent is reactive enough to be attacked by the carboxylate anion, generating a mixed anhydride that in turn can be attacked by another glycine, resulting in a dipeptide.



Scheme IV.23: Formation of AllocGlyGlyOH.

This can be prevented by *in situ* transforming the chloroformate into the less reactive acylazide (**Scheme IV.24**).¹⁰¹ In our hands, the desired compound was obtained using this protocol, but ¹³C-NMR analysis showed the presence of another glycine derivative. Coupling of this Alloc-glycine to the tripodal scaffold however, gave only one detectable compound with the right mass.



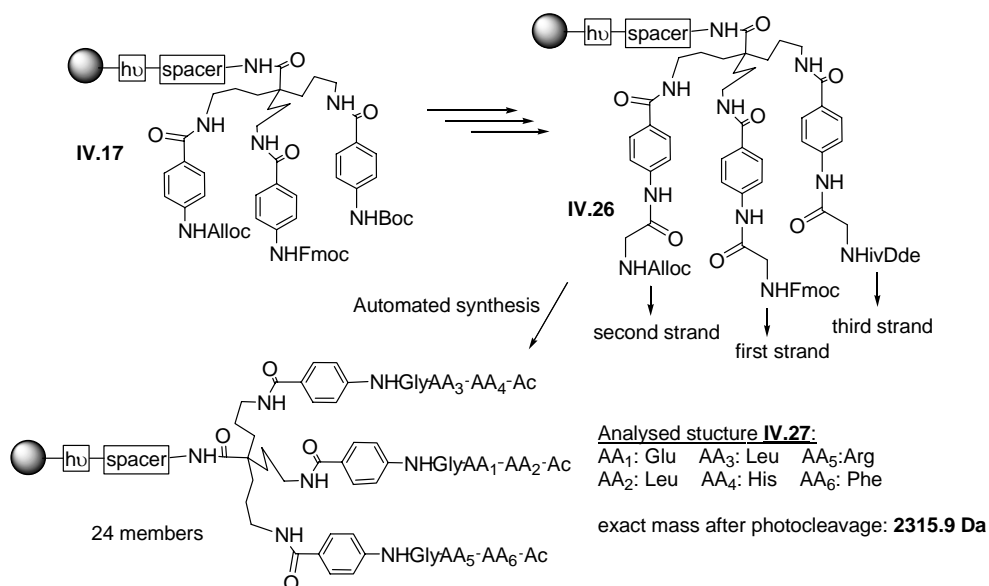
Scheme IV.24: Alloc protection of glycine.

To illustrate the problems that were still encountered with the Alloc group, we focussed is on the synthesis of 24 library members. The choice of amino acids and the details of the synthesis are explained stage in this chapter. The starting point is construct **IV.26** (**Scheme IV.25**) to which three different peptide strands are attached. To clarify the encountered problems, a specific sequence **IV.27** is chosen as example.

The synthesis was started by first deprotecting the Fmoc group of **IV.26** and thus generating a free glycine amino group which was subsequently acetylated with a Glu

¹⁰¹ Cruz, L. J.; Beteta, N. G.; Ewenson, A.; Albericio, F. *Org. Process Res. Dev.* **2004**, 8, 920-924.

residue. The second incorporated AA was Leu and the first peptide strand was capped with Ac_2O . For the Alloc deprotection, PhSiH_3 was manually added to each reaction vessel followed by the addition of catalytic amounts of Pd^0 in DCM. The reaction was vortexed by the synthesiser for 60 min and the sequence was repeated once. After the Alloc deprotection, no more manual steps had to be included. The coupling of Leu and His and subsequent capping was automatically followed by *ivDde* removal. The third strand consisted of Arg and Phe and was capped with Ac_2O .



Scheme IV.25: Automated synthesis of 24 library members.

The identity of the obtained compound was checked via analysis of the product after photocleavage. Because the polar side chains of His, Arg and Glu were still protected,

resulting in a mass of the photocleaved product of 2315.9 Da, analysis was only possible via MALDI-TOF.¹⁰²

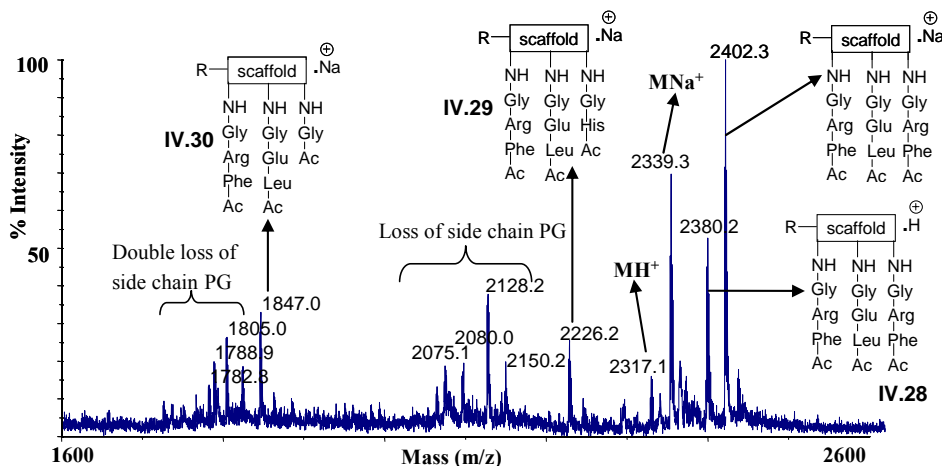


Figure IV.16: MALDI analysis of IV.27 after photocleavage.

The obtained MALDI spectrum (**Figure IV.16**) was at start a little bit puzzling. The correct mass of the compound (2317.1 [M+H]^+) was observed, but it was not the main peak. Clearly, a product that was heavier than the target compound had been synthesised (2380.2, 2402.3). Besides the loss of side chain protecting groups, which is due to the acidic sample preparation for MALDI analysis, other peaks with a lower mass were observed.

The key to solving this spectrum was found in the mass difference between 2226.2 and 2339.3 $[\text{M}+\text{Na}]^+$ which corresponded with a missing Leu residue. This deletion could come from the first Fmoc strand or from the second Alloc strand. Taking into account the previous problems encountered with the Alloc group, it was assumed that the Leu was missing in the second strand. In this way, the peak at 1847.0 could be explained as a double deletion: no Leu and His were present. The higher masses of

¹⁰² For ESI, current equipment does not allow the analysis of masses higher than 2000 Da.

2380.2 and 2402.3 could eventually be correlated to a double insertion of the third strand, implying that instead of the insertion of a Leu and His, an Arg and a Phe were incorporated.

Similar spectra were obtained when other samples were analysed and the same trend was observed after the side chain protecting groups were removed.

One way for explaining this was by assuming that after the Alloc deprotection, the free glycine amine was reversibly blocked. Indeed, only a fraction of the unprotected product was coupled to the first AA (Leu) after Alloc deprotection. This compound would eventually lead to the desired product with the observed masses of 2317.1 $[M+H]^+$ and 2339.3 $[M+Na]^+$.

Nevertheless, the peak of 2226.2 $[M-Leu+Na]^+$ suggests that after the Leu coupling, the glycine amine was partially unblocked and able to react in the subsequent His coupling forming **IV.29** (**Figure IV.16**). Moreover, this also explains the existence of **IV.30** and **IV.28**. It seems that after every treatment with a nitrogen base like piperidine for the Fmoc deprotection, DIEA during the AA coupling or pyridine during the capping step, the temporarily blocked glycine generated during the Alloc deprotection, is partially deprotected.

What can be the nature of this blocked glycine amine? The following possibilities are suggested (**Figure IV.17**):

a) *The formed carbamic acid is silylated and does not decompose (IV.26a)*. When using silyl or tin based scavengers, it is thought that the intermediate carbamic acid binds with the Lewis acid. The formed adduct readily decomposes in the presence of traces water.¹⁰⁰ In this context, it should be noted that when working in an automated fashion, it is impossible to work under dry circumstances, so there is always some water present in the reaction mixture.

b) *The liberated amine forms a complex with Pd (IV.26b)*. Though Pd^0 was only added in catalytic amounts (20 mol %), the deprotection was repeated once and so partial blocking of the glycine can result from a glycine-Pd complex formation. This complex could then be dissociated by adding another N-ligand like piperidine or pyridine.

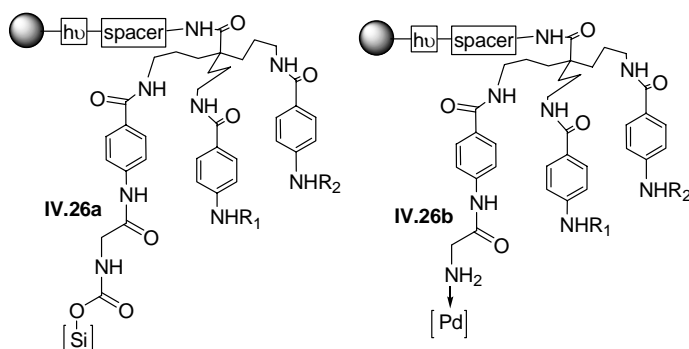


Figure IV.17: The two suggested possibilities for the partial blocking of Gly.

Whatever the chemical answer to these questions may be, one fact is sure from these and previous experiments: the Alloc group is an unreliable protecting group lacking the robustness needed for the synthesis of a library of tripodal receptors.

IV.2.5.3. In search of a new protecting group: azidoglycine

Faced with the practical drawbacks of the Alloc group, a new literature search was started to find a new protecting group for α -amines which is compatible with the Fmoc and *iv*Dde group. Luckily, at that time click chemistry had become a chemical hype and azides were in the spotlight. The idea grew of using the azido derivative of glycine in our synthetic scheme.

Using the azide as a protective group in peptide synthesis is surprisingly enough discarded in most reviews about protecting group strategies.⁸⁹ A few examples are known where azido derivatives of amino acids are used.¹⁰³ Probably the inherent instability of azides has prevented widespread use of the azido derivatives of amino

¹⁰³ a) Debaene, F.; Winssinger, N. *Org. Lett.* **2003**, 5, 4445-4447. b) Zhang, Z. S.; Carter, T.; Fan, E. K. *Tetrahedron Lett.* **2003**, 44, 3063-3066. c) Yan, R. B.; Yang, F.; Wu, Y. F.; Zhang, L. H.; Ye, X. S. *Tetrahedron Lett.* **2005**, 46, 8993-8995.

acids. When working with a specific azide, the following equation should be kept in mind.¹⁰⁴

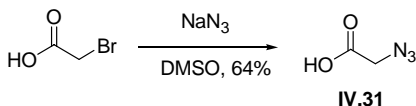
$$\frac{N_C + N_O}{N_N} > 3 \quad \text{Azidoglycine IV.31} \quad \frac{2 + 2}{3} = 1.33$$

Equation I

Figure IV.18: Safety aspects of azidoglycine. Equation I gives the ratio of the number of C and O atoms to the number of N atoms.

Only azides with a ratio larger than 3 can be handled like a normal non-explosive organic compound. If the calculation is done for azidoglycine **IV.31**, a value of 1.33 is found. Nevertheless, several articles report about the synthesis and applications of this small, energy rich molecule.¹⁰⁵ All the articles mention that care must be taken in handling this compound but no accidents have ever been reported using azidoglycine. One article even discusses the thermal decomposition of azidoglycine and the characterisation of the formed products.¹⁰⁶ In light of these examples, it was decided to synthesise azidoglycine and to incorporate it into the synthetic strategy.

The azide group could be easily introduced via an S_N2 reaction in DMSO (**Scheme IV.26**).



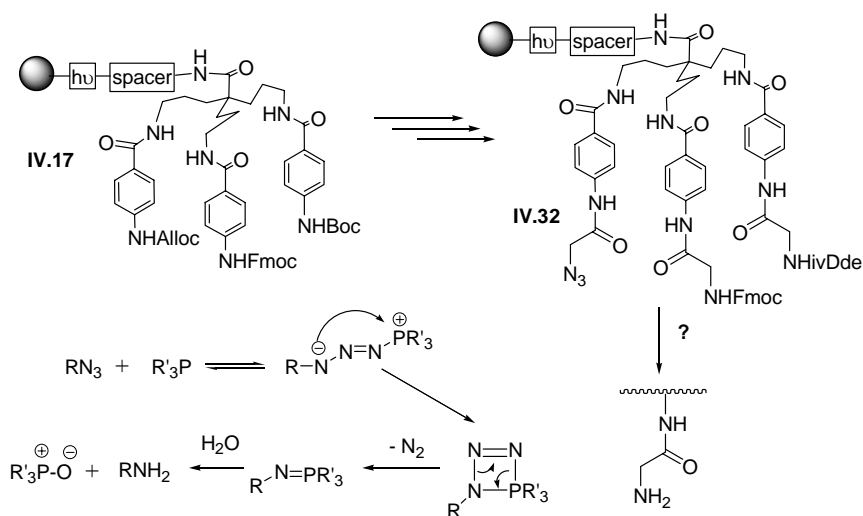
Scheme IV.26: Synthesis of azidoglycine IV.31.

¹⁰⁴ Kolb, H. C.; Finn, M. G.; Sharpless, K. B. *Angew. Chem. Int. Ed.* **2001**, *40*, 2004-2021.

¹⁰⁵ a) Cai, J. F.; Li, X. X.; Yue, X.; Taylor, J. S. *J. Am. Chem. Soc.* **2004**, *126*, 16324-16325. b) Banaszynski, L. A.; Liu, C. W.; Wandless, T. J. *J. Am. Chem. Soc.* **2006**, *128*, 15928-15928.

¹⁰⁶ Dyke, J. M.; Groves, A. P.; Morris, A.; Ogden, J. S.; Dias, A. A.; Oliveira, A. M. S.; Costa, M. L.; Barros, M. T.; Cabral, M. H.; Moutinho, A. M. C. *J. Am. Chem. Soc.* **1997**, *119*, 6883-6887.

The deprotection was optimised on construct **IV.32** (Scheme IV.27). Though reduction of the azide is possible via $\text{SnCl}_2/\text{ArSH}/\text{base}$ ¹⁰⁷ it was decided to use the more classical Staudinger conditions to avoid reduction of the nitro group of the photolinker.¹⁰⁸



Scheme IV.27: Staudinger reduction of azide **IV.32**.

The first step of the Staudinger reduction consists of the nucleophilic attack of the phosphine nucleophile on the azide. The kinetics of this first step are dependent on the donating properties of the phosphine substituents and the electron deficiency of the azide.¹⁰⁹ In the second step, both steric and electronic properties play a role. The kinetics for the second step are presumably in favour for phosphines with little sterical hindrance like Me_3P rather than bulkier nucleophiles like Ph_3P . After nitrogen loss, an iminophosphorane or [N-P]-ylide is obtained which can subsequently be hydrolysed.

¹⁰⁷ Zhang, Z. S.; Carter, T.; Fan, E. K. *Tetrahedron Lett.* **2003**, *44*, 3063-3066.

¹⁰⁸ Wu, Z.; Rea, P.; Wickham, G. *Tetrahedron Lett.* **2000**, *41*, 9871-9874.

¹⁰⁹ Nyffeler, P. T.; Liang, C. H.; Koeller, K. M.; Wong, C. H. *J. Am. Chem. Soc.* **2002**, *124*, 10773-10778.

The iminophosphoranes of Ph_3P are more stable than those of Me_3P and thus more difficult to hydrolyse.

From these considerations Me_3P can be considered to possess the best properties for reducing the azide. Nevertheless, both Me_3P and Ph_3P were tested because the former is more readily oxidised and has the practical disadvantage of an irritant, persistent smell.

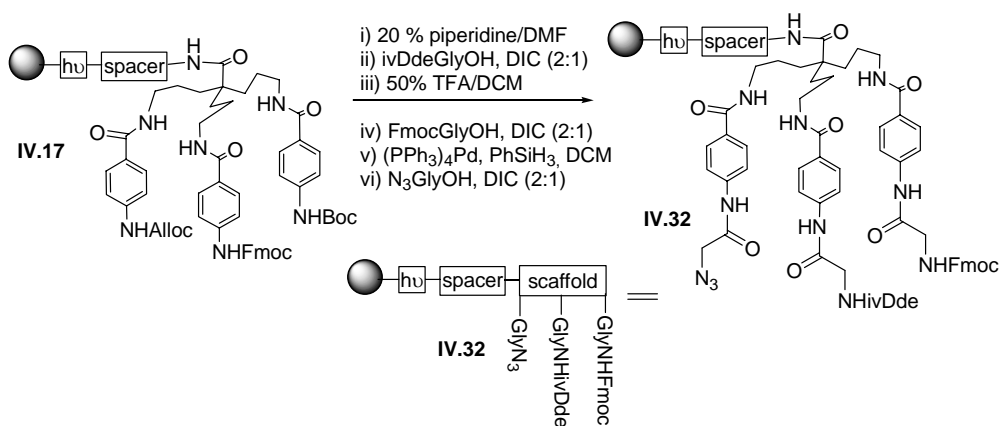
Looking at the results depicted in **Table IV.4** it is clear that the more hindered and less nucleophilic Ph_3P is not suited for a fast reduction of the azide (**entry 1 & 2**). First results obtained with Me_3P however (**entry 3 & 4**), did not give a complete reduction but this was due to the low viscosity of the organic solvent system. It appeared that after 10 min, the solution containing the reagent had leaked through the filter, explaining the bad results. It must be noted that this approach is not compatible with a Fmoc group in the molecule, so the azide cannot be deprotected as the first protecting group. The viscosity was increased by using a 1:1 mixture of THF/ H_2O (**entry 5**) and indeed, after two times 1 h the reduction was complete. In a final experiment, reaction times could be reduced to two times 10 min, establishing the azide as a robust protecting group, ideally suited for the current orthogonality scheme.

Table IV.4: Optimising the Staudinger reduction.

Entry	Nucleophile	Conc.	Solvent	Time	Remarks
1	Ph ₃ P	1 M	dioxane	2 h	- Incomplete azide reduction. - Stable [N-P]-ylide present.
2	Ph ₃ P	1 M	dioxane/H ₂ O (4:1)	2 h	- Incomplete azide reduction. - Stable [N-P]-ylide present.
3	Me ₃ P	1 M	THF	2 h	- Solvent leaks through filter. - Incomplete azide reduction. - Concurrent Fmoc deprotection.
4	Me ₃ P	0.8 M	THF/H ₂ O (4:1)	2 h	- Solvent leaks through filter. - Incomplete azide reduction. - Concurrent Fmoc deprotection.
5	Me ₃ P	0.5 M	THF/H ₂ O (1:1)	2x 1 h	- Complete azide reduction.
6	Me ₃ P	0.5 M	THF/H ₂ O (1:1)	2x 10'	- Complete azide reduction.

IV.2.6. Incorporation of the new glycine derivatives

Starting from construct **IV.17**, the three differently protected glycine derivatives were attached via their symmetrical anhydrides (**Scheme IV.28**). First the Fmoc group was deprotected and the corresponding amine was acylated with *ivDdeGlyOH*. Then the Boc group was removed and subsequent coupling of FmocGlyOH was followed by the Alloc deprotection. Finally, azidoglycine was attached to yield construct **IV.32**.



Scheme IV.28: Construction of the starting material for automated synthesis.

Each coupling was carefully monitored via LC-MS after photocleavage of a small sample. Sometimes, a double coupling had to be performed to make sure that all the starting material had reacted. The azide derivative was coupled last to prevent any undesired reduction by the phosphine ligands of the Pd^0 catalyst during the Alloc deprotection. **IV.32** was obtained in a good purity (**Figure IV.19**) and will serve as the starting point for the synthesis of the receptor library.

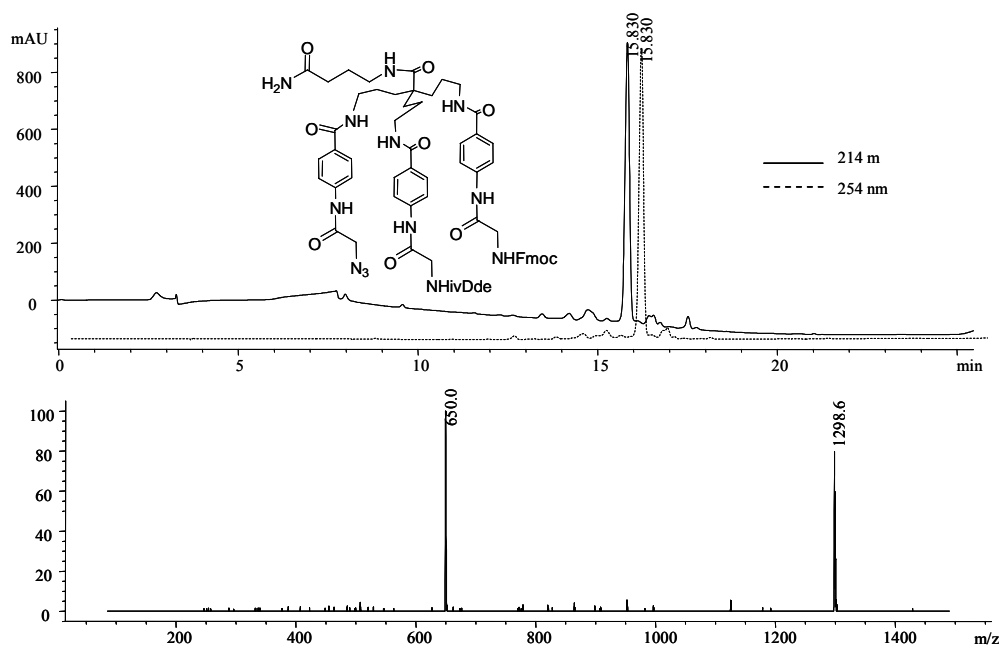


Figure IV.19: LC-MS of IV.32 after photocleavage in EtOH (exact mass = 1297.6)

IV.2.7. Selection of the key amino acids

Now that the protocols for the solid phase synthesis of a library based on the tripodal scaffold **IV.1** are established, the right AAs have to be chosen in order to efficiently mimic the HBD of the hER. The choice was made based on X-ray structures of the HD of the hER with different ligands.¹¹⁰ A schematic representation of the HBD of hER α in complex with estradiol is depicted in **Figure IV.20**.¹¹¹

¹¹⁰ The X-ray structures downloaded from The Protein Data Bank consist of the HBD of hER in complex with Genistein (PDB ID: 1QKM), estradiol (PDB ID: 1ERE and 1A52) and bisphenol-A (PDB ID: 2P7G).

¹¹¹ a) Tanenbaum, D. M.; Wang, Y.; Williams, S. P.; Sigler, P. B. *PNAS* **1998**, 95, 5998-6003. b) Pike, A. C.; Brzozowski, A. M.; Hubbard, R. E.; Bonn, T.; Thorsell, A. G.; Engstrom, O.; Ljunggren, J.; Gustafsson, J. A.; Carlquist, M. *EMBO J* **1999**, 18, 4608-18.

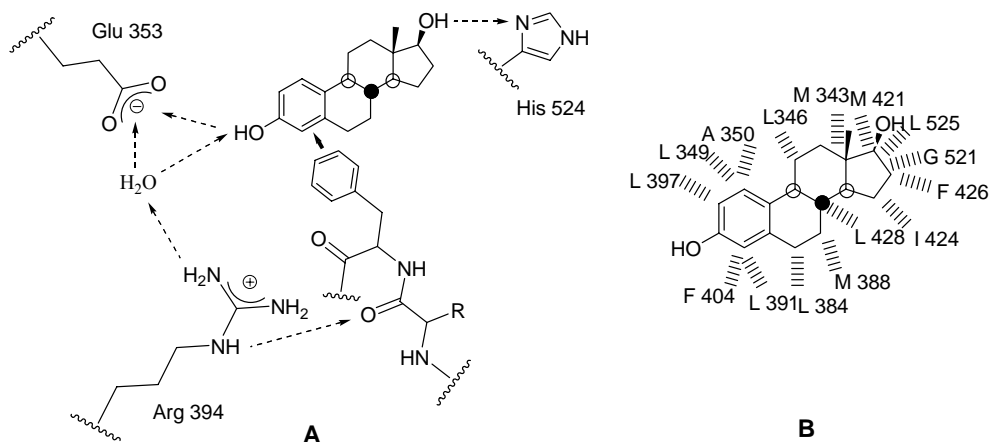


Figure IV.20: Schematic representation of A) hydrogen bonding network and B) hydrophobic interactions between the AAs of the HBD of the hER and its natural ligand estradiol.

The hormone is orientated by two types of contacts: hydrogen bonding at the two ends (A) and van der Waals contacts along the body of the hormone (B).

The hydroxyl group of the phenol is H-bonded to a Glu residue while the aliphatic hydroxyl interacts with the imidazole ring of His₅₂₄. The glutamate is oriented and positioned through a hydrogen bonding network involving a highly polarised water molecule and an Arg side chain. This Arg is braced by a hydrogen bond to the carbonyl of the residue preceding a Phe which in its turn is fixed by an aromatic interaction with the phenolic ring of the ligand.

The body of estradiol interacts with various apolar side chains. The flat A ring is caught in a pincer like environment created by the bulky side chains of different Leu residues.

From these data, six AA were selected to be incorporated into the tripodal backbone. For mimicking the hydrogen bond network, His, Arg and Glu were chosen. The apolar environment of the receptor would be mimicked by choosing Leu, Phe and Met as building blocks.

IV.2.8. Size of the parallel library

When applying a split-and-mix or combinatorial approach (**Figure IV.21**), all the possible combinations with the six selected AA on the six different positions of the scaffold would be made. The number of synthesised molecules would be 6^6 or 46656, a very big number indeed. The disadvantage of these combinatorial libraries is that while generating a very large diversity, it is practically impossible to make 10 or even 1 mg of resin for each member. Generally, the libraries contain only 10 beads carrying the same peptide. This of course has its implications on the screening for activity. Usually, a marked ligand, coloured or fluorescent, is added and after incubation of the whole library, the beads that are coloured or fluorescent are selected and analysed to find out the identity of the peptides.⁵⁹ The identity of the active compound can be determined using techniques such as radio frequency tagging,¹¹² chemical tagging, Edman degradation or other available methods.¹¹³ In view of the small amounts available, it remains difficult to identify the active members.¹¹⁴ Moreover, it is impossible to check the purity of the synthesised compounds which implies that one is never sure whether the whole spectrum of desired molecules has actually been made.

To avoid these problems, a larger amount of the different compounds should be synthesised. This is possible via parallel libraries, where the identity of the compound is determined by the fixed position of the reaction vessel. Though molecular diversity can be generated with automated synthesis, it is practically impossible to synthesise a library of more than 46000 members. For example, if it takes 1 working day to make 24 members, then 1944 days are needed to make 46656 members in a parallel fashion.

¹¹² Nicolaou, K. C.; Xiao, X. Y.; Parandoosh, Z.; Senyei, A.; Nova, M. P. *Angew. Chem. Int. Ed.* **1995**, *34*, 2289-2291.

¹¹³ Czarnik, A. W. *PNAS* **1997**, *94*, 12738-12739.

¹¹⁴ Schmuck, C.; Wich, P. *New J. Chem.* **2006**, *30*, 1377-1385.

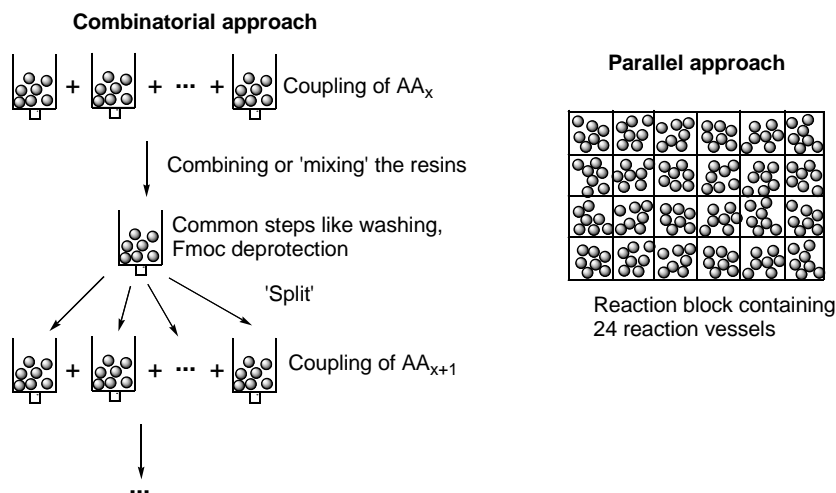


Figure IV.21: Combinatorial vs parallel libraries.

The size of the theoretically possible library was substantially decreased by applying some preconditions. A first simplification was made by leaving out the combinations where it seems that one strand is traded in place with another strand (**Figure IV.22**). In other words, the tripodal structure is treated like a D_3 -symmetrical structure. Consequently, the size of the original library ($6^6 = 46656$) was reduced to a number of 8436 (according to $(x^{(3n)} + 2x^n)/3$ where x is the total number of AAs that can be incorporated and where n is the number of AAs per arm). A second restriction was made by inserting each AA only once into the tripodal structure. In this way, a small sized library of 120 members was designed.¹¹⁵

¹¹⁵ The possible sequences of the library of 8436 members were listed in an Excel File by the Sequence V1.5 software developed by James E. Redman (Redman, J.E., Wilcoxon, K.M and Ghadiri M.R, *J. Comb. Chem.* **2003**, 5, 33-40). The 120 compounds with 6 different AAs were selected by a specially written Visual Basic Application (VBA) protocol.

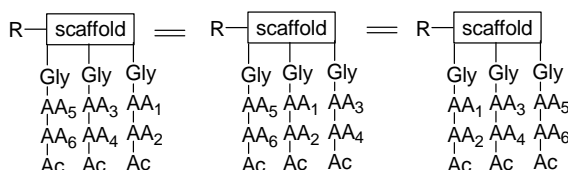
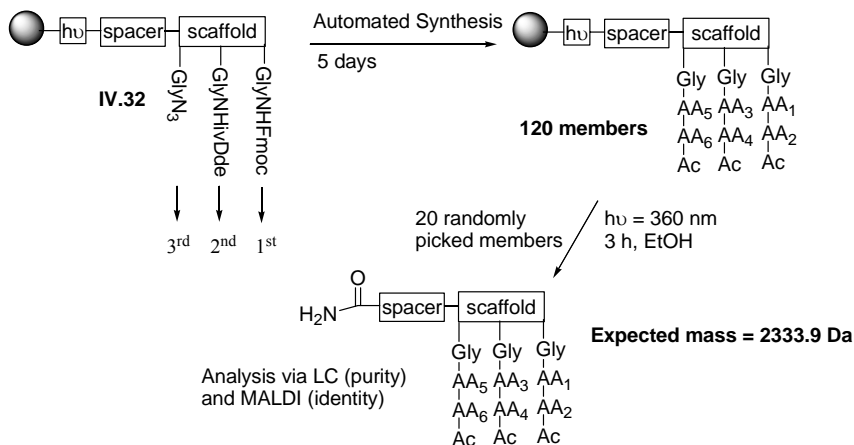


Figure IV.22: Simplifying the library composition.

IV.2.9. Automated solid phase synthesis of 120 receptors

For the automated synthesis, a SYRO I robot setup was used. This device consists of a pipetting arm that simply adds different mixtures to the reaction vessel containing the resin. Via the software, the sequence of the desired peptide is inserted and in this way the robot arm knows when a specific AA_x has to be coupled.

The solutions used for peptide coupling are a 0.5 M HBTU/DMF solution, a 0.5 M AA_x/DMF solution and a 2 M DIEA/NMP solution. In total, 5 equivalents of AA_x and HBTU are added next to 10 equivalents of DIEA. Next to these solutions, also a 40 % piperidine/DMF mixture, and a capping solution (Ac₂O/pyridine/NMP (1:3:10) are prepared. For the *iv*Dde deprotection a 2 % H₂NNH₂.H₂O/DMF is made and for the azide reduction a solution of 0.5 M Me₃P in THF/H₂O is prepared.



Scheme IV.29: Automated synthesis of the library.

Once the different solutions are prepared and the correct sequence is inserted in the software, the resin has to be weighed in the different reaction vessels. After pressing the start button, everything proceeds automatically. Coupling times are typically 40 min and the Fmoc deprotection takes 15 min. Since there are 24 reaction vessels and it takes 20 h to finish the synthesis of 24 members, the whole library was prepared in only 5 days.

For each member, 1-3 mg of resin bound **IV.32** (Scheme IV.29) was weighed in a reaction vessel. The purity and identity were checked by randomly picking 20 members throughout the library and analysing the compounds after photocleavage via MALDI and LC.

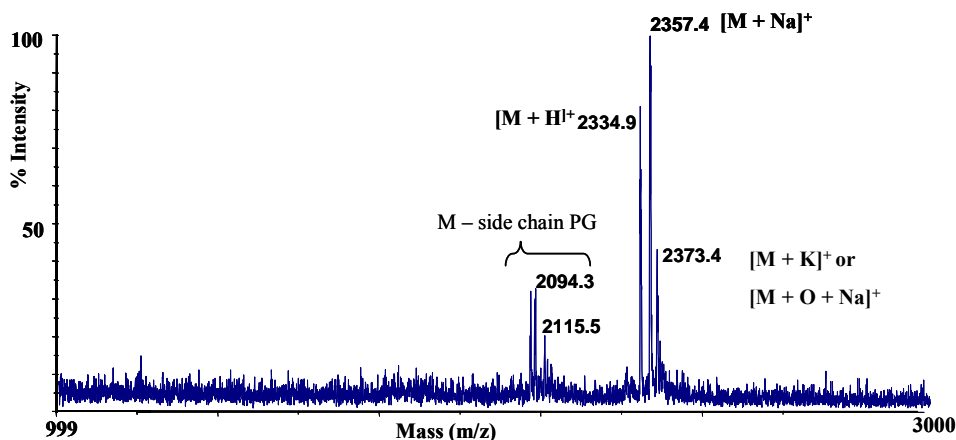


Figure IV.23: MALDI analysis of a library member.

The MALDI spectrum (Figure IV.23) looked very nice at first sight, but when the purity was checked (Figure IV.24), two main peaks were observed. A more careful analysis of the mass spectrum revealed a small peak of 2350.7 (not shown) corresponding to the desired product + an extra oxygen. In this view, the peak of 2373.4 could now also be seen as the Na⁺ adduct of [M + O], what would explain the relative large intensity of this peak (normally K⁺ adducts are observed in lower intensity).

An explanation was found by assuming that the incorporated Met was oxidised during synthesis, causing a hydrophilic shift in the HPLC chromatogram. Normally, this oxidation only happens under acid catalysed conditions. The purity of the starting

compound FmocMetOH was checked via HPLC and only one peak was observed, so this showed that the oxidation happened during the automated synthesis. This is probably due to the fact that the suspension of the beads and the reaction mixture are vortexed intensely during synthesis. No inert atmosphere is applied, so oxygen is really mixed into the solution.

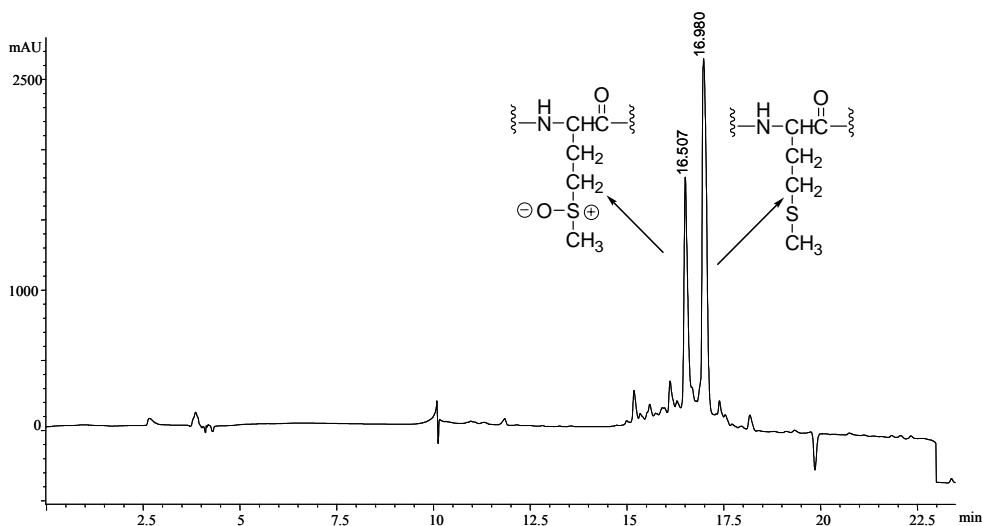


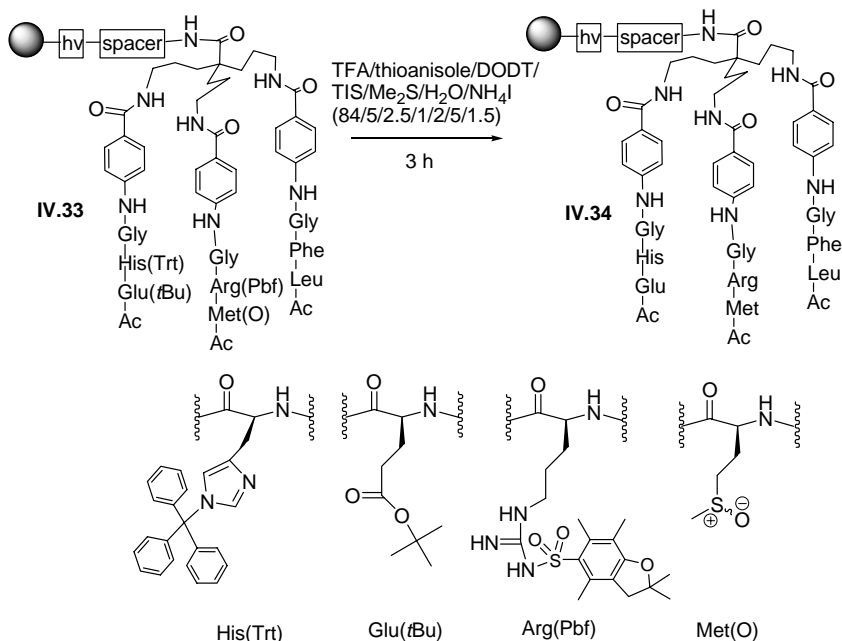
Figure IV.24: HPLC chromatogram at 214 nm of a library member.

The oxidised Met can be regarded as a protected amino acid. Indeed, sometimes Met is fully oxidised before using it as a building block for peptide synthesis. This extra protecting group should now be taken into account when the other side chains are deprotected.

IV.2.10. Side chain deprotection

The side chain protecting groups of His, Glu and Arg can be removed using TFA. During the deprotection, several carbocations are generated and these can cause undesired alkylations of the synthesised molecule. Generally, the cations are trapped by

adding scavengers to the reaction mixture. Based on previous experience in the lab, thioanisole, triisopropylsilane (TIS), 3,6-dioxa-1,8-octanedithiol (DODT)¹¹⁶ and water are added as scavengers. For the reduction of the sulfoxide, NH_4I (1.5 w/w%) and Me_2S (2 %) are added to the cleavage cocktail.¹¹⁷ In **Scheme IV.30** library member **IV.33** is taken as an example.



Scheme IV.30: Deprotection of the side chain protecting groups.

Because a lot of scavengers are added, the amount of TFA and thus the acidity or reactivity of the mixture is lowered. The acidity of the cleavage mixture is also lowered by using Tentagel as a solid phase. The polyethylene glycol chains tend to be

¹¹⁶ Teixeira, A.; Benckhuijsen, W. E.; de Koning, P. E.; Valentijn, A.; Drijfhout, J. W. *Protein and Peptide Letters* **2002**, *9*, 379-385.

¹¹⁷ Hackenberger, C. P. R. *Org. Biomol. Chem.* **2006**, *4*, 2291-2295.

protonated by the acid, hence lowering the effective $[H^+]$. By prolonging the standard reaction time of 1 h to 3 h these effects can be compensated.

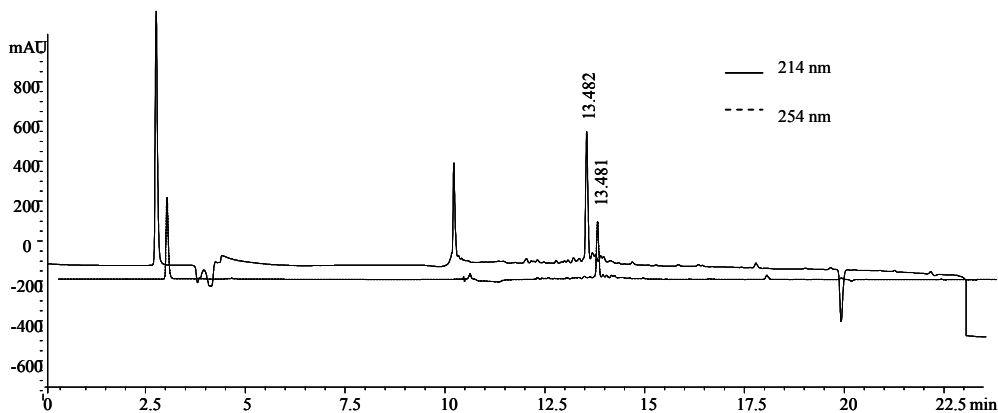


Figure IV.25: HPLC of IV.34 after photocleavage in H_2O .

The HPLC chromatogram looked very clean (**Figure IV.25**) and this result was confirmed by ESI. No trace of oxidised product was observed anymore. The analysis was repeated for the 18 other randomly picked members and besides having the right mass, all of them displayed a purity similar to **IV.34** (for the LC chromatograms of the 18 members, see **Chapter VIII.3.5**).

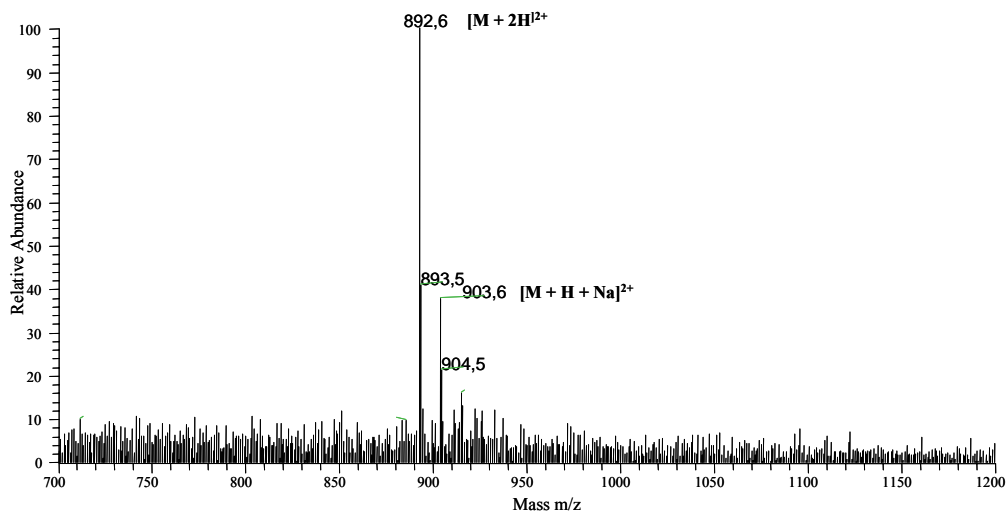
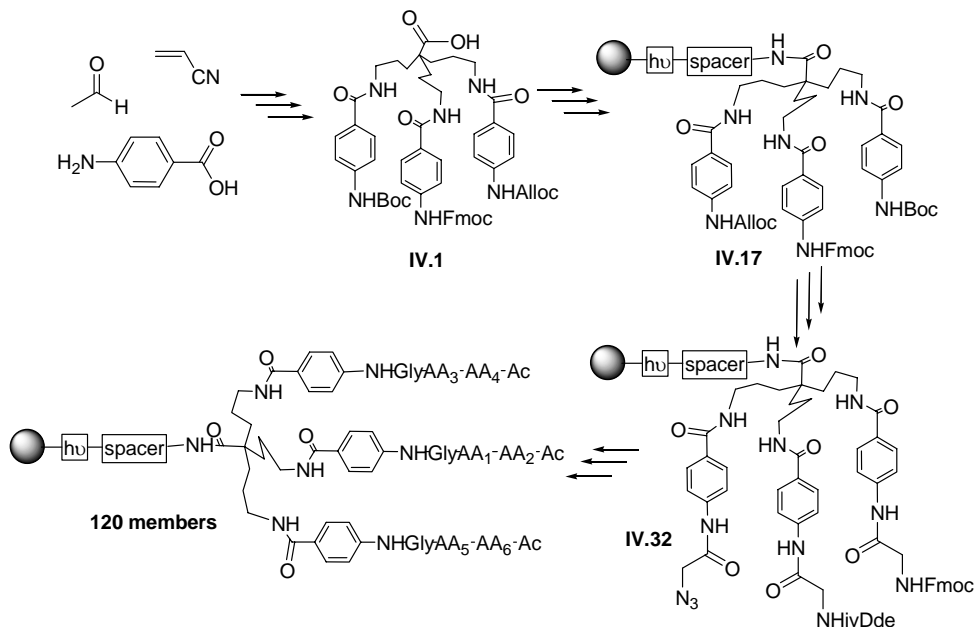


Figure IV.26: ESI (+ mode) of IV.34 after photocleavage in H_2O .

IV.3. Conclusion

In this chapter a synthetic protocol for small sized libraries of possible EDC receptors was established. Starting from simple commercial building blocks the tripodal scaffold **IV.1** was synthesised (Scheme IV.31). After optimisation of the coupling of **IV.1** to Tentagel the weak nucleophilicity of the aromatic amines was bypassed and at the same time the whole orthogonality scheme was reconsidered. Starting from **IV.32**, this new strategy enabled the synthesis of 120 library members in a short period of time. Moreover, after analysis, it was proven that the overall quality of the synthesised library was very good.



Scheme IV.31: Summary of chapter IV.

The next chapter will discuss the screening of the library and the different problems encountered will be addressed.

V. Screening of the library

Synthesising a lot of molecules is one thing, finding out which one has the desired properties is a completely different story. With combinatorial and parallel libraries, screening for affinity has generally been achieved by incubating the library with a labelled ligand. The ligand can be marked with a coloured substrate¹¹⁸, a fluorescent label^{53a,59} or a radioactive marker.⁵¹

The first two options inherently possess some drawbacks. The main problem is that the ligand used for screening is very different from the unlabelled substrate. Usually, the possible interactions with the label itself are then further investigated either by incubating the unligated label with the library or by screening the library with the same substrate but differently labelled.

Considering the estradiol-hER interaction, it is clear that besides hydrogen bonding at both sides of the molecule, hydrophobic interactions, and more specifically aromatic interactions, will play a key role in molecular recognition. Hence, this recognition can be influenced by coupling an aromatic coloured or fluorescent label to the substrate.

These problems can be solved by using a radioactive ligand like [³H]-labelled estradiol in the work of Tozzi et al.⁵¹ With this approach, the changes to the ligand are minor but the molecule still is detectable at very low concentrations. The only drawback is that neither the equipment nor the experience needed for the successful implementation of this method is present in our lab.

For this reason, alternative screening methods were explored during this PhD that focussed on using unmodified ligands and on a direct multi-residue screening of the library. This was only possible thanks to the strong collaboration with the Laboratory of Separation Sciences of Prof. Dr. P. Sandra, and more specifically the scientific aid of Dr. F. Lynen and Drs. E. Van Hoeck. Also a significant contribution was made in

¹¹⁸ Shepherd, J.; Gale, T.; Jensen, K. B.; Kilburn, J. D. *Chem. Eur. J.* **2006**, *12*, 713-720.

solving this problem by Drs. S. Figaroli, who had joined our team in the context of the European Marie Curie sEnDiChem project.¹¹⁹

V.1. SPE tests

V.1.1. Tentagel based SPE material

In first instance, it was decided to use an approach similar to the one described by Tozzi et al.⁵¹ In the work of Tozzi, a radioactive ligand was incubated with the different resin-bound library members. By analysing the amount of ligand remaining on the beads after draining the solution, the most active member could be selected.

In our case, the concentration of the ligand before and after incubation was checked via LC-MS, making the use of radioactive ligands unnecessary. The concentration of a ligand could be determined by adding an internal standard, estradiol-d₃, to the incubation mixture. Another big advantage of this method was that the library members could be screened for affinity towards different EDCs in one and the same experiment. Surely, the different compounds were first separated on a C₁₈ column before the intensity of the mass signal was correlated to the concentration of the specific compounds.

Before screening the actual library, the affinity of Tentagel towards the EDC mixture was examined. Certainly, the data obtained from screening of the library can only be interpreted if suitable blank data are available. These blank data were obtained by adding a mixture of bisphenol-A (BPA), diethylstilbestrol (DES), estrone, estradiol (E₂), ethinylestradiol (EE₂) and testosterone (Tes) in water to the unmodified Tentagel beads. Testosterone, a non-estrogenic compound, was added to test for possible selectivity of the beads towards estrogenic compounds.

¹¹⁹ For more info about the sEnDiChem project please visit <http://www.sendichem.ugent.be>.

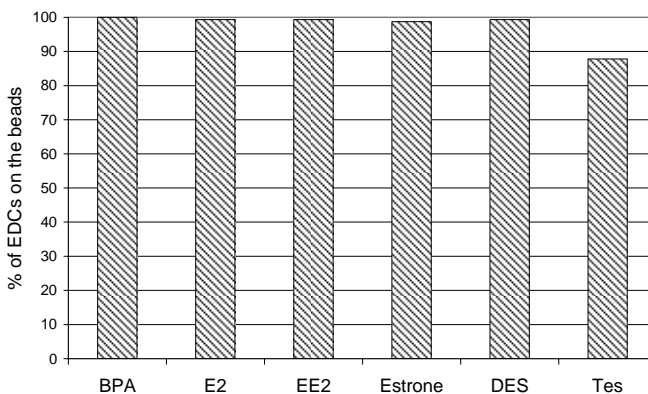
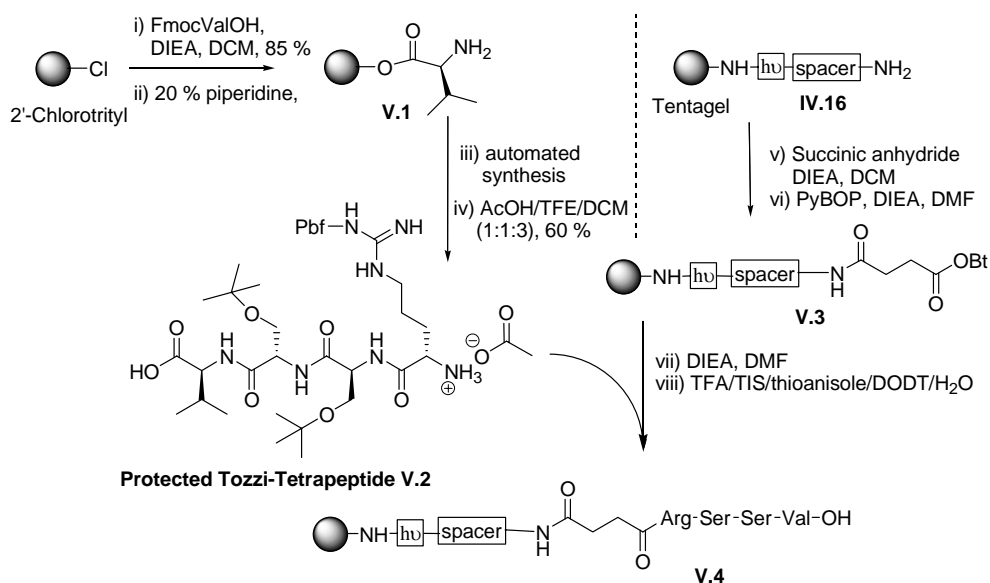


Figure V.1: Testing of Tentagel (▨) for affinity towards EDCs.

From **Figure V.1** it is clear that Tentagel is not a good solid support for affinity SPE testing. The Y-axis represents the percentage of EDCs that sticking to the beads. In the case of bisphenol-A, everything seems to be absorbed by the Tentagel. In general, 88 % to 100 % of the selected EDCs are trapped on the beads. Consequently, it will be difficult to see whether a receptor attached to Tentagel is able to bind EDCs because of this high background absorbance.

In order to tackle this problem, a way had to be found to wash away the non specific interactions without disturbing the specific [receptor-ligand] interactions. The difference between specific and non-specific interactions could only be seen if the data obtained with unmodified Tentagel were compared to Tentagel modified with a known EDC receptor. For this reason, the protected Tozzi-tetrapeptide $\text{H}_2\text{N-GABA-Arg-Ser-Ser-Val-OH}$ **V.2 (Chapter II.2.7.3)** was synthesised and attached to Tentagel. This linear peptide was described by Tozzi to have a K_d of 17 μM for estradiol in water (**Table II.1**).



Scheme V.1: Preparation of resin bound construct V.4.

Because Tozzi et al used a rather unusual N → C build up for their peptides and no experience with this synthesis approach was present in our lab, the Tozzi-tetrapeptide was first synthesised on 2'-chlorotritylresin via the standard C → N build up (**Scheme V.1**). Cleavage with AcOH/TFE/DCM generated the protected peptide segment that could be coupled to the pre-activated construct **V.3**. Finally, the side chains were deprotected and the product was characterised by ESI and HPLC.

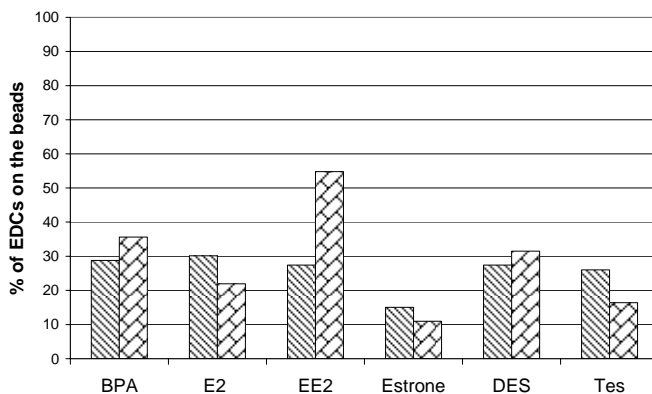


Figure V.2: Washing away the non specific interactions with 60 % MeCN in H₂O. The results for Tentagel (▨) and construct V.4 (▩) are shown.

As can be seen from **Figure V.2**, a washing step would be unsuccessful. The amount of EDCs that stay on construct **V.4** after washing with 60 % MeCN/H₂O, are not significantly higher than the amount of EDCs left on Tentagel. Hence, it was not possible to selectively wash away the non-specific interactions from the specific ones.

V.1.2. Alternatives for Tentagel

In order to circumvent the high background adsorption caused by the Tentagel matrix, a new resin was needed for these affinity SPE tests. A lot of well and less well known resins were tested for affinity towards EDCs (**Figure V.3**). Among them, the classical Merrifield resin, the polar polyacrylamide PEGA beads, a polyester CLEAR support (**Figure V.4**) and an amine-functionalised silica material. It appeared that Merrifield, silica and, in a lesser extent, CLEAR did not retain the EDCs too much.

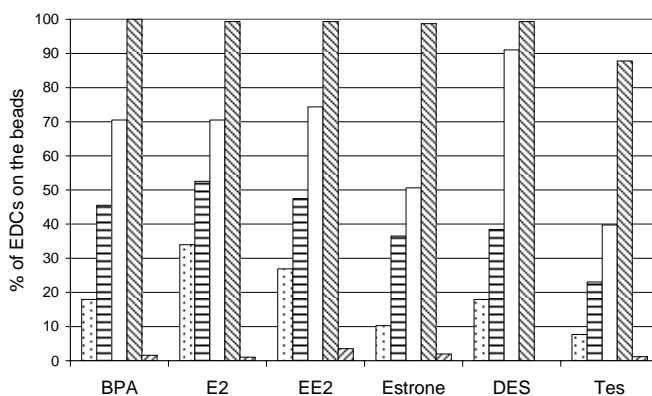


Figure V.3: Testing of the affinity towards EDCs of Merrifield (▤), CLEAR (▨), PEGA (□), Tentagel (▧) and aminopropylsilica (▩).

For the Merrifield resin, an explanation can probably be found in the fact that this apolar resin does not swell in aqueous media. Hence, the EDCs cannot penetrate the core and interact with the bulk of the polymer.

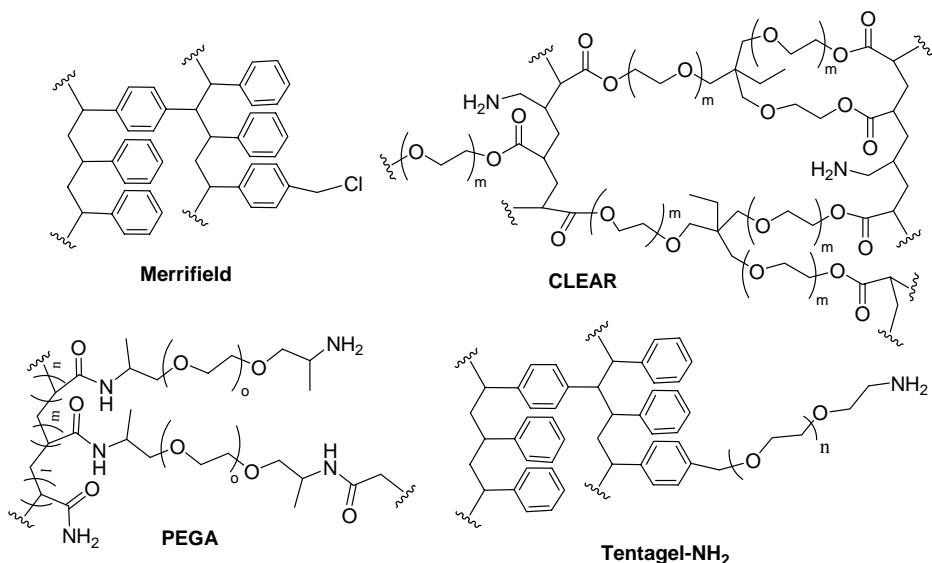


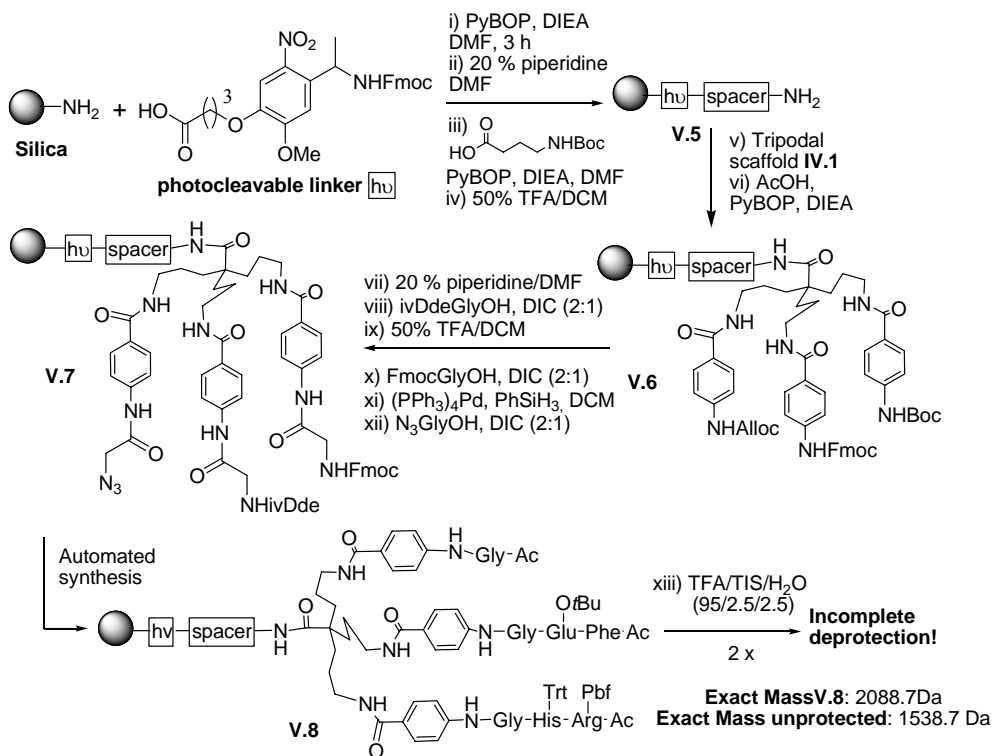
Figure V.4: Structures of different solid supports.

CLEAR is a resin constituted of polyethylene glycol chains linked via ester bonds resulting in a highly polar polymer swelling in a broad range of solvents, including water.¹²⁰ Though it has been described as a useful alternative to Tentagel, it was found that the synthesis on this CLEAR resin was more difficult. Certain acetylations failed to proceed quantitatively and for this reason no further effort was put in optimising the use of this resin.

Besides the fact that the tested EDCs already stick to a high degree to PEGA, this resin was not used due to its tendency to become statically charged. PEGA is provided as a suspension in MeOH but upon drying, the resin becomes impossible to handle and basic actions like weighing are very difficult.

Via this elimination process, aminopropylsilica remained the only suitable solid support. In a test sequence, the tripodal scaffold was coupled to photolinker-modified silica and one member of the library was synthesised (**Scheme V.2**). Not only was the overall purity of the protected member less than on Tentagel (due to a major deletion of Leu and Met sequences) but more importantly, deprotection of the side chains was unsuccessful (**Figure V.5**). Even after a second treatment with a higher percentage of TFA, the deprotection was not complete. This is probably due to the oxygen rich backbone of silica. These oxygens can be protonated by TFA lowering the effective $[H^+]$.

¹²⁰ Kempe, M.; Barany, G. *J. Am. Chem. Soc.* **1996**, *118*, 7083-7093.



Scheme V.2: Testing silica as a suitable solid phase.

In view of these results, it became clear that there was no solid support available that combines good synthetic properties with a low background absorbance of EDCs. Consequently, a completely different approach was needed to screen the library for affinity towards EDCs.

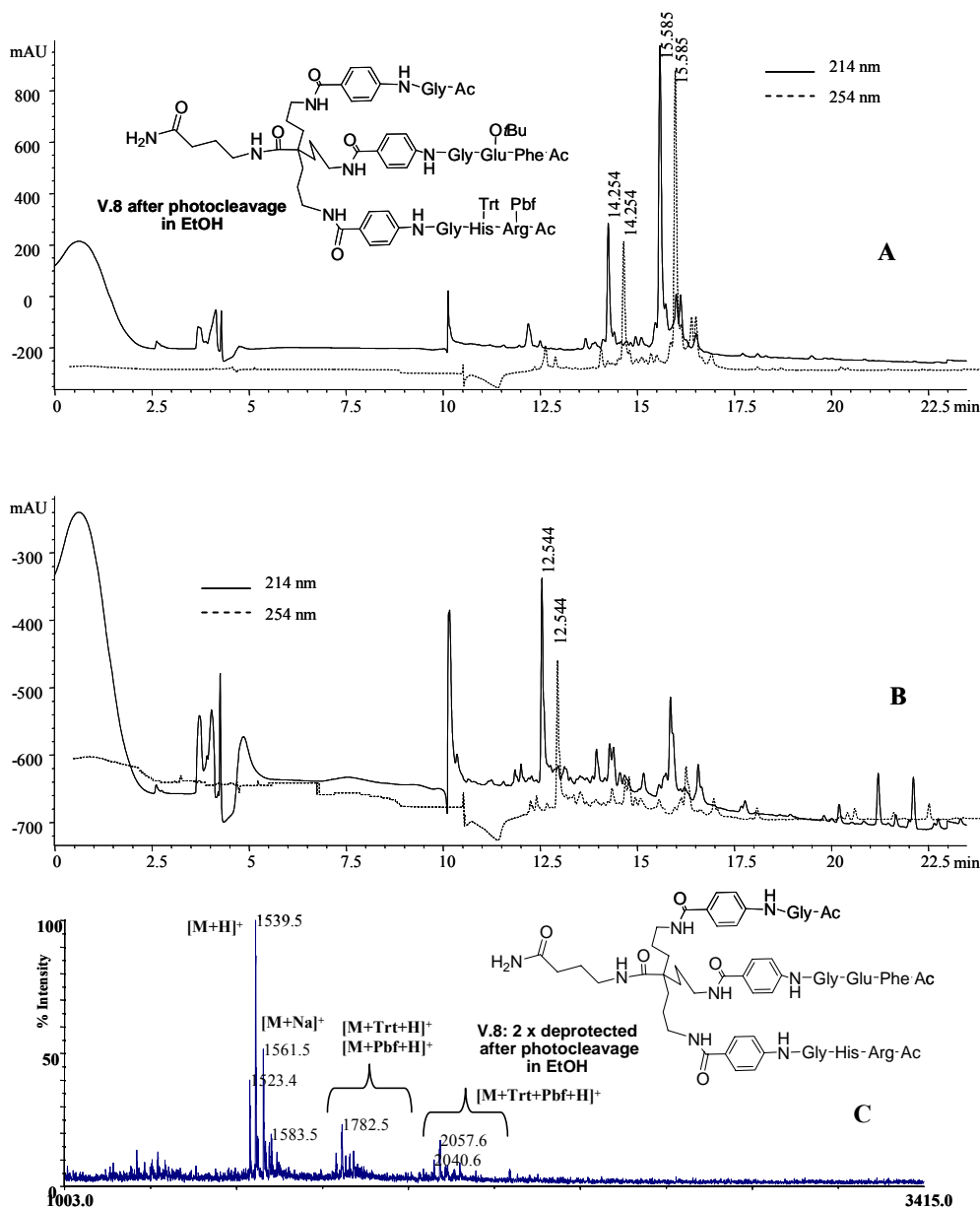


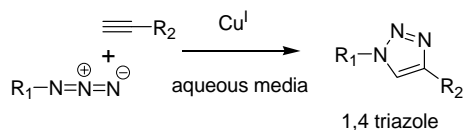
Figure V.5: HPLC of protected V.8 after photocleavage in EtOH (A). HPLC of 2x deprotected V.8 after photocleavage in EtOH (B). MALDI-TOF of 2x deprotected V.8 after photocleavage in EtOH (C).

V.2.Affinity LC

V.2.1. Development of a new estradiol column

In the previous experiments, the receptor was immobilised on the solid support while the ligands were present in solution. It was decided to reverse this order by binding a ligand to a solid support. More specifically, if silica is used as a solid phase, a column can be packed using this silica-bound substrate. Consequently, when the receptors are sent over the column, the one that shows the highest retention time should have the strongest affinity towards the ligand. This principle is called affinity LC.

For the development of a new column material, a suitable ligation reaction had to be developed to couple a ligand to the silica material. The copper(I)-catalyzed azide-alkyne cycloaddition seemed very interesting for this purpose (**Scheme V.3**). This Cu^{I} catalysed addition received considerable attention during the past 7 years as it is one of the click reactions described by Sharpless et al.¹⁰⁴ In this paper, the Cu^{I} catalysed azide-alkyne cycloaddition is described as the ‘cream of the crop’ of a class of reactions giving high yields, are very specific and can proceed in benign solvents like H_2O .

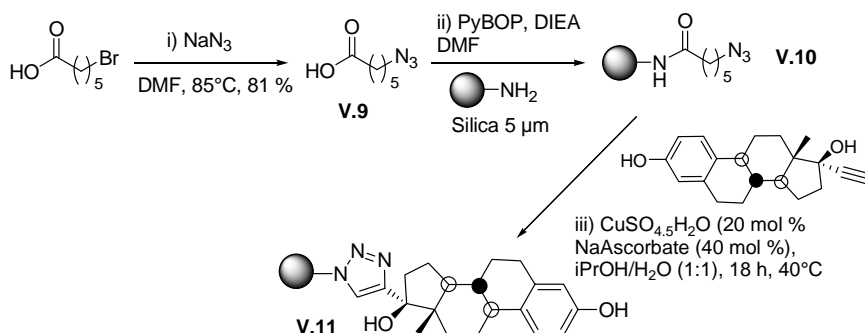


Scheme V.3: Cu^{I} catalysed addition of an azide to an alkyne.

Applied to our specific situation, it was decided to attach the alkyne-bearing ethinylestradiol (EE_2) to an azido-functionalised silica material via the Cu^{I} catalysed addition (**Scheme V.4**). The azido-functionalised silica was obtained after acetylation of aminopropylsilica with 6-azido-hexanoic acid **V.9**. This azide was prepared via a $\text{S}_{\text{N}}2$ substitution of 6-bromo-hexanoic acid with NaN_3 in good yields.¹²¹

¹²¹ Grandjean. *J. Org. Chem.* **2005**, *70*, 7123-7132.

The click reaction itself was performed in a 1:1 *i*PrOH/H₂O mixture at 40 °C using catalytic amounts of Cu^{II} that was reduced *in situ* to Cu^I by an excess of sodium ascorbate. After overnight reaction, the addition was finished as witnessed by the disappearance of the azide peak (~ 2100 cm⁻¹) in the corresponding IR spectrum.



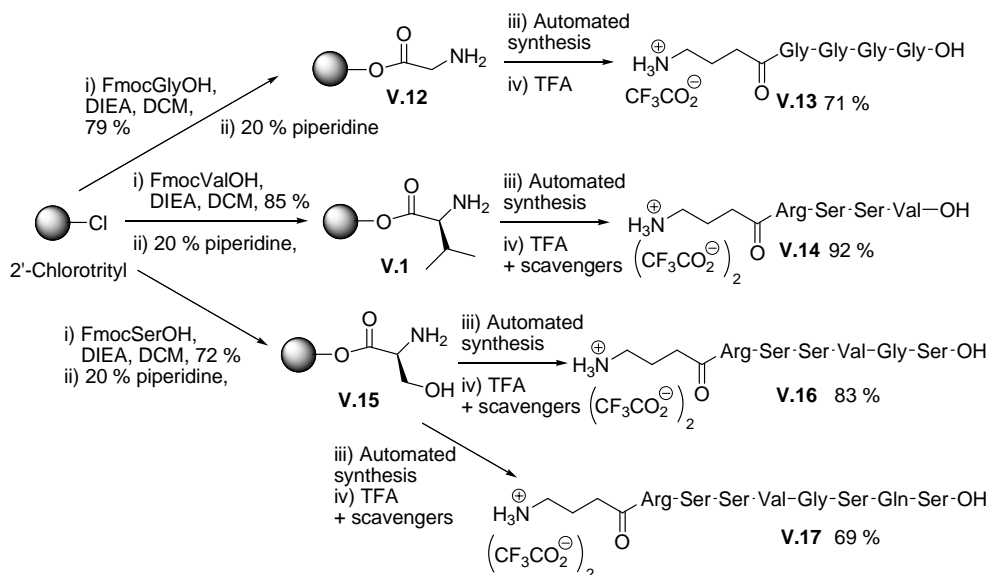
Scheme V.4: Preparation of an estradiol column.

By packing the silica material **V.11** into a column (2.1 x 150 mm), an estradiol affinity column was obtained that could be used for the screening of the library.

V.2.2. Evaluation of the estradiol column

Because this approach was quite new, no real literature precedents existed and it was decided to first validate this column. This could be achieved by testing the peptides described by Tozzi et al.⁵¹ For this reason, they were synthesised on the 2'-chlorotrityl resin via automated synthesis (**Figure IV.3**). Serving as a 'blank peptide', the tetraglycine derivative **V.13** was synthesised in a similar fashion.

The retention times of the peptides were monitored via LC-MS. A flow of 0.2 mL/min was applied under isocratic conditions. Buffered H₂O at pH 7.4 was used as eluent.



Scheme V.5: Synthesis of the different Tozzi peptides.

It was expected from **Table II.1** that the Tozzi-hexapeptide **V.16** should elute first followed by the Tozzi-octapeptide **V.17** and then the Tozzi-tetrapeptide **V.14**. It must be noted that the differences in K_d values of the different peptides are small and the error margins were not taken into account.

Figure V.6 clearly shows that an increase in retention times is observed when the data of the Tozzi peptides are compared to the retention of the 'blank' tetraglycine derivative **V.13**.

The reversed order of elution ($V.14 < V.16 < V.17$ instead of $V.16 < V.17 < V.14$) probably can be ascribed to the poor difference in K_d values of the three peptides. Nevertheless, based on these results, it should be possible to recognise compounds with a certain affinity for estradiol.

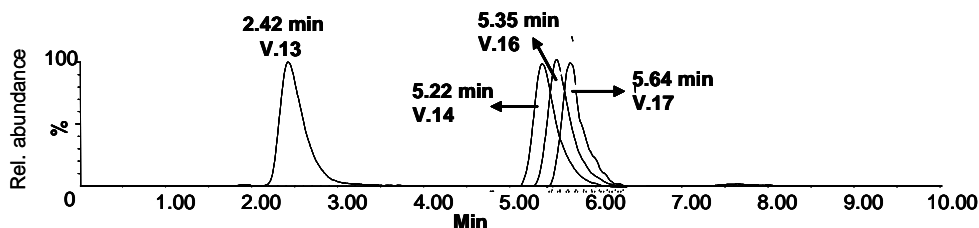


Figure V.6: Retention times of the different Tozzi peptides compared with the blank tetraglycine peptide. The retention times were monitored via LC-MS.

V.2.3. Testing of the library via affinity LC

The 120 members could easily be tested using the developed affinity method. For each member, a small sample (1 mg resin or less) was suspended in 100 μ L H_2O and irradiated at 360 nm for 3 h. After the photocleavage, the resin was washed with water and the resulting 400 μ L was diluted 10 times before transferring it into a HPLC vial. These vials were collected in the rack of an auto sampler allowing a rapid screening of the 120 members.

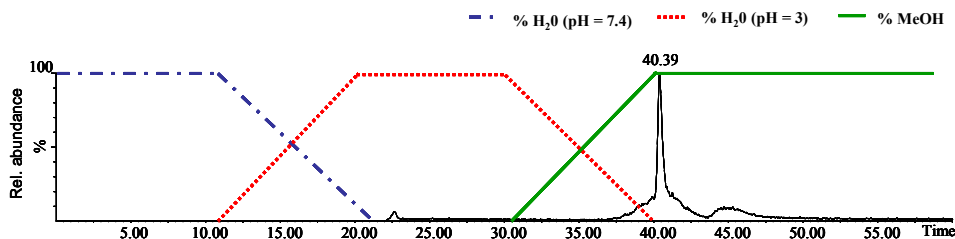


Figure V.7: Optimisation of the elution conditions for one library member. Retention time was monitored via LC-MS.

Before the whole library was screened, the elution and detection parameters were optimised by injecting one member (Figure V.7). Using the same isocratic conditions as for the screening of the Tozzi peptides, no signal was observed. The receptor

seemed-to be sticking to the estradiol column. In an attempt to disturb the hydrogen bonding, the pH was lowered to 3 but still no signal was observed. More drastic elution conditions were then applied by a gradient to 100 % MeOH. Changing the solvent from H₂O to MeOH implied that the hydrophobic interactions were disturbed. This eventually led to the elution of the receptor.

Excited by these preliminary results, a big increase in affinity compared to the Tozzi peptides was observed, the next step was taken by screening the whole library. Another ‘blank’ molecule was prepared by attaching six glycine residues to construct **IV.17** via automated synthesis to evaluate the effect of the scaffold.

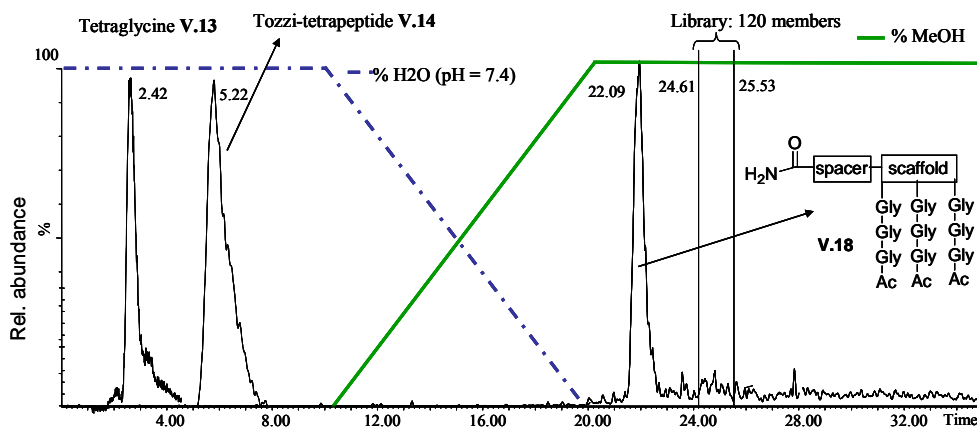


Figure V.8: Screening of the library. Retention times were monitored via LC-MS.

The results obtained from these screening are shown in **Figure V.8**. The first surprising fact is that blank peptide **V.18** has a higher retention time than the Tozzi-tetrapeptide **V.14**. This would mean that the tripodal scaffold, substituted with six glycines is a better receptor than the Tozzi peptide? In addition, there is no member of the library that really jumps out, all the receptors have a similar retention time and elute between 24.61 min and 25.53 min.

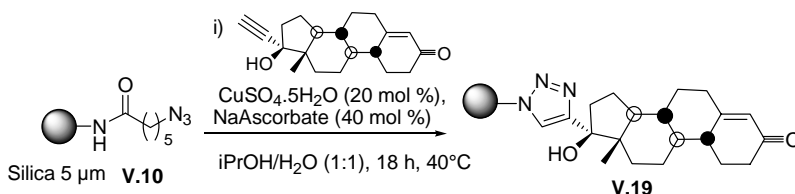
When looking at these data, the excitement disappeared and made place for doubt. Questions rose about what really was happening on the column. The initial thought was that the receptors would form a complex with the silica-bound estradiol and depending

on the strength of this complex, a shift in retention time would be observed. However, it should be taken into account that a separation based on polarity is also possible. Certainly, a new stationary phase is formed when clicking the EE₂ to the azido-functionalised silica particles. According to our results, instead of an estradiol affinity column, this new phase can best be compared with a standard C₁₈ phase but with different properties.

These indecisive results made it necessary to design a new set of experiments to determine if the separation is based on polarity and/or affinity.

V.2.4. Development of a norethindrone column

The first alternative experiment that crossed our mind was the preparation of a new type of column, to which the receptors should have no or weak affinity. By clicking the progesteron 19-norethindrone to azido-functionalised silica material (**Scheme V.6**), a new non-estrogenic column was prepared.



Scheme V.6: Preparation of a norethindrone column.

The library was designed to show no or weak affinity towards non-estrogenic compounds, so low retention times should be obtained when injected over the norethindrone column. However, the same window in retention times was observed. In **Figure V.9** the example is shown for one library member. Of course, this could be due to a lack of selectivity. But when the Tozzi-tetrapeptide **V.14** was injected, a similar retention time as on the estradiol column was observed.

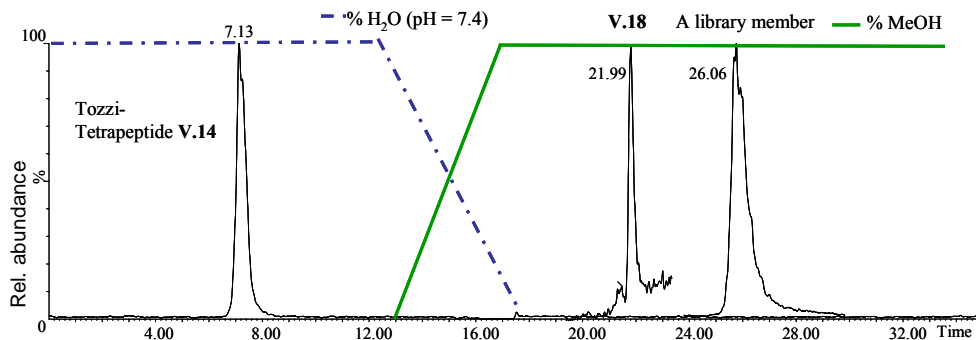


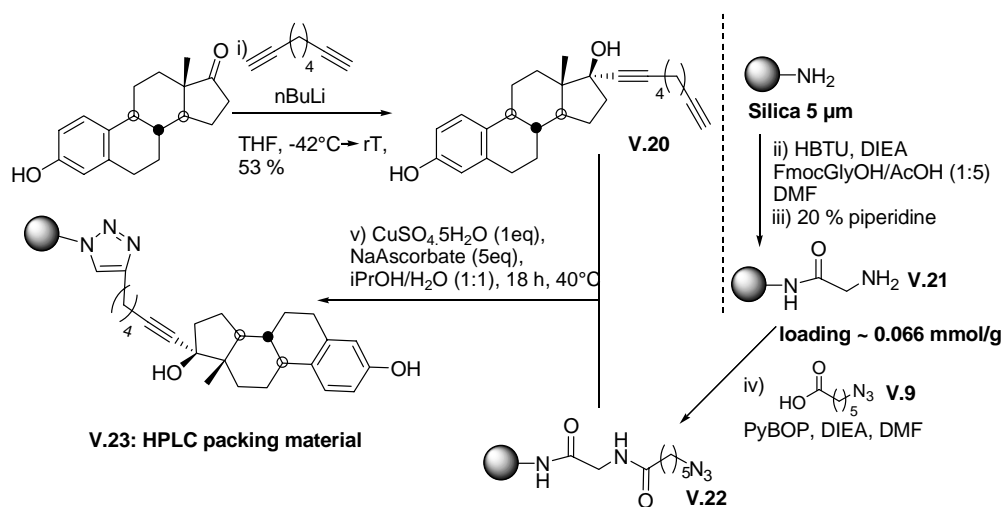
Figure V.9: Screening on the norethindrone column. Retention times were monitored via LC-MS.

Confused by the fact that even the Tozzi-tetrapeptide **V.14** failed to show any selectivity, alternative methods were explored to determine the exact nature of this chromatographic experiment.

V.2.5. Competition experiments

Assuming that the retention time of a library member is the consequence of a complex formation between the silica-bound-estradiol and the receptor, then this retention time should be influenced when there is less [estradiol_{silica}-receptor] complex. This can be achieved in the same experimental set up but now some estradiol has to be added to the eluent. Indeed, then a [estradiol_{solution}-receptor]-complex can be formed, complexing the receptor up in the eluent and consequently causing a decrease in retention time.

No shift was however observed upon adding estradiol to the aqueous buffer. The poor solubility of estradiol in H₂O limited the amount that could be added. Maybe there was just not enough estradiol present in the eluent to be able to compete with the large amount of silica-bound-estradiol (loading ~ 0.6-0.7 mmol/g). These problems could be tackled if a new column was developed with a lower loading.



Scheme V.7: Development of a new estradiol column with a lower loading.

Next to lowering the loading of the new column, it was also decided to insert a spacer between estradiol and the triazole function to minimise possible effects of the triazole on complex formation. This was done by first deprotonating 1,7-octadiyne with $n\text{BuLi}$ (Scheme V.7).¹²² An excess of this carbon nucleophile was added to estrone yielding 53 % of the desired derivative **V.20**. It seemed impossible to separate the estradiol derivative **V.20** from the starting compound, however, since estrone does not possess an alkyne function, separation between the two compounds was unnecessary.

The loading of the aminopropylsilica was lowered by first coupling FmocGlyOH in the presence of 5 equivalents of AcOH, yielding a loading of only 0.066 mmol/g. After deprotection of the Fmoc group, the azido-hexanoic acid was coupled using PyBOP.

Clicking again proceeded very smoothly as monitored by IR spectroscopy. After washing the silica thoroughly, the material was packed into an HPLC column.

¹²² Ali, H.; Ahmed, N.; Tessier, G.; van Lier, J. E. *Bioorg. Med. Chem. Lett.* **2006**, *16*, 317-319.

Sadly enough, the new material appeared to possess too little estradiol to be able to retain our library members. A few compounds were tested and they all eluted with the solvent peak, showing little or no retention. Hence, further competition experiments were made impossible.

V.3. Reconsidering the SPE test

Though the developed affinity LC method allowed a fast screening of the synthesised library while only a small sample of each compound was needed, it failed to deliver decisive results. It was not clear whether the obtained retention times could be related to a certain affinity for estradiol. In search of a second screening method that could evaluate these results, we looked back at the initial experiments in **Chapter V.1**. There the problem was the high background EDC adsorbance by Tentagel. On the other hand, materials that showed less retention of the EDCs, could not be used due to practical drawbacks concerning the synthesis of the library on these materials.

One way of dealing with this situation is by performing the synthesis on Tentagel and then transferring the members to an inert solid phase, like silica. In this way, the library members could be synthesised via the already established protocols on Tentagel, but their activity in an SPE cartridge could be tested on silica, bypassing any background absorption by the solid phase.

V.3.1. General strategy

Until now, a photocleavable linker was used to cleave the synthesised compounds from the beads. Photocleavage, however, yields a carboxamide that offers few possibilities for recoupling to another solid support (**Figure V.10**). Consequently, recoupling to another solid phase like silica is impossible unless a new chemical functionality is introduced. This anchor moiety should not only ensure a smooth coupling but at the same time it has to be inert to the applied protocols for synthesising a library member. An extra requirement is that the ligation reaction has to be compatible with the unprotected side chain functionalities of the library members.

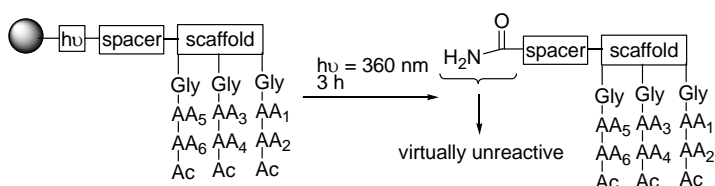


Figure V.10: Photocleavage yields an unreactive carboxamide.

All these stringent conditions are fulfilled when the Cu^{I} -catalysed cycloaddition between an azide and an alkyne is used. Since a protocol for the synthesis of azide-functionalised silica was already established, the library members had to be equipped with an alkyne functionality.

To test if the affinity LC method was able to identify the best receptor, two members of the library were scaled up for subsequent coupling to silica. From the affinity LC experiments, the member with the lowest and the member with the highest retention time were chosen (**Figure V.11**). In this way, the data obtained from the affinity LC could be correlated to the SPE behaviour of our two compounds. In other words, library member **V.25** should retain less EDCs than member **V.24** when coupled to silica.

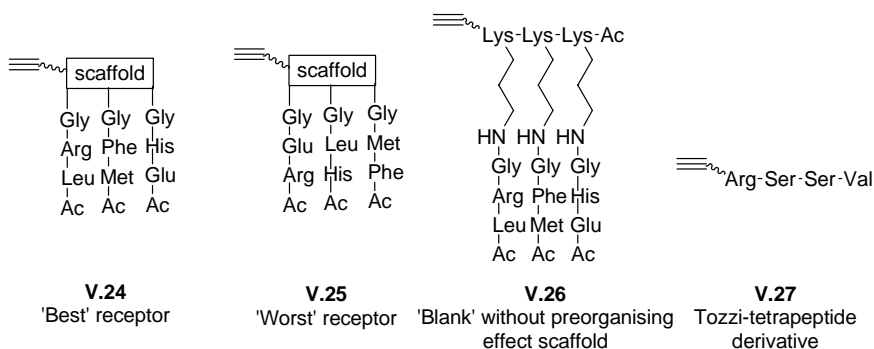


Figure V.11: The 'best' and the 'worst' receptor as determined via affinity LC.

To determine the effect of the tripodal scaffold on the efficiency of the receptors, a derivative of the 'best' receptor **V.24** should be synthesised. In derivative **V.26**, the three benzylic cores are replaced by the side chains of a Lys residue. Any aromatic interaction is thus excluded, resulting in three peptide chains that are not spatially

constrained. By comparing the SPE results obtained with **V.24** and **V.26**, the influence of the scaffold should become clear.

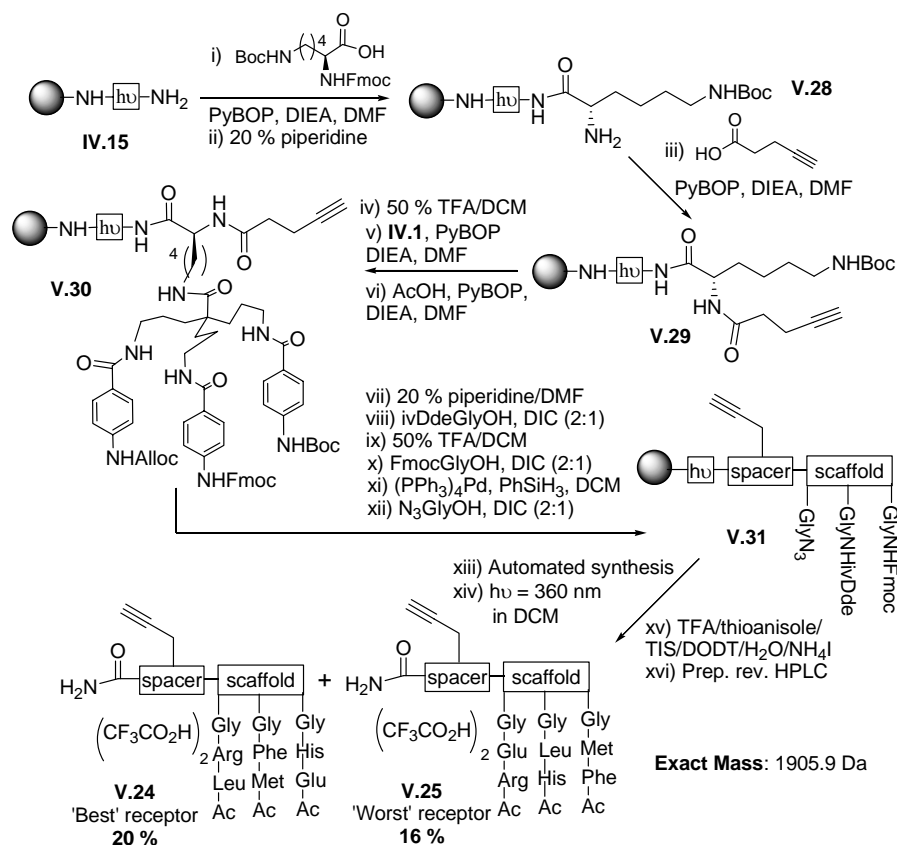
To correctly interpret the data obtained with the SPE tests, an alkyne derivative of the Tozzi-tetrapeptide (**V.27**) should be synthesised. After clicking it to silica, the construct can serve as a calibration point for the SPE tests.

V.3.1.1. Synthesis of V.24 and V.25: incorporating an alkyne via the Lys approach

One way of incorporating an alkyne is by replacing the current spacer with a Lys residue. Indeed, the side chain of Lys can be regarded as a distancing arm while the α -amine group can be used to couple pentynoic acid.

Starting from Tentagel equipped with the photocleavable linker, first a FmocLys(Boc)OH residue was coupled (**Scheme V.8**). After Fmoc deprotection of the α -amine, the alkyne moiety was introduced via coupling of pentynoic acid. This was followed by removing the Boc group with TFA, yielding a free ϵ -amine that could be used as anchoring point for the tripodal scaffold **IV.1**.

After selectively capping the remaining free Lys- ϵ -amines with AcOH and PyBOP, the orthogonality scheme was adapted by coupling the Gly derivatives as their symmetrical anhydrides. Construct **V.31** was then used as the starting point for the automated synthesis. Only the ‘best’ and the ‘worst’ members (as determined via affinity LC, *vide supra*) were synthesised.



Scheme V.8: Synthesis of the alkyne modified receptors.

Once the two receptors were prepared on bead, they still had to be cleaved from the resin. For this purpose, the resin was suspended in DCM and irradiated with light at $\lambda = 360$ nm for 18 h. This was repeated five times in order to obtain yields as high as possible. After pooling the organic fractions, the solvent was removed in vacuo. Subsequently, the side chain protecting groups, including the oxidised Met, were deprotected with TFA and scavengers.

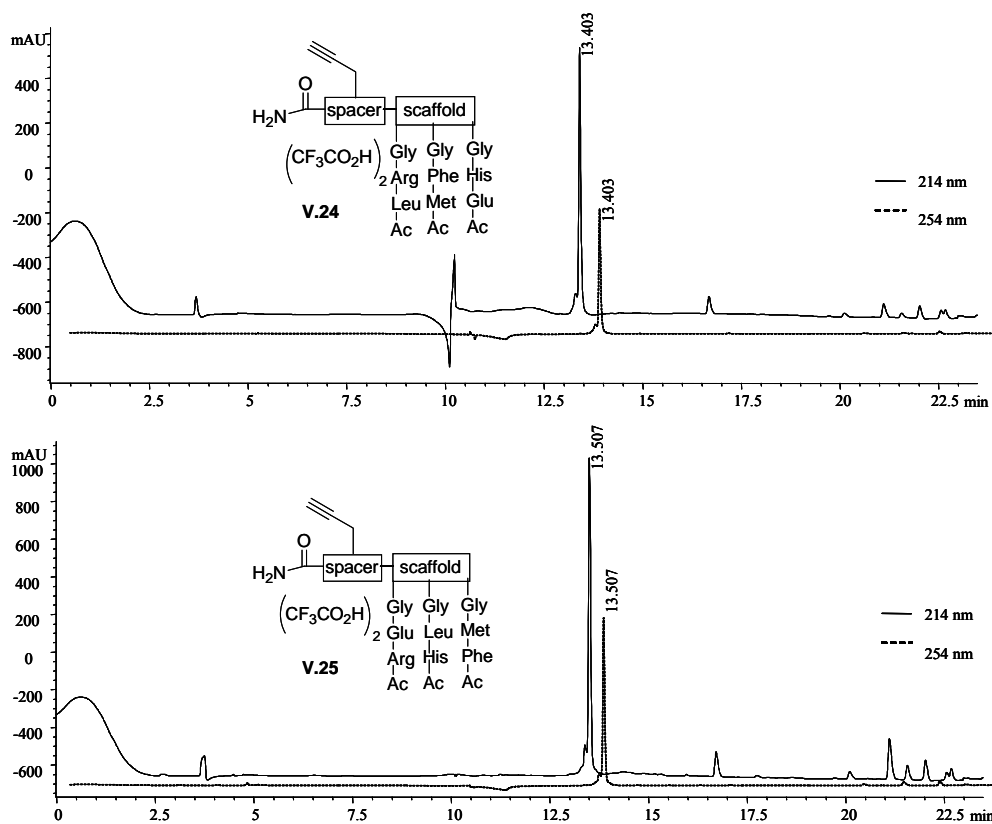


Figure V.12: HPLC chromatogram of V.24 and V.25 after prep. HPLC.

Finally the two receptors were purified by preparative reversed phase HPLC. At the end 4.2 mg (20 % yield) of the ‘best’ receptor **V.24** and 3.5 mg (16 % yield) of the ‘worst’ receptor **V.25** were obtained in good purity (**Figure V.12**) and their identity was confirmed by MALDI-TOF (**Figure V.13**).

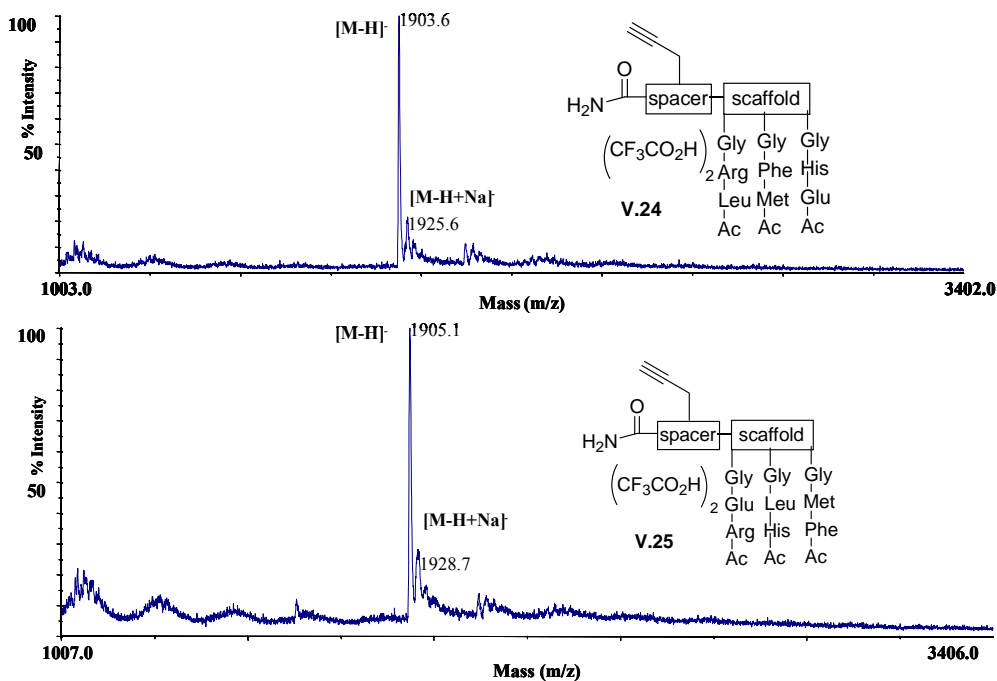


Figure V.13: MALDI-TOF spectrum of V.24 and V.25 after prep. HPLC.

V.3.1.2. Synthesis of V.26: the hydrazine linker approach

A little bit disappointed by the yields obtained in **Scheme V.8**, it was decided to develop a new route for the synthesis of the non-constrained **V.26**. Though the photocleavable linker is an excellent tool for monitoring reactions on solid phase, it becomes less efficient when an up-scaling is necessary, in view of the lower cleavage yields.

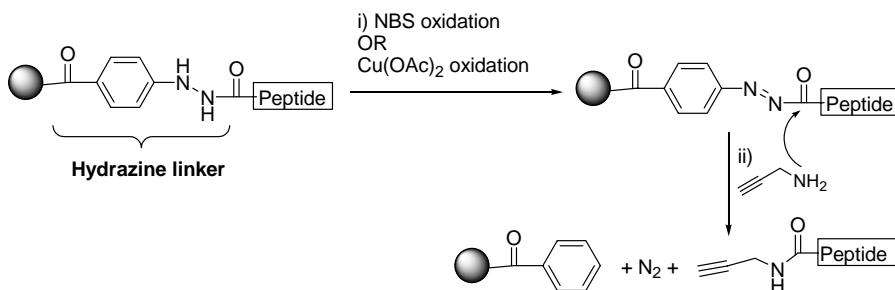
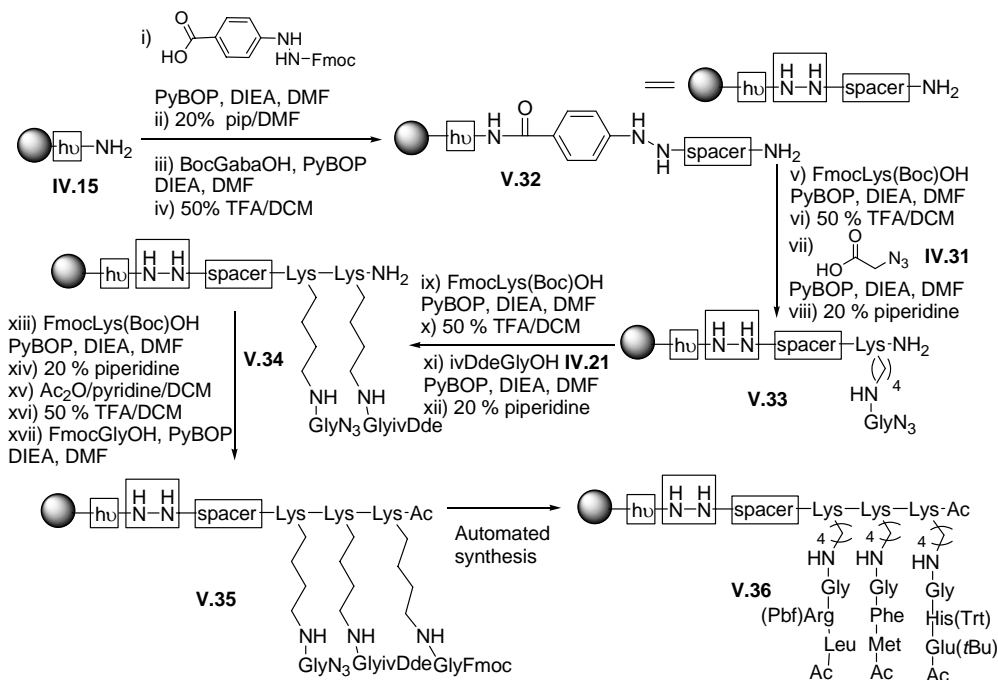


Figure V.14: Hydrazine linker: principle of cleavage.

To overcome this problem, a hydrazine linker was tested for the synthesis of **V.36**. As shown in **Figure V.14**, the synthesised peptide can be cleaved from the resin after oxidation of the hydrazine.¹²³ The obtained activated carbonyl reacts readily with a great variety of nucleophiles.¹²⁴ In this way, not only can good cleavage yields be obtained but at the same time the desired alkyne moiety can be introduced if propargylamine is used as the nucleophile.

¹²³ a) Millington, C. R.; Quarrell, R.; Lowe, G. *Tetrahedron Lett.* **1998**, 39, 7201-7204. b) Stieber, F.; Grether, U.; Waldmann, H. *Angew. Chem. Int. Ed.* **1999**, 38, 1073-1077.

¹²⁴ Woo, Y. H.; Mitchell, A. R.; Camarero, J. A. *Int. J. Pept. Res. Therap.* **2007**, 13, 181-190.



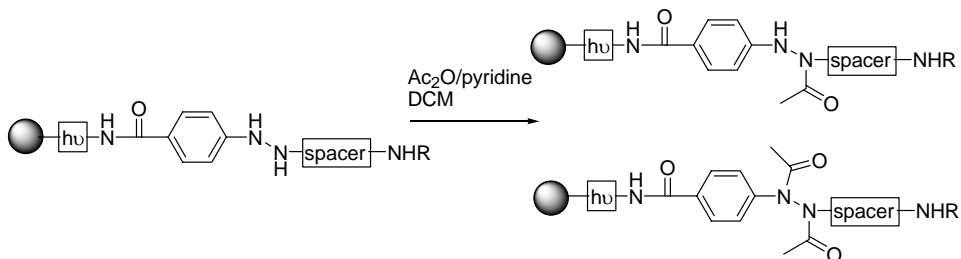
Scheme V.9: Preparation of the non-constrained construct V.36.

For the solid phase synthesis of **V.36**, a dual linker strategy was used (**Scheme V.9**). Though the hydrazine linker was used for the quantitative cleavage from the resin, the photocleavable linker still was incorporated to allow fast reaction monitoring.

Starting from construct **IV.15**, the hydrazine linker was introduced by coupling Fmoc-hydrazinobenzoic acid with PyBOP. Subsequently, a spacer arm was attached and next the first FmocLys(Boc)OH was coupled. After deprotection of the side chain, azidoglycine **IV.31** could be coupled. Another FmocLys(Boc)OH was then coupled and when the Boc group of this side chain was removed, ivDdeGlyOH (**IV.21**) was coupled. The incorporation of the final FmocLys(Boc)OH was followed by Fmoc deprotection of the α -amine. This was first capped before the side chain was removed with TFA and FmocGlyOH could be finally coupled to give Tentagel-bound **V.35**.

By implementing the photocleavable linker, a side reaction that occurred during the capping step (xv in **Scheme V.9**) could be characterised. Indeed, MALDI-TOF analysis showed that mono- and especially di-acetylation of the hydrazine linker itself had

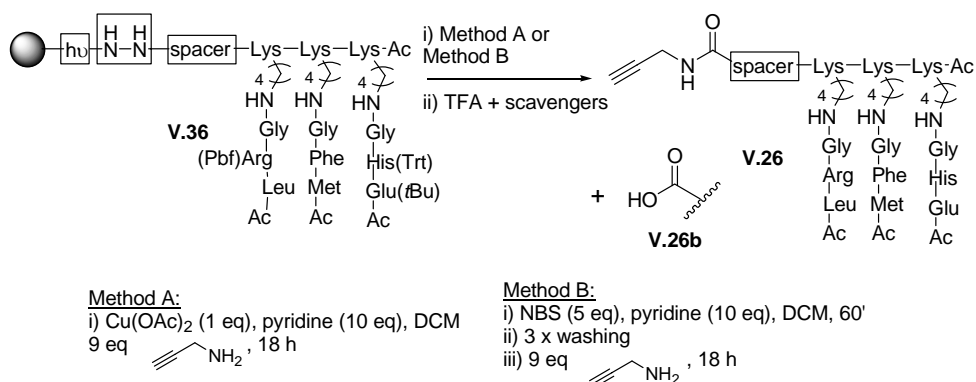
occurred during the capping step. This side reaction is mentioned in literature and future capping should proceed with the more sterically hindered pivalic anhydride.¹²⁵



Scheme V.10: Acetylation of the hydrazine linker.

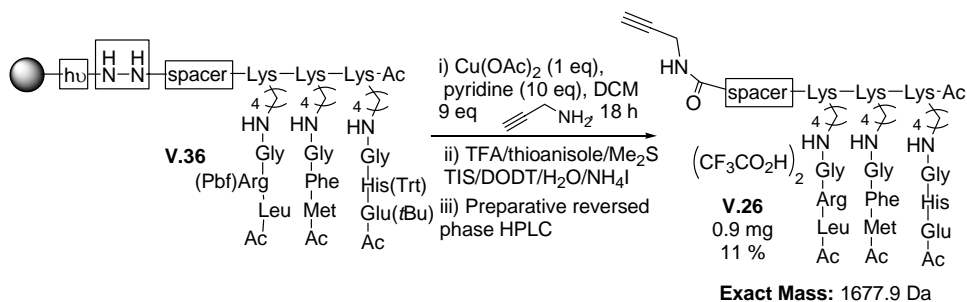
The oxidative cleavage can be carried out by using a one-step process with Cu(OAc)₂ in the presence of a suitable nucleophile (method A), or in a two-step process with N-bromosuccinimide and subsequent addition of the nucleophile (method B). In both cases, the reactions are performed open to the air. Both procedures were examined (**Scheme V.11**) and it was found that in the two cases, the hydrolysed side product **V.26b** was present. However, the two step process gave rise to a much more substantial amount of free carboxylic acid **V.26b** than the Cu^{II} mediated cleavage. This is probably due to the intermediate washing steps needed to remove the excess of NBS.

¹²⁵ Peters, C.; Waldmann, H. *J. Org. Chem.* **2003**, 68, 6053-6055.



Scheme V.11: Optimising the cleavage conditions.

Based on these results, method A was chosen for the cleavage of **V.36**. Though it is possible that the thioether of Met is oxidised during the cleavage and consequently consumes some of the Cu^{II} needed for the cleavage, this does not cause a problem because the Cu^{I} is re-oxidised by oxygen from the air.



Scheme V.12: Cleavage, side chain deprotection and purification.

After side chain deprotection and reduction of the Met(O), the peptide was purified by preparative reversed phase HPLC to give 0.9 mg (11 %) of the desired compound (**Scheme V.12**). The identity of the compound was confirmed via MALDI-TOF analysis (**Figure V.15**) but due to the low amount of obtained product, no HPLC analysis was performed to evaluate the purity.

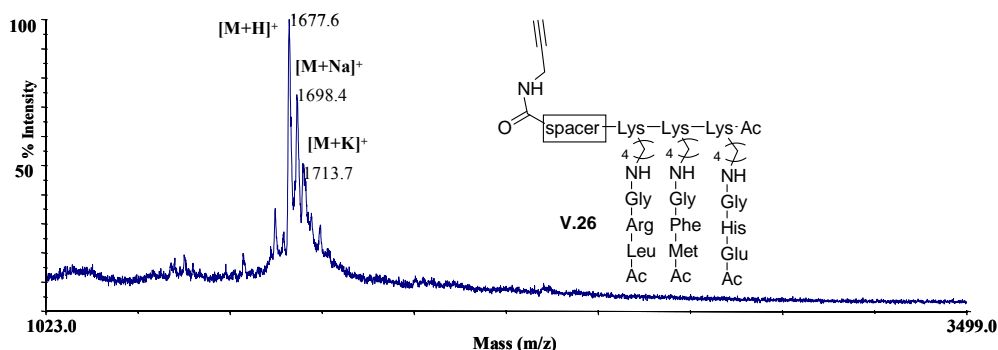
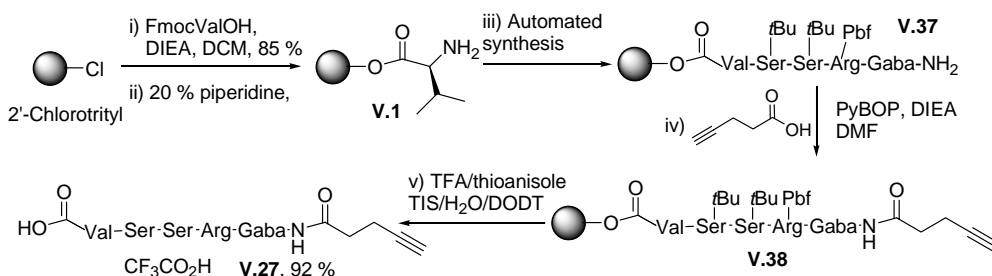


Figure V.15: MALDI-TOF spectrum of compound V.26.

In conclusion, the at first sight promising hydrazine linker did not give a significant improvement in yield. Certain factors can be invoked for this ineffectiveness: a) capping and thus deactivation of the linker by Ac_2O and b) hydrolysis of the oxidised linker during the cleavage. Nevertheless, the desired compound **V.26** was obtained in a sufficient amount and purity for further ligation experiments.

V.3.1.3. Synthesis of the Tozzi-tetrapeptide V.27

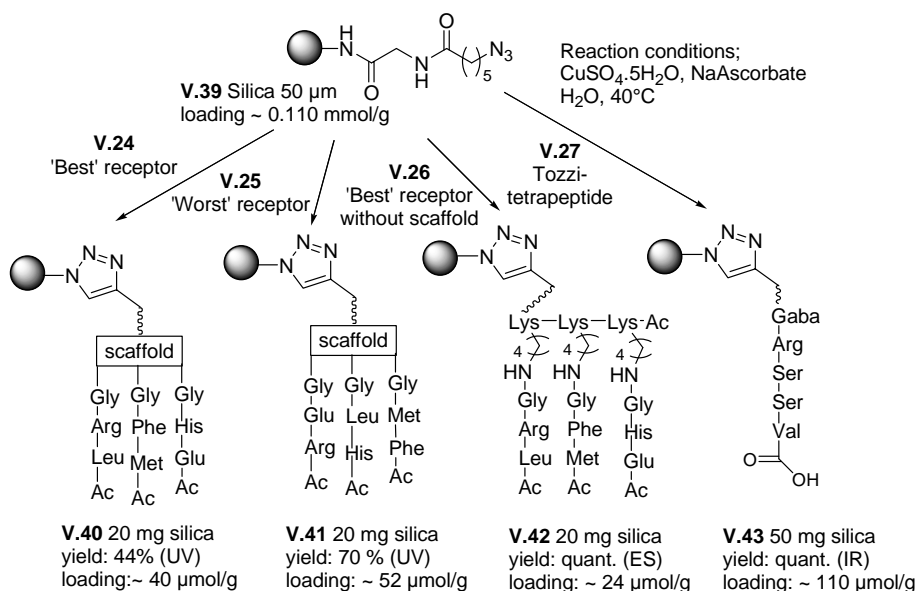
The alkyne containing tetrapeptide **V.27** could be synthesised via standard automated synthesis. The alkyne group was introduced in the final step by a manual capping of the sequence with pentynoic acid (**Scheme V.13**). Cleavage with TFA and scavengers yielded peptide **V.27** in a very good yield (92 %).



Scheme V.13: Synthesis of tetrapeptide V.27.

V.3.2. 'Clicking' of the alkyne derivatives to silica

Scheme V.14 shows the preparation of four different SPE materials based on a silica framework. Starting from azido-functionalised silica with a controlled loading of 0.110 mmol/g, the four alkyne components were attached via the Cu^I-catalysed cycloaddition. The difficulty resided in the determination of the loading of the obtained materials, which is necessary for the correct interpretation of the results.



Scheme V.14: 'Clicking' of the alkyne derivatives to silica.

Only in the case of the alkyne Tozzi-tetrapeptide **V.27** sufficient material was available to use an excess of alkyne. This resulted in a quantitative reaction as proved by a complete disappearance of the azide absorption in the IR spectrum. Consequently, a loading of $110\text{ }\mu\text{mol/g}$ was obtained.

Because there was not enough material to use an excess of **V.24** and **V.25** in the 'click' reaction, the corresponding loading values were determined with UV-spectroscopy. First a UV calibration curve was determined at $\lambda = 265$ nm. Using this calibration curve, the concentration of the two receptors in the remaining solution could be determined after the reaction. In this way, an estimate of the amount of compound that was covalently linked to the silica material could be made. This resulted in a loading of $\sim 40\text{ }\mu\text{mol/g}$ for **V.40** and $\sim 52\text{ }\mu\text{mol/g}$ for **V.41**.

This approach could not be applied when **V.26** was coupled to the silica material. Due to the presence of only one aromatic moiety (Phe), the absorbance at 254 nm was too weak to give accurate UV measurements. The calibration curve was thus recorded at 214 nm. However, the Cu^{II} and sodium ascorbate matrix of the reaction resulted in a

high background at this wavelength, making concentration determination via UV impossible.

In an attempt to tackle this problem, the amount of catalyst added was raised (20 eq instead of 0.2 eq) and the mixture was shaken for 4 days. The reaction was followed by ESI and after 4 days, no signal of **V.26** was observed anymore. From this, the conclusion was drawn that all of the starting alkyne component had reacted leading to a loading of $\sim 24 \mu\text{mol/g}$.

V.4. Results of the SPE tests

The different materials (**V.40** \rightarrow **V.43**) were tested by incubating them with an aqueous solution containing bisphenol-A (BPA), diethylstilbestrol (DES), estrone, estradiol (E_2), ethinylestradiol (EE_2) and testosterone (Tes). Testosterone, a non-estrogenic compound, was added to test for possible selectivity of the SPE materials towards estrogenic compounds. After incubation, the concentrations of the different compounds in the solution were determined by LC-UV. From these values, the amount that was trapped on the SPE materials was calculated. For each material, the loading and the amount of tested material were taken into account.

The properties of the synthesised materials were compared with OASIS. This commercial SPE cartridge is used universally in the clean-up of samples containing EDCs.¹²⁶

¹²⁶ Lopez de Alda, M. J.; Barcelo, D. *J. Chromatogr. A* **2001**, 938, 145-153.

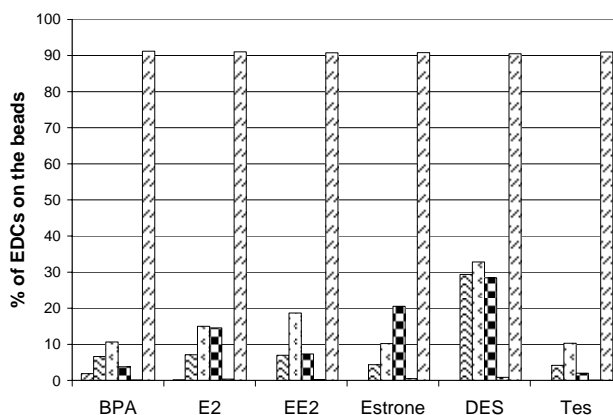


Figure V.16: SPE results: silica (▨), V.40 (▩), V.41 (▧), V.42 (▣), V.43 (▤) and OASIS (▨).

From **Figure V.16** it is clear that the materials loaded with the two receptors (**V.40** and **V.41**) show an increased affinity towards estrogenic compounds when compared to the unmodified silica. More surprising is that the receptors withhold the various EDCs better than the Tozzi-tetrapeptide compound **V.43**, which does not trap any compound what so ever.

However, it is more likely that these effects are the result of non-specific interactions (**Figure V.17**) and that there is no real complex formation between the receptors and the various ligands. Indeed, when looking at compound **V.42** that lacks the scaffold but has the same amino acid build up as **V.40**, it is clear that there is no significant difference between the two materials. This is probably due to a combined effect of non-specific hydrogen and Van der Waals bonding between the estrogenic compounds and the amino acids of the compounds.

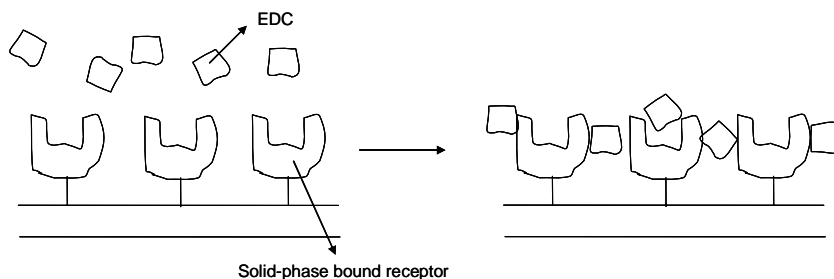


Figure V.17: non-specific interactions between EDCs and the solid-phase bound receptor.

The fact that there is no selective complex formation between the receptors and the estrogenic compounds is confirmed by the amount of testosterone which is trapped. Though lower amounts of Tes are being retained, there is no big discrepancy between these values and those from BPA.

From these data, it can be confirmed that the results obtained from the screening with the estradiol column (**Paragraph V.2**) cannot be correlated with affinity properties of the tested library members. Whereas compound **V.41** should retain the compounds to a lesser extent than compound **V.40**, **Figure V.16** shows that no significant difference, but rather a reversed trend is visible.

Figure V.16 above all raises questions about the effectiveness of the Tozzi-tetrapeptide. Compound **V.43** does not show any affinity towards the tested compounds, although with the published K_d of 17 μM a different trend was expected. In retrospect, until now the published Tozzi peptides have served as a calibration point to assess the observed affinities towards estrogenic compounds, but the data for **V.43**, indicate that properties of the Tozzi peptides are not reproducible.

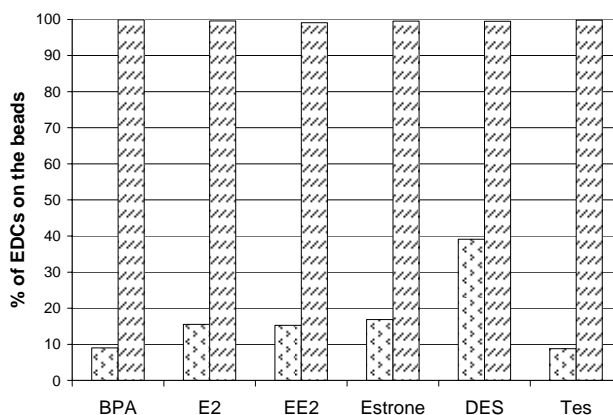


Figure V.18: SPE of hospital water spiked with EDCs.
Tested materials: V.41 (□) and OASIS (▨).

In a last experiment, the potential of **V.41** to extract EDCs from a more complex matrix was compared to OASIS. In this experiment, a sample from the waste water of the UZ hospital in Ghent was spiked with the EDC mixture and then sent over the two SPE materials. Maybe now an increased efficiency towards OASIS could be obtained, but it is clear from **Figure V.18** that OASIS is still performing better. Nevertheless, the ability of **V.41** to extract EDCs from a more complicated matrix remain unchanged when compared to data of **Figure V.16** obtained in deionised water.

V.5. Conclusion

This chapter dealt with the difficult task of screening the synthesised library of 120 members towards affinity for various estrogenic compounds.

In a first attempt, the solid-phase bound members were treated as small SPE cartridges but the high background absorption of Tentagel made this approach not meaningful. A different material was sought that was compatible with the developed synthesis protocols and at the same time showed no affinity towards EDCs. However, it appeared that a suitable solid support combining these two properties could not be found.

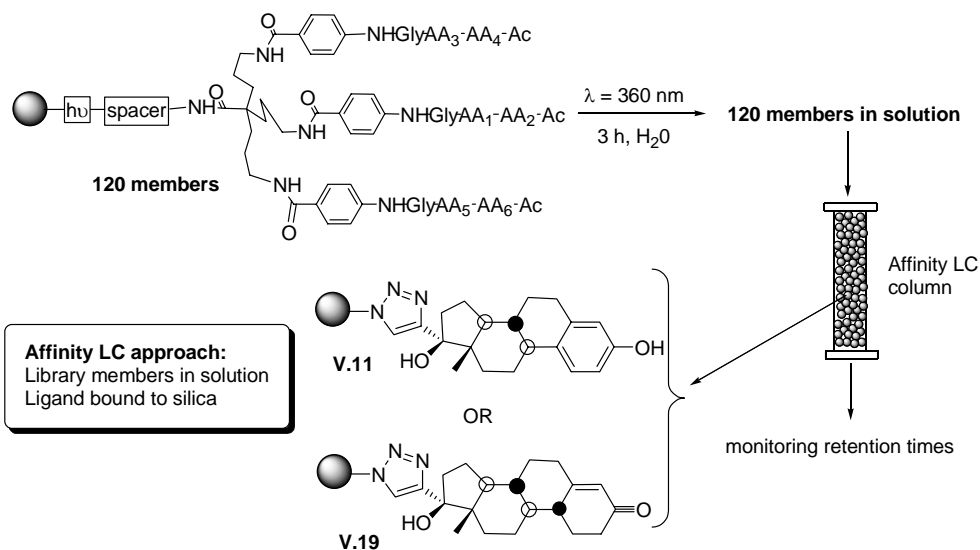


Figure V.19: Affinity LC approach.

A completely different approach was then investigated by using an affinity LC based method (**Figure V.19**). For this purpose, ethinylestradiol was ‘clicked’ to silica and from this material a HPLC column was packed. Though first results looked promising, screening of the library did not yield decisive results.

The selectivity of the library was tested by screening it via a second, non estrogenic norethindron column. The data obtained however, were similar as with the EE_2 column indicating that the difference in retention times may not be due to a difference in affinity but to a difference in polarity. In other words, instead of an affinity column, a new type of reversed phase material was developed.

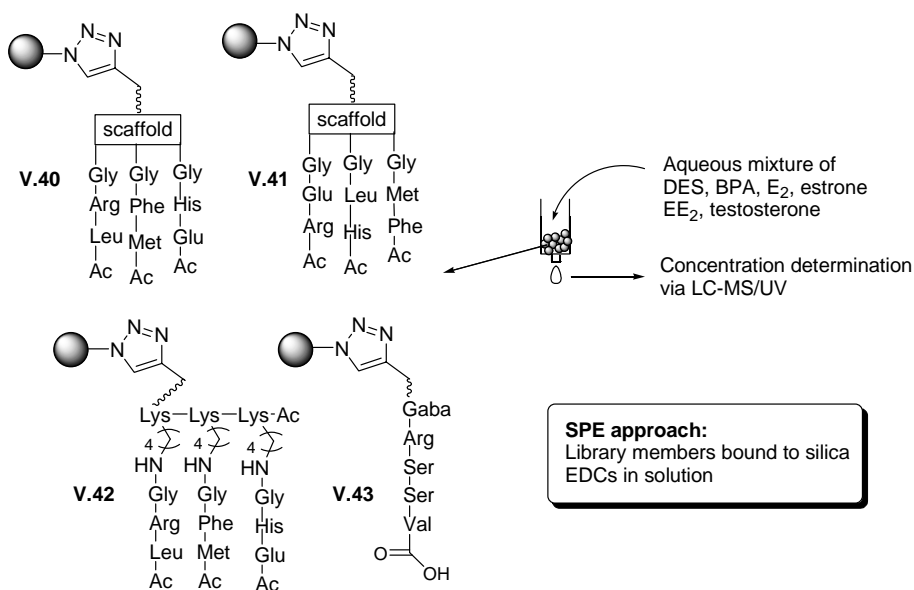


Figure V.20: SPE approach.

These preliminary conclusions were confirmed by another set of experiments where two receptors, **V.24** and **V.25** were scaled up and ‘clicked’ to silica. These materials could now be used as SPE cartridges (**Figure V.20**). Incubation with a mixture of EDCs showed that there was no significant difference between the two members, on the contrary, a slight opposite trend was observed.

To conclude, it can be said that though materials have been made which can retain EDCs from an aqueous mixture, a comparison with known SPE cartridges like OASIS shows that the amounts trapped are not sufficient to justify their use as a clean-up procedure before actual chemical analysis.

VI. Considering the chirality of the scaffold

The skeleton of the tripodal scaffold **IV.1** inherently possesses a chiral quaternary centre at the foot of the carboxylic acid (**Figure VI.1**). This implies that at the stage of **IV.1**, a racemic mixture is generated. Consequently, two diastereomers are formed by building in a chiral amino acid. As a result, the generated library consists of 240 members instead of 120 members.

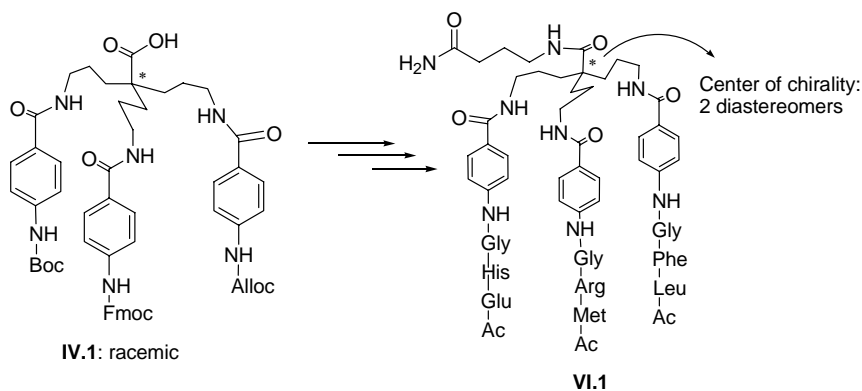


Figure VI.1: Chirality issues.

The impact of the chiral quaternary centre on the 3D structure of the overall molecule was assessed via modelling. The modelling was performed by ir. J. Goeman in the Laboratorium of Organic and Bio-organic synthesis of Prof. Dr. J. Vandereycken. The conformations of the two diastereomers of **VI.1** were optimised in water via the OPLS-AA force field, part of the Macro Model V.6 software.

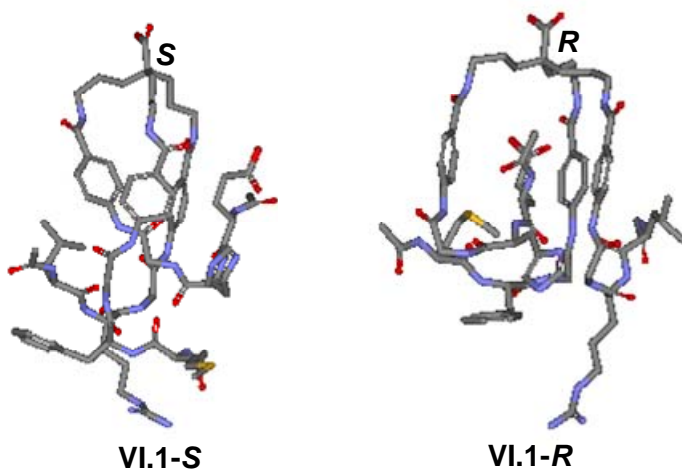


Figure VI.2: Conformational analysis of VI.1 in water.

The structures of the two epimers in **Figure VI.2** clearly show that the chirality of the quaternary centre has a significant impact on the conformational behaviour of the chains. With **VI.1-S**, the three aromatic cores are in close contact with each other, leaving no free space in between them. With **VI.1-R** on the other hand, the three aromatic moieties create a space that is filled by an amino acid (Glu) from the peptide chains. In the structure of the **S** epimer, this Glu is floating next to the aromatic cores.

The fact that the two epimers have a distinct different conformation can have the following consequences:

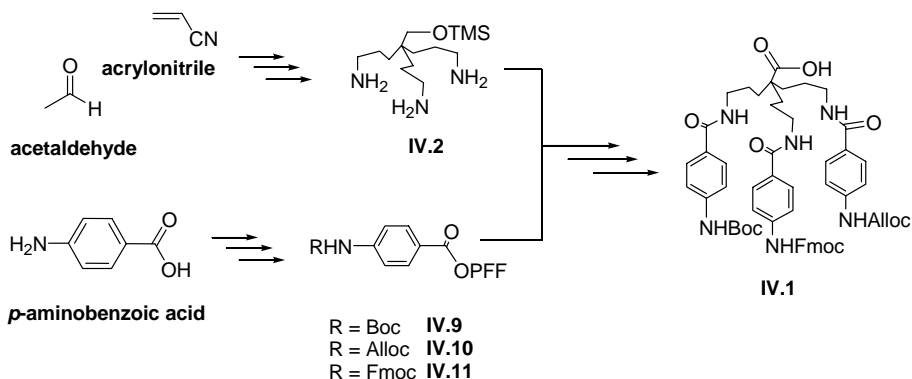
- Only one of the two diastereomers shows affinity.
- The two both show affinity resulting in a synergetic effect.
- None of the two epimers show any affinity.

When the affinity is tested with the SPE approach, no differentiation between the two epimers can be seen. The observed affinity is the overall affinity. With the affinity LC approach however, it should be possible to separate the two epimers if there is a difference in affinity. This effect was not observed.

When designing a tripodal scaffold, it is difficult to bypass the chirality problem and make an enantiomerically pure compound. Designing an enantiomerically pure version of the scaffold would require quite some extra effort. Therefore, the obtained data and results should be looked at with great care, keeping in mind that two different sets of compounds are made and that this can (or cannot) have a significant effect on the obtained results.

VII. General conclusions

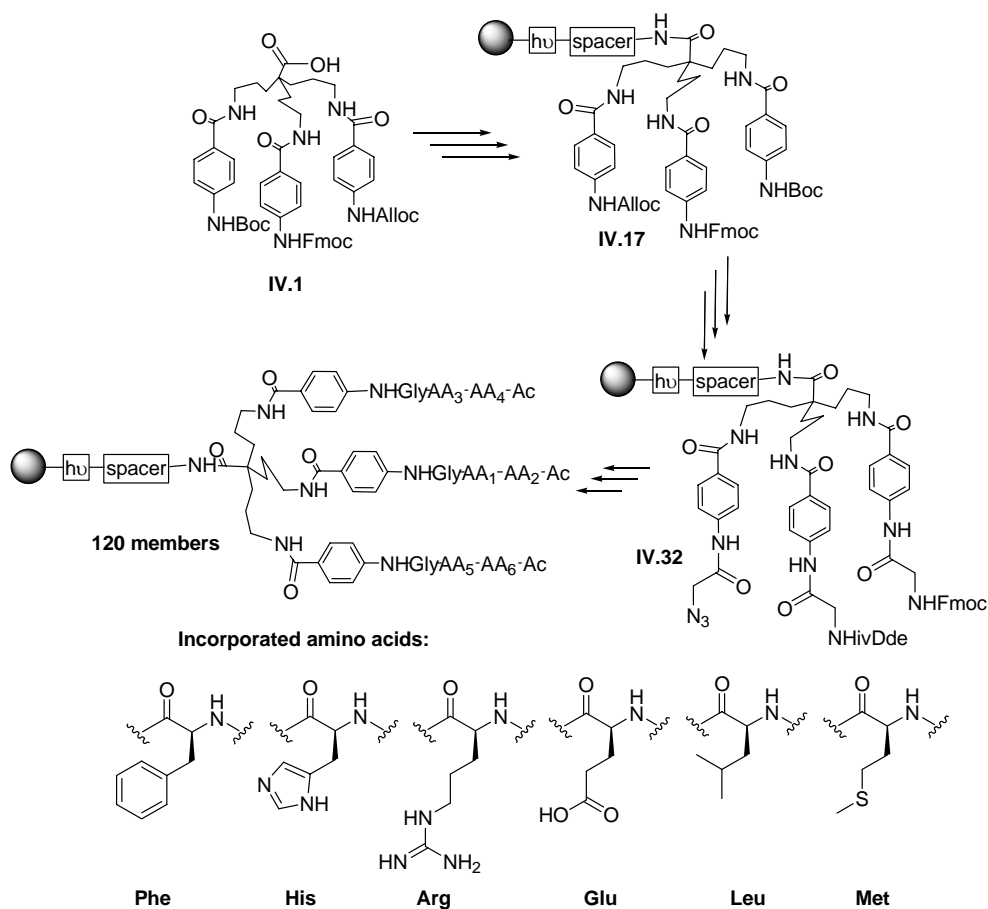
The first goal of this PhD to find a protocol to synthesise possible hER mimics, was accomplished by starting with the synthesis of tripodal scaffold **IV.1**. Derived from simple commercial building blocks, the tripodal scaffold **IV.1** was synthesised in gram quantities (**Scheme VII.1**). Acetaldehyde and acrylonitrile were used to generate the triamine backbone **IV.2**. The differently protected arms were synthesised from *p*-aminobenzoic acid and subsequently activated as their PFF-esters. After coupling the active esters to the triamine backbone, the silyl ether was deprotected and the resulting alcohol oxidised to give the desired tripodal scaffold **IV.1**.



Scheme VII.1: Synthesis of tripodal scaffold IV.1.

Once **IV.1** was synthesised, the synthetic protocols for the solid-phase synthesis of the library had to be established (**Scheme VII.2**). First, coupling of **IV.1** to Tentagel was optimised to such an extent that only 1.5 equivalents of scaffold were consumed. Next, the weak nucleophilicity of the aromatic amines was bypassed by coupling glycines as their symmetrical anhydrides. In the same time the whole orthogonality scheme was reconsidered by replacing the Boc and the Alloc group with the *iv*Dde and azide group respectively. This new strategy enabled the fully automated synthesis of 120 library members in a short period of time. The incorporated amino acids were

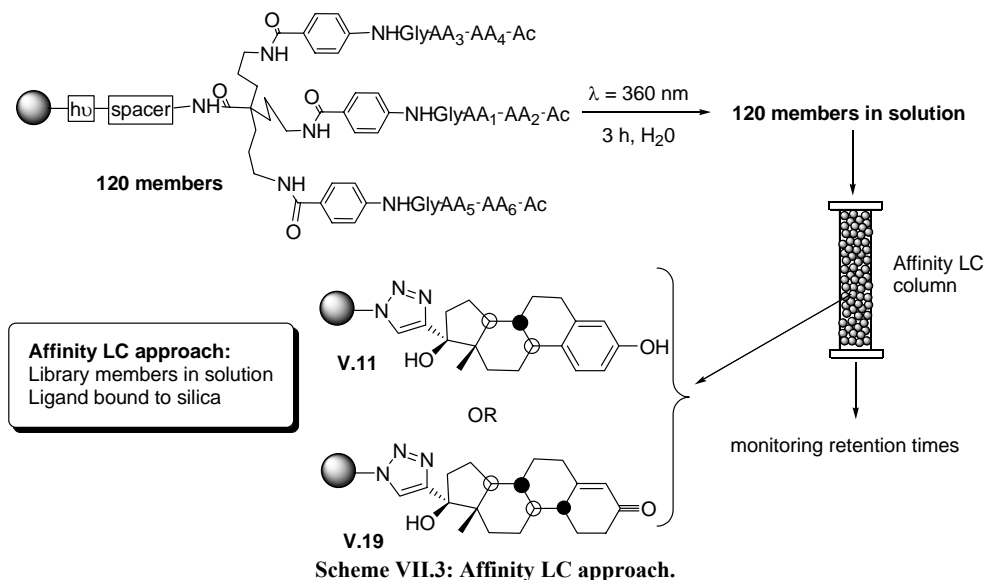
chosen based upon the X-ray structures of the hER complexed with various ligands. During the synthesis however, the thioether of Met was oxidised, but this problem could be solved during the acidic side chain deprotection. After analysis, it was proven by LC and MS techniques that the overall quality of the synthesised library was very good.



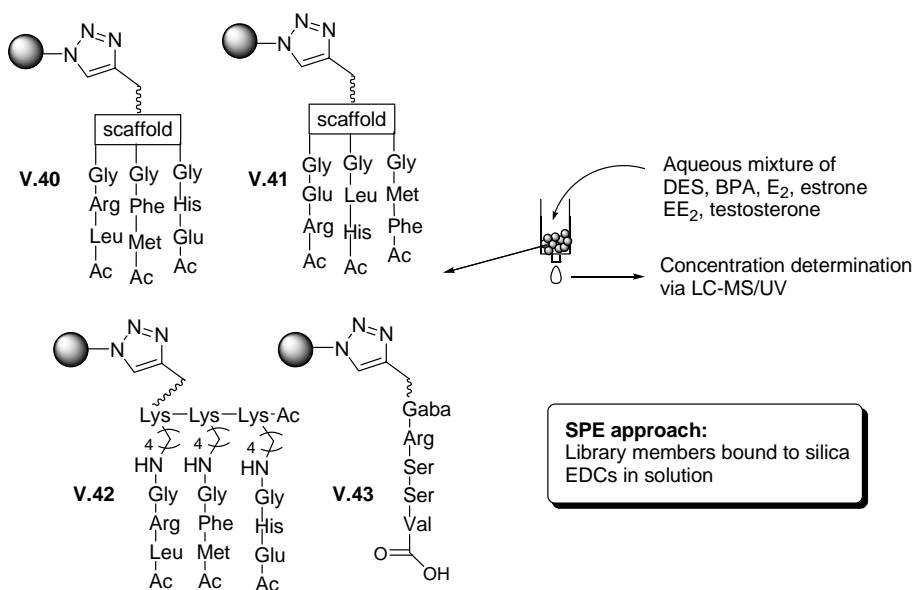
Scheme VII.2: Solid-phase synthesis of the library.

The second goal of selecting the most active receptor proved to be more difficult. Due to the high background adsorbance of Tentagel, it was impossible to use the resin-bound members directly as a SPE cartridge. An alternative was investigated by

‘clicking’ EE_2 to azido functionalised silica material. This material was used to pack an HPLC column. By passing the different members separately over this column, the retention times were monitored (**Scheme VII.3**). These retention times were compared with the ones obtained in a similar experiment but with a non-estrogenic compound, norethindrone, ‘clicked’ to silica. However, from these experiments, no clear connection between the retention behaviour of the different library members and the possible affinity towards estradiol could be established.



In order to evaluate the results from the affinity LC, the ‘best’ and the ‘worst’ receptor as determined by affinity LC were provided with an alkyne moiety and scaled up. In the same manner, a compound with the same AA content but without the scaffold and a derivative of the Tozzi-tetrapeptide were prepared. Though the scaling-up process was hindered by the low yield obtained with the photocleavable and the hydrazine linker, the different alkyne substituted compounds were obtained in sufficient amount and purity to be ‘clicked’ to silica (**Scheme VII.4**).



Scheme VII.4: SPE approach.

The obtained SPE materials were subsequently tested by incubating them with an aqueous mixture of EDCs. From the results depicted in **Figure VII.1**, it can be seen that the results obtained with the affinity LC method do not correlate with any kind of affinity towards EDCs. The ‘best’ and the ‘worst’ receptor **V.40** and **V.41** show a similar affinity towards most EDCs and it even can be said that a reversed trend is visible.

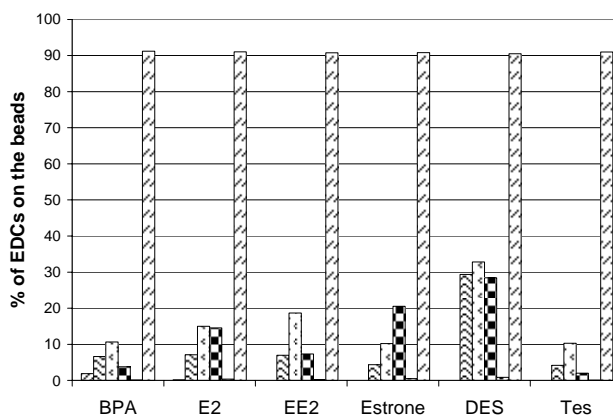


Figure VII.1: SPE results: silica (▨), V.40 (▩), V.41 (▧), V.42 (▣), V.43 (▤) and OASIS (▨).

Nevertheless, an increase in affinity towards EDCs is obtained when compared with unmodified silica and even when compared with Tozzi-tetrapeptide modified silica **V.43**.

However, the observed affinity does probably not stem from a complex formation between the receptors and the estrogenic compounds and is more likely the result of non-specific interactions. Indeed, when looking at compound **V.42** that lacks the scaffold but has the same amino acid build up than **V.40**, it is clear that there is no significant difference between the two materials. Also the fact that the amount of trapped testosterone is similar to the amounts of trapped BPA, indicate that the different receptor mimics do not entangle the compounds. The compounds rather stick randomly to the modified silica surfaces (**Figure VII.2**).

Finally, the new materials were compared to commercial SPE systems, like OASIS, which are known to possess good enrichment qualities for various EDCs. This material withholds more than 90 % of all the EDCs making it a valuable tool in solid-phase extraction. The newly developed materials **V.40** and **V.41** clearly do not possess the same qualities as the OASIS cartridge as only up to 35 % is retained in the case of DES.

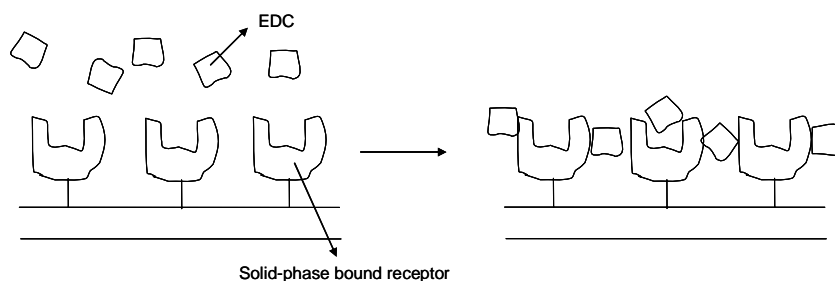


Figure VII.2: non-specific interactions between EDCs and the solid-phase bound receptor.

To conclude, it can be said that though materials have been made that can withhold EDCs from an aqueous mixture, a comparison with known SPE cartridges like OASIS show that the amounts trapped are not sufficient to justify their use as a clean-up procedure before actual chemical analysis.

VIII. Experimental part

VIII.1. Methods and materials

Methods: All solution phase reactions were conducted under an inert atmosphere of argon gas in oven dried glassware. The reactions were monitored by thin layer chromatography (TLC) using SIL G-25 UV₂₅₄ pre-coated silicagel plates (0.25 mm thickness). The TLC plates were visualized using an anisaldehyde (5% anisaldehyde in ethanol with 1% sulfuric acid) or a PMA (5% phosphomolybdic acid in ethanol) solution. Flash column chromatography was performed using BIOSOLVE silica gel (0.063-0.200 mm particle size).

Peptide synthesis: All solid phase reactions on 20 mg resin or less were performed in polypropylene Chromabond columns of 1 mL with a polyethylene frit, closed at the bottom with a B7 septum from Aldrich. Solid phase reactions on a bigger scale were performed in a peptide vessel protected against light with aluminium foil and comprising a sintered glass funnel and a 3-way stopcock for easy filtration and washing. The solid phase reactions were performed on a shaker (Selecta Vibromatic) or on a Yellow Line TTS 2 vortexer. Automated peptide syntheses were performed on a 24 reactor block SYRO Multiple Peptide Synthesiser equipped with a vortexing unit (from Multisyntech, Witten, Germany). Aqueous peptide solutions were lyophilised using a Heto Drywinner lyophiliser connected to a Thermoelectron corporation Savant SPD111V Speedvac concentrator (Milford, MA, USA).

Analysis: *NMR spectra* were recorded at 500 MHz or 300 MHz for proton and at 125 MHz or 75 MHz for carbon nuclei in chloroform-*d*, DMSO-*d*₆, MeOD-*d*₄ or aceton-*d*₆. Chemical shifts are reported in units of parts per million (ppm), referenced relative to the residual ¹H or ¹³C peaks of the used solvent as internal standards (chloroform-*d*: ¹H 7.26 and ¹³C 77.16; DMSO-*d*₆: ¹H 2.50 and ¹³C 39.52; MeOD-*d*₄: ¹H 3.31 and ¹³C 49.00; aceton-*d*₆: ¹H 2.05 and ¹³C 29.84 and 206.26). The following abbreviations were used to explain the multiplicities: s, singlet; d, doublet; t, triplet; q, quadruplet; m, multiplet; br, broadened.

Infrared spectra (IR) were recorded on a PERKIN-ELMER 1600 series FTIR spectrometer and reported in wave numbers (cm^{-1}). Samples were prepared as a thin film (neat) on KBr plate or used directly with the Horizontal Attenuated Total Reflection (HATR) adaptor.

Elemental analyses were performed by SIARE at the Université Pierre & Marie Curie, Paris, France.

High-Resolution Mass Spectra (HRMS) were recorded by Amberlab at Ghent University on a Thermo Finnigan MAT95XP-Trap tandem mass spectrometer or by the Rega institute at the University of Leuven on a ThermoFinnigan LCQ MSn ion trap.

Low Resolution Mass Spectra were recorded with LCQ MS (Thermo Finnigan, San Jose, CA, USA) equipped with an electrospray ionisation source.

MALDI-TOF spectra were recorded on an Applied Biosystems Voyager-DE STR Biospectrometry Workstation. For the sample preparation, a mixture of 2,5-dihydrobenzoic acid and TFA was used as the matrix.

LC-MS data were obtained on an Agilent 1100 series instrument with a Phenomenex Luna C18(2) column (250x 4.6 mm, 5 μm at 35 $^{\circ}\text{C}$) and an ES-MSD type VL mass detector using the following systems: 5 mM NH_4OAc in H_2O (A) and MeCN (B). Unless otherwise stated the column was flushed for 2 min with 100% A, then a gradient from 0 to 100% B over 15 min was used, followed by 5 min of flushing with 100% B.

HPLC analyses were performed on an Agilent 1100 Series instrument with a Phenomenex Luna C18(2) column (250 x 4.6 mm, 5 μ at 35 $^{\circ}\text{C}$) using a flow rate of 1 ml/min and with the following solvent systems: 0.1% TFA in H_2O (A) and MeCN (B). Unless otherwise stated the column was flushed for 3 min with 100% A, then a gradient from 0 to 100% B over 15 min was used, followed by 5 min of flushing with 100% B.

UV-spectra were recorded on a Varian Cary 300 Bio UV-VIS spectrophotometer.

Photolyses were carried out with a 4W Bioblock Scientific compact UV lamp set at 365 nm.

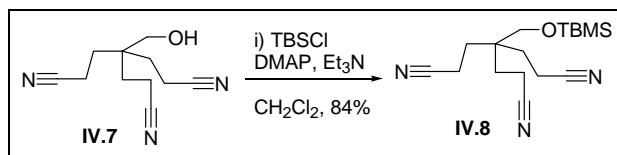
Melting point ranges were determined with an Electrothermal 9100 melting point apparatus.

Materials. All chemicals were purchased from Sigma Aldrich or Acros except the amino acids that were bought at IRIS Biotech GmbH. Tentagel-S-NH₂ was purchased from NovaBiochem. Extra dry DMF was purchased from Acros. DMF peptide grade was purchased from Biosolve. All chemicals were purchased and used without any further purification, except tetrahydrofuran (THF), which was distilled from Na/benzophenone prior to use and dichloromethane, which was distilled from CaH₂.

VIII.2. Synthesis of the Tripodal Scaffold IV.1

VIII.2.1. Synthesis of the triamine core IV.2

VIII.2.1.1. Protection of the alcohol IV.7



In a dry flask of 25 ml, 865 mg (4.21 mmol, 1eq.) of **IV.7** is dissolved in dry dichloromethane. To this solution *tert*-butyldimethylsilyl chloride (0.699 g, 4.64 mmol, 1.1 eq.), 4-dimethylaminopyridine (0.514 g, 4.21 mmol, 1 eq.) and triethylamine (587 μ l, 4.21 mmol, 1 eq.) are added. The solution is refluxed overnight. Afterwards, the solution is poured into a separating funnel and washed three times with a saturated sodium chloride solution and further three times with a 1M hydrochloric acid solution. The organic phase is dried on magnesium sulfate, filtered off and evaporated under reduced pressure providing 1.130 g (80%) of **IV.8** as white crystals.

Molecular Formula: C₁₇H₂₉N₃OSi

MW.: 319.52 g/mol

RF. (DCM:MeOH 9:1): 0.28

Melting Point: 72-73 °C

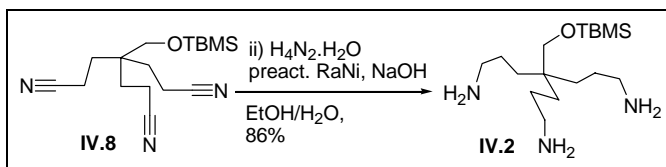
IR. (KBr-plate): 2952 (m), 2927 (m), 2882 (m), 2857 (m), 2248 (m), 1466 (m), 1450 (m), 1424 (m), 1374 (w), 1297 (w), 1262 (m), 1132 (m), 1102 (s), 1084 (s), 1006 (w), 940 (w), 858 (s), 840 (s), 782 (m), 748 (w), 674 (m) cm^{-1} .

ES. (m/z): 337.2 $[\text{M}+\text{NH}_4]^+$

^1H -NMR (500 MHz, CDCl_3): δ 3.40 (2H, s), 2.36 (6H, t, $J = 7.9$ Hz), 1.73 (6H, t, $J = 7.9$ Hz), 0.90 (9H, s), 0.08 (6H, s) ppm.

^{13}C -NMR + APT (75 MHz, CDCl_3): δ 119.06 (C), 65.87 (CH_2), 39.84 (C), 29.50 (CH_2), 25.73 (CH_3), 18.01 (C), 11.81 (CH_2), -5.73 (CH_3) ppm.

VIII.2.1.2. Reduction of the nitriles

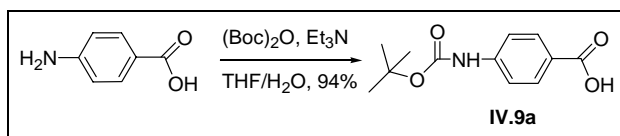


In a two necked flask of 500 ml, **4** (22.0 g, 68.9 mmol) was dissolved in 250 ml of pure ethanol and 13.2 ml of water. To this mixture, NaOH (10.6 g, 26.0 mmol) was added, after which the mixture was cooled down to 0°C . After stirring for half an hour, hydrazine monohydrate (26.4 ml, 544 mmol) was added. In the meantime a Raney Nickel-slurry (6.2 g, 53 mmol, Merck, 50% active catalyst in water) was washed thoroughly with water and pure ethanol in a little flask. This suspension was added to the reaction mixture over a period of 2 h, after which the solution was allowed to warm up to rT. After 1 h of stirring, the reaction mixture was refluxed during 2 h. The reaction mixture was filtered off over celite and the filtrate was concentrated under reduced pressure. Toluene was added to the residue to precipitate the NaOH . The base was filtered off and the filtrate was evaporated under reduced pressure. This action was repeated until no more precipitation was formed. A light yellow oil was obtained (19.6 g, 59.2 mmol, 86%).

Molecular Formula: C₁₇H₄₁N₃OSi**MW.:** 331.61 g/mol**RF.** (MeOH/NH₃): 0.30**Melting Point:** 72-73 °C**IR.** (KBr-plate): 3358 (s), 2929 (s), 28571568 (m), 1472 (m), 1386 (w), 1328 (m), 1252 (w), 1098 (m), 1006 (w), 836 (m), 774 (m), 739 (w), 668 (w) cm⁻¹.**ES.** (m/z): 332.3 [M+H]⁺**¹H-NMR** (300 MHz, CDCl₃): δ 3.12 (s, 2H), 3.10 (br. s, 6H), 2.64 (t, *J* = 6.8 Hz, 6H), 1.34 (m, 6H), 1.15 (m, 6H), 0.84 (s, 9H), 0.03 (s, 6H) ppm.**¹³C-NMR + APT** (75 MHz, CDCl₃): δ 66.4 (CH₂), 43.0 (CH₂), 39.3 (C), 31.1 (CH₂), 27.4 (CH₂), 25.8 (CH₃), 18.1 (C), -5.7 (CH₃) ppm.

VIII.2.2. Synthesis of the arms

VIII.2.2.1. Boc-protection of *p*-aminobenzoic acid



In a flask of 1 L, 4-aminobenzoic acid (17.5 g, 0.128 mol, 1eq) was dissolved in 153 mL water and 306 mL dioxane. The Et₃N (36 mL, 0.256 mol, 2 eq) was then added followed by the addition of di-*tert*-butyl dicarbonate (56.0 g, 0.256 mol, 2 eq). After stirring for 24 h the solution was evaporated under reduced pressure. Subsequently, a 3 N HCl solution was added drop wise until there was no more precipitate formed. Finally, the white powder was filtered off and dried over P₂O₅ under vacuum (28.5 g, 94 %)

Molecular Formula: C₁₂H₁₅NO₄**MW.:** 237.25 g/mol**RF.** (DCM:MeOH 1:1): 0.45**Melting point:** 198–200 °C

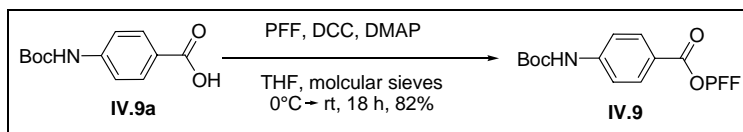
IR. (KBr-plate): 3366 (m), 1705 (s), 1678(s), 1609 (m), 1524 (s), 1506 (m), 1409 (w), 1366 (w), 1311 (w), 1285 (w), 1234 (m), 1160 (s), 1056 (w), 941 (w), 839 (w), 801 (w), 774 (w), 694 (w), 644 (w) cm^{-1} .

ES. (m/z): 236.2 [M-H]⁻

¹H-NMR (500 MHz, DMSO-d₆): δ 9.71 (1H, br. s), 7.84 (2H, ddd, $J = 9.5/2.3/1.9$ Hz), 7.75 (2H, ddd, $J = 9.5/2.4/2.0$ Hz), 1.49 (9H, s) ppm.

¹³C-APT (75 MHz, DMSO-d₆): δ 167.0 (C), 125.5 (C), 143.7 (C), 130.3 (CH), 124.0 (C), 117.2 (CH), 79.6 (C), 28.0 (CH₃) ppm.

VIII.2.2.2. Activation of IV.9a



To a solution of **IV.9a** (10.0 g, 42.0 mmol) in THF (65 mL) was added pentafluorophenol (9.37 g, 50.4 mmol), DMAP (260 mg, 2.11 mmol) and molecular sieves. After stirring the solution for 10 min at 0 °C the coupling reagent DCC (10.5 g, 50.4 mmol) was added and the ice-bath was allowed to warm up at rT. After 18 h the reaction mixture was filtered off and the filtrate was concentrated under reduced pressure. The resulting orange precipitate was chromatographed with pentane/ DCM (1:1) to give **IV.9** (13.9 g, 82%) as a white powder.

Molecular Formula: C₁₈H₁₄F₅NO₄ **MW.:** 403.30 g/mol

RF. (DCM): 0.64

Melting Point: 124-126°C

IR. (KBr-plaatjes): 3355 (w), 2983 (w), 2936 (w), 1758 (m), 1736 (m), 1607 (m), 1592 (m), 1521 (s), 1414 (m), 1370 (w), 1320 (w), 1256 (s), 1236 (s), 1145 (s), 1046 (s), 1011 (s), 996 (m), 901 (w), 853 (w), 758 (w), 615 (w) cm^{-1}

E.S. (m/z): 402.7 [M-H]⁻

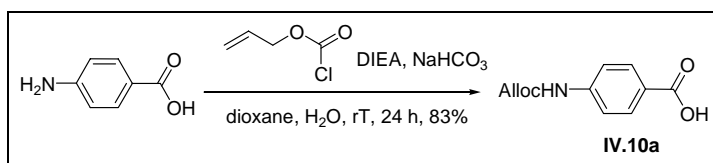
CH-Analysis: calculated: C (53.61%), H (3.50%), N (3.47%)

found: C (53.71%), H (3.67%), N (3.30%)

¹H-NMR (500 MHz, CDCl₃): δ 8.12 (2H, ddd, *J* = 8.4/2.4/1.8 Hz), 7.54 (2H, ddd, *J* = 9.3/2.3/1.9 Hz), 6.77 (1H, br. s), 1.52 (9H, s) ppm.

¹³C-APT (75 MHz, CDCl₃): δ 162.1 (C), 151.9 (C), 144.4 (C), 132.2 (CH), 120.7 (C), 117.6 (CH), 81.7 (C), 28.2 (CH₃) ppm.

VIII.2.2.3. Alloc protection of *p*-aminobenzoic acid



In a 2 L flask, 4-aminobenzoic acid (1 g, 7.29 mmol) was dissolved in 10 mL of dioxane and 10 mL of water. DIEA (2.6 mL, 14.9 mmol) and NaHCO₃ (1.8 g, 21.8 mmol) were added. Finally, allyl chloroformate (0.78 mL, 7.33 mmol) was added and the reaction is stirred overnight. A 1N HCl solution was added drop wise until there was no more precipitate forming. The white powder was filtered off and dried over P₂O₅ under reduced pressure to provide **IV.10a** (1.35 g, 83%).

Molecular Formula: C₁₁H₁₁NO₄ **MW.:** 221.21 g/mol

RF. (DCM:MeOH 1:1): 0.45

Melting Point: 199-201 °C

IR. (KBr-plate): 3334 (w), 1702 (w), 1685 (m), 1600 (m), 1532 (m), 1425 (w), 1411 (w), 1315 (m), 1230 (s), 1175 (m), 1132 (w), 1055 (m), 985 (w), 938 (w), 856 (w), 771 (w), 694 (w), 590 (w) cm⁻¹.

E.S. (m/z): 220.2 [M-H]⁻

CH analysis: calculated: C (59.73%), H (5.01%), N (6.33%)

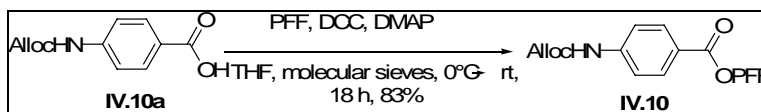
found: C (59.43%), H (4.95%), N (6.58%)

¹H-NMR (500 MHz, DMSO-d₆): δ 10.07 (1H, br. s), 7.83 (2H, ddd, *J* = 9.3/2.3/1.8 Hz), 7.74 (2H, ddd, *J* = 9.3/2.3/1.9 Hz), 5.95 (1H, ddt, *J* = 17.3/10.5/5.5 Hz), 5.35 (1H, ddd,

$J = 17.3/3.3/1.6$), 5.21 (1H, ddd, $J = 10.4/2.9/1.3$ Hz), 4.58 (2H, ddd, $J = 5.5/1.3/1.3$ Hz) ppm.

^{13}C -APT (50 MHz, acetone- d_6): δ 167.3 (C), 153.9 (C), 144.5 (C), 133.9 (CH), 131.6 (CH), 125.3 (C), 118.3 (CH), 117.9 (CH₂), 66.0 (CH₂) ppm.

VIII.2.2.4. Activation of IV.10a



To a solution of **IV.10a** (19.2 g, 83.6 mmol) in THF (225 mL) was added pentafluorophenol (19.2 g, 104.5 mmol), DMAP (480 mg, 3.93 mmol) and molecular sieves. After stirring the solution for 10 min at 0 °C the coupling reagent DCC (21.6 g, 104.5 mmol) was added and the ice-bath is allowed to melt. After 18 h the reaction mixture was filtered off and the filtrate was concentrated under reduced pressure. The resulting powder was chromatographed with pentane/EtOAc (9:1) to give **7** (26.8 g, 83%) as a white powder.

Molecular Formula: C₁₇H₁₀F₅NO₄ **MW.:** 387.26 g/mol

RF. (DCM): 0.64

Melting Point: 138°C

IR. (KBr-plate): 1759 (w), 1596 (w), 1522 (s), 1414 (s), 1314 (w), 1255 (m), 1214 (m), 1178 (m), 1143 (w), 1046 (s), 1002 (m), 850 (w), 806 (m), 702 (s), 573 (w), 503 (w) cm⁻¹

E.S. (m/z): 386.1 [M-H]⁻

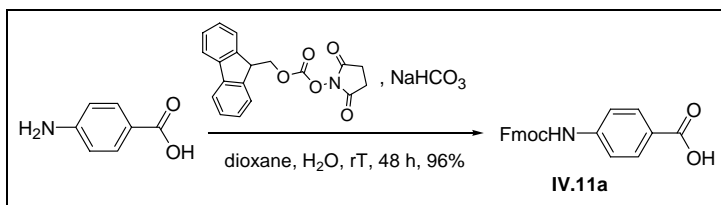
C.H. Analysis: calculated: C (52.73%), H (2.60%), N (3.62%)

found: C (52.65%), H (2.78%), N (3.45%)

^1H -NMR (500 MHz, CDCl₃) δ 8.17 (2H, ddd, $J = 9.4/2.4/2.0$ Hz), 7.75 (2H, ddd, $J = 9.4/2.4/2.0$ Hz), 5.97 (1H, ddt, $J = 17.3/10.5/5.7$ Hz), 5.40 (2H, ddd, $J = 17.1/2.9/1.5$), 5.30 (2H, ddd, $J = 10.4/2.4/1.2$ Hz), 4.70 (2H, ddd, $J = 5.9/1.3/1.3$ Hz) ppm.

^{13}C -APT (75 MHz, CDCl_3): δ 162.1 (C), 152.6 (C), 143.9 (C), 132.3 (CH), 131.9 (CH), 121.3 (C), 118.3 (CH_2), 117.9 (CH), 66.4 (CH_2) ppm.

VIII.2.2.5. Fmoc protection of *p*-aminobenzoic acid



In a 5 L flask, 4-aminobenzoic acid (40.7 g, 0.297 mol) was dissolved in 810 mL water. NaHCO_3 (68.0 g, 0.809 mol) was then added, followed by the addition of 810 mL of dioxane and FmocOSu (100 g, 0.297 mol). After stirring for 4 h, 400 mL water was added. The solution was stirred for another 44 h and was then acidified with 1N HCl solution until pH 3 was reached. The white precipitate was filtered off and dried over P_2O_5 under vacuum (102.9 g, 96%).

Molecular Formula: $\text{C}_{22}\text{H}_{17}\text{NO}_4$ **MW.:** 359.37 g/mol

RF. (DCM): 0.43

Melting Point: 276-278 °C

I.R. (KBr-plate): 3342 (w), 1711 (s), 1678 (m), 1608 (w), 1590 (w), 1529 (s), 1443 (w), 1408 (w), 1378 (w), 1308 (m), 1279 (m), 1238 (s), 1179 (w), 1108 (w), 1085 (w), 1054 (m), 979 (w), 850 (w), 812 (w), 739 (s), 691 (w), 544 (w), 450 (w) cm^{-1} .

ES. (m/z): 358.5 $[\text{M-H}]^-$, 717 $[2\text{M-H}]^-$

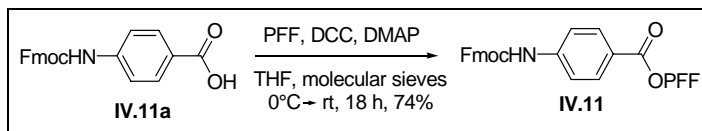
CH analysis: calculated: C (73.53%), H (4.77%), N (3.90%)

found: C (73.40%), H (4.93%), N (3.93%)

^1H -NMR + COSY (500 MHz, DMSO-d_6): δ 10.0 (1H, br. s), 7.91 (2H, d, $J = 7.5$ Hz), 7.84 (2H, d, $J = 8.1$ Hz), 7.75 (2H, d, $J = 7.5$ Hz), 7.54 (2H, br. s), 7.43 (2H, dd, $J = 7.4/7.4$ Hz), 7.35 (2H, ddd, $J = 7.4/7.4/0.9$ Hz), 4.53 (2H, d, $J = 6.4$ Hz), 4.33 (1H, t, $J = 6.4$ Hz) ppm.

^{13}C -APT + HSQC + HMBC (75 MHz, DMSO- d_6): δ 166.9 (C), 153.2 (C), 143.7 (C), 143.2 (C), 140.8 (C), 130.4 (CH), 127.7 (CH), 127.2 (CH), 125.2 (CH), 125.1 (C), 120.2 (CH), 117.4 (CH), 65.8 (CH_2), 46.5 (CH) ppm.

VIII.2.2.6. Activation of IV.11a



To a solution of **IV.11a** (10.0 g, 27.8 mmol, 1 eq) in THF (45 mL) was added pentafluorophenol (7.23 g, 38.9 mmol), DMAP (173 mg, 1.40 mmol) and molecular sieves. After stirring the solution for 10 min at 0 °C, the coupling reagent DCC (8.11 g, 38.9 mmol) was added and the ice-bath was allowed warm until rT. After 18 h the reaction mixture was filtered off and the filtrate was concentrated under reduced pressure. The resulting light-yellow precipitate was recrystallised in EtOAc. Then the precipitate was taken into THF and refluxed. When everything was dissolved, the solution was slowly cooled in an ice-bath. The white precipitate was filtered off and the filtrate was evaporated to give **IV.11** (10.8 g, 74%) as a white powder.

Molecular Formula: C₂₈H₁₆F₅NO₄

MW.: 525.42 g/mol

R.F. (DCM): 0.59

Melting Point: 195 °C

IR. (KBr-plate): 3343 (w), 1755 (m), 1708 (m), 1593 (w), 1525 (s), 1451 (w), 1414 (w), 1310 (w), 1265 (w), 1242 (w), 1223 (m), 1178 (w), 1090 (w), 1062 (m), 995 (m), 848 (w), 757 (w), 737 (m), 702 (w), 645 (w), 507 (w) cm⁻¹

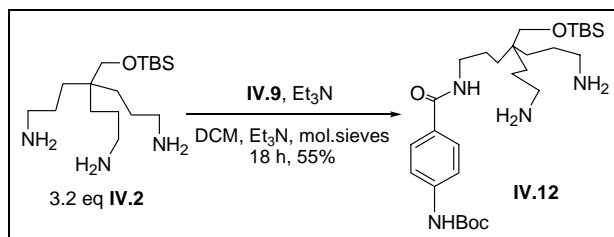
E.S. (m/z): 590.4 [M+MeCN+Na]⁺

¹H-NMR (500 MHz, CDCl₃): δ 8.14 (2H, ddd, J = 8.8/2.4/1.8 Hz), 7.80 (2H, d, J = 7.5 Hz), 7.63 (2H, d, J = 7.5 Hz), 7.55 (2H, d, J = 8.6), 7.44 (2H, dd, J = 7.2/7.2 Hz), 7.35 (2H, ddd, J = 7.5/7.5/1.1 Hz), 6.90 (1H, s), 4.62 (2H, d, J = 6.4 Hz), 4.28 (1H, t, J = 6.4 Hz) ppm.

^{13}C -APT + HSQC + HMBC (75 MHz, CDCl_3): δ 162.1 (C), 152.8 (C), 143.7 (C), 143.5 (C), 141.4 (C), 132.3 (CH), 128.0 (CH), 127.2 (CH), 124.8 (CH), 121.3 (C), 120.2 (CH), 117.9 (CH), 67.2 (CH_2), 47.0 (CH) ppm.

VIII.2.3. Coupling of the arms to the triamine core

VIII.2.3.1. Attachment of the first Boc protected arm



To a solution of **IV.2** (11.182 g, 33.7, 3.2 eq mmol) in DCM (70 mL) was added Et₃N (1.475 mL, 10.5 mmol, 1 eq) and molecular sieves. To the resulting mixture, a solution of the activated ester **6** (4.247 g, 10.5 mmol, 1 eq) in DCM (60 mL) was slowly added via the syringe pump over a period of 8 h. The solution was then stirred overnight and afterwards concentrated under reduced pressure. The residual oil was chromatographed with gradient elution where the amount of MeOH(NH₃) in DCM was varied from 5% to 25%. The desired diamine **IV.12** was obtained as a light-yellow foam (3.182 g, 55%). At the end the column was washed with pure MeOH(NH₃) to recover the excess starting material (6.512 g or 55%).

Molecular Formula: C₂₉H₅₄N₄O₄Si **MW.:** 550.85 g/mol

RF. (DCM:MeOH/NH₃ 9:1): 0.28 **Melting Point:** 67-68 °C

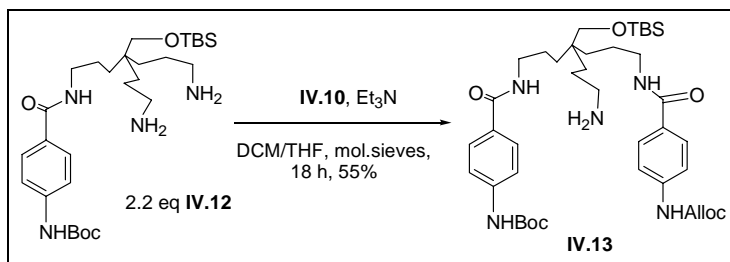
IR. (KBr-plaatjes): 3304 (N-H stretch, br s), 2924 (s), 2854 (s), 1728 (m), 1662 (m), 1634 (m), 1607 (m), 1538 (m), 1506 (m), 1463 (m), 1367 (m), 1317 (m), 1249 (m), 1161 (m), 1097 (m), 1053 (m), 855 (m), 836 (m), 774 (m), 668 (w) cm⁻¹.

ES. (m/z): 551.3 [M+H⁺]

¹H-NMR+COSY (300 MHz, CDCl₃): δ 8.26 (1H, br. s), 7.63 (2H, d, *J* = 8.8 Hz), 7.36 (2H, d, *J* = 8.6 Hz), 6.77 (1H, t, *J* = 5.6 Hz), 3.25 (2H, m), 3.16 (2H, s), 2.53 (4H, t, *J* = 6.6 Hz), 1.43-1.36 (11H, m), 1.28-1.05 (10H, m), 0.77 (9H, s), -0.10 (6H, s) ppm.

^{13}C -NMR + APT + DEPT (75 MHz, CDCl_3): δ 167.1 (C), 152.9 (C), 142.0 (C), 128.5 (C), 128.0 (CH), 117.6 (CH), 80.3 (C), 66.4 (CH_2), 42.9 (CH_2), 40.7 (CH_2), 39.2 (C), 31.1 (CH_2), 28.3 (CH_3), 27.1 (CH_2), 25.8 (CH_3), 23.4 (CH_2), 18.1 (C), -5.6 (CH_3) ppm.

VIII.2.3.2. Attachment of the second Alloc arm



To a solution of the diamine **IV.12** (6.176 g, 11.2 mmol, 2.2 eq) in DCM (60 mL) was added Et_3N (0.72 mL, 5.1 mmol, 1 eq) and molecular sieves. To the resulting mixture, a solution of activated ester **7** (1.974 g, 5.1 mmol, 1 eq) in THF (14 mL) was slowly added via the syringe pump over a period of 8 h. The solution was then stirred overnight and afterwards concentrated under reduced pressure. The residual oil was chromatographed with gradient elution where the amount of $\text{MeOH}(\text{NH}_3)$ in DCM was varied from 3% to 10%. The desired mono-amine was obtained as a light-yellow foam with a 54% (2.091 g).

Molecular Formula: $\text{C}_{40}\text{H}_{63}\text{N}_5\text{O}_7\text{Si}$ **MW.:** 754.04 g/mol

RF. (DCM:MeOH/ NH_3 97:3): 0.18 **Melting Point:** 114-116 °C

IR. (KBr-plate): 3304 (br s), 3179 (m), 3099 (m), 3039 (m), 2930 (s), 2856 (s), 1729 (s), 1639 (s), 1609 (s), 1460 (m), 1408 (m), 1391 (w), 1368 (m), 1317 (s), 1232 (s), 1160 (s), 1100 (m), 1054 (m), 936 (m), 851 (w), 771 (s), 668 (w) cm^{-1} .

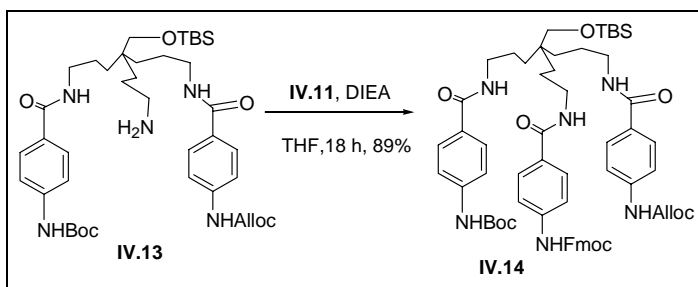
ES. (m/z): 755.0 $[\text{MH}]^+$

^1H -NMR+COSY (500 MHz, CDCl_3): δ 7.78 (1H, br. s) 7.73 (2H, d, $J = 8.6$ Hz), 7.70 (2H, d, $J = 8.6$ Hz), 7.42 (2H, d, $J = 8.3$ Hz), 7.38 (2H, d, $J = 8.6$ Hz), 7.15 (1H, br. s),

6.64 (1H, br. s), 6.57 (1H, br. s), 5.96 (1H, ddt, $J = 17.2/10.5/5.7$ Hz), 5.36 (1H, ddd, $J = 17.2/2.9/1.5$ Hz), 5.26 (1H, ddd, $J = 10.3/2.4/1.3$ Hz), 4.66 (2H, ddd, $J = 5.6/1.3/1.3$ Hz), 3.38-3.31 (4H, m), 3.22 (2H, s), 2.62 (2H, t, $J = 6.8$ Hz), 1.53-1.43 (13H, m), 1.35-1.18 (8H, m), 0.84 (9H, s), -0.03 (6H, s) ppm.

$^{13}\text{C-NMR}$ + **APT** (75 MHz, CDCl_3): δ 167.2 (C), 167.1 (C), 153.2 (C), 152.6 (C), 141.5 (C), 141.0 (C), 132.3 (CH), 129.3 (C), 128.8 (C), 128.1 (CH), 128.0 (CH), 118.4 (CH_2), 118.2 (CH), 118.0 (CH), 80.9 (C), 66.6 (CH_2), 66.0 (CH_2), 42.9 (CH_2), 40.8 (CH_2), 39.4 (C), 31.5 (CH_2), 30.8 (CH_2 or C), 28.3 (CH_3), 27.1 (CH_2), 25.8 (CH_3), 23.3 (CH_2), 18.1 (C), -5.6 (CH_3) ppm.

VIII.2.3.3. Attachment of the third Fmoc arm



To a solution of the mono-amine **IV.13** (2.09 g, 2.77, 1eq mmol) in THF (34 mL) was added DIEA (0.48 mL, 2.76 mmol, 1eq) and **IV.11** (2.90 g, 5.52 mmol, 2 eq). The solution was then stirred overnight and afterwards concentrated under reduced pressure. The residual yellow foam was chromatographed using gradient elution where the amount of MeOH in DCM was varied from 2 % to 4 %. In this way the product **IV.14** was collected as a white powder (2.70 g, 89 %).

Molecular Formula: $\text{C}_{62}\text{H}_{78}\text{N}_6\text{O}_{10}\text{Si}$

MW.: 1095.40 g/mol

RF. (DCM:MeOH 97:3): 0.18

Melting Point: 135-136 °C

IR. (KBr-plaatjes): 3296 (w), 2930 (w), 2846 (w), 1714 (m), 1634 (m), 1609 (m), 1530 (s), 1447 (w), 1408 (w), 1365 (w), 1317 (m), 1223 (s), 1183 (w), 1158 (m), 1101 (w), 1056 (w), 851 (w), 770 (w) cm^{-1} .

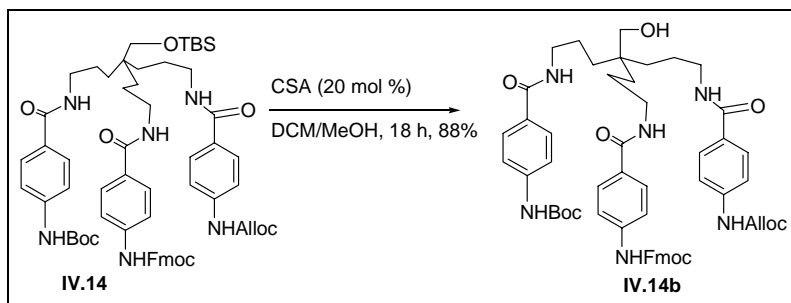
ES. (m/z): 1095.5 $[\text{M}+\text{H}]^+$

^1H -NMR+COSY (500 MHz, CDCl_3): δ 7.81 (1H, br. s), 7.74 (2H, d, $J = 7.7$ Hz), 7.72-7.65 (6H, m), 7.63 (1H, br. s), 7.59 (2H, d, $J = 7.5$ Hz), 7.45-7.30 (8H, m), 7.26 (2H, ddd, $J = 7.4/7.4/0.9$ Hz), 7.15 (1H, br. s), 6.95 (2H, br. s), 6.86 (1H, t, $J = 5.5$ Hz), 5.86 (1H, ddt, $J = 17.2/10.6/5.7$ Hz), 5.28 (1H, ddd, $J = 17.2/3.0/1.5$ Hz), 5.18 (1H, $J = 10.4/2.5/1.2$ Hz), 4.58 (2H, ddd, $J = 5.7/1.4/1.4$ Hz), 4.46 (2H, d, $J = 6.6$ Hz), 4.21 (1H, t, $J = 6.9$ Hz), 3.26 (6H, br. s), 3.13 (2H, s), 1.46 (9H, s), 1.36 (6H, br. s), 1.09 (6H, br. s), 0.77 (9H, s), -0.08 (6H, s) ppm.

^{13}C -NMR + APT + HSCQ (75 MHz, CDCl_3): δ 167.4 (C), 153.5 (C), 152.6 (C), 143.7 (C), 141.5 (C), 141.3 (C), 141.0 (C), 132.3 (CH), 129.1 (C), 128.6 (C), 128.1 (CH), 127.9 (CH), 127.2 (CH), 125.0 (CH), 120.1 (CH), 118.4 (C), 118.4 (CH), 118.3 (CH), 118.1 (CH), 81.0 (C), 67.1 (CH_2), 66.6 (CH_2), 65.6 (CH_2), 47.0 (CH), 40.8 (CH_2), 39.3 (C), 30.8 (CH_2), 28.3 (CH_3), 25.8 (CH_3), 23.1 (CH_2), 18.1 (C), -5.63 (CH_3) ppm.

VIII.2.4. Establishing the anchor point

VIII.2.4.1. Deprotection of the silyl ether



The silyl ether **IV.14** (2.95 g, 2.70 mmol, 1 eq) was dissolved in a 1:1 mixture of DCM (45 mL) and MeOH (45 mL). Then (\pm)-CSA (125 mg, 0.539 mmol, 20 mol %) was added and the reaction mixture is stirred overnight. The reaction was monitored by reversed-phase HPLC at 262 nm and if there was more than 6 % starting material, then an extra portion (\pm)-CSA (31 mg, 0.13 mmol, 5 mol %) was added. After another 4h the mixture is concentrated under reduced pressure in the presence of silica gel. The light-yellow powder is chromatographed with a gradient elution where the amount of MeOH is varied from 5 to 6 % to give the alcohol (2.33 g, 88%).

Molecular Formula: C₅₆H₆₄N₆O₁₀

MW.: 981.14g/mol

RF. (DCM:MeOH 94:6): 0.28

Melting Point: 154-155 °C

IR. (KBr-plaatjes): 3367 (w), 2932 (w), 2867 (w), 2474 (w), 2355 (w), 1714 (m), 1608 (s), 1567 (w), 1523 (w), 1446 (s), 1393 (w), 1356 (m), 1316 (w), 1243 (m), 186 (w), 1072 (m), 848 (w), 767 (w) cm⁻¹.

ES. (m/z): 981.4 [M+H]⁺

¹H-NMR+COSY (500 MHz, MeOD): δ 7.81 (2H, d, J = 7.5 Hz), 7.75-7.65 (8H, m), 7.56-7.42 (6H, m), 7.38 (2H, dd, J = 7.4/7.4 Hz), 7.29 (2H, ddd, J = 7.4/7.4/0.9 Hz),

5.96 (1H, ddt, $J = 17.2/10.6/5.5$ Hz), 5.34 (1H, ddd, $J = 17.2/3.1/1.6$ Hz), 5.20 (1H, ddd, $J = 10.5/2.6/1.5$ Hz), 4.60 (2H, ddd, $J = 5.7/1.4/1.4$ Hz), 4.48 (2H, d, 6.4 Hz), 4.27 (1H, t, 6.6 Hz), 3.30 (8H, m), 1.59-1.50 (6H, m), 1.48 (9H, s), 1.33-1.22 (6H, m) ppm.

^{13}C -APT+DEPT+HSQC+HMBC: δ 169.8 (C), 155.5 (C), 155.3 (C), 154.8 (C), 145.2 (C), 143.9 (C), 143.5 (C), 143.4 (C), 142.7 (C), 134.1 (CH), 129.8 (C), 129.3 (C), 129.2 (CH), 129.1 (CH), 128.9 (CH), 128.2 (CH), 126.2 (CH), 121.0 (CH), 119.1 (CH), 119.0 (CH), 118.9 (CH), 118.0 (C), 81.7 (C), 67.9 (CH₂), 66.6 (CH₂), 48.4 (CH), 41.7 (CH₂), 40.3 (C), 32.0 (CH₂), 28.7 (CH₃) 24.2 (CH₂) ppm.

¹H-NMR+COSY (300 MHz, DMSO-d₆): δ 12.17 (1H, br. s), 9.96 (1H, s), 9.91 (1H, s), 9.56 (1H, s), 8.33 (3H, br. s), 7.96 (2H, d, *J* = 7.4 Hz), 7.80-7.68 (8H, m), 7.55-7.45 (6H, m), 7.41 (2H, dd, *J* = 7.4/7.4 Hz), 7.33 (2H, ddd, *J* = 7.4/7.4/1.1 Hz), 5.97 (1H, ddt, *J* = 17.0/10.4/5.5 Hz), 5.36 (1H, ddd, *J* = 17.2/3.3/1.7 Hz), 5.23 (1H, ddd, *J* = 10.4/2.8/1.4 Hz), 4.61 (2H, ddd, *J* = 5.4/1.3/1.3 Hz), 4.49 (2H, d, 6.9 Hz), 4.31 (1H, t, 6.9 Hz), 3.15 (6H, s), 1.51-1.41 (6H, m), 1.40-1.28 (15H, s), 1.40-1.28 (6H, s) ppm.

¹³C-APT+DEPT (75 MHz, MeOD): δ 180.4 (C), 169.7 (C), 155.5 (C), 154.8 (C), 145.2 (C), 144.0 (C), 143.5 (C), 143.4 (C), 142.7 (C), 134.1 (CH), 129.7 (C), 129.2 (CH), 128.9 (CH), 128.2 (CH), 126.2 (CH), 121.0 (CH), 119.1 (CH), 119.0 (CH), 118.8 (CH), 118.0 (C), 81.2 (C), 67.9 (CH₂), 66.6 (CH₂), 48.4 (CH), 41.2 (CH₂), 32.9 (CH₂), 28.7 (CH₃), 25.5 (CH₂) ppm.

VIII.3. Solid phase synthesis

VIII.3.1. Standard operating protocols

Swelling: The resin is swollen by adding a solvent (10 mL/g) of choice (usually DMF or DCM) to the beads and shaking the suspension for 5 min. To remove the solvent, the resin is filtered at the end.

Washing: Unless stated other wise, the resin is washed with DMF (3x), MeOH (3 x) and DCM (3 x). Finally, the resin can be dried by washing it with ether (3 x) or pentane (3 x).

Fmoc deprotection: A 20 % piperidine/DMF solution is added to the resin (10 mL/g resin). The suspension is shaken for 1 min after which the suspension is filtered. This step is repeated for 5 min and 10 min. Finally, the resin is washed with DMF (3 x), MeOH (3 x) and DCM (3 x).

Boc deprotection: The resin is treated with a 50 % TFA/DCM solution for 5 min. After filtration; the same solution is applied and the suspension is shaken for 25 min. Finally, the beads are washed with DCM (3 x), MeOH (3 x), 10 % DIEA/DCM (3 x), DCM (3 x).

Capping: The free amines are capped by adding a mixture of Ac₂O/pyridine/DCM (1:3:16) to the beads. After 1 h, the resin is filtered and washed.

Loading determination: A known amount (typically ~10 mg) of the resin is treated with a 20 % piperidine/DMF solution for 30 min. After occasional swirling, the resin was left to settle. Subsequently, an amount of the solution was transferred to two UV cuvettes (~3 mL). By measuring the absorbance value at $\lambda = 300$ nm, the concentration of the piperidine-fulvene adduct could be determined by applying the following formula: “Abs = 8.0618 x conc.- 0.047”. This concentration could be correlated to the loading by taken into account the amount of resin used for the loading test.

Automated synthesis: The automated synthesis is performed on a Syro I automated peptide synthesiser from MultiSyntech (Witten, Germany). All reactions are performed at ambient temperature and without protective atmosphere. First, the resin is weighed

into 2, 5 or 10 mL syringes, depending on the amount of resin. The syringes are placed in a reaction block that has 24 positions. This reaction block ensures vortexing of the suspensions and subsequent filtration.

Fmoc deprotection is done in two steps. First a 40 % piperidine solution is added to the resin for 3 min. After filtration and washing with DMF, a second volume of 40 % piperidine/DMF solution is added, which is immediately diluted until 20 % by adding the same amount of DMF. This time, the suspension is vortexed for 12 min after which the solution is drained and the resin is washed 6 times with DMF.

The *iv*Dde group is deprotected by adding a 2 % $\text{H}_2\text{NNH}_2\cdot\text{H}_2\text{O}$ /DMF solution to the resin for 2 times 10 min.

The azide group is reduced by adding a solution of 0.5 M Me_3P in THF/ H_2O (1:1) to the resin. After vortexing the suspension for 10 min, the solution is drained and the step is repeated once.

Amino acids are coupled by adding a 0.5 M solution of AA_x /DMF¹²⁷ to the resin, followed by the addition of a 0.5 M solution of HBTU/DMF. Finally, a 2 M DIEA/NMP solution is added in such a manner that the ratio AA_x /HBTU/DIEA is 1:1:2. In total, 5 equivalents of AA_x are added. The resulting suspension is vortexed for 40 min after which the solution is drained and the resin is washed 6 times with DMF.

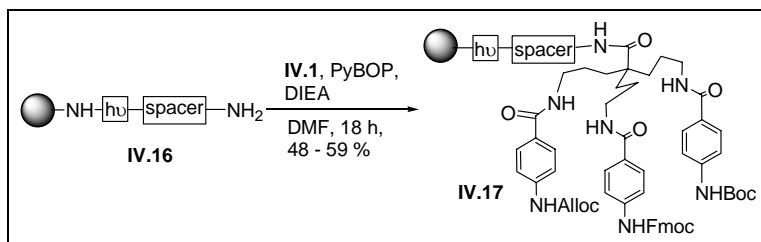
Capping is performed by adding a solution of Ac_2O /pyridine/NMP (1:3:10) to the resin. An equal amount of DMF is subsequently added and the resulting suspension is vortexed for 40 min, after which the solution is drained and the beads are washed.

¹²⁷ Except in the case of FmocPheOH which is dissolved in NMP for solubility reasons.

shaken for 3 h. After draining and washing the resin, approximately 1 mg of the beads were subjected to a NF31 test which was negative.

Finally, the Boc group was deprotected.

VIII.3.2.3. Coupling of scaffold IV.1 and subsequent capping



A solution of **IV.1** (4.5 mg, 4.5 μmol) and PyBOP (2.3 mg, 4.5 μmol) in 0.15 mL DMF was prepared. When homogeneous, the solution was transferred to the pre-swollen resin and after adding DIEA (2.4 μL , 13.5 μmol) the suspension was shaken for 18 h. The resin was drained and washed thoroughly. The TNBS test turned the beads dark-yellow and with NF31 we got red beads. The remaining free spacer-amino groups were capped for 1 h with a 0.1 M solution of AcOH and PyBOP in the presence of 2 eq DIEA. The ninhydrin test was negative. The loading was 0.075 mmol/g and the amount of Fmoc-deprotection was 12%. Thus the total loading was 0.085 mmol/g which correlated (maximal theoretical loading is 0.173 mmolg⁻¹) to a yield of 49%.

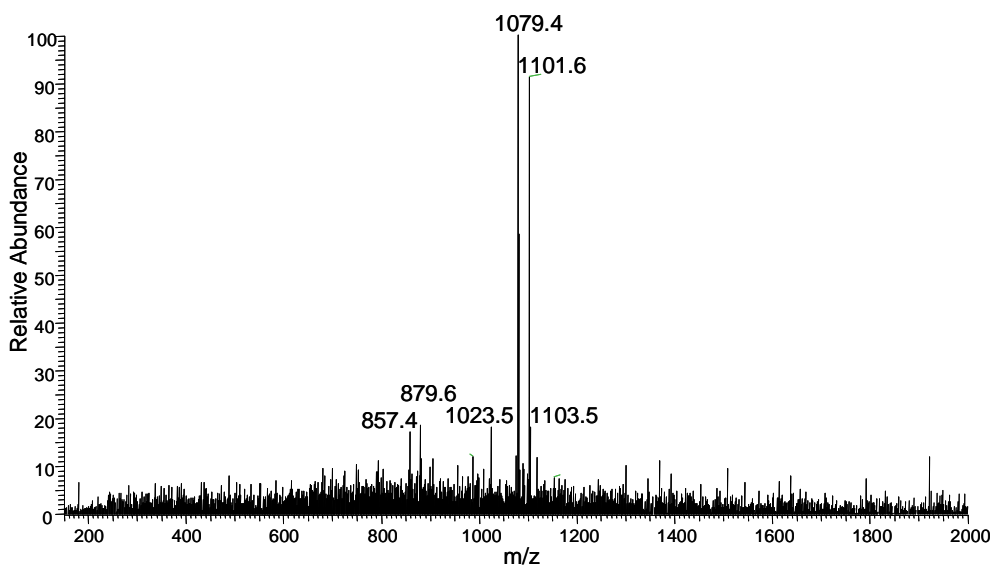
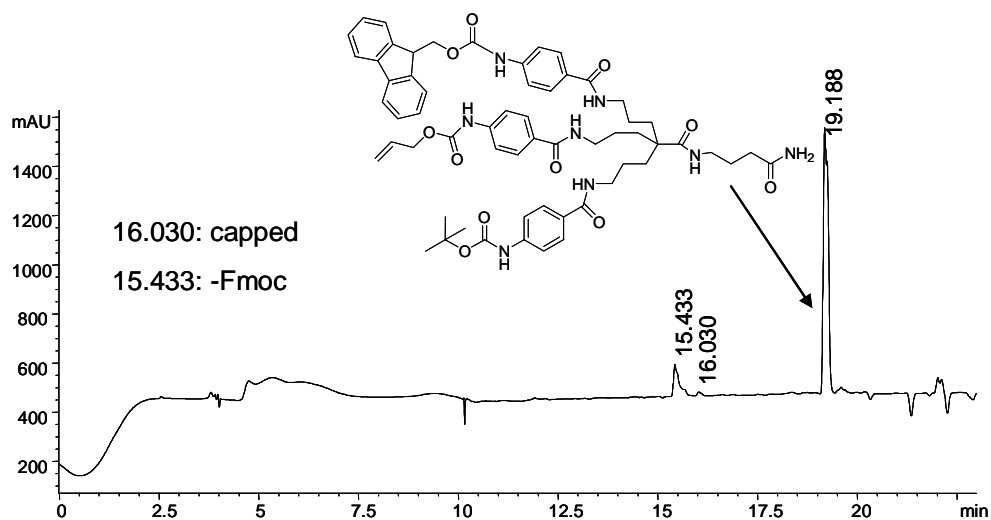
Molecular Formula: C₆₀H₇₀N₈O₁₁

MW.: 1079.2 g/mol

Exact mass: 1078.5 Da

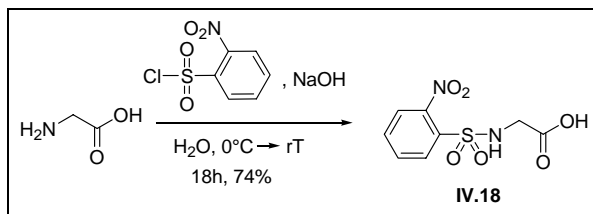
ES. (after photocleavage in MeCN): 857.4 [M-Fmoc+H]⁺, 879.6 [M-Fmoc+Na]⁺, 1023.5 [M-tBu+H]⁺, 1079.4 [M+H]⁺; 1101.6 [M+Na]⁺.

HR-ES (after photocleavage in MeCN, calculated for the Fmoc deprotected **IV.17**): [C₄₅H₆₀N₈O₉ + H]⁺: 857.45556, found: 857.45427.



VIII.3.3. Synthesis of new glycine derivatives

VIII.3.3.1. Synthesis of *o*NBSGlyOH



Glycine (1 g, 13 mmol) was dissolved in a 100 mL aqueous NaOH (0.640 g) solution. After putting the flask in an ice bath, *o*NBSCl (0.754 g, 16 mmol, 1.2 eq) and NaOH (0.150 g) were added. This step was repeated 4 times over a period of 4h. Then the reaction was stirred overnight. Upon acidifying with NaHSO₃H, a white precipitate was formed. This precipitate was filtered and dissolved in a mixture of water and methanol. The solution was then lyophilised to give a white powder (2.51 g, 74 %)

Molecular Formula: C₈H₈N₂O₆S

MW.: 260.22 g/mol

RF. (DCM:MeOH 95:5 + drop AcOH): 0.36

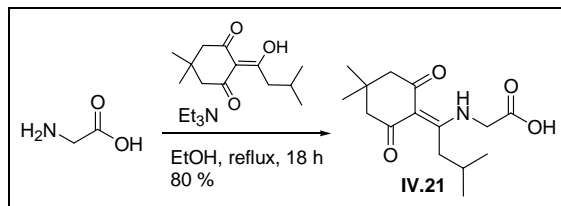
Melting Point: 154-156 °C

IR.: 3472 (br.), 3319 (m), 3096 (m), 2874 (m), 1712 (s), 1534 (s), 1434 (s), 1384 (s), 1347 (s), 1313 (s), 1260 (s), 1166 (s), 1107 (s), 887 (s) cm⁻¹.

E.S. (m/z): 259.3 [M-H]⁺

¹H-NMR (500 MHz, DMSO-d₆): δ 12.55 (1H, br. s), 8.37 (1H, 7, *J* = 5.4 Hz), 8.04-8.00 (1H, m), 7.97-7.92 (1H, m), 7.86-7.80 (2H, m), 3.75 (2H, d, *J* = 5.4 Hz) ppm.

APT (75 MHz, DMSO-d₆): δ 170.3 (C), 147.3 (C), 133.9 (CH), 133.5 (C), 132.6 (CH), 129.7 (CH), 124.3 (CH), 43.9 (CH₂) ppm.

VIII.3.3.2. Synthesis of *iv*DdeGlyOH

Et₃N (1.74 mL, 12.5 mmol, 1.5 eq) and *iv*DdeOH (2.36 mL, 10.8 mmol, 1.3 eq) were added to a suspension of glycine (623 mg, 8.30 mmol, 1 eq) in EtOH (16 mL). The suspension was refluxed overnight under inert atmosphere. After 18 h the clear, yellow solution was evaporated under reduced pressure to give a yellow residue. After redissolving the residue in a 1:1 dioxane/water mixture, a 4N HCl solution was added drop wise until no more precipitation occurred. The white precipitate was dissolved in water/MeOH and was subsequently lyophilised to give a white powder (1.86 g, 80 %).

Molecular Formula C₁₅H₂₃NO₄ **MW.:** 281.35 g/mol

RF. (DCM:MeOH 8:2 + drop AcOH): 0.57

Melting Point: 234-237 °C

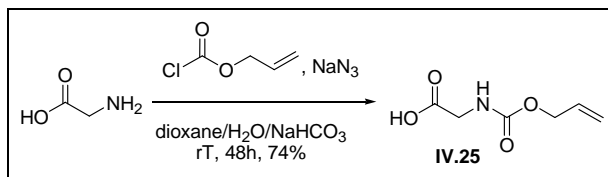
I.R.: 2959 (m), 2866 (m), 1834 (w), 1725 (s), 1642 (s), 1578 (s), 1534 (s), 1455 (m), 1429 (m), 1414 (m), 1218 (s), 1181 (m), 1146 (m), 918 (m) cm⁻¹.

ESI-MS. (m/z): 280.3 [M-H]⁻

¹H-NMR (500 MHz, DMSO-d₆): δ 13.63 (1H, t, *J* = 4.8 Hz), 13.24 (1H, br.s.), 4.33 (2H, d, *J* = 5.0 Hz), 2.94 (2H, s), 2.28 (4H, s), 1.81 (1H, sep, *J* = 6.8 Hz), 0.93 (6H, s), 0.89 (6H, d, *J* = 6.9 Hz) ppm.

APT + HSQC + HMBC (75 MHz, DMSO-d₆): δ 175.0 (C), 169.8 (C), 106.7 (C), 52.6 (CH₂), 45.0 (CH₂), 36.7 (CH₂), 29.5 (C), 28.2 (CH), 27.8 (CH₃), 22.0 (CH₃) ppm.

VIII.3.3.3. Synthesis of AllocGlyOH



An aqueous solution (3 mL) of NaN_3 (1.04 g, 16 mmol, 1.2 eq) was added to a solution of AllocCl (1.2 mL, 11 mmol, 0.8 eq) in dioxane (3 mL). The resulting mixture was stirred for 1 h. Meanwhile, glycine (1 g, 13 mmol, 1 eq) was dissolved in a 1% Na_2CO_3 solution (38 mL). When this solution was added to the *in situ* activated allylchloroformate, the pH was kept between 8 and 10 by adding some extra Na_2CO_3 . After 48 h, the mixture was extracted 3 times with MTBE, acidified until pH 1 and subsequently extracted with EtOAc (3X). This organic phase was dried on MgSO_4 and evaporated to give a yellow oil (2.86 g, 74%).

Molecular Formula: $\text{C}_6\text{H}_9\text{NO}_4$

MW.: 159.14 g/mol

RF. (DCM:MeOH 9:1 + drop AcOH): 0.34

Melting Point: 28-30 °C

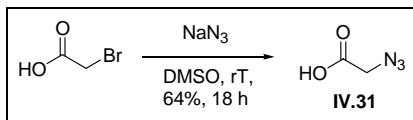
IR.: 3375 (br.), 2942 (w), 1713 (m), 1523 (m), 1412 (m), 1221 (m), 1055 (m), 991 (m), 905 (s), 725 (s)

ES. (m/z): 158.1 $[\text{M}-\text{H}]^-$

^1H -NMR (500 MHz, CDCl_3): δ 9.99 (1H, br. s), 6.67 (1H, br. s), 5.87 (1H, m), 5.62 (1H, s), 5.27 (1H, d, $J = 17.0$ Hz), 5.18 (1H, d, $J = 10.1$ Hz), 4.56 (2H, d, $J = 4.7$ Hz), 3.96 (2H, s) ppm.

APT (75 MHz, CDCl_3): δ 174.1 (C), 156.7 (C), 132.3 (CH), 118.0 (CH_2), 66.1 (CH_2), 42.4 (CH_2) ppm.

VIII.3.3.4. Synthesis of azidoglycine



NaN_3 (5.13 g, 78.9 mmol, 2 eq) was dissolved in DMSO (210 mL) and stirred for 90 min. Bromoacetic acid (5.17 g, 37.4 mmol, 1 eq) was then added in a solution of DMSO (2 mL). After stirring for another 18 h, the solution was diluted with H_2O (170 mL) and acidified with 6 N HCl (33 mL). The aqueous phase was then 3 times extracted with MTBE. The organic phases were pooled and extracted with a 0.1 N HCl solution saturated with NaCl. After drying and subsequent evaporation of the organic phase, an oil (2.40 g, 64%) was obtained.

Molecular Formula $\text{C}_2\text{H}_3\text{N}_3\text{O}_2$

M.W.: 101.02 g/mol

I.R.: 3452 (br.), 2927 (w), 2111 (s), 1726 (m), 1623 (w), 1420 (m), 1282 (m), 1217 (m) cm^{-1} .

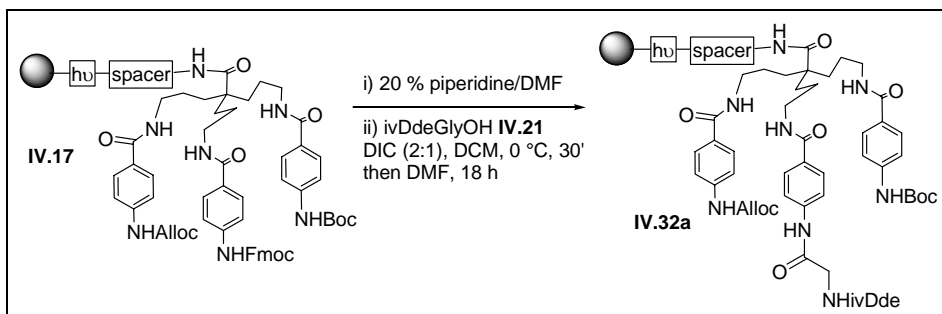
EI (m/z): 101 [M^+], 45 [CHO_2^+]

$^1\text{H-NMR}$ (300 MHz, CDCl_3): δ 9.62 (1H, br.s), 3.97 (1H, br.s.) ppm.

APT (75 MHz, CDCl_3): δ 174.2 (C), 50.1 (CH_2) ppm.

VIII.3.4. Incorporation of the glycine derivatives

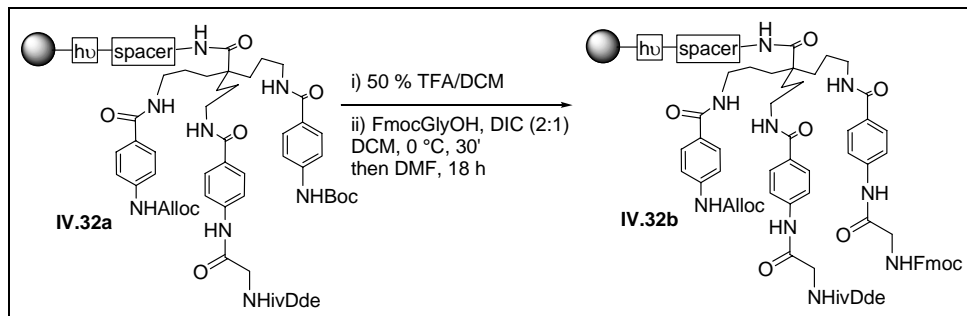
VIII.3.4.1. Attachment of *iv*DdeGlyOH



First the resin **IV.17** (1.6 g, 0.100 mmol/g, 0.19 mmol, 1 eq) was Fmoc deprotected. During the Fmoc deprotection, *iv*DdeGlyOH (646 mg, 2.3 mmol, 12 eq) was dissolved in DCM (4 mL) and the solution was cooled down until 0 °C. After adding DIC (170 μ L, 1.1 mmol, 6 eq), the mixture was stirred for 30 min and subsequently added to the Fmoc deprotected **IV.17**. To ensure complete solubility of the symmetrical anhydride, DMF (4 mL) was added. The resulting suspension was shaken for 18 h and after filtering the resin, the beads were thoroughly washed.

A small sample was photocleaved in EtOH and analysed via LC which show the presence of a small amount of starting material. The coupling was thus repeated once and no more starting material was observed.

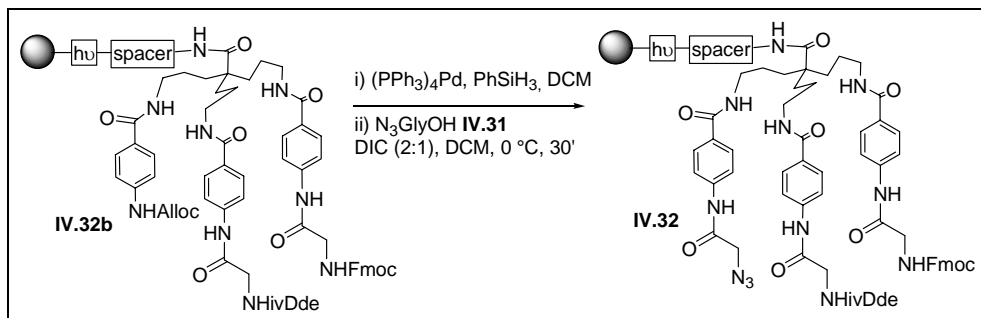
VIII.3.4.2. Coupling of FmocGlyOH



First, the Boc group was deprotected. In the mean while, FmocGlyOH (683 mg, 2.3 mmol, 12 eq) was dissolved in DCM (4 mL) and cooled down until 0 °C. After adding DIC (170 μ L, 1.1 mmol, 6 eq), the mixture was stirred for 30 min and subsequently added to the Boc deprotected **IV.32a**. To ensure complete solubility of the symmetrical anhydride, DMF (4 mL) was added. The resulting suspension was shaken for 18 h and after filtering the resin, the beads were thoroughly washed.

A small sample was photocleaved in EtOH and analysed via LC which show the presence of a small amount of starting material. The coupling was thus repeated once and no more starting material was observed.

VIII.3.4.3. Coupling of azidoglycine



The resin was suspended in DCM. First, the scavenger PhSiH_3 (585 μL , 4.75 mmol, 25 eq) was added to this suspension followed the Pd^0 catalyst (22 mg, 19 μmol , 10 mol %). The resulting brown mixture was shaken for 1 h and subsequently filtered and washed 3 times with DCM. After repeating this procedure once, the Alloc group was fully removed as monitored by HPLC after photocleavage in EtOH.

Next, azidoglycine **IV.31** (230 mg, 2.3 mmol, 12 eq) was dissolved in DCM (8 mL) and cooled down until 0 °C. After adding DIC (170 μL , 1.1 mmol, 6 eq), the mixture was stirred for 30 min and subsequently added to the Alloc deprotected **IV.32b**. The resulting suspension was shaken for 18 h and after filtering the resin, the beads were thoroughly washed.

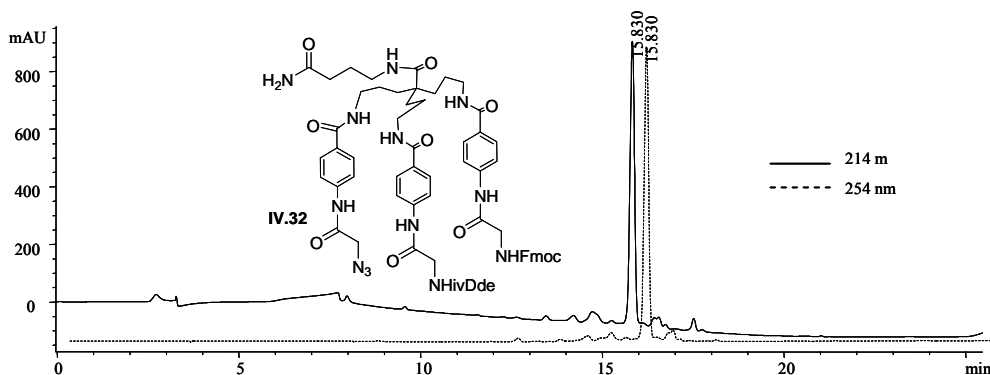
A small sample was photocleaved in EtOH and analysed via LC which show the presence of a small quantity of starting material. The coupling was thus repeated once and no more starting material was observed.

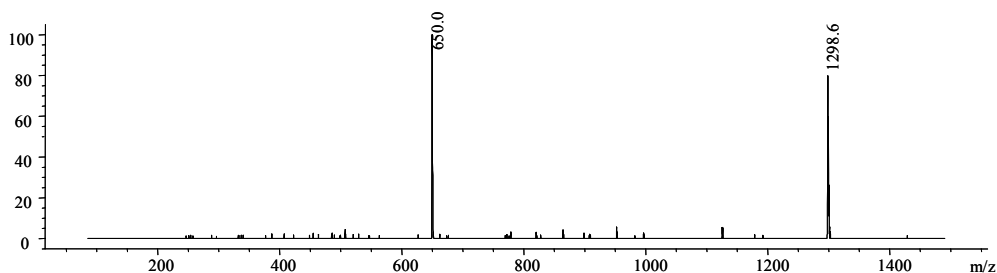
Molecular Formula: $\text{C}_{70}\text{H}_{83}\text{N}_{13}\text{O}_{12}$

MW.: 1298.5 g/mol

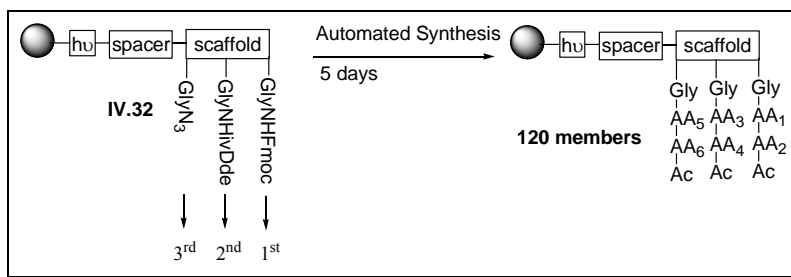
Exact mass: 1297.6 Da

LC-MS. (after photocleavage in EtOH): 650 $[\text{M}+2\text{H}]^{2+}$, 1298.6 $[\text{M}+\text{H}]^+$





VIII.3.5. Automated synthesis of 120 members



In 24 plastic syringes of 2 mL, a small amount of resin **IV.32** (1 to 3 mg, 0.09 μmol to 0.27 μmol) was weighed. These syringes were placed into the reaction block of the Syro I.

After inserting the correct sequences in the software program and preparing the AA_x, HBTU, DIEA, piperidine and capping solutions, the sequence was started.

First the Fmoc group was deprotected. The first AA was coupled by adding a 0.5 M solution of AA_x (60 μL) to the resin. Then, each syringe was filled with a 0.5 M HBTU solution (60 μL) and a 2 M DIEA solution (30 μL). The suspension was vortexed for 40 min, after which it was drained and washed. This procedure was repeated once. The first strand was terminated by adding the capping mixture (120 μL) and DMF (120 μL) to the resin.

The ivDde group was removed by adding a 2 % H₂N.NH₂.H₂O/DMF (180 μL) to the syringes. After vortexing for 10 min, the resin was shortly washed with DMF and the

deprotection was repeated once. Then the subsequent AA_x were coupled as already described. The second strand was terminated by capping the free amine with A₂O.

Finally, the azide was reduced by adding 0.5 M Me₃P in THF/H₂O (180 μL) for 10 min to the syringes. The reduction was repeated once and then the resin was drained and washed thoroughly with DMF and *i*PrOH. Then the subsequent AA_x were coupled as already described. The synthesis was terminated by capping the free amine.

After the synthesis, the resins were washed with *i*PrOH (3 x) and pentane (3 x).

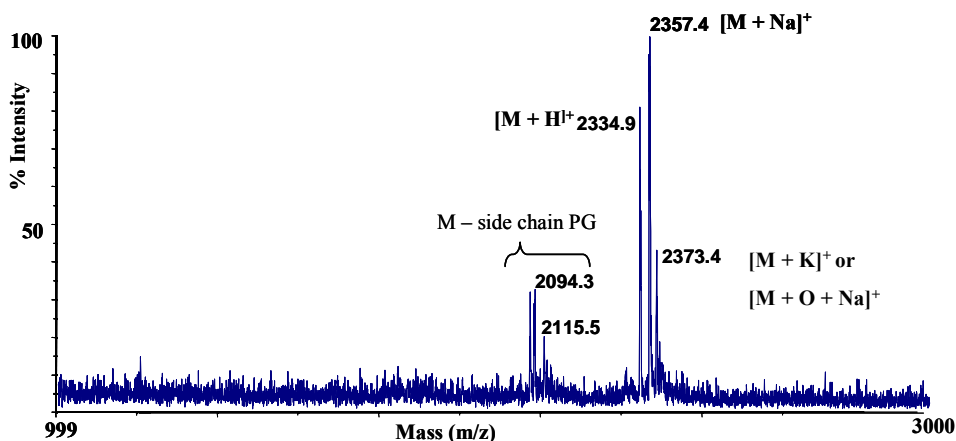
In total, 120 members were synthesized by repeating this overall procedure 5 times.

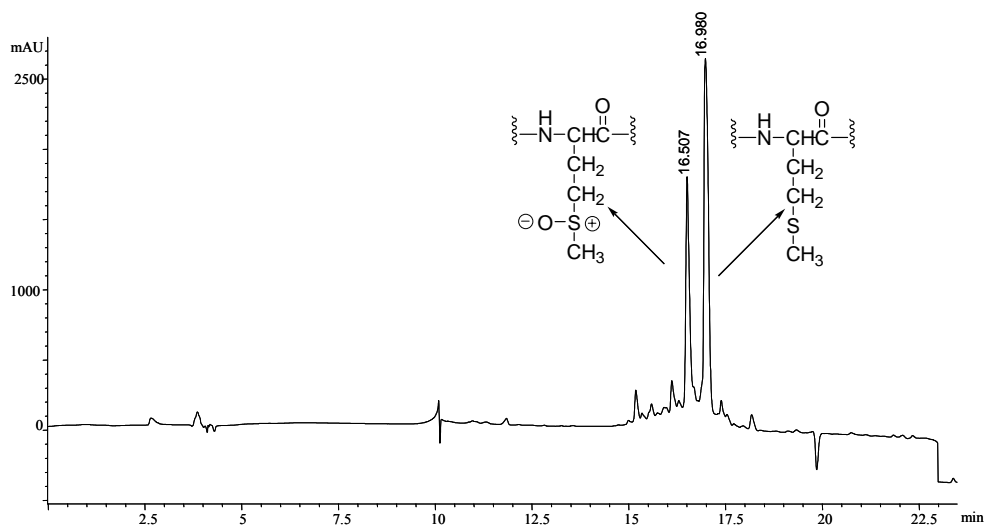
Molecular Formula: C₁₂₁H₁₅₇N₂₂O₂₂S₂

MW.: 2335.8 g/mol

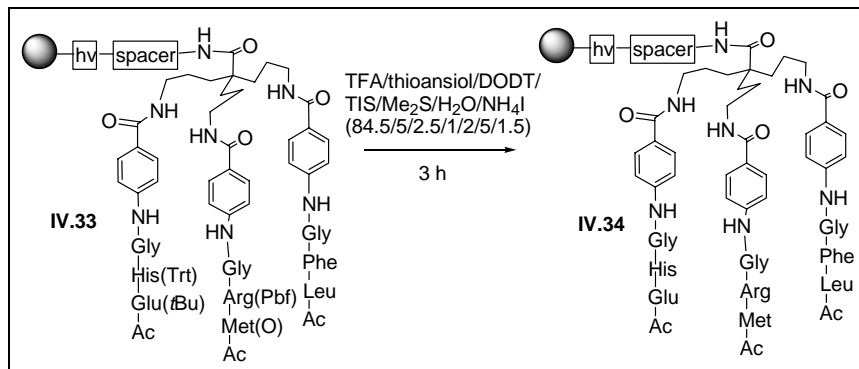
Exact mass: 2334.1 Da

MALDI-TOF. (after photocleavage in EtOH): 2094.3 [M-Trt+H]⁺, 2115.5 [M-Trt+Na]⁺, 2334.9 [M+H]⁺, 2350.7 [M+O+H]⁺, 2357.4 [M+Na]⁺, 2373.4 [M+O+Na]⁺ or [M+K]⁺





VIII.3.6. Side chain deprotection of the library



The procedure is described for the specific case of **IV.33** but was applied on all of the 120 members.

The TFA cleavage mixture was prepared by mixing TIS (100 μ L), DODT (250 μ L), Me₂S (200 μ L) and thioansole (500 μ L) with TFA (8.45 mL). For the reduction of Met(O), NH₄I (230 mg) was dissolved in H₂O (500 μ L).

First, the NH₄I_{aq} (10 μ L) was added to each member followed by the addition of the TFA cleavage mixture (190 μ L). The suspension was left for 3 h, after which the beads were drained and washed thoroughly.

From this library, 20 randomly picked members were photocleaved in H₂O and analysed via HPLC (*vide infra*). The identity of all the 120 members was confirmed in the affinity chromatography experiments where the reaction times were monitored via LC-MS.

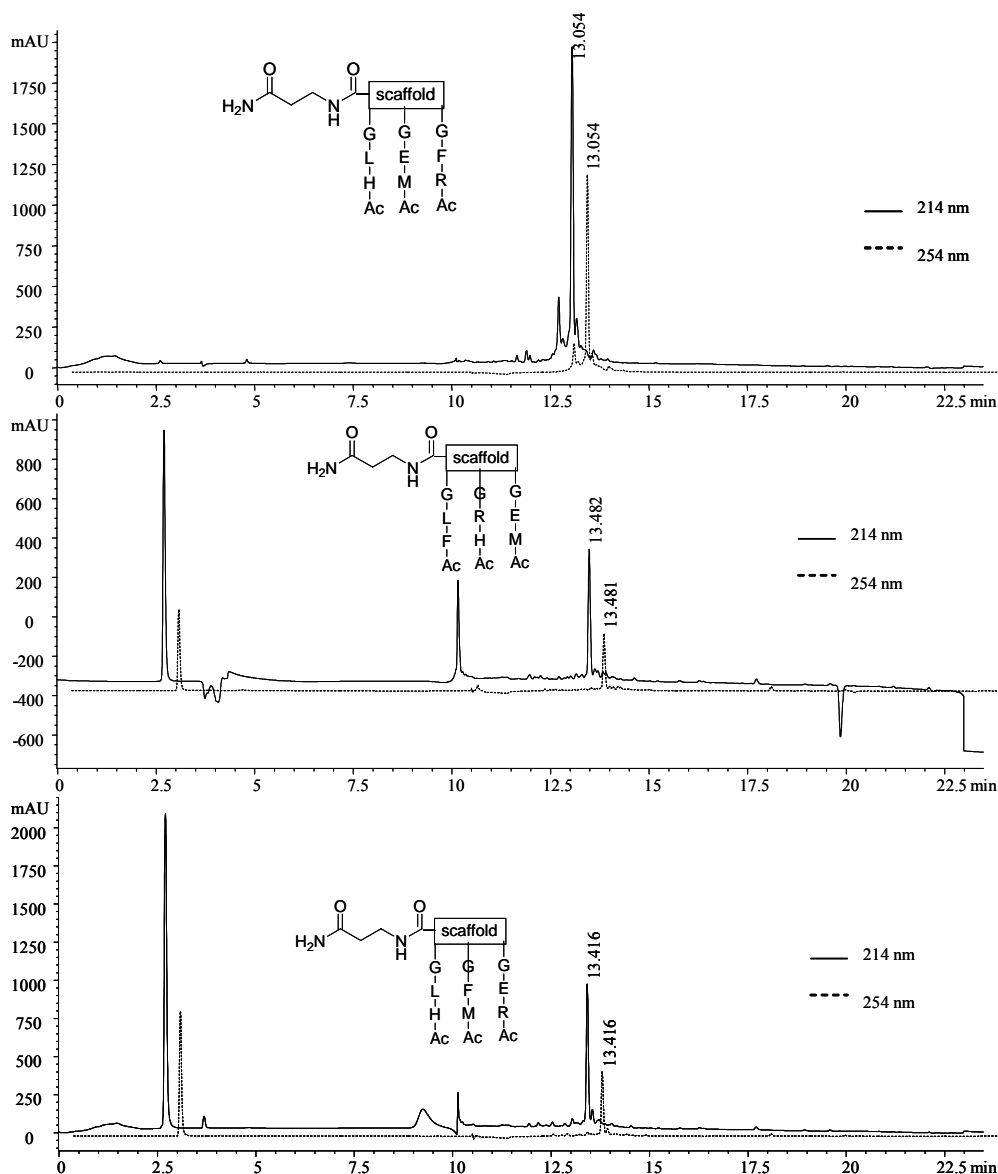
Molecular Formula: C₈₅H₁₁₉N₂₂O₁₉S

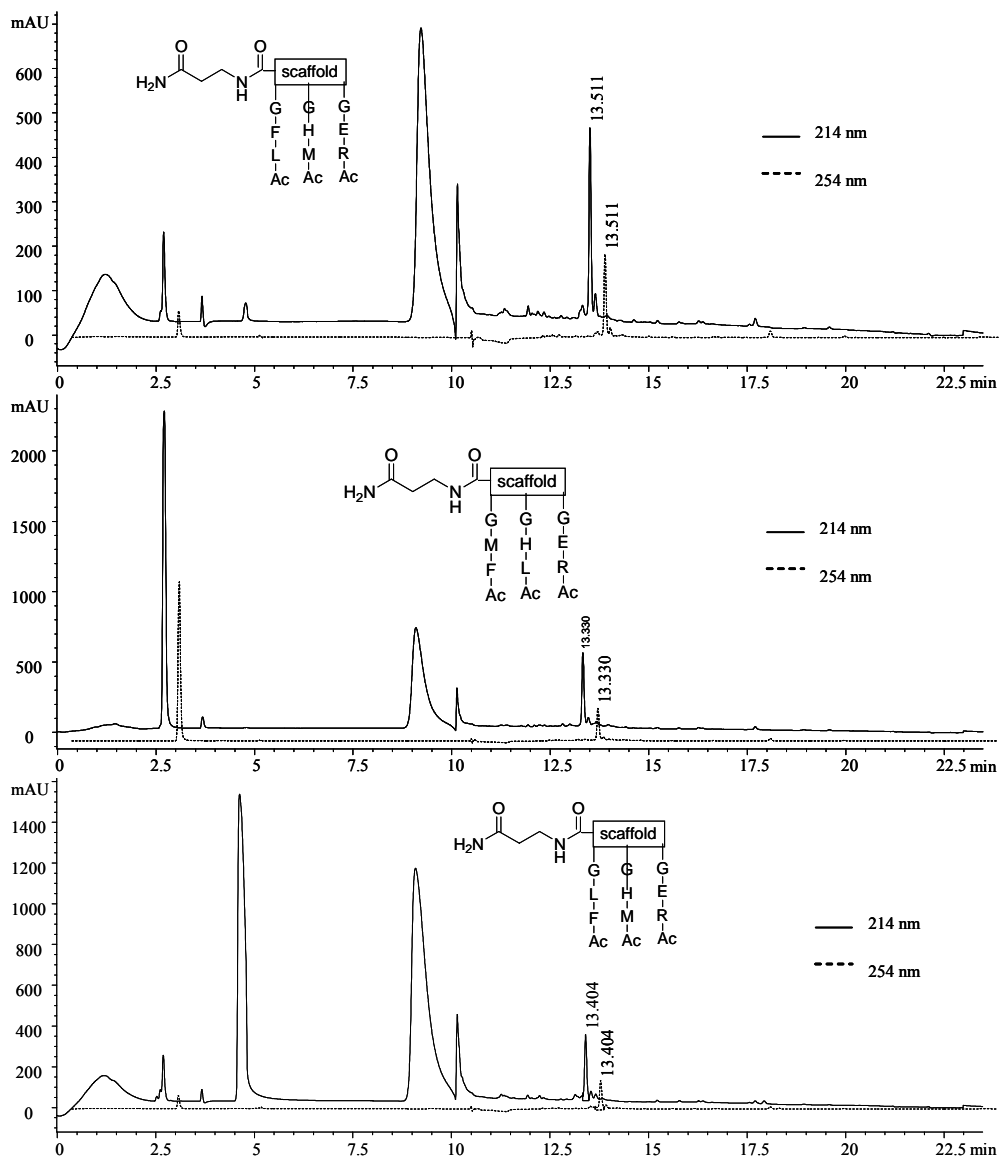
MW.: 1785.1 g/mol

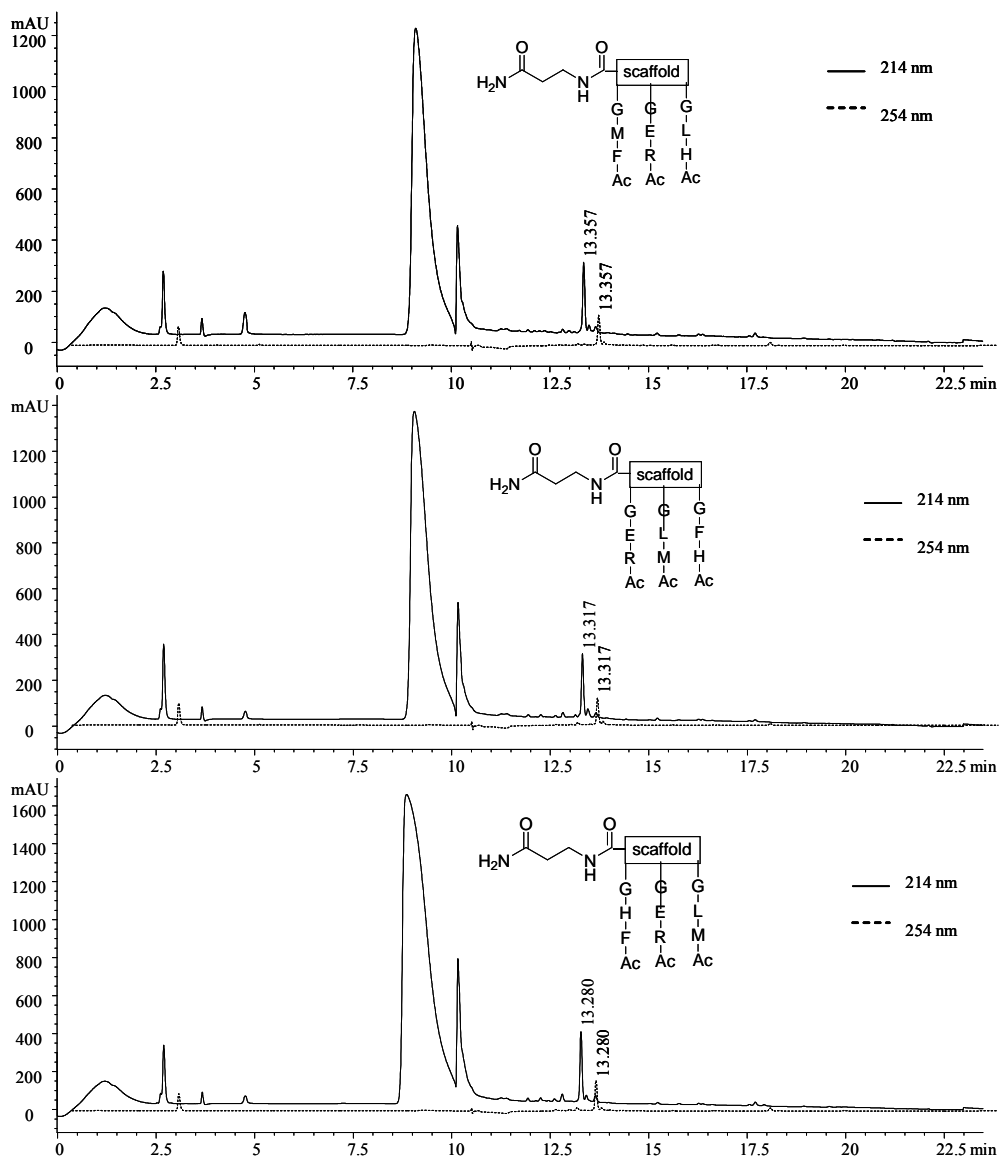
Exact Mass: 1783.9 Da

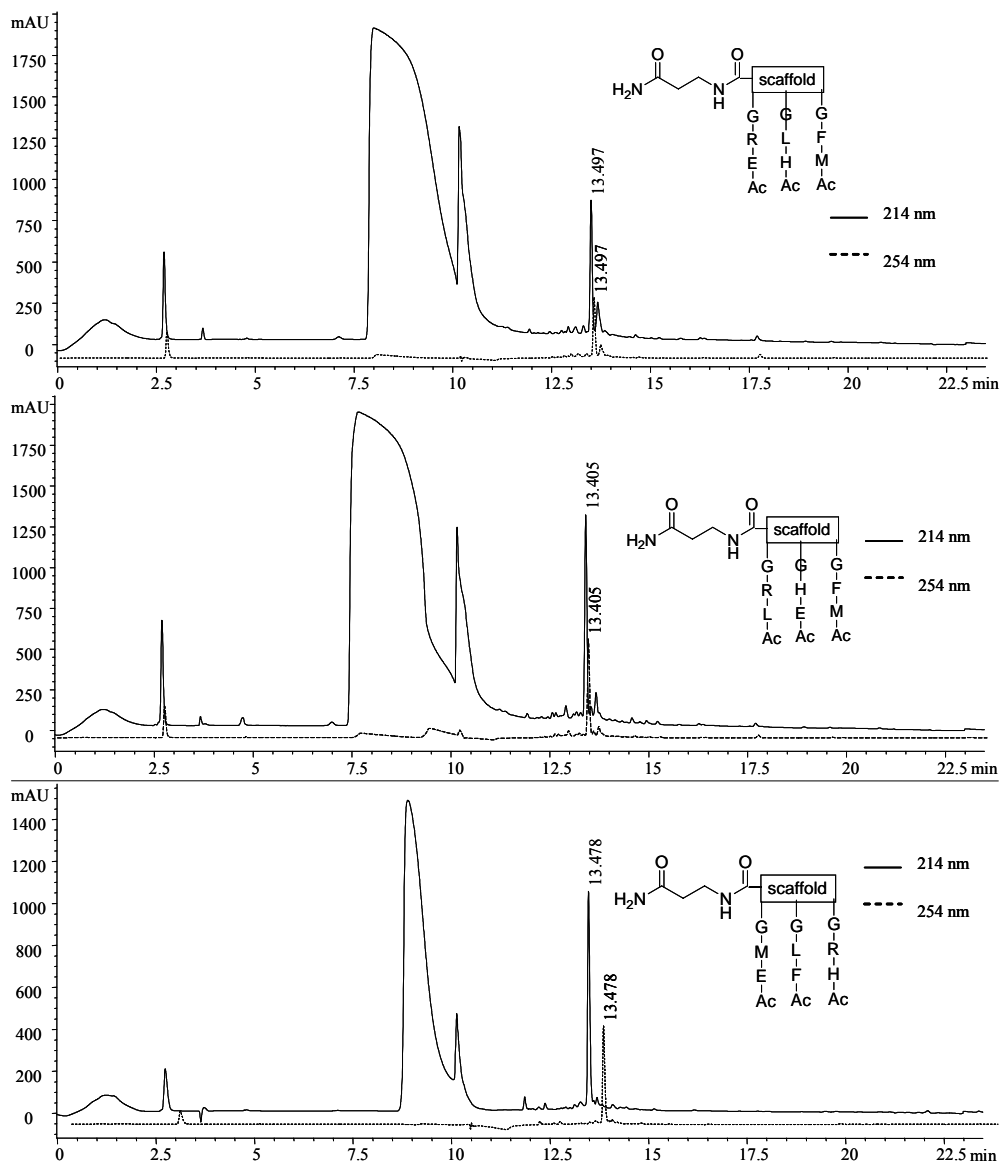
ES. (after photocleavage in H₂O): 892.6 [M+2H]²⁺, 903.6 [M+Na+H]²⁺

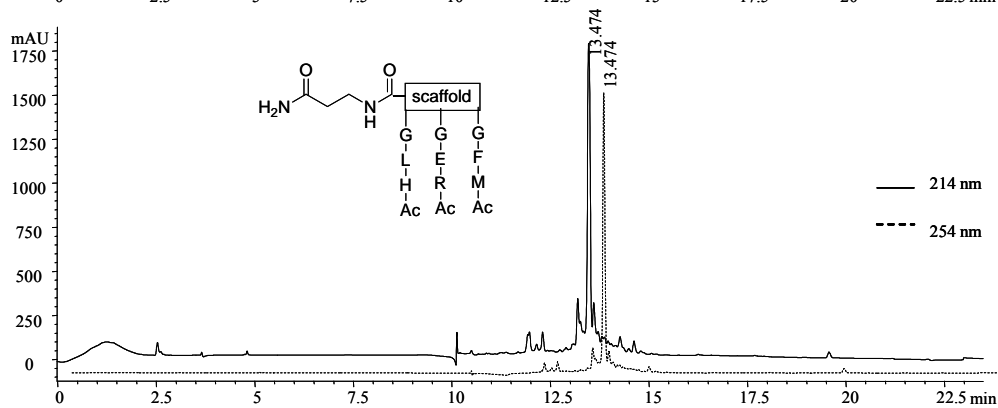
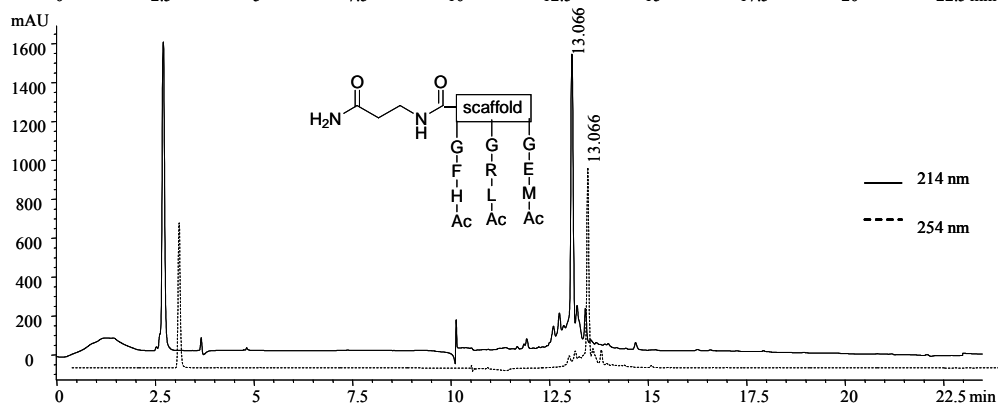
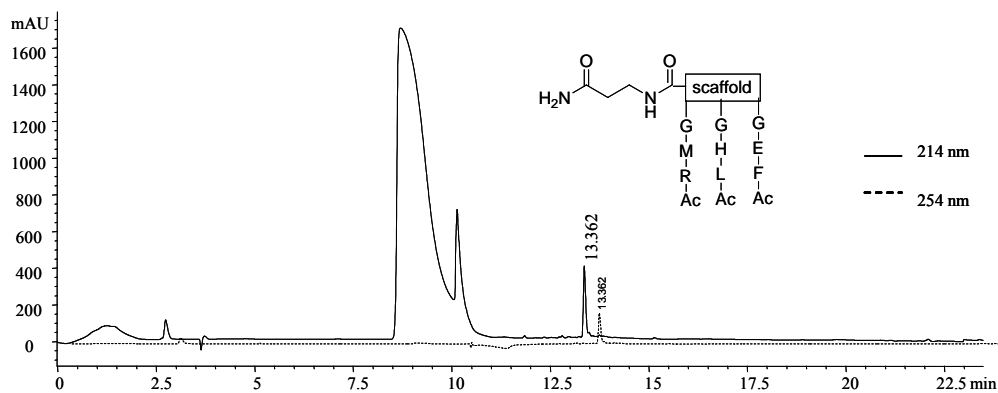
Confirming the overall purity of the library:

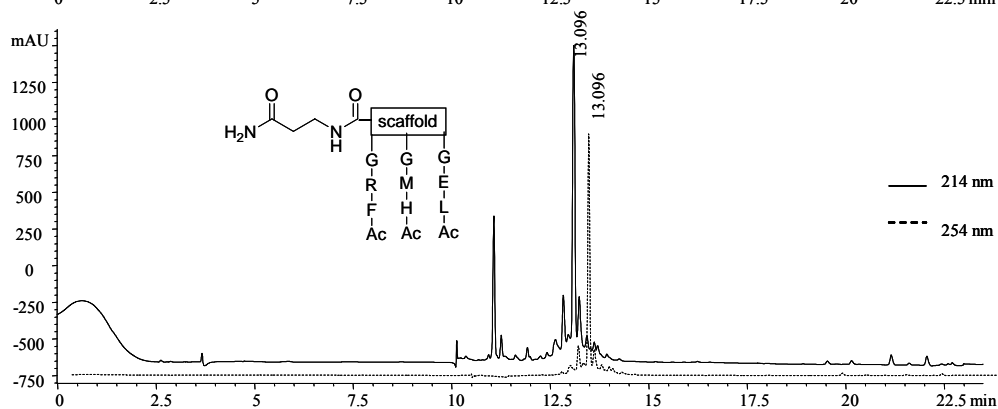
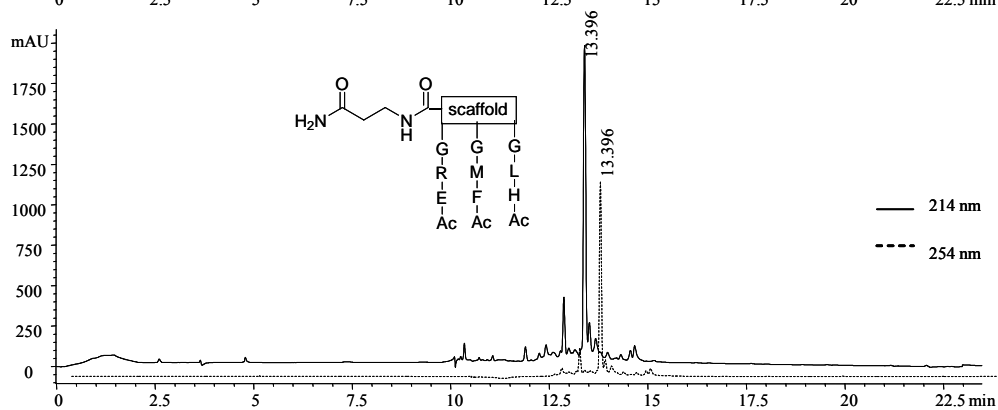
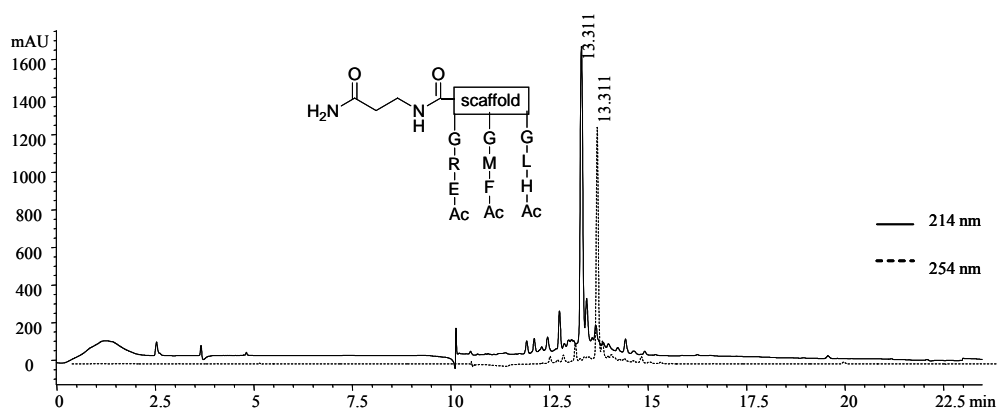








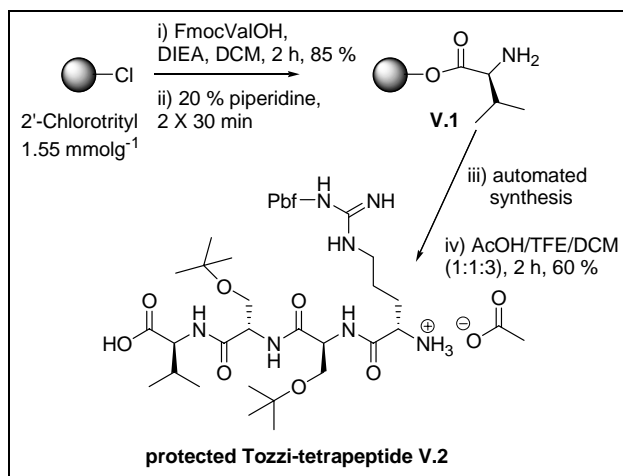




VIII.4. Screening of the library: development of the first SPE tests

VIII.4.1. Preparation of Tentagel-bound Tozzi-tetrapeptide

VIII.4.1.1. Synthesis of protected Tozzi-tetrapeptide



This work was done in cooperation with Drs. S. Figaroli.

FmocValOH (210 mg, 0.62 mmol, 2 eq) was added to the preswollen 2'-chlorotritylresin (200 mg, 0.31 mmol, 1 eq). Next, DCM (2 mL) was added and the suspension was shaken until all of the FmocValOH was dissolved. After adding DIEA (108 μ L, 0.62 mmol, 2 eq), the suspension was shaken for 2 h after which the solution was drained and the beads thoroughly washed with DMF (3 x), 10 % DIEA/MeOH (3 x), MeOH (3 x) and DCM (3 x). A loading value of 1.06 mmol⁻¹ was determined which corresponded with a yield of 85 %.

The Fmoc group was deprotected using a 20 % piperidine/DMF solution for two times 30 min.

Subsequently an amount of resin (17 mg, 18 μmol) was weighed into a syringe of 2 mL and put into the reaction block of the Syro I.

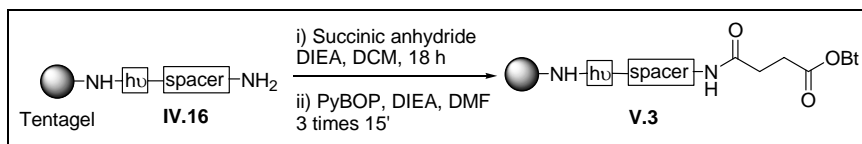
After the automated synthesis, the desired peptide was cleaved from the resin with 400 μL AcOH/TFE/DCM (1:1:3) for 2 h. The resin was subsequently washed 3 times with the cleavage mixture and the combined organic fractions were pooled and evaporated. The residual oil was co-evaporated 3 times with hexane, yielding 9.4 mg of the protected peptide (60 %)

Molecular Formula: $\text{C}_{38}\text{H}_{65}\text{N}_7\text{O}_{10}\text{S}$

MW.: 812.0 g/mol

ES.: 811.6 [M-H]⁻

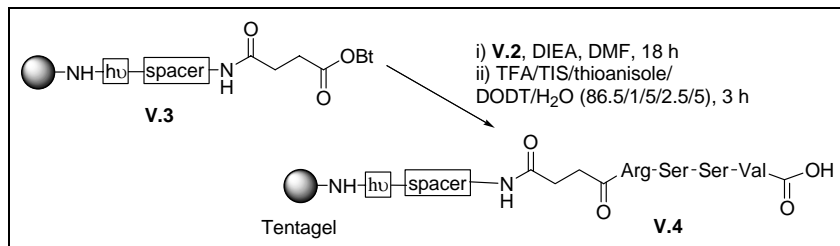
VIII.4.1.2. Reversing the synthesis order (from C→N to N→C)



A solution of succinic anhydride (8.6 mg, 86 μmol , 10 eq) in DCM (400 μL) was added to preswollen to IV.16 (40 mg, 8.4 μmol) and after addition of DIEA (30 μL , 170 μmol , 20 eq), the suspension was shaken for 18 h. Subsequently, the resin was drained and washed.

The free carboxylic acid on the resin (10 mg, 2.1 μmol) was then activated by adding 100 μL of a 0.5 M solution PyBOP in DMF (50 μmol , 24 eq) and 25 μL of a 2 M solution of DIEA in NMP (100 μmol , 48 eq). The resulting suspension was shaken for 15 min, after which the solution was filtered and the beads were washed (3 x DMF, 3 x DCM, 3 x DMF). This activation was repeated 3 times.

VIII.4.1.3. Coupling of V.2 to the preactivated V.3



The protected peptide **V.2** (7.4 mg, 8.5 μmol , 4 eq) was dissolved in DMF (100 μL) and added to resin **V.3**. Next, DIEA (2 μL , 11.5 μmol , 5.5 eq) was added and the suspension was vortexed for 18 h. Then, the beads were drained and washed. A cleavage mixture containing TFA/TIS/thioanisole/DODT/H₂O (86.5/1/5/2.5/5) was prepared and 100 μL of this mixture was added to the resin. After 3 h, the beads were drained and washed with DMF (3 x), 10 % DIEA/DCM (3 x), MeOH (3 x) and DCM (3 x) to give resin bound peptide **V.4**.

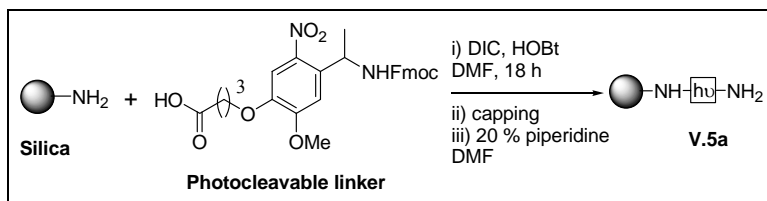
Molecular Formula: C₂₅H₄₅N₉O₁₀

MW.: 631.7 g/mol

ES. (after photocleavage in H₂O): 630.4 [M-H]⁻

VIII.4.2. Synthesis on silica

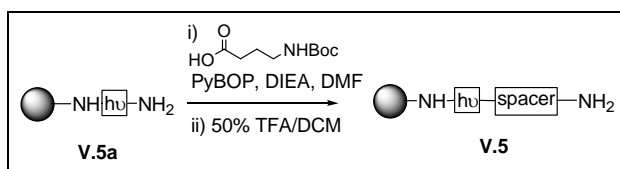
VIII.4.2.1. Coupling of the photocleavable linker on silica



The photocleavable linker (37 mg, 72 μmol) was dissolved in 2 mL DMF and the solution was added to the silica material (114 mg). The coupling reagent DIC (10 μL , 69 μmol) and HOBT (10 mg, 72 μmol) were added. The suspension was shaken for 18 h. After draining, the silica was washed. Next, the material was capped for 3 h. The loading was determined to be 0.471 mmol g^{-1} .

For the next reaction, the silica material was Fmoc deprotected.

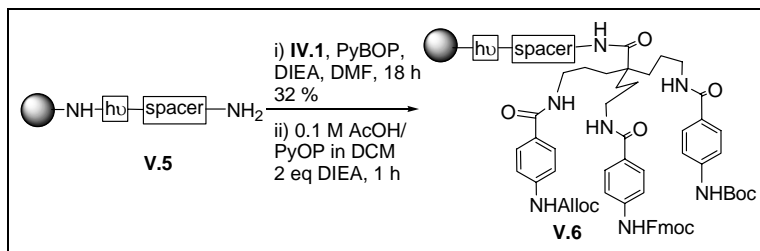
VIII.4.2.2. Coupling of the spacer Boc-GABA to construct IV.15



The spacer Boc-GABA (53 mg, 0.26 mmol, 5 eq) and the coupling reagent PyBOP (135 mg, 0.26 mmol, 5 eq) were added to the silica material (110 g, 52 μmol , 1 eq). DMF (1 mL) was added and the suspension was shaken until the reagents were dissolved. The base DIEA (90 μL , 0.52 mmol, 10 eq) was added whereafter the suspension was shaken for 3 h.

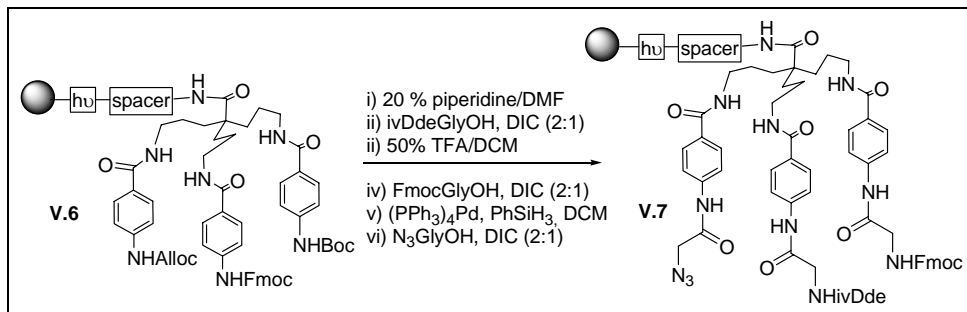
After draining and washing the silica the Boc group was deprotected.

VIII.4.2.3. Coupling of scaffold IV.1 and subsequent capping



A solution of **IV.1** (21 mg, 21 μmol) and PyBOP (11 mg, 21 μmol) in 0.4 mL DMF was prepared. When homogeneous, the solution was transferred to the silica material in a eppendorf tube. After adding DIEA (11 μL , 63 μmol) the suspension was vortexed for 18 h. The silica was isolated via centrifugation and subsequently drained and thoroughly washed.. The remaining free spacer-amino groups were capped for 1 h with a 0.1 M solution (300 μL) of AcOH and PyBOP in the presence of 2 eq DIEA. The ninhydrin test was negative. The loading was 0.060 mmol/g and the amount of Fmoc-deprotection was 44% (as determined by HPLC). Thus the total loading was 0.107 mmol/g which correlated (maximal theoretical loading is 0.330 mmol g^{-1}) to a yield of 32%.

VIII.4.2.4. Attachment of the glycine derivatives to V.6



For the incorporation of the glycine derivatives, the same protocol as described in VIII.3.4 was applied. The amount of silica construct **V.6** used was 40 mg (4.3 μmol).

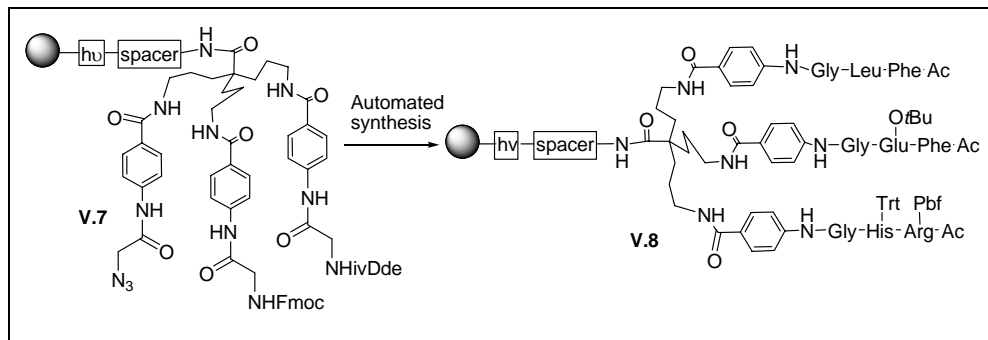
Molecular Formula: $\text{C}_{70}\text{H}_{83}\text{N}_{13}\text{O}_{12}$

MW.: 1298.5 g/mol

Exact mass: 1297.6 Da

LC-MS. (after photocleavage in EtOH): 1299.2 $[\text{M}+\text{H}]^+$

VIII.4.2.5. Synthesis of one library member on silica



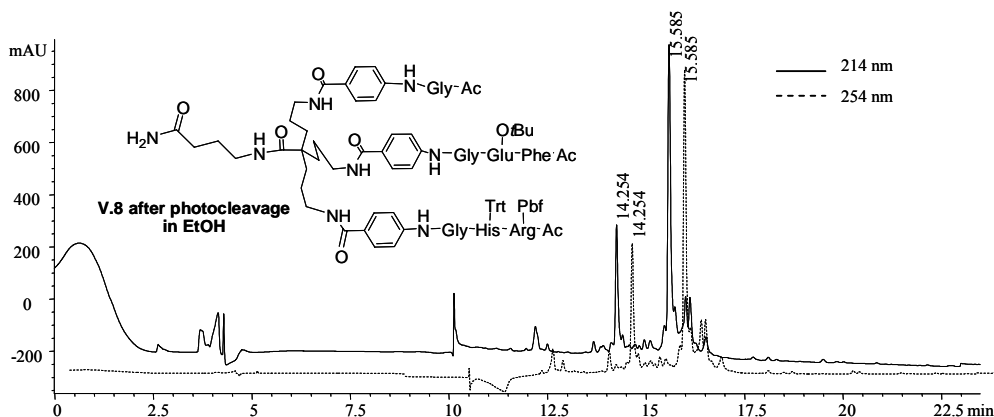
The automated synthesis was performed in a manner similar to the protocol described in **Paragraph VIII.3.5**. An amount of 10 mg of construct **V.7** (1.1 μmol) was subjected to this protocol. MALDI-TOF analysis after photocleavage in EtOH showed that a major deletion of the Leu and Met residues had occurred.

Molecular Formula: $\text{C}_{125}\text{H}_{156}\text{N}_{22}\text{O}_{22}\text{S}$

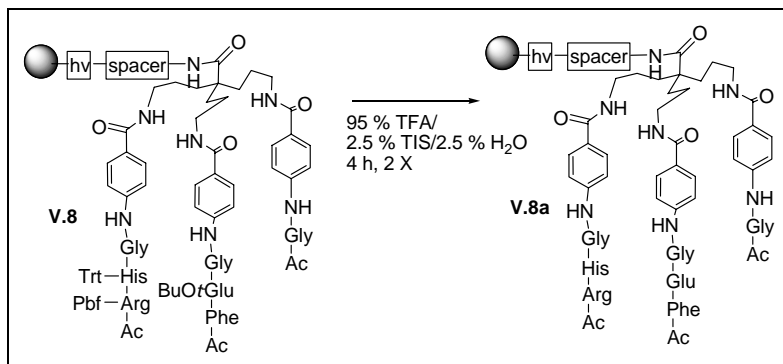
MW.: 2353.8 g/mol

Exact mass: 2349.2 Da

MALDI-TOF. (after photocleavage in EtOH): 2096.7 $[\text{M-Leu-Phe-Pbf}+\text{H}]^+$, 2112.7 $[\text{M-Leu-Phe}+\text{Na}]^+$, 2127.7 $[\text{M-Leu-Phe}+\text{K}]^+$



VIII.4.2.6. Side chain deprotection of V.8



The TFA cleavage mixture was prepared by mixing TIS (250 μ L) and H₂O (250 μ L) with TFA. The mixture (200 μ L) was then added to the silica construct **V.8** (10 mg). The suspension was left standing for 4 h. After draining the solution, the resin was washed and the deprotection was repeated once.

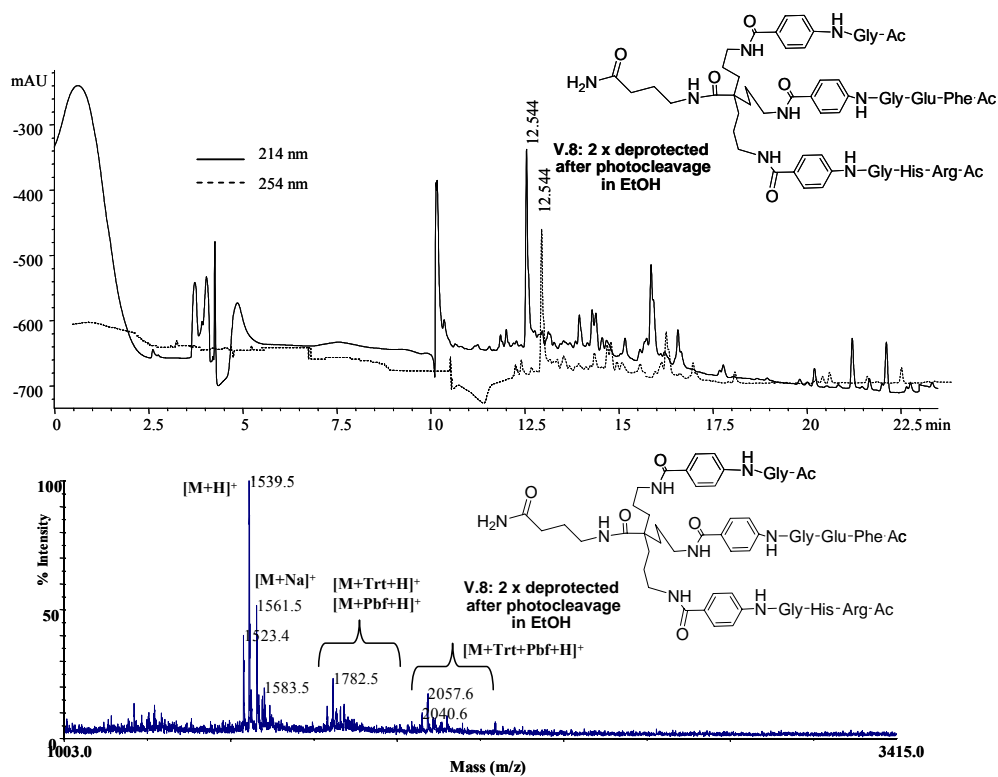
Analysis after photocleavage in EtOH revealed that the deprotection of the Trt and the Pbf group were not fully completed, even after a doubled deprotection.

Molecular Formula: C₇₄H₉₈N₂₀O₁₇

MW.: 1538.7 g/mol

Exact mass: 1539.7 Da

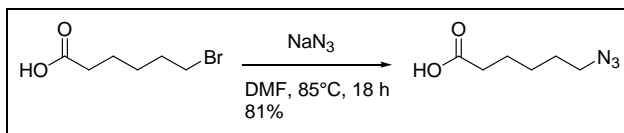
MALDI-TOF. (after photocleavage in EtOH): 1539.5 [M + H]⁺, 1561.5 [M + Na]⁺, 1782.5 [M + Trt + H]⁺, 2057.6 [M + Trt + Pbf + Na]⁺



VIII.5. Screening of the library: development of affinity LC

VIII.5.1. Development of the estradiol column V.11

VIII.5.1.1. Synthesis of azidohexanoic acid V.9



Bromohexanoic acid (6g, 31 mmol, 1 eq) was dissolved in 20 mL DMF. After adding NaN_3 (4g, 62 mmol, 2eq) the solution was refluxed for 18 h at an oil bath temperature of 85°C . After cooling down the solution, DMF was evaporated under vacuum to give an oil that was redissolved in DCM. This organic phase was then extracted 3 times with a 0.1 N HCl solution. After drying the organic phase on MgSO_4 and evaporation, 3.96 g of light yellow oil was obtained (81% yield).

Molecular Formula: $\text{C}_6\text{H}_{11}\text{N}_3\text{O}_2$ **MW.:** 157.09 g/mol

RF. (DCM + drop AcOH): 0.17

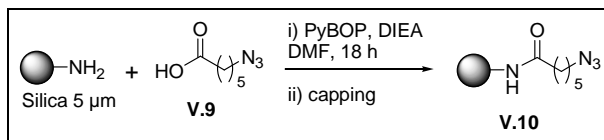
IR. (KBr-plate): 3075 (br.), 2939 (m), 2866 (m), 2093 (s), 1706 (s), 1254 (m), 910 (m), 731 (s) cm^{-1} .

ES. (m/z): 156.5 $[\text{M}-\text{H}]^-$

APT (75 MHz, CDCl_3): δ 179.5 (C), 51.2 (CH_2), 33.8 (CH_2), 28.5 (CH_2), 26.1 (CH_2), 24.1 (CH_2) ppm.

^1H -NMR + COSY (500 MHz, CDCl_3): δ 10.37 (1H, br. s), 3.26 (2H, t, $J = 6.9$ Hz), 2.86 (2H, t, $J = 7.4$ Hz), 1.69-1.64 (2H, m), 1.62-1.58 (2H, m), 1.45-1.39 (2H, m) ppm.

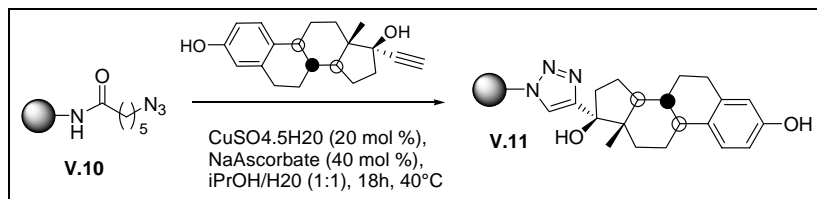
VIII.5.1.2. Coupling of V.9 to silica



The silica material (2 g, max. loading 0.73 mmol g^{-1}) was suspended in DMF (10 mL) and azidoheptanoic acid **V.9** (691 mg, 4.4 mmol, 3 eq) was then added to this suspension. After addition of PyBOP (2.3 g, 4.4 mmol, 3 eq) and DIEA (1.53 mL, 8.8 mmol, 6 eq) the suspension was shaken for 18 h. Subsequently, the solution was drained and the remaining powder was washed thoroughly. After capping, the ninhydrine test gave a colourless result, indicating that there was no more free amine left.

IR. (KBr-plate): 3414 (br. s), 2104 (s), 1642 (m), 1111 (br. s), 810 (s) cm^{-1}

VIII.5.1.3. ‘Clicking’ of ethinylestradiol to V.10



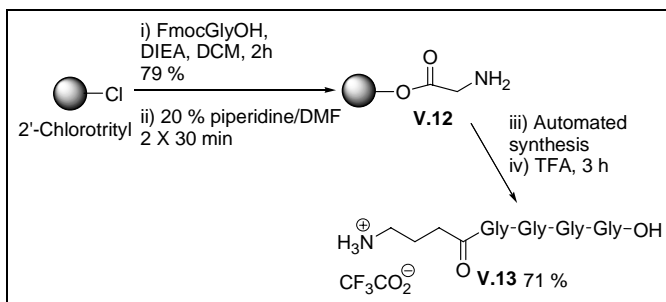
The silica material **V.10** (6 g) was suspended in an *i*PrOH/ H_2O (60 mL in a ratio of 1:1) solution. Ethinylestradiol (4.45 g, 15 mmol, 1 eq) was added to this suspension followed by $\text{CuSO}_4 \cdot 5\text{H}_2\text{O}$ (749 mg, 3 mmol, 20 mol %) and NaAscorbate (1.2 g, 6 mmol, 40 mol %). The resulting orange solution was stirred gently in an oil bath of 40°C . After overnight reaction, the suspension was filtered and the remaining silica material was washed with MeOH (3 x), EDTA_{aq} (3 x), MeOH (3 x) and ether (3 x). All the azide functions had reacted as witnessed by the disappearance of the azide

absorption ($\sim 2100\text{ cm}^{-1}$) in the IR-spectrum. Finally, the silica material **V.11** was dried at an oven temperature of $60\text{ }^{\circ}\text{C}$ for overnight.

IR. (KBr-plate): 3399 (br. s), 2936 (s), 1670 (s), 1050 (br. s), 800 cm^{-1} (s)

VIII.5.2. Synthesis of the Tozzi peptides

VIII.5.2.1. Synthesis of a 'blanc' tetraglycine peptide **V.13**



FmocGlyOH (92 mg, 0.31 mmol, 2 eq) was added to the preswollen 2'-chlorotritylresin (100 mg, 0.16 mmol, 1 eq). Next, DCM (1 mL) was added and the suspension was shaken until all of the FmocGlyOH was dissolved. After adding DIEA (323 μL , 0.31 mmol, 2 eq), the suspension was shaken for 2 h after which the solution was drained and the beads thoroughly washed with DMF (3 x), 10 % DIEA/MeOH (3 x), MeOH (3 x) and DCM (3 x). A loading value of 1.23 mmol g^{-1} was determined which corresponded with a yield of 79 %.

The Fmoc group was deprotected using a 20 % piperidine/DMF solution for two times 30 min. Then the resin was weighed into a syringe of 10 mL and put into the reaction block of the Syro I.

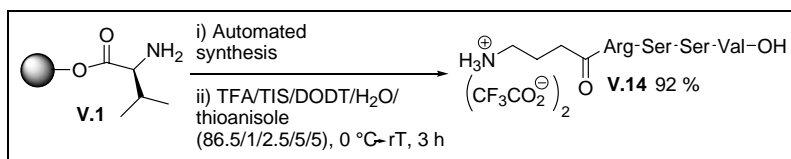
After the automated synthesis, the desired peptide was cleaved from the resin with TFA for 3 h and precipitated with ice cold MTBE. After centrifugation, the residue was dissolved in H₂O. Lyophilisation gave 39.1 mg (96 %) of white powder.

Molecular Formula: $C_{12}H_{21}N_5O_6$

MW.: 331.2 g/mol

LC-MS: 288.5 $[M-CO_2+H]^+$, 332.5 $[M+H]^+$

VIII.5.2.2. Synthesis of the Tozzi-tetrapeptide V.14



Starting from construct **V.1**, the tetrapeptide **V.14** was synthesised by weighing 200 mg of **V.1** into a syringe of 10 mL. This syringe was put into the reaction block of the Syro I.

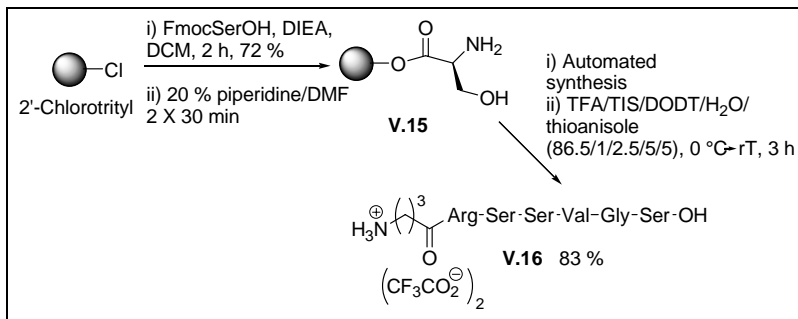
After the automated synthesis, an ice cold mixture of TFA/TIS/DODT/ H_2O /thioanisole (86.5/1/2.5/5/5) was added to the resin. After 3 h, the suspension was dried by applying an Ar stream over the syringe. From the resulting oil, the desired peptide was precipitated with ice cold MTBE. To remove all the scavengers, this precipitation was repeated 3 times. Centrifugation gave a residue that was redissolved in H_2O . Lyophilisation gave 149 mg (92 %) of a white powder.

Molecular Formula: $C_{21}H_{41}N_8O_8$

MW.: 533.6 g/mol

ES: 534.5 $[M+H]^+$

VIII.5.2.3. Synthesis of the Tozzi-hexapeptide V.16



FmocSerOH (363 mg, 0.95 mmol, 2 eq) was added to the preswollen 2'-chlorotritylresin (300 mg, 0.47 mmol, 1 eq). Next, DCM (3 mL) was added and the suspension was shaken until all of the FmocSerOH was dissolved. After adding DIEA (153 μL , 0.95 mmol, 2 eq), the suspension was shaken for 2 h after which the solution was drained and the beads thoroughly washed with DMF (3 x), 10 % DIEA/MeOH (3 x), MeOH (3 x) and DCM (3 x). A loading value of 0.721 mmolg⁻¹ was determined which corresponded with a yield of 72 %.

The Fmoc group was deprotected using a 20 % piperidine/DMF solution for two times 30 min. Then the resin (100 mg) was weighed into a syringe of 10 mL and put into the reaction block of the Syro I.

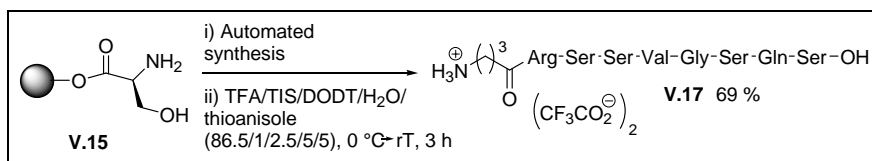
After the automated synthesis, an ice cold mixture of TFA/TIS/DODT/H₂O/thioanisole (86.5/1/2.5/5/5) was added to the resin. After 3 h, the suspension was dried by applying an Ar stream over the syringe. From the resulting oil, the desired peptide was precipitated with ice cold MTBE. To remove all the scavengers, this precipitation was repeated 3 times. Centrifugation gave a residue that was redissolved in H₂O. Lyophilisation gave 54 mg (83 %) of a white powder.

Molecular Formula: C₂₆H₄₈N₁₀O₁₁

MW.: 676.7 g/mol

ES: 339.3 $[M+2H]^{2+}$, 677.3 $[M+H]^+$

VIII.5.2.4. Synthesis of the Tozzi-octapeptide



Starting from construct **V.15**, the Tozzi-octapeptide **V.17** was synthesised on the Syro I. The resin (100 mg) was weighed into a syringe of 10 mL and put into the reaction block of the Syro I.

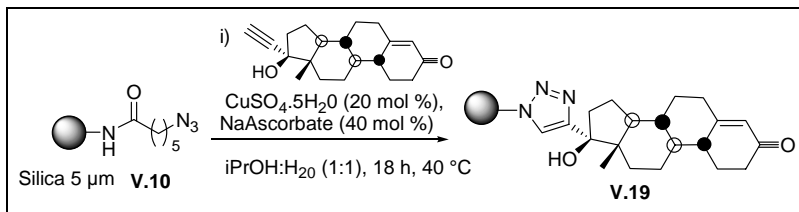
After the automated synthesis, an ice cold mixture of TFA/TIS/DODT/H₂O/thioanisole (86.5/1/2.5/5/5) was added to the resin. After 3 h, the suspension was dried by applying an Ar stream over the syringe. From the resulting oil, the desired peptide was precipitated with ice cold MTBE. To remove all the scavengers, this precipitation was repeated 3 times. Centrifugation gave a residue that was redissolved in H₂O. Lyophilisation gave 56 mg (69 %) of a white powder.

Molecular Formula: C₃₄H₆₁N₁₃O₁₅

MW.: 891.9 g/mol

ES: 446.9 $[M+2H]^{2+}$

VIII.5.3. Development of the norethindrone column V.19



The silica material **V.10** (1 g) was suspended in an $i\text{PrOH}/\text{H}_2\text{O}$ (10 mL in a ratio of 1:1) solution. Norethindrone (756 mg, 2.5 mmol, 1 eq) was added to this suspension followed by $\text{CuSO}_4 \cdot 5\text{H}_2\text{O}$ (125 mg, 0.5 mmol, 20 mol %) and NaAscorbate (198 mg, 1.0 mmol, 40 mol %). The resulting orange solution was stirred gently in an oil bath of 40 °C. After overnight reaction, the green suspension was filtered and the remaining silica material was washed with MeOH (3 x), EDTA_{aq} (3 x), MeOH (3 x) and ether (3 x). Finally, the silica material **V.19** was dried at an oven temperature of 60 °C for overnight.

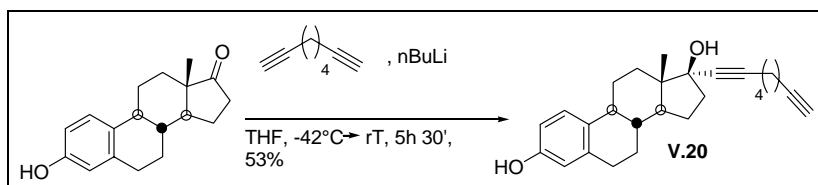
The filtrate was extracted three times with DCM. The organic phases were pooled, extracted once with a 10 % Na_2CO_3 solution and subsequently dried over Na_2SO_4 . After filtration, the organic phase was evaporated under reduced pressure to yield 524 mg of a white powder. LC-MS and ^1H -NMR analysis showed that this was pure norethindrone. From this, it was calculated that 232 mg (0.744 mmol) was coupled to the silica; resulting in a final loading of 0.609 mmol/g.

All the azide functions had reacted as witnessed by the disappearance of the azide absorption ($\sim 2100 \text{ cm}^{-1}$) in the IR-spectrum.

IR. (KBr-plate): 3430 (br. s), 2947 (m), 1647 (s), 1092 (br. s), 802 (s) cm^{-1}

VIII.5.4. Development of a second generation estradiol column V.23

VIII.5.4.1. Synthesis of estradiol derivative V.20



A solution of 1,7-octadiyne (1 mL, 8.29 mmol, 5eq) under Ar was cooled down until -42°C (MeCN/ CO_2). The subsequent addition of a 1 M solution of nBuLi in hexane (3.52 mL, 8.29 mmol, 5eq) resulted in a white precipitate. After stirring the suspension for 30 min, estrone (445 mg, 1.65 mmol, 1eq) was added and the reaction was allowed to warm up at rT for 5h. Then the mixture was diluted with $\text{NH}_4\text{Cl}_{\text{aq}}$ and extracted 3 times with DCM. The combined organic phases were dried with Na_2SO_4 , filtered and evaporated. The residue was purified via flash chromatography with *i*octane/EtOAc (8:2 – 7:3) to yield a white solid (479 mg). However, LC-MS analysis showed that the isolated material consisted of 30% estrone and 70% of the desired product. This corresponded with the ^1H -NMR integration of the two CH_3 -18 singlets. Thus the overall yield was 53%.

Molecular Formula: $\text{C}_{26}\text{H}_{32}\text{O}_2$

M.W.: 376.53 g/mol

R.F. (*i*octane/EtOAc 1:1): 0.48

Melting Point: 120–122 $^{\circ}\text{C}$

I.R.: 3400 (br.), 3303 (s), 2930 (s), 2864 (s), 2245 (w), 2116 (w), 1724 (m), 1610 (s), 1584 (w), 1499 (s), 1452 (s), 1379 (w), 1355 (w), 1326 (w), 1286 (s), 1246 (s), 910 (s), 731 (s)

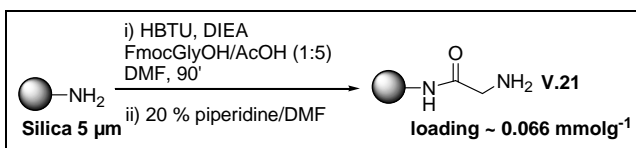
E.S.-M.S. (m/z): 375.2 $[\text{M}-\text{H}]^-$

^1H -NMR (500 MHz, CDCl_3): δ 7.20-7.09 (m), 6.67-6.59 (m), 4.78 (s), 4.73 (s), 2.93-2.73 (m), 2.55-2.43 (m), 2.43-2.30 (m), 2.30-2.24 (m), 2.24-2.15 (m), 2.15-2.08 (m), 2.08-1.93 (m), 1.93-1.90 (m), 1.90-1.80 (m), 1.79-1.71 (m), 1.71-1.68 (m), 1.68-1.57

(m), 1.57-1.50 (m), 1.50-1.46 (m), 1.46-1.43 (m), 1.43-1.29 (m), 1.28-1.23 (m), 0.90 (s), 0.86 (s) ppm.

^{13}C -APT (75 MHz, CDCl_3): δ 153.3 (C), 138.3 (C), 132.7 (C), 126.5 (CH), 115.2 (CH), 112.7 (CH), 85.8 (C), 84.1 (C), 80.1 (C), 68.5 (alkyne-CH), 50.4 (CH), 49.5 (CH), 47.2, 43.6 (CH), 39.4 (CH), 35.9, 32.9, 31.6, 29.6, 27.7, 27.2, 26.5, 25.9, 22.8, 21.6, 18.3, 17.9, 13.8 (CH_3), 12.8 (CH_3) ppm.

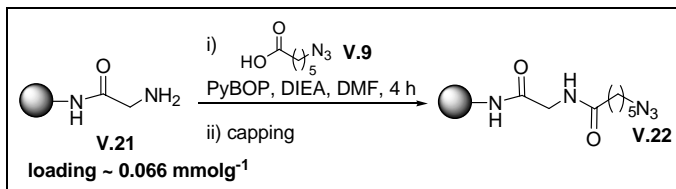
VIII.5.4.2. Lowering the loading of silica



The silica particles (2.1 g) were put in a plastic falcon tube. Subsequently, DMF (6 mL) was added followed by the addition of FmocGlyOH (119 mg, 0.4 mmol, 20 mol%), AcOH (92 μL , 1.6 mmol, 80 mol%), HBTU (759 mg, 2 mmol, 1 eq) and DIEA (700 μL , 4 mmol, 2 eq). After shaking for 90 min, the suspension was centrifuged and washed thoroughly. Determination of the loading gave a value of $0.066 \text{ mmol g}^{-1}$.

Next, the Fmoc group was deprotected to give **IV.21**. The presence of free amine groups was confirmed by a positive TNBS test.

VIII.5.4.3. Preparation of construct V.22: coupling of azidohexanoic acid

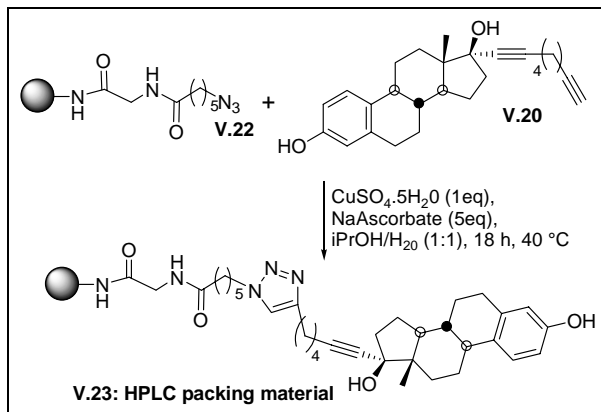


The silica material **V.21** (1 g, 0.066 mmol, 1 eq) was suspended in DMF (4 mL). PyBOP (260 mg, 0.5 mmol, 7.6 eq), azidohexanoic acid **V.9** (79 mg, 0.5 mmol, 7.6 eq) and DIEA (174 μL , 1 mmol, 15.2 eq) were subsequently added to this suspension. After shaking for 4 h, the solution was drained and the particles were thoroughly washed.

Though no free amines were detected by the TNBS test, a capping step was still performed to make sure that there were no more free amines.

After subjecting a small sample of the silica material **V.22** to a solution of 0.5 M Ph_3P in THF/ H_2O at 70 °C for 10 min, the TNBS test turned the particles red, thereby proving that the azides were present on the surface.

VIII.5.4.4. Preparation of construct V.23: ‘clicking’ of V.20 to V.22

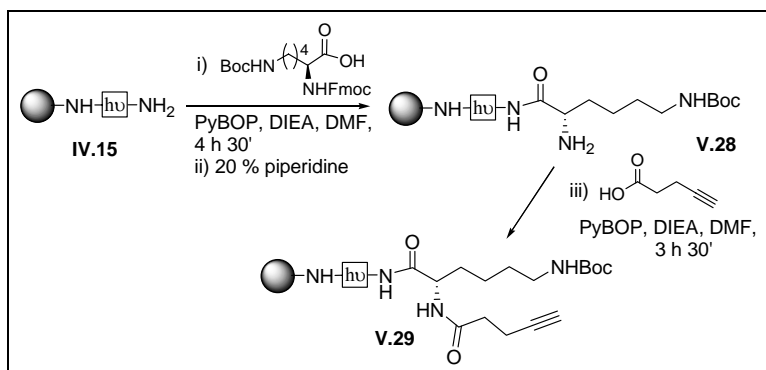


The silica material **V.22** (1 g, 0.066 mmol, 1 eq) was suspended in a solution of *i*PrOH/ H_2O (10 mL in a ratio of 1:1). Estradiol derivative **V.20** (269 mg, 0.5 mmol, 7.6 eq) was added to this suspension followed by $\text{CuSO}_4 \cdot 5\text{H}_2\text{O}$ (25 mg, 0.1 mmol, 1.5 eq) and NaAscorbate (99 mg, 0.5 mmol, 7.6 eq). The resulting orange solution was stirred gently in an oil bath of 40 °C. After overnight reaction, the green suspension was filtered and the remaining silica material was washed with MeOH (3 x), EDTA_{aq} (3 x), MeOH (3 x) and ether (3 x). Finally, the silica material **V.23** was dried at an oven temperature of 60 °C for overnight.

VIII.6. Screening of the library: development of new SPE cartridges

VIII.6.1. Synthesis of alkyne substituted components

VIII.6.1.1. Synthesis of alkyne modified construct V.29



The resin **IV.15** (1g, 0.21 mmol, 1 eq) was weighed into a reaction vessel. After the addition of DMF (4.6 mL), FmocLys(Boc)OH (539 mg, 1.15 mmol, 5.5 eq) and PyBOP (598 mg, 1.15 mmol, 5.5 eq) were added to this suspension. Subsequently, DIEA (400 μ L, 2.30 mmol, 11 eq) was added and the suspension was shaken for 4 h 30' after which the solution was drained and the beads were thoroughly washed. Ninhydrine test on a small sample was negative.

Then the Fmoc group was deprotected to give construct **V.28**.

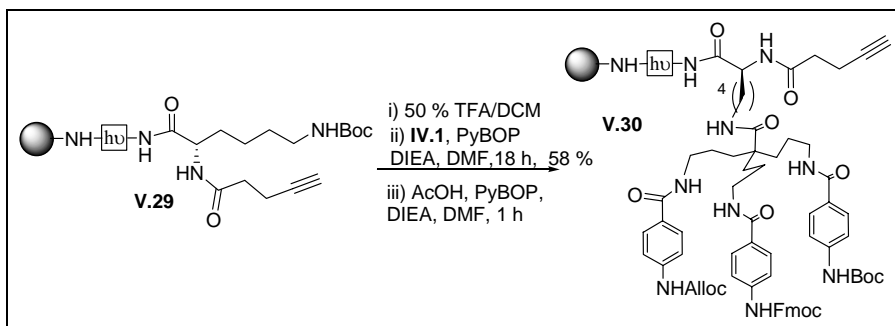
Next, pentynoic acid (68 mg, 0.69 mmol, 3.3 eq), PyBOP (359 mg, 0.69 mmol, 3.3 eq) and DIEA (241 μ L, 1.38 mmol, 6.6 eq) were added to a suspension of **V.28** in DMF (4.6 mL). The suspension was shaken for 3 h 30 min, drained and the remaining beads were washed. Ninhydrine test was negative

Molecular Formula: C₁₆H₂₇N₃O₄

MW.: 325.4 g/mol

ES. (after photocleavage in EtOH): 348.0 $[M+Na]^+$

VIII.6.1.2. Coupling of scaffold IV.1 to construct V.29

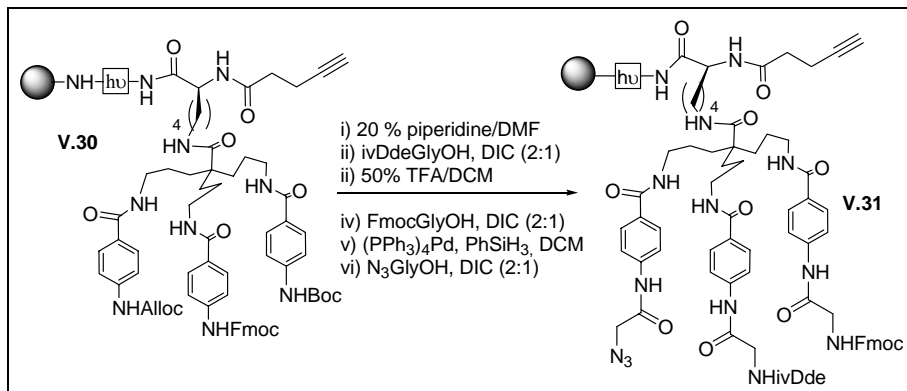


Resin **V.29** (1.1 g, 0.23 mmol, 1 eq) was weighed into a reaction vessel and Boc deprotected.

A solution of **IV.1** (345 mg, 0.35 mmol, 1.5 eq) and PyBOP (180 mg, 0.35 mmol, 1.5 eq) in 15 mL DMF was prepared. When homogeneous, the solution was transferred to the pre-swollen resin and after adding DIEA (181 μ L, 1.04 mmol), the suspension was shaken for 18 h. The resin was drained and washed thoroughly. The TNBS test turned the beads dark-yellow and with NF31 we got red beads. The remaining free spacer-amino groups were capped for 1 h with a 0.1 M solution of AcOH and PyBOP in the presence of 2 eq DIEA. The ninhydrin test was negative.

The total loading was $0.101 \text{ mmol g}^{-1}$ which corresponded (maximal theoretical loading is $0.173 \text{ mmol g}^{-1}$) to a yield of 58 %.

VIII.6.1.3. Attachment of the glycine derivatives to V.30



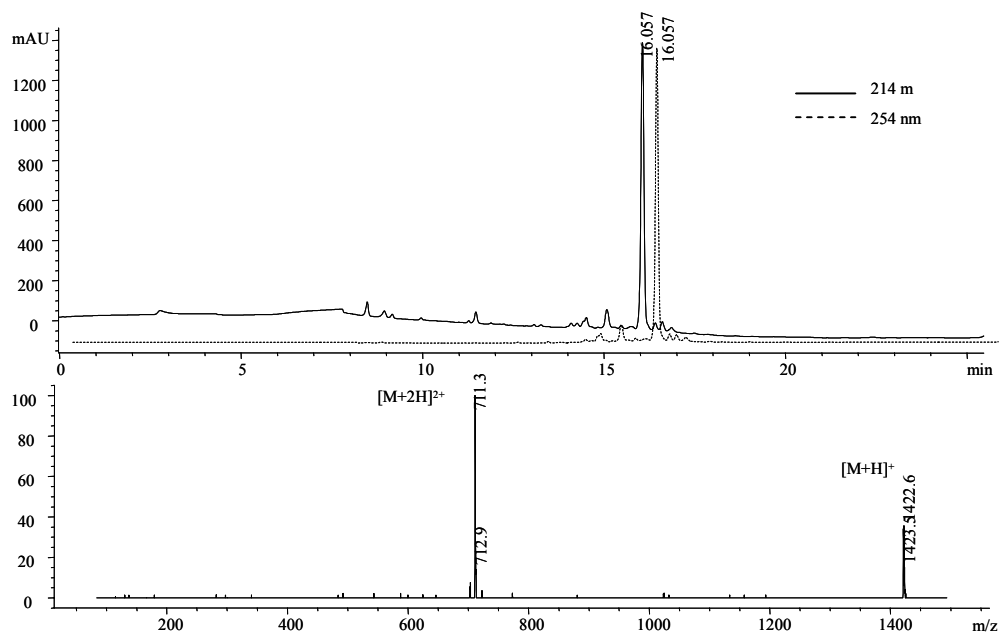
For the incorporation of the glycine derivatives, the same protocol as described in VIII.3.4 was applied. The amount of resin **V.30** used was 1.1 g (110 μmol).

Molecular Formula: $\text{C}_{77}\text{H}_{92}\text{N}_{14}\text{O}_{13}$

MW.: 1421.6 g/mol

Exact mass: 1420.7Da

LC-MS. (after photocleavage in EtOH): 711.3 $[\text{M}+2\text{H}]^{2+}$, 1422.6 $[\text{M}+\text{H}]^+$



The residue was subsequently dissolved in 10 % AcOH/H₂O and this aqueous fraction was extracted 3 times with MTBE ether. The water fraction was then lyophilised.

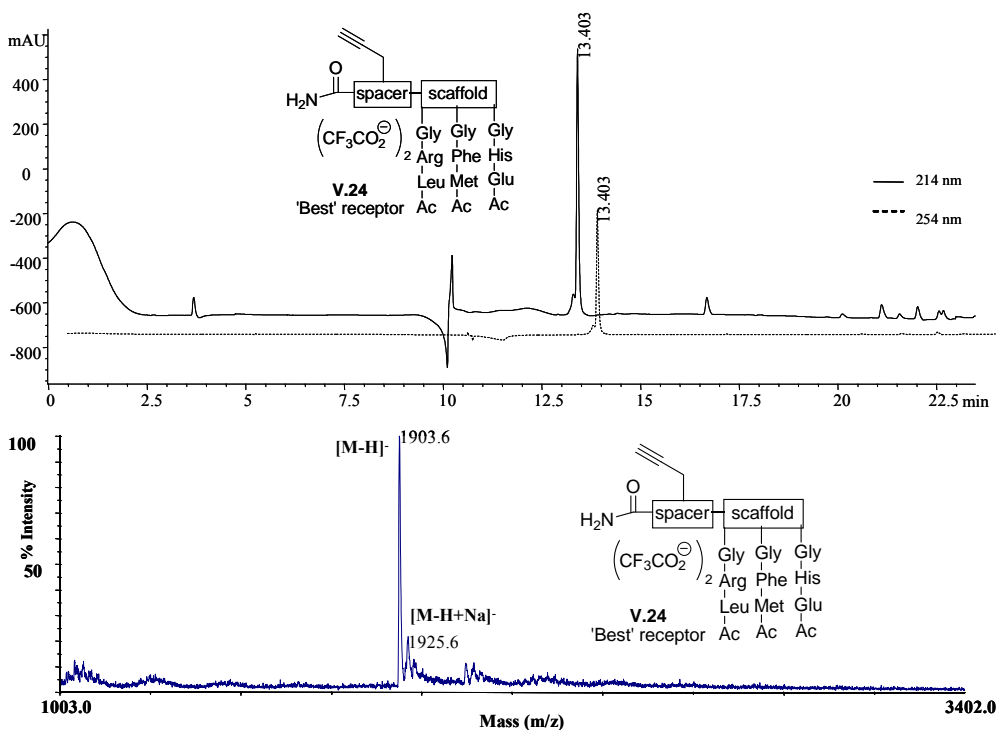
The residue obtained after lyophilisation was redissolved in 10 % AcOH/H₂O (1 mL). The desired compound was then purified by injecting 500 µL of this mixture on a preparative HPLC system (C₁₈ column). A gradient from 0 to 40 % MeCN in 40 min was used in combination with a 0.1 % TFA_{aq} solution (from 100 % to 60 % in 40 min). After lyophilisation, 4.2 mg (20 %) of **V.24** was obtained.

Molecular Formula: C₉₂H₁₂₇N₂₃O₂₀S

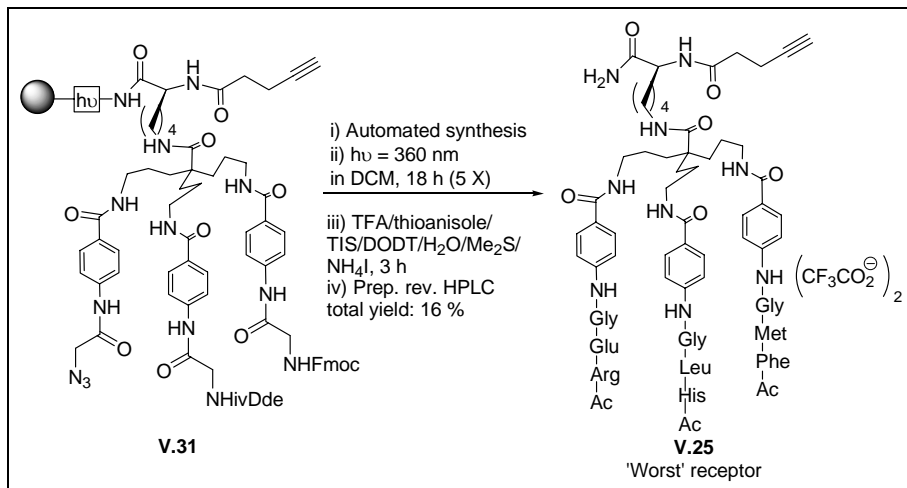
MW.: 1907.1 g/mol

Exact mass: 1905.9 Da

MALDI. (after photocleavage in H₂O): 1903.6 [M-H]⁻, 1925.6 [M-H+Na]⁻, 1940.5 [M-H+K]⁻



VIII.6.1.5. Synthesis of the ‘worst’ receptor V.25



Starting from 100 mg **V.31** (11 μmol), the ‘worst’ receptor **V.25** was prepared according to the protocol outlined in **Paragraph VIII.6.1.4**.

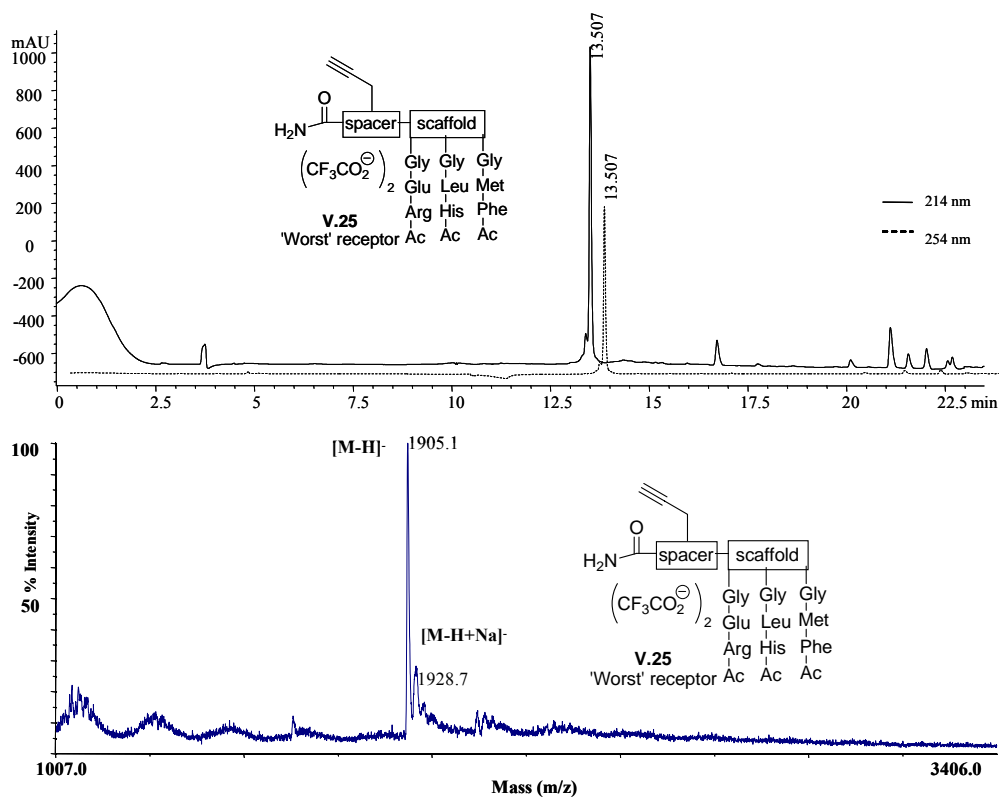
Purification yielded 3.5 mg (16 %).

Molecular Formula: C₉₂H₁₂₇N₂₃O₂₀S

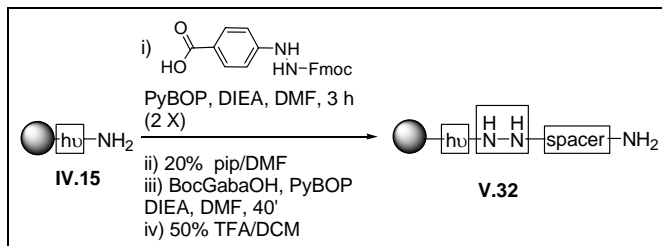
MW.: 1907.1 g/mol

Exact mass: 1905.9 Da

MALDI : 1905.1 [M-H]⁻, 1928.7 [M-H+Na]⁻, 1942.9 [M-H+K]⁻



VIII.6.1.6. Synthesis of construct V.32



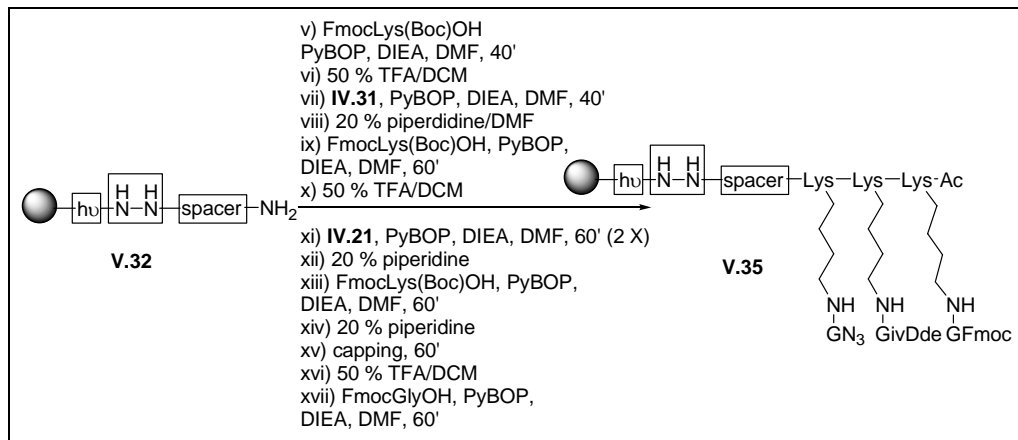
Resin **IV.15** (118 mg, 25 μ mol, 1 eq) was weighed into a reaction vessel. Fmoc-hydrazinobenzoic acid (31 mg, 82 μ mol, 3.3 eq) was dissolved in DMF (500 μ L) together with PyBOP (43 mg, 82 μ mol, 3.3 eq). This mixture was added to the beads and after the addition of DIEA (28 μ L; 164 μ mol, 6.6 eq), the suspension was shaken for 3 h. Subsequently, the resin was drained and washed. A positive NF31 test indicated the presence of unreacted amines. The reaction was repeated once.

Next, the Fmoc group was deprotected.

Then, the spacer Boc- γ -aminobutyric acid (21 mg, 105 μ mol, 5 eq) was added to a suspension of the resin (100 mg, 21 μ mmol, 1 eq) in DMF (210 μ L). PyBOP (210 μ L of a 0.5 M solution in DMF, 5 eq) and DIEA (110 μ L of a 2 M solution in NMP, 10 eq) were added and the resulting suspension was shaken for 40 min. After draining and washing, the NFR31 and TNBS test were negative.

Finally, the Boc group was deprotected.

VIII.6.1.7. Synthesis of construct V.35



FmocLys(Boc)OH (210 μL , 0.5 M in DMF, 5 eq) was added to resin **V.32** (100 mg, 21 μmol , 1 eq). After adding PyBOP (210 μL , 0.5 M in DMF, 5 eq) and DIEA (110 μL , 2 M in NMP, 10 eq) the suspension was shaken for 40 min. After draining and washing of the beads, a NF31 and TNBS test were negative.

Then the Boc group was deprotected.

Azidoglycine **IV.31** (11 mg, 108 μmol , 5 eq) was dissolved in DMF (210 μL) and added to the resin. After adding PyBOP (210 μL , 0.5 M in DMF, 5 eq) and DIEA (110 μL , 2 M in NMP, 10 eq) the suspension was shaken for 40 min. After draining and washing of the beads, a NF31 and TNBS test were negative.

Next, the Fmoc group was deprotected.

FmocLys(Boc)OH (210 μL , 0.5 M in DMF, 5 eq) was added to the resin. After adding PyBOP (210 μL , 0.5 M in DMF, 5 eq) and DIEA (110 μL , 2 M in NMP, 10 eq) the suspension was shaken for 60 min. After draining and washing of the beads, a NF31 and TNBS test were negative.

Then, the Boc group was deprotected.

ivDdeGlyOH **IV.21** (30 mg, 107 μmol , 5 eq) was dissolved in DMF (210 μL) and added to the resin. After adding PyBOP (210 μL , 0.5 M in DMF, 5 eq) and DIEA (110 μL , 2 M in NMP, 10 eq) the suspension was shaken for 60 min. After draining and washing of the beads, the NF31 test was positive. Consequently, the reaction was repeated once to give a negative NF31 test.

Next, the Fmoc group was deprotected.

FmocLys(Boc)OH (210 μL , 0.5 M in DMF, 5 eq) was added to the resin. After adding PyBOP (210 μL , 0.5 M in DMF, 5 eq) and DIEA (110 μL , 2 M in NMP, 10 eq) the suspension was shaken for 60 min. After draining and washing of the beads, a NF31 and TNBS test were negative.

Then, the Fmoc group was deprotected.

The free amine was capped with Ac_2O /pyridine/DCM (1:3:16) for 60 min. The subsequent NF31 and TNBS test were both negative.

Next, the Boc group was deprotected.

Finally, FmocGlyOH (31 mg, 105 μmol , 5 eq) was dissolved in DMF (210 μL) and added to the resin. After adding PyBOP (210 μL , 0.5 M in DMF, 5 eq) and DIEA (110 μL , 2 M in NMP, 10 eq) the suspension was shaken for 60 min. After draining and washing of the beads, the NF31 test was positive. Consequently, the reaction was repeated once to give a negative NF31 test.

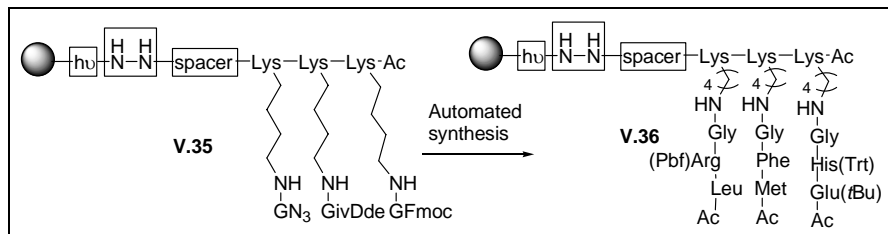
Molecular Formula: $\text{C}_{65}\text{H}_{89}\text{N}_{15}\text{O}_{13}$

MW.: 1288.5 g/mol

Exact mass: 1287.7 Da

LC-MS (after photocleavage in EtOH): 1288.7 $[\text{M}+\text{H}]^+$, 1371.7 $[\text{M}+2\text{Ac}+\text{H}]^+$

VIII.6.1.8. Synthesis of V.36



The automated synthesis was performed in a manner similar to the protocol described in **Paragraph VIII.3.5**. An amount of 41 mg (4.3 μ mol) of construct **V.35** was subjected to this protocol.

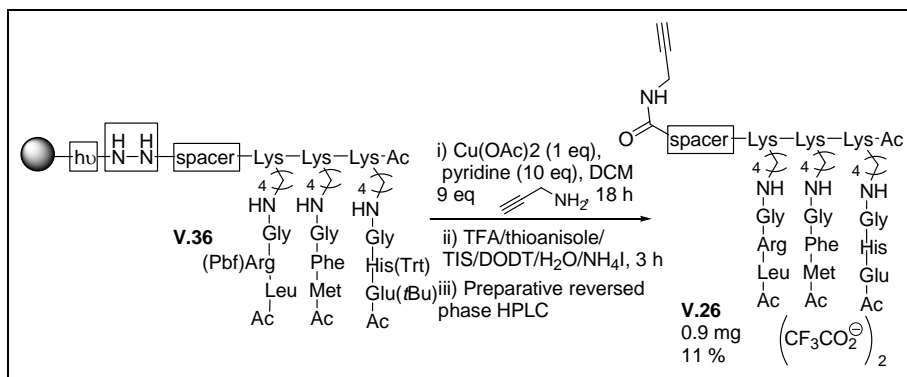
Molecular Formula: C₁₁₆H₁₆₃N₂₄O₂₃S₂

MW.: 2325.8 g/mol

Exact mass: 2324.2 Da

MALDI (after photocleavage in EtOH): 2324.5 [M+H]⁺, 2339.6 [M+O+H]⁺, 2345.9 [M+Na]⁺, 2363.0 [M+K]⁺, 1371.7 [M+2Ac+H]⁺

VIII.6.1.9. Cleavage of V.36 from the resin with propargylamine and subsequent side chain deprotection



The resin **V.36** (4.3 μmol) was suspended in DCM (500 μL). Propargylamine (2.7 μL , 39.3 μmol , 9 eq) was added followed by $\text{Cu}(\text{OAc})_2$ (anhydrous, 0.8 mg, 4.3 μmol , 1 eq) and pyridine (3.5 μL , 43 μmol , 10 eq). The resulting suspension was left overnight open to the air. Then the beads were drained and washed with DCM (3 x). The organic fractions were combined and evaporated.

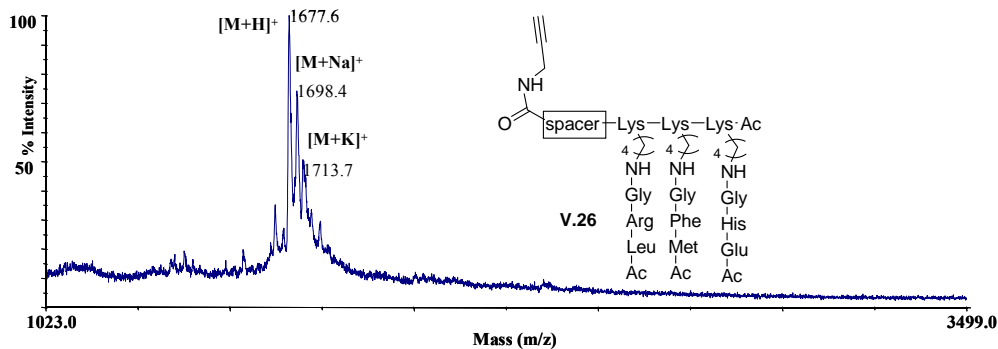
The residual oil was dissolved in 950 μL cleavage mixture consisting of TFA/TIS/DODT/ Me_2S /thioanisole (89.5/1/2.5/2/5) and then $\text{NH}_4\text{I}_{\text{aq}}$ (50 μL , 460 mg/mL) was added. This yellow mixture was shaken for 3 h and blown to dryness with Ar.

The black residue was dissolved in 10 % $\text{AcOH}/\text{H}_2\text{O}$ and filtered over a small piece of cotton wool in a pasteur pipette before purifying via preparative HPLC. The desired compound was then purified using a gradient from 0 to 40 % MeCN in 40 min in combination with a 0.1 % TFA_{aq} solution (from 100 % to 60 % in 40 min). After lyophilisation, 0.9 mg (11 %) of **V.26** was obtained.

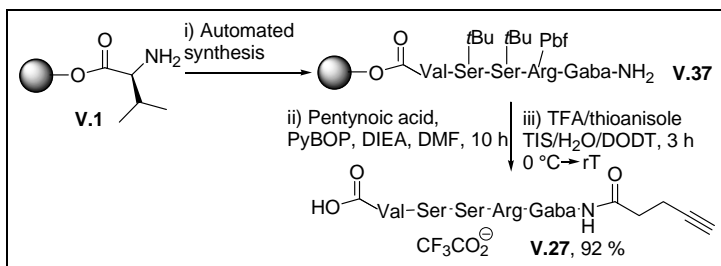
Molecular Formula: $\text{C}_{76}\text{H}_{121}\text{N}_{22}\text{O}_{19}\text{S}$

MW.: 1679.0 g/mol

Exact mass: 1677.9 Da

MALDI.: 1677.6 $[M+H]^+$, 1698.4 $[M+Na]^+$, 1713.7 $[M+K]^+$ 

VIII.6.1.10. Synthesis of alkyne modified Tozzi-tetrapeptide V.27



Resin **V.1** (235 mg, 0.25 mmol) was weighed into a 10 mL syringe, that was placed in the reaction block of the Syro I. The automated synthesis was performed in a manner similar to the protocol described in **Paragraph VIII.3.5**. The process was stopped at the stage of **V.37**. Then, pentynoic acid (74 mg, 0.75 mmol, 3 eq) was added manually to the syringe followed by HBTU (284 mg, 0.75 mmol, 3 eq), DIEA (0.75 mL, 1.50 mmol, 6 eq) and DMF (2. mL). Next, the suspension was shaken for 10 h after which the solution was drained and the beads were washed.

Subsequently, the resin was transferred to a flask, mixing it with 5 mL of freshly prepared TFA/thioanisole/TIS/H₂O/DODT (86.5/5/1/5/2.5) at 0 °C. The resulting

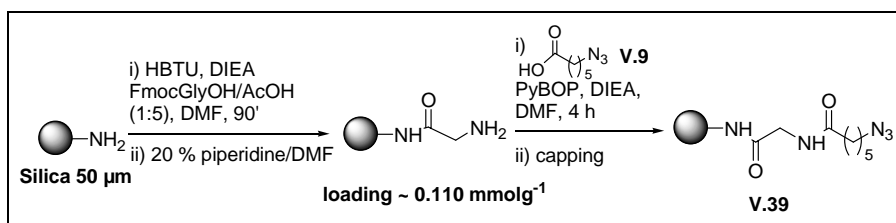
suspension was stirred gently and after 5 min the ice bath was removed and the suspension was stirred for 3 h at ambient temperature. Then the filtrate was isolated and blown to dryness with Ar. From the residual oil, the peptide **V.27** was precipitated 3 times with cold MTBE. After isolation, the peptide was dissolved in H₂O and lyophilised to give **V.27** as a white foam (176 mg, 92 %).

Molecular Formula: C₂₆H₄₄N₈O₉

MW.: 612.3 g/mol

ES.: 611.5 [M-H]⁻

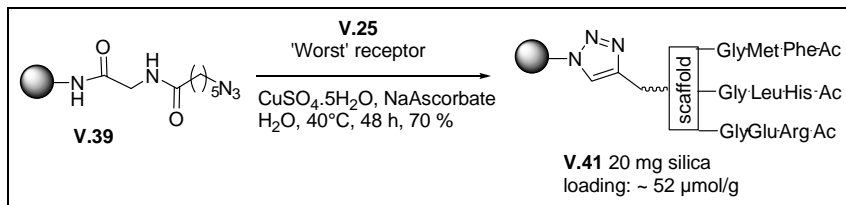
VIII.6.1.11. Lowering the loading of silica (particle size 50 µm)



A protocol similar as described in **Paragraph VIII.5.4.2** was applied on 2.35 g of aminopropylsilica with a particle size of 50 µm.

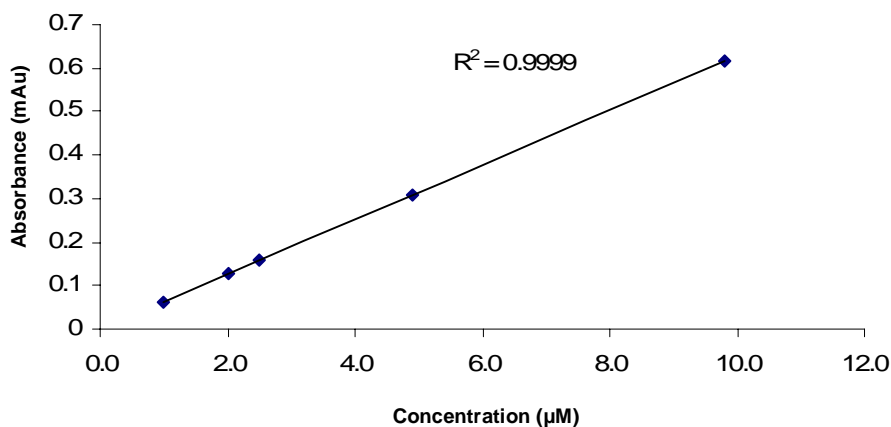
IR. (KBr): 3450 (br. s), 2106 (m), 1643 (s), 1089 (br. s), 798 (s)

VIII.6.1.12. 'Clicking' of V.25 to silica



First, a UV-calibration curve was determined by making different concentrations (9.8 μM , 4.9 μM , 2.5 μM , 2.0 μM and 1.0 μM) of **V.25** in H_2O . By measuring the absorbance of the different concentrations, the following equation was determined:

$$\text{Abs} = 63.082 \times [\text{V.25}]_{\text{aq}} - 0.0544 \quad (R^2 = 0.9999)$$

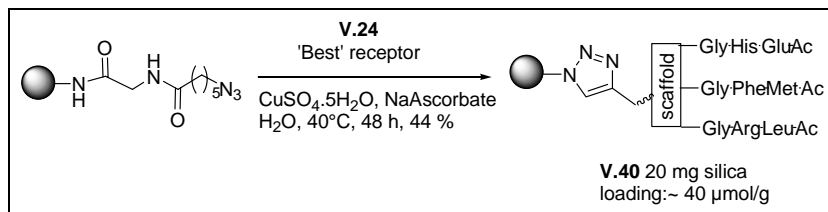


Next, $\text{CuSO}_4 \cdot 5\text{H}_2\text{O}$ (5.5 mg, 22 μmol) and NaAscorbate (8.71 mg, 44.0 μmol) were dissolved in H_2O (20 mL). From this stock solution, 200 μL (16 mol % $\text{CuSO}_4 \cdot 5\text{H}_2\text{O}$ and 32 mol % NaAscorbate) was pipetted in an eppendorf containing **V.25** (3.5 mg, 1.64 μmol , 8.2 mM 1 eq) and **V.39** (20 mg, 2.20 μmol). The resulting mixture was vortexed at 40 °C.

After 48 h, 3 μL of the reaction mixture was transferred to a UV cuvette and 2997 μL H_2O was added. For the blanc sample, 3 μL from the $\text{CuSO}_4 \cdot 5\text{H}_2\text{O}$ stock solution was diluted up to 3 mL in a UV cuvette. The absorbance from this sample was 0.121 mAu, correlating to a concentration of 2.8 mM. From this value, a loading of ~ 52 $\mu\text{mol/g}$ was determined.

The silica material **V.41** was isolated via centrifugation and subsequent decantation of the liquid. The material was washed thoroughly water (3 x), EDTA_{aq} (3 x) and *i*PrOH (3 x).

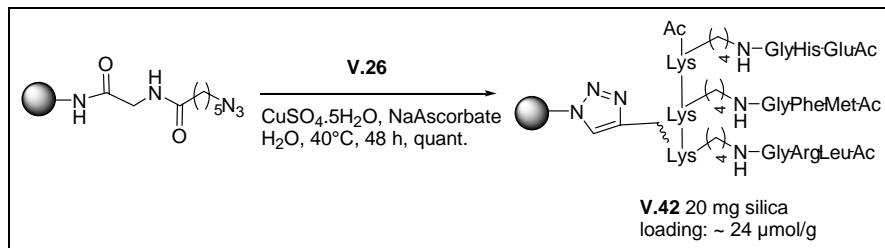
VIII.6.1.13. Clicking of V.24 to silica



An approach similar as in **Paragraph VIII.6.1.12** was applied on 20 mg silica **V.39** and 4.2 mg **V.24** (1.97 μmol , 9.9 mM, 1 eq).

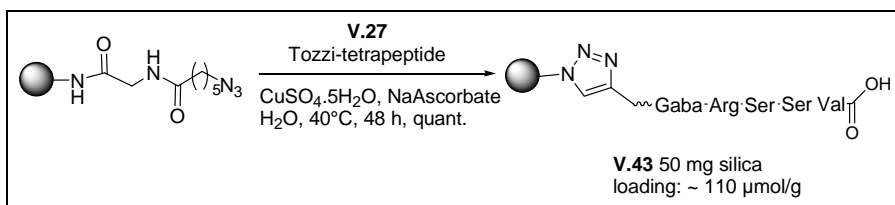
After 48 h, an absorbance of 0.313 mAu was measured, correlating to a concentration of 5.8 mM. From this value, a loading of ~ 40 $\mu\text{mol/g}$ was determined.

VIII.6.1.14. 'Clicking' of V.26 to silica



An approach similar as in **Paragraph VIII.6.1.12** was applied on 20 mg silica **V.39** and 0.9 mg **V.26** (0.47 μmol , 2.4 mM, 1 eq). In 200 μL H_2O was added $\text{CuSO}_4 \cdot 5\text{H}_2\text{O}$ (2.3 mg, 9.4 μmol , 20 eq) and NaAscorbate (3.72 mg, 18.8 μmol , 40 eq). After 48 h, no ES-signal of **V.26** was observed anymore when 2.5 μL of the reaction mixture was injected directly. Therefore, a loading value of ~ 24 $\mu\text{mol/g}$ was obtained.

VIII.6.1.15. 'Clicking' of V.27 to silica



An approach similar as in **Paragraph VIII.6.1.12** was applied on 50 mg silica **V.39** (5.5 μmol , 1 eq) and 21 mg **V.27** (28 μmol , 5 eq). A solution of $\text{CuSO}_4 \cdot 5\text{H}_2\text{O}$ (0.6 μmol , 20 mol%) and NaAscorbate (1.2 μmol , 40 mol%) in 500 μL H_2O was added and the suspension was vortexed for 48 h. The reaction proceeded quantitatively as witnessed by the disappearance of the azide absorption in the IR spectrum. The new material **V.43** was obtained with a loading of ~ 0.110 $\mu\text{mol/g}$.

IR. (Kbr): 3466 (br. s), 2106 (m), 1643 (s), 1093 (br. s), 803 (s)

IX. List of publications

IX.1. Poster presentations

- 10th BOSS congress, Ghent, Belgium (14/07/2008 – 18/07/2008), *poster*
- HPLC 2008, Baltimore, USA (10/05/2008 -16/05/2008), *poster*
- 9th KVCV congres, Antwerp, Belgium (4/4/2008), *poster*
- 11th Sigma-Aldrich symposium for organic synthesis, Sol Cress, Spa, Belgium (6/12/2007 - 7/12/2007), *poster*.
- International Symposium organised in honour of Prof. Léon Ghosez, Louvain-La-Neuve, Belgium (10/04/2007 - 13/04/2007), *poster*.
- 8th Tetrahedron Symposium, Berlin, Germany (26/06/2007 - 29/06/2007), *poster*
- 10th Sigma-Aldrich symposium for organic synthesis, Sol Cress, Spa, Belgium (7/12/2006 - 8/12/2006), *poster*.
- 9th Sigma-Aldrich symposium for organic synthesis, Sol Cress, Spa, Belgium (1/12/2005 - 2/12/2005), *poster*.

IX.2. Peer reviewed publications

- 1) **Fast and easy detection of aromatic amines on solid support.**
Van der Plas, S. E.; De Clercq, P. J.; Madder, A. *Tetrahedron Lett.* **2007**, 48, 2587-2589.
- 2) **Synthesis of a tripodal scaffold for solid phase synthesis of artificial receptors.**
Van der Plas, S. E.; Gea, A.; Figaroli, S.; De Clercq, P. J.; Madder, A. *Eur. J. Org. Chem.* **2008**, 1582-1588.
- 3) **Towards a new SPE material for EDCs: Fully automated synthesis of a library of tripodal receptors followed by a fast screening via affinity LC.**
Van der Plas, S.E.; Van Hoeck, E.; Lynen, F.; Sandra, P.; Madder A. *Eur. J. Org. Chem.* submitted.

- 4) **Click chemistry used as an efficient strategy for the manufacturing of dedicated stationary phases for LC and SFC.**

Van Hoeck, E.; Van der Plas, S.E.; Dunkle, M.; Lynen, F.; Madder, A.; Sandra, P. article in preparation.